Disertační práce

Univerzita Karlova v Praze
1. lékařská fakulta

STUDIJNÍ PROGRAM: Fyziologie a patofyziologie člověka

PharmDr. Vladimír, Farár

Adaptace centrálního nervového systému na chybění acetylcholinesterázy

Adaptation of the central nervous system to the absence of acetylcholinesterase

Školitel: doc. MUDr. Jaromír Mysliveček, Ph.D.
Spoluškolitel: Dr. Eric Krejci, Ph.D.

Praha, 2013

Vladimír FARÁR

Adaptace centrálního nervového systému na chybění acetylcholinesterázy
Adaptation of the central nervous system to the absence of acetylcholinesterase

Abstrakt

Acetylcholinesteráza (AChE) účinně hydrolyzuje acetylcholin (Ach). Inhibice AChE je letální a myši s chyběním AChE ve všech tkáních (AChE KO) jsou těžce poškozeny. AChE je v CNS kotvena na prolin bohatou kotvou - proline-rich membrane anchor (PRiMA), zatímco ve svalech je kotvena kolagenem Q (ColQ). V této disertaci popisujeme že u PRiMA KO myší, u nichž je AChE v CNS eliminována, nedochází k významným změnám v chování i přes nadbytek ACh a adaptaci cholinergních receptorů podobnou té, která byla pozorována u AChE KO myší. Kromě toho u myší, u nichž AChE nemůže interagovat s PRiMA i ColQ, je fenotyp podobný jako u AChE KO myší, ale biochemické změny v CNS jsou podobné změnám u PRiMA KO jedinců. PRiMA KO myší se také od ostatních AChE deficitních myší liší svou reakcí na AChE inhibitory. Naše výsledky nasvědčují, že AChE v periferních tkáních je hlavním cílem inhibitorů AChE a že chybění AChE v periferii je hlavní příčinou fenotypických charakteristik AChE KO myší.

Nervová soustava, acetylcholin, mozek, knockout myši, donepezil

Abstract

Acetylcholinesterase (AChE) effectively hydrolyzes acetylcholine (ACh). The inhibition of AChE is generally lethal and mice without AChE in all tissues (AChE KO) have severe impairments. In the brain, AChE is anchored in the plasma membrane by proline-rich membrane anchor (PRiMA), while in the muscles, AChE is anchored by collagen Q (ColQ) in the basal lamina. We report here that the PRIMA KO mice, in which AChE is essentially eliminated in the brain, show very little changes in behavior despite an excess of ACh in the brain and adaptation of ACh receptors comparable to those seen in AChE KO mice. Moreover, when AChE cannot interact with ColQ and PRIMA, the phenotype resembles that of AChE KO mice, but the biochemical changes in the brain are similar to those in PRiMA KO mice. PRiMA KO mice also differ from other AChE-deficit mice strains in their responses to AChE inhibitor. Our results suggest that AChE in the peripheral tissues is the major target of AChE inhibitors and AChE absence in the peripheral tissues is the leading cause of the phenotype of AChE KO mice.

Nervous System, acetylcholine, brain, knockout mice, donepezil

- **Prohlášení**

Prohlašuji, že jsem závěrečnou práci zpracoval samostatně a že jsem řádně uvedl a citoval všechny použité prameny a literaturu. Současně prohlašuji, že práce nebyla využita k získání jiného nebo stejného titulu.
Souhlasím s trvalým uložením elektronické verze mé práce v databázi systému meziuniverzitního projektu Theses.cz za účelem soustavné kontroly podobnosti kvalifikačních prací.

V Praze, 18.06.2013

VLADIMÍR FARÁR

Podpis

- **Identifikační záznam**

FARÁR, Vladimír. *Adaptace centrálního nervového systému na chybění acetylcholinesterázy. [Adaptation of the central nervous system to the absence of acetylcholinesterase].* Praha, 2013. 198 s., 3 příl. Disertační práce (Phd.). Univerzita Karlova v Praze, 1. lékařská fakulta, Fyziologický ústav. Školitel Mysliveček, Jaromír.

- **Acknowledgements**

I would like to thank my tutors dr. Eric Krejci and dr. Jaromír Mysliveček for undertaking the daunting task of a shared guidance over a PhD student, and for being my support and motivation not only in the scientific, but also in the personal sphere. My special thanks goes to dr. Anna Hrabovská who introduced me to the enchanting world of science. In addition to all the foregoing I would like to thank to my family, especially to my mother, close friends, Matej Ďurík and Kamil Stratený for the support in the difficult moments.

• TABLE OF CONTENTS

- **FIGURES** **85**

- **Abbreviation index**

A, asymmetric form of ChE

AC, auditory cortex

acetyl-CoA, acetyl coenzym A

AChE, acetylcholinesterase

AChE del E5, allele with deletion of exon 5

AChE del E6, allele with deletion of exon 6

AChE del E5+6, allele with deletion of exons 5 and 6

AChE H, hydrophobic or hematopoietic variant of AChE

AChE 1irr, alelle with a deletion in intron 1

AChE KO, allele with deletion of catalytic domain

AChE R, readthrough variant of AChE

AChE S, snake variant of AChE

AChE T, tailed variant of AChE

ACh, acetylcholine

AC, adenylatcyclase

ATR, atropine

BChE, butyrylcholinesterase

BChE KO, allele with the deletion of catalytic domain

BF, basal forebrain

bp, base pair

cAMP, 3‘5‘-cyclic adenosine monophosphate

CA1, CA1 field of hippocampus

CA3, CA3 field of hippocampus

CgC, cingulatae cortex

Ch, choline

ChAT, choline acetyltransferase

ChE, cholinesterase

ChI, striatal cholinergic interneurons

ChR, cholinergic receptors

ChT, high-affinity choline transporter

CICR, calcium-induced calcium release

CNS, central nervous system

ColQ, collagen like tail

ColQ KO, allele with deletion of the PRAD domain

CPu, caudate putamen

Cx, cortex

DAG, diacylglycerol

DG, dentate gyrus

EPP, evoked endplate potential

ERAD, endoplasmic reticulum-associated degradation

ER, endoplasmic reticulum

ERK, extracellular signal-regulated kinases

GABA, gamma-aminobutyric acid

GA, Golgi apparatus

GDP, guanosine 5‘-diphosphate

GIRK, G-protein gated inwardly rectifying potassium channels

GPCR, G-protein-coupled receptors

GPI, glycosylphosphatidylinositol

G-protein, GTP-binding protein

GTP, guanosine 5‘-triphosphate

HACU, high-affinity choline uptake

HDBn, horizontal diagonal band nucleus

Het, heterozygote

Hipp, hippocampus

Hth, hypothalamus

I_{AHP}, afterhyperpolarization current

I_{cat}, Ca^{2+} dependent nonspecific cation current

I_h, hyperpolarization-activated current

I_{leak}, leak K^+ current

I_M, voltage and time-dependent K^+ current

Ipn, interpenducular nucleus

IP_3, 1,4,5-trisphosphate

Kir, inwardly rectifying potassium channels

KO, knockout

LdTn, laterodorsal tegmental nucleus

LHth, lateral hypothalamus

MC, motor cortex

MEPP, miniature endplate potential

MH, medial habenula

MHC-1, slow myosin heavy chains

MR, muscarinic receptors

MPn, magnocellular preoptic nucleus

MSn, medial septum nucleus

MSN, medium spiny sized neurons

MWM, Morris water matez

NAc, nucleus accumbens

NMJ, neuromuscular junction

NR, nicotinic receptor

NBM, nucleus basalis magnocellularis

OT, olfactory tubercle

OXO, oxotremorine

Pbn, parabigeminal nucleus

$PIP_{2,}$ phosphatidylinositol-4,5-bisphosphate

PKC, protein kinase C

PIL, pilocarpine

PLC, phopholipase C

PNS, peripheral nervous system

Pptn, penduculopontine nucleus

PRAD, proline rich attachment domain

PRiMA, proline rich membrane anchor

PRiMA KO, allele with the deletion of the PRAD domain

PrlC, prelimbic cortex

RsC, retrosplenial cortex

SC, somatosensory cortex

SCO, scopolamine

SG, sympathetic ganglia

SI, substantia inominata

SN, substantia nigra

SNc, substantia nigra pars compacta

Str, striatum

Th, thalamus

t peptide, C terminal peptide of AChE T

VAChT, vesicular acetylcholine transporter

VC, visual cortex

VGCC, voltage-gated calcium channels

VDBn, vertical diagonal band nucleus

VTA, ventral tegmental area

WAT, tryptophan amphiphilic tetramerization domain

• INTRODUCTION

AChE is a well-known enzyme that has been a subject of intense research for decades. The well-established role of AChE is to hydrolyse ACh synthetized and released by cholinergic neurons in the central (CNS) and peripheral nervous system (PNS).

Previously, many concepts describing the function of AChE in the brain have been extrapolated from the results of intense research of cholinergic transmission at the neuromuscular junction (NMJ) (Fig. 1). This junction was used as a model of cholinergic synapse and it is commonly accepted that the role of AChE in the brain, as at NMJ, is to rapidly terminate the cholinergic transmission. At NMJ, the depolarization of motor neuron results in the release of ACh from multiple active zones that covers a large surface of the postsynaptic membrane. ACh diffuses trough the narrow synaptic cleft. Two ACh molecules bind to a nicotinic receptor (NR), a ligand gated ion channel, which is present at high density. The synchronous opening of NRs depolarize the postsynaptic membrane. When the depolarization attains the threshold, the action potential is generated and propagates along the muscle. At the transverse tubule, the excitation-contraction coupling and the release of intracellular calcium from sarcoplasmic reticulum result in the muscle contraction. AChE is mainly present at the postsynaptic membrane and its role is to clear the released ACh to prevent rebinding of ACh to NRs, thus allowing the sustained high-frequency stimulation of muscle

However, there are substantial differences between the nature of ACh transmsission at NMJ and in the brain, that might place different demands on ACh hydrolysis in the brain compared to NMJ. Several lines of evidence indicate that the synaptic transmission of ACh in the brain is rather rare and a substantial portion of ACh operates in the so-called volume transmission mode. While the synaptic transmission occurs within the borders of synapses, the volume transmission mode assumes that neurotransmitter released from varicosity with or without post-synaptic specialization is able to travel a relatively long distance to reach multiple targets. Moreover, the persistent presence of an ambient ACh level that undergoes physiological changes has been proposed. In such situation, the spatial and temporal demands on ACh hydrolysis by AChE are only poorly understood. On the other hand it is widely believed that disregarding where and when the hydrolysis of ACh by AChE does occur, AChE is indispensable for proper function of the brain.

As a common tool to study AChE physiological function is the pharmacological inhibition of the enzyme and more recently new light has been shed by the use of genetic approaches. Toxicology and pharmacology studies led to the conclusion that AChE function is essential both to the PNS and CNS. The acute profound inhibition of AChE leads to retarded removal of ACh, its build-up and overstimulation of cholinergic receptors resulting in a wide range of pathological manifestations and eventually in death due to the respiratory failure. With respect to the toxicological studies it was a big surprise that mice with genetic lack of AChE (AChE KO), even though with strongly changed phenotype, are viable. A body of research has unraveled several compensatory

mechanisms and the vialability of AChE KO mice has been best explained by preserved activity of BChE, a second ChE, that is able, although less efficiently, to hydrolyse ACh.

Among many features, AChE KO mice are smaller, have persistent tremor, abnormal gait and die from epileptic seizures. As the AChE is absent in the whole organism it has remained a question which phenotypical signs of AChE are solely dependent either on the absence of AChE in muscles, vegetative nervous system, other peripheral locations or on the AChE lack in the brain. Similarly, some signs of intoxications by AChE inhibitors could be consequences of peripherial or central action or of the combination of both. To answer the contribution of central inhibition of AChE vs. peripheral to general phenotype of AChE KO mice or long-lasting intoxications called for more specific approach.

AChE is encoded by a single gene, but possesses remarkable polymorphism in its molecular forms. One of the origins of such diversity is different anchoring of AChE at the cell surface. While at NMJ the prevalent form of functional AChE are tetramers anchored in the basal lamina of NMJ by ColQ, in the brain the majority of active AChE is tethered to the plasma membrane of neurons by PRiMA, a small transmembrane protein. This intriguing difference in the way of attachment of CHE in the brain and muscles, has allowed for generation of mouse model with more selective lack of AChE than the general absence as in AChE KO. By knocking out the domain of PRiMA required to associate AChE, we generated mice with a profound deficit of AChE and BChE in the brain, while preserving those in the periphery (PRiMA KO).

Interestingly, PRiMA KO mice do not show any obvious abnormalities in their phenotype. This is in striking contrast to what has been deduced from the phenotype of AChE KO mice or toxicological studies. To understand how the cholinergic system responds to the virtual absence of active ChE in the brain and search for specific phenotype of PRiMA KO mice to progress in our understanding of AChE roles in the brain is the aim of the thesis.

• The central cholinergic system

* Neuroanatomical distribution of the brain cholinergic system

The central cholinergic neurons widespread and are clustered in distinct brain areas which are located mainly ventrally (Fig. 2). Based on their neuroanatomical distribution they can be divided in cholinergic projection neurons located in the mesopontine region, in epithalamus and in the basal forebrain. In addition to these neurons which are characterized by remote projections, a class of cholinergic interneurons are present in caudate putamen, nucleus accumbens, olfactory tubercle and in the islands of the Cajella complex (Woolf and Butcher, 2011). Moreover, a population of intrinsic cholinergic neurons are found in the hippocampus (Hipp) (Frotscher et al., 2000) and cerebral cortex (Cx) (Consonni et al., 2009).

The mesopontine cholinergic neurons are localized in three nuclei: penduculopontine nucleus (Pptn), laterodorsal tegmental nucleus (LdTn) and parabigeminal nucleus (Pbn). These cholinergic neurons project to the thalamus (Th), hypothalamus (Hth), basal forebrain (BF), medial frontal cortex as well as to the brainstem and spinal cord (Mesulam et al., 1983; Woolf and Butcher, 1986, 1989). Pbn provide major cholinergic input to superior colliculus (Mufson et al., 1986).

The basal forebrain cholinergic neurons are located to the medial septum nucleus (MSn), vertical diagonal band nucleus (VDBn), horizontal diagonal band nucleus (HDBn), nucleus basalis magnocellularis (NBM) (of Meynert), magnocellular preoptic nucleus (MPn) and substantia inominata (SI). They provide cholinergic projections to the entire Cx, to amygdala, olfactory bulb and to the Hipp including CA1 to CA4 regions as well as dentate gyrus (DG) (Ichikawa et al., 1997; Mesulam et al., 1983; Satoh et al., 1983; Woolf et al., 1984). The cholinergic neurons of MSn and VDBn project to Hipp in the so-called septohippocampal pathway. NBM is the major source of cholinergic projection to the cortical mantle and to amygdala (Mesulam et al., 1983). HDBn and MPn are sending their axons to olfactory bulb, amygdala and different cortex areas (Woolf et al., 1984).

The epithalamic cholinergic neurons are represented by cholinergic cells in the medial habenula (MH) and project mainly to interpenducular nucleus (Ipn).

According to the nomenclature introduced by Mesulam, MS is referred to as CH1, VDBn as CH2, HDBn as CH3, NBM as CH4, Pptn as CH5, LdTn as CH6, MH and Pbn to as CH7 and CH8 cholinergic group, respectively (Mesulam et al., 1983; Mufson et al., 1986).

* Central cholinergic synapse

Cholinergic neurons in both divisions of nervous system release ACh and share the common pathways of ACh synthesis and storage (Fig. 3).

ACh is synthesized in varicosities of cholinergic neurons from its precursors choline (Ch) and acetyl coenzym A (acetyl-CoA) in a reaction catalyzed by the enzyme choline acetyltransferase (ChAT) (Brandon et al., 2003; Oda, 1999). Upon the synthesis, ACh is pumped from the cytosol by vesicular acetylcholine transporter (VAChT) and concentrated into the synaptic vesicles for storage (de Castro et al., 2009a; Prado et al., 2002). Acetyl-CoA for ACh synthesis is provided by the basal metabolism of neurons which is common to all cell types (Szutowicz et al., 1996; Tucek, 1983), but Ch required for sustainable cholinergic neurotransmission has to be captured from the extracellular space and this uptake is mediated by a high-affinity choline transporter (ChT) (Ferguson et al., 2004). Ch uptake is sodium dependent, sensitive to hemicholinium-3, specific to cholinergic neurons and is referred to as high-affinity choline uptake (HACU) with Km values for choline 0.5-5 μM (Ferguson et al., 2003; Guyenet et al., 1973; Murrin and Kuhar, 1976; Yamamura

and Snyder, 1972). Studies in vitro, ex vivo and in vivo suggest that the rate of HACU is directly coupled to the neuronal activity (Antonelli et al., 1981; Apparsundaram et al., 2005; Murrin and Kuhar, 1976; Parikh et al., 2013; Simon and Kuhar, 1975). In the brain cholinergic neurons, the majority of ChT protein is co-localized with VAChT on ACh containing vesicles. Almost 50% of VAChT positive vesicles bear ChT (Ferguson et al., 2003). Supported by, the biochemical evidence for plasma membrane increase of CHT protein following depolarization and necessity of vesicle fusion to increase HACU, Fergusson and co-workers have proposed that incorporation of ChT containing ACh vesicles into the membrane underlies the coupling of HACU to the cholinergic neuronal activity (Ferguson et al., 2003). Similarly to central cholinergic neurons, ChT is also enriched on synaptic vesicles at NMJ (Nakata et al., 2004).

In addition to HACU, choline is recruited also by low affinity Ch transport systems which are not cell-specific, have low Km for Ch (20-200 μM) and provide Ch for synthesis of plasma membrane phospholipids (Michel et al., 2006).

The released ACh is subjected to the enzymatic degradation by ChE: AChE and BChE, while AChE is the prominent player in the hydrolysis of ACh. 40-60% of Ch derived from hydrolysis of ACh is taken up by HACU and reused in the synthesis of new ACh (Collier and Katz, 1974; Parikh and Sarter, 2006).

The released ACh binds and activates two distinct classes of cholinergic receptors (ChR): NRs which are ligand-gated ion channels and muscarinic receptors (MR), G-protein-coupled receptors (GPCR).

A substantial difference between cholinergic transmission in the brain and PNS (at autonomic ganglia and NMJ) is the mode of ACh transmission.

There are two general concepts for neurotransmitter transmission – the wired or synaptic (Fig. 4) and the volume transmission (Fig. 5). The wired transmission is fast, short-distance, restricted to synaptic cleft of classical synapses with one to one ratio and activating receptors at postsynaptic membrane facing the release sites of neurotransmitter. The volume transmission is slower; assumes the escape of neurotransmitter from synaptic cleft to activate non-synaptic receptors or the release of neurotransmitter at sites not forming the synapses. The volume transmission thus allows for affecting many targets (Sarter et al., 2009).

In the periphery at NMJ and autonomic ganglia ACh mediate fast synaptic transmission which is ensured by establishing tight synaptic contact between presynaptic nerve terminals and postsynaptic membrane, where ACh travel short distance to activate NR. This is particularly evident at NMJ where a single nerve terminal with multiple active zones releases ACh over a large postsynaptic muscle membrane (Fagerlund and Eriksson, 2009; Ruff, 2003). At mammalian paravertebral ganglia, in addition to synaptic boutons a significant portion of vesicle containing boutons that are in contact with target neurons do not form synapse (Gibbins and Morris, 2006). However, the putative volume transmission and activation of extrasynaptic MR is not sufficient to

ameliorate the silencing of transmission in the absence of NRs (Krishnaswamy and Cooper, 2009; Rassadi et al., 2005).

Contrary to autonomic ganglia and NMJ where fast synaptic transmission is principal, in the brain a substantial portion of ACh has been proposed to signal via volume transmission mode (Descarries, 1998; Descarries et al., 1997; Lendvai and Vizi, 2008). The often contradictory findings, however, preclude drawing the conclusions and the relative proportion of synaptic and nonsynaptic transmission is open to debate (Sarter et al., 2009).

The idea that beyond direct synaptic communication a substantial portion of ACh signals by the means of volume transmission, at least in some brain areas, is mainly based on the results of studies elaborating the frequency of cholinergic varicosities forming synapses and ultrastructural localisation of cholinergic receptors (Descarries et al., 1997, 2004; Lendvai and Vizi, 2008; Yamasaki et al., 2010).

Studies that aimed at estimating the synaptic incidence of cholinergic varicosities (the percent of varisocities forming synapses) indicate that in some brain regions the population of varicosities with synaptic specialization is small, thus suggesting that volume transmission prevails (Descarries et al., 1997, 2004). On the other hand, some brain areas present much higher synaptic incidence, thus favoring the wired transmission mode (Holmstrand et al., 2010; Parent and Descarries, 2008; Turrini et al., 2001). In addition there are also conflicting observations regarding the synaptic incidence in the same brain region (Turrini et al., 2001; Umbriaco et al., 1994).

In rat cortex, 14% and 17% of cholinergic varicosities show synaptic specialization in adult and 32 days old rats respectively (Mechawar et al., 2002; Umbriaco et al., 1994). Very low rate of synaptic incidence is found also in striatum (Str) (9%) and in Hipp of adult (7%) and 32 days old rats (7%) (Aznavour et al., 2005; Contant et al., 1996; Umbriaco et al., 1995). Even lower frequency of varicosities with synaptic specialization has been indicated in mouse hippocampus. In CA1 field of Hipp as low as 3% of cholinergic varicosities appear to form synapse (Yamasaki et al., 2010). Contrary to studies reporting low synaptic incidence, Turrini et al. found 66% synaptic incidence in rat parietal cortex (Turrini et al., 2001). Higher values have been reported also in primates. In human cortex, the synaptic incidence is 67% (Smiley et al., 1997) and in macaque prefrontal cortex 44% of varicosities form synaptic specialization (Mrzljak et al., 1995). The relatively high synaptic incidence on one hand and frequent coincidence of nonsynaptic cholinergic varicosities and putative excitatory synapses at the same spines and dendrites of cortical neurons on the other hand, has been suggested to indicate importance of both modes of cholinergic transmission (Mrzljak et al., 1995). A relatively high occurrence of varicosities with synaptic specialization is found in rodent ventral tegmental area (VTA) and in various Th nuclei. In rat VTA, anteroventral Th, reticular nucleus of Th and dorsolateral geniculate nucleus 47%, 36%, 33%, 39% of cholinergic varicosities possess synaptic specialization, respectively (Holmstrand et al., 2010; Parent and Descarries, 2008). In striking contrast, the synaptic incidence in parafascicular nucleus of Th is 100 % (Parent and Descarries, 2008).

In addition to low synaptic incidence in some brain areas, the idea of volume transmission has also been suggested from ultrastructural localisation of ChR (Jones and Wonnacott, 2004; Jones et al., 2001; Yamasaki et al., 2010). Various types of noncholinergic neurons possess ChR at their axon terminals, where they modulate the release of neurotransmitters and since the axo-axonic synapses are mostly absent, it has been assumed that ACh reaches the presynaptic ChR by non-synaptic transmission (Lendvai and Vizi, 2008). Moreover, the postsynaptic ChR are often found extrasynaptically or at postsynaptic membrane of noncholinergic synapses, suggesting that these receptors sense ACh delivered by volume transmission (Duffy et al., 2009; Hersch et al., 1994; Jones and Wonnacott, 2004; Yamasaki et al., 2010). While it seems unlikely that ChR could be activated by ACh released from remote release sites a model has been proposed of more restricted volume transmission in which ACh released from nonsynaptic terminals targets ChR located only a short-range distance from ACh release sites (Lendvai and Vizi, 2008). This proposition is in line with observations that cholinergic varicosities - even though without synaptic specialization - directly contact asymmetrical synapses or are directly apposed to neuronal profiles containing ChR (Duffy et al., 2009; Yamasaki et al., 2010).

The transmission mode of ACh has also been studied by means of electrophysiology, with the data suggesting that the volume transmission, as well as synaptic transmission, might be of physiological importance (Alkondon et al., 1998; Arroyo et al., 2012; Bell et al., 2011; Frazier et al., 1998; Grybko et al., 2011; Hatton and Yang, 2002; Hefft et al., 1999; Lamotte d'Incamps et al., 2012; Ren et al., 2011). For instance, a brief selective stimulation of cortical cholinergic afferents using an optogenetic approach generated slow NR excitatory currents in a subset of cortical GABAergic interneurons, possibly reflecting the volume transmission mode of ACh (Arroyo et al., 2012). In addition to the slow response, the fast nicotinic response was observed in some types of GABAergic interneurons (Arroyo et al., 2012), which is in accordance with other works demonstrating fast nicotinic transmission also in other brain regions (Alkondon et al., 1998; Frazier et al., 1998; Grybko et al., 2011; Hatton and Yang, 2002; Hefft et al., 1999).

An optogenetic approach has also been used to study cholinergic signaling at MH - Ipn cholinergic pathway and has revealed two modes of transmission provided by cholinergic neurons (Ren et al., 2011). The tetanic photostimulation resulted in slow, largely NR-dependent excitatory responses, indicating the volume transmission of ACh. The brief photostimulation generated fast excitatory response. The fast response was NR-independent and mediated by glutamatergic receptors, suggesting glutamatergic synaptic transmission (Ren et al., 2011). The assumption that glutamatergic transmission carried by cholinergic neurons could be more common is supported by findings that also striatal cholinergic interneurons (ChI) mediate fast glutamatergic transmission (Cachope et al., 2012; Higley et al., 2011).

The brain region differences in cholinergic synaptic incidence, spatial relationship between ACh release sites and ChR localization, synaptic vs. volume transmission mode and finally the use of glutamate, in addition to ACh, by cholinergic neurons to convey information point to the highly complex nature of the central cholinergic transmission.

* Central cholinergic receptors

- *Muscarinic receptors*

MRs are prototypical members of the superfamily of GPCR characterized by a single protein unit that spans plasma membrane 7 times, creating 7 transmembrane domains interconnected with three extracellular and three intracellular hydrophilic loops. The N-terminus is positioned in the extracellular and C-terminus in the intracellular space (Felder, 1995). 5 subtypes of MR encoded by 5 distinct genes were identified (M1-M5) (Caulfield and Birdsall, 1998; Dencker et al., 2012).

MRs are distributed throughout the whole brain, with the highest densities in the forebrain structures (Oki et al., 2005). All five subtypes of MR are found in the brain (Levey, 1996; Wolfe and Yasuda, 1995). M1 represents the predominant type of MRs in the brain accounting to almost 50% of the overall MRs (Hamilton et al., 1997) and serve primarily as postsynaptic receptor (Levey, 1996). M2 is expressed at relatively low densities at presynaptic and postsynaptic sites (Csaba et al., 2013; Hersch et al., 1994; Levey, 1996; Wolfe and Yasuda, 1995). M3 is expressed in many brain regions but only at low levels (Levey, 1996; Wolfe and Yasuda, 1995). M4 is enriched in Str while in Hipp and cortex shows moderate density (Gomeza et al., 1999a). M4 is localized both presynapticaly and postsynapticaly (Hersch et al., 1994; Levey, 1996; Wolfe and Yasuda, 1995). M5 is found at very low levels in Hipp, Str and midbrain (Levey, 1996; Wolfe and Yasuda, 1995).

As a member of GPCR, MR initiate their signaling by activating the preferred GTP-binding proteins (G-proteins), consisting of three subunits - α, β and γ. GDP bound to α subunit is replaced by GTP, which destabilizes the complex with receptor and G-protein dissociates into α and βγ subunits. Both subunits can than influence the functional state of different effector molecules, including second messenger enzymes, protein kinases and ion channels (Felder, 1995; Lanzafame et al., 2003; Nathanson, 2000).

The odd numbered MRs are positively coupled to phopholipase Cβ (PLC) through G-proteins of the Gq/G11 family. PLC hydrolyse phosphatidylinositol-4,5-bisphosphate (PIP2) into inositol 1,4,5-trisphosphate (IP3) and diacylglycerol (DAG) which in turn mobilize intracellular calcium and activate protein kinase C (PKC), respectively (Wess, 1996).

The even numbered MRs are negatively coupled to adenylatcyclase (AC) through G proteins of Gi/Go class which leads to the decrease of intracellular concentration of cAMP (Jeon et al., 2010).

MRs has been suggested to modulate the neuronal circuits by several mechanisms, including the regulation of neurotransmitters release, neuronal excitability, transcription and translation (Brown, 2010; Calabresi et al., 2000; Kimura and Baughman, 1997; McCoy and McMahon, 2007;

Power and Sah, 2002; Rosenblum et al., 2000; Zhang et al., 2002).

MRs exert their modulatory action on neuronal excitability through regulation of various ion conductances. Depending on ion channel involved, MRs activation can either enhance or decrease the neuronal excitability (Brown, 2010). MRs coupled to PLC can provide the postsynaptic excitation by suppression of several potassium currents including the voltage and time-dependent K+ current (IM / KCNQ channel current), the Ca2+ activated K+ current that generates afterhyperpolarization (IAHP) and a leak K+ current (Ileak) (Brown, 2010; Rouse et al., 2000a; Shen et al., 2005). Moreover, the presynaptic inhibition of KCNQ by M1 increases action potential independent glutamate release at Schaffer collateral-CA1 pyramidal synapses (Sun and Kapur, 2012).

Activation of putative M1 can inhibit also inwardly rectifying potassium channels Kir2 resulting in depolarization and enhanced summation of stimulatory input (Carr and Surmeier, 2007; Shen et al., 2007). This suppressor effect on Kir2 depends on activation of PLC and depletion of PIP2, which reduces the probability of the opened conformation of the channel (Carr and Surmeier, 2007). Similar to Kir2, the suppression of KCNQ currents and IAHP also depend on depletion of PIP2 (Brown, 2010; Shen et al., 2005; Villalobos et al., 2011).

In addition to regulation of potassium conductances, M1 activation can induce depolarization by increasing the mixed Na+/K+ hyperpolarization-activated current (Ih) and Ca2+ dependent nonspecific cation current (Icat) (Fisahn et al., 2002).

The postsynaptic inhibition of neuronal excitability is achieved via direct activation of G-protein gated inwardly rectifying potassium channels (GIRK) by Gβγ dimer upon stimulation of MRs coupled to Gi/Go (Brown, 2010; Lüscher and Slesinger, 2010). The postsynaptic suppression of neuronal excitability through activation of GIRK might serve as a sorting mechanism for small, less relevant stimuli (Seeger and Alzheimer, 2001).

A prominent role ascribed to MRs is the feedback control of ACh release (Dolezal and Tucek, 1999; Dolezal and Wecker, 1990). This appears to be mediated primarily - if not exclusively - by presynaptic M2 and M4 as indicated by the use of mice devoid of M2 and M4 MRs (Zhang et al., 2002). M4 is the main subtype involved in controlling ACh release in striatum, while M2 inhibit ACh release primarily in the cortex and Hipp (Zhang et al., 2002). As predicted, the lack of autoinhibitory MR leads to an increased level of ACh in several brain regions (Tzavara et al., 2003, 2004).

Despite it being now firmly established that M2/M4 serve the autoinhibition of ACh release, less clear is how the control of ACh release is exerted. This might involve the inhibition of N and P/Q calcium channels through a membrane-delimited pathway, presumably by direct action of βγ dimer on ion channels (Brown, 2010; Yan and Surmeier, 1996) as well as the activation of GIRK resulting in hyperpolarization of cholinergic neurons (Bonsi et al., 2008; Calabresi et al., 1998; Ding et al., 2006). On the other hand, evidence also suggests that the responsible mechanisms might

lie downstream to the calcium entry and involve direct interaction with the exocytic machinery (Blackmer et al., 2001, 2005; Kupchik et al., 2011).

In addition to providing feedback control of ACh release, MRs appear to be directly involved in the kinetics of ACh release directing the initiation and duration of ACh release (Kupchik et al., 2011; Slutsky et al., 2003).

The modulatory role of MRs on neurotransmitters release is not restricted to autocontrol of ACh liberation. MRs and particularly M2 and M4 are often found as heteroreceptors at glutamatergic and GABAergic terminals (Hersch et al., 1994; Rouse et al., 2000b) and their activation can decrease the release of glutamate and GABA (Calabresi et al., 2000; Carr and Surmeier, 2007; Koós and Tepper, 2002; Seeger et al., 2004). The regulation of glutamate and GABA release can be achieved also indirectly by regulation of endocanabionid retrograde signaling. For instance, in Str, evidence suggests that M1 tonically inhibits endocannabionid release at glutamatergic synapses on one hand (Wang et al., 2006) and constitutively upregulates the endocannabinoid-mediated retrograde suppression of inhibitory GABAergic transmission on the other hand (Narushima et al., 2007).

The modulation of neurotransmitters release (Seeger et al., 2004; Wang et al., 2006) and neuronal excitability by MRs (Buchanan et al., 2010; Petrovic et al., 2012) has been linked to the ability of MRs to trigger long-term changes of synaptic strength - the synaptic plasticity - which is considered to be the molecular mechanism underlying learning and memory (Gkogkas et al., 2010; Malenka and Bear, 2004; Whitlock et al., 2006). In addition, MRs-dependent forms of synaptic plasticity have been associated with activation of extracellular signal-regulated kinases (ERK) (McCoy and McMahon, 2007; Rosenblum et al., 2000) and generation of IP3 mediated calcium signals by MR (Fernández de Sevilla et al., 2008; Power and Sah, 2002).

The pharmacological studies have pointed to an important role of MRs in several brain processes including learning and memory (Anagnostaras et al., 1995; Ohno et al., 1994; Quirion et al., 1995), attention (Chen et al., 2004; Mirza and Stolerman, 2000; Pattij et al., 2007), locomotion (Bushnell, 1987; Mathur et al., 1997; Sipos et al., 1999), thermoregulation (Lomax and Jenden, 1966), sleep and wakefulness (Coleman et al., 2004; Sanford et al., 2006), food intake (Perry et al., 2010; Pratt and Blackstone, 2009) and reward (Crespo et al., 2006; Mark et al., 2006; Shabani et al., 2010). The poor selectivity of commonly used MRs ligands and the overlapping pattern of distribution of particular MR, however, have precluded the definition of MR subtype specific roles in these processes (Wess et al., 2007). To overcome this problem a genetics has been employed to help in delineation of MR subtype specific roles (Dencker et al., 2012; Wess et al., 2007). For instance, M1 KO mice are hyperactive (Gerber et al., 2001; Miyakawa et al., 2001), show enhanced contextual fear acquisition, but impaired contextual, working and social discrimination memory (Anagnostaras et al., 2003). M1 KO mice have also deficits in cue detection task, indicating impaired attention (Gulledge et al., 2009). The hyperactivity of M1 KO mice has been associated with enhanced dopaminergic transmission in Str, possibly having origin in the suppression of

striatal feedback inhibition of midbrain dopaminergic neurons (Gerber et al., 2001). The cognitive deficits of M1 KO mice has been linked to the impairment of cholinergic control of neuronal excitability and synaptic plasticity (Anagnostaras et al., 2003; Gulledge et al., 2009; Shinoe et al., 2005).

The deletion of M2 gene does not interfere with basal locomotor activity in the open field or with motor coordination as assessed by rotarod (Gomeza et al., 1999b) but M2 KO mice present deficits in behavioural flexibility and working memory that have been associated with profound changes in neuronal plasticity (Seeger et al., 2004). The loss of M2 results also in increased basal ACh efflux in hippocampus and might, in addition to impairment in synaptic plasticity, underlie the impaired performance of M2 KO mice in the passive avoidance test, a measure of learning and memory (Tzavara et al., 2003).

Similar to M1 KO mice, M4 KO mice show enhanced locomotion and elevated dopaminergic tone in Str (Gomeza et al., 1999a; Tzavara et al., 2004). However, after backcrossing (10 times) of the original line maintained on the mixed genetic background into an inbred strain background, M4 KO mice did not differ from WT mice in terms of locomotion (Schmidt et al., 2011). There are only sparse data concerning cognitive function of M4 KO mice, but distinct to M2 KO mice, M4 KO mice do not present deficits in the passive avoidance test (Tzavara et al., 2003).

- ***Nicotinic receptors***

NRs have attracted a considerable interest due to their key role in nicotine addiction (Maskos et al., 2005). However, often overlooked, the endogenous ligand of NRs is ACh (Maskos, 2010)

NRs are pentameric ligand gated ion channels permeable for monovalent and divalent cations present both in the CNS and in the periphery (Gotti and Clementi, 2004). According to the subunit composition that determines pharmacological and functional properties of NRs, NRs can be formed as homomeric or heteromeric subunit associations (Le Novère et al., 2002). In mammals, fifteen different NR subunits encoded by distinct genes were identified (α1-α7, α9-α10, β1-β4, γ, δ and ε) (Le Novère et al., 2002). In the CNS, the expression of six α (α2-α7) and three β (β2-β4) have been found, giving the possibility of presence of an array of subunit associations (Yakel, 2012). The central homomeric NRs are represented by α7 NR and the majority of heteromeric NRs are composed at least from α4 and β2 subunits (Baddick and Marks, 2011; Gotti et al., 2009; Marks et al., 2010). The diversity of native NRs can be illustrated by NR subtypes that have been identified on dopaminergic nerve terminals. The evidence demonstrates that at least 5 different subunit associations are present on dopaminergic terminals in Str (α4β2, α4α5β2, α6β2, α4α6β2β3 and α6β2β3) (Grady et al., 2007).

NRs are widely expressed throughout the whole brain and can be found at presynaptic, preterminal, postsynaptic and nonsynaptic neuronal loci, thus allowing for contribution to

neuronal signaling by multiple mechanisms (Dani and Bertrand, 2007). A large body of evidence employing diverse experimental approaches has implicated the presynaptic NRs in modulation of neurotransmitters release (Dani and Bertrand, 2007; Wonnacott, 1997; Wonnacott et al., 2006). The electrophysiological experiments in various experimental preparations have revealed that stimulation of presynaptic NRs can enhance the spontaneous as well as stimulus evoked glutamatergic and GABAergic transmission (Gray et al., 1996; Léna and Changeux, 1997; McGehee et al., 1995; Radcliffe and Dani, 1998; Radcliffe et al., 1999). Even in the absence of incoming action potentials, longer stimulation of presynaptic NRs can increase the release of glutamate enough to drive postsynaptic firing (Sharma and Vijayaraghavan, 2003; Sharma et al., 2008).

The modulatory role of presynaptic NRs on neurotransmitters release has also been widely studied in synaptosomes prepared from various brain areas and stimulation of synaptosomal NRs has been shown to enhance the release of multiple neurotransmitters including glutamate, GABA, dopamine, serotonin, noradrenalin and ACh (Azam and McIntosh, 2006; Grady et al., 2001, 2010; Reuben and Clarke, 2000; Zappettini et al., 2010, 2011).

As recently demonstrated, activation of presynaptic NRs by endogenously released ACh can directly evoke dopamine release in dorsal striatum and nucleus accumbens (Cachope et al., 2012; Threlfell et al., 2012). Using an optogenetic approach to selectively drive ChI, both research groups showed acute and NR-dependent release of dopamine following synchronous activation of a group of ChI (Cachope et al., 2012; Threlfell et al., 2012). Moreover, Cachope and co-workers extended their in vitro observations also to in vivo model (Cachope et al., 2012).

The modulatory role of presynaptic NRs on neurotransmitters release has been associated with their ability to generate calcium signals. NRs can provide calcium signals directly by influx of calcium through NRs themselves and indirectly by local depolarization and reccruitment of voltage-gated calcium channels (VGCC). The primary calcium signal can be than amplified by mobilization of calcium from intracellular calcium stores, calcium-induced calcium release (CICR) (Dajas-Bailador and Wonnacott, 2004; Shen and Yakel, 2009). While the direct influx of Ca2+ through NR and the subsequent involvement of CICR and downstream signaling pathways is typically reported for α7 NR, heteromeric NRs are mainly associated with recruitment of VGCC (Dickinson et al., 2008; Kulak et al., 2001; Sharma et al., 2008; Zappettini et al., 2010, 2011). In some instances, however, evidence indicates that NRs might provide Ca2+ signals solely by influx through NRs themselves without contribution of indirect mechanisms (Kalappa et al., 2011; Léna and Changeux, 1997).

In addition to presynaptic NRs, the modulatory role has been ascribed to somatodentritic NRs. For instance, the putative heterosynaptic NRs can decrease the inhibitory GABAergic transmission by modulation of postsynaptic GABAA receptors (Wanaverbecq et al., 2007; Zhang and Berg, 2007). As for presynaptic NRs, the generation of calcium signals and subsequent downstream signaling cascades underlie this modulatory effect (Wanaverbecq et al., 2007; Zhang

and Berg, 2007). On the other hand, the properly-timed activation of postsynaptic NRs together with presynaptic NRs can result in long-lasting enhancement of the strength of glutamatergic transmission or boost the preexisting synaptic plasticity (Ge and Dani, 2005; Gu and Yakel, 2011; Ji et al., 2001).

At autonomic ganglia and NMJ the principal role of NR is to mediate the fast cholinergic neurotransmission. An increasing body of evidence demonstrates that the fast nicotinic transmission does also occur in the CNS. The fast and α7 NR dependent synaptic transmission has been demonstrated in different brain areas and between cholinergic inputs and various target cells (Alkondon et al., 1998; Arroyo et al., 2012; Frazier et al., 1998; Grybko et al., 2011; Hatton and Yang, 2002; Hefft et al., 1999). In addition to the fast cholinergic neurotransmision mediated by α7 NR, NRs can provide the target cells by excitatory responses that likely originate from nonsynaptic mode of ACh transmission. The putative nonsynaptic nicotinic excitatory responses characterized by slow time course have been shown for instance in Ipn, in cortical GABAergic interneurons and hippocampal CA1 neurons (Arroyo et al., 2012; Bell et al., 2011; Ren et al., 2011). While the Ipn neurons are excited by NR only following tetanic stimulation of cholinergic inputs originating in MH and blocked by mixture of nonselective NR antagonists, in Cx and Hipp the responses are dependent on β2 NRs and readily observable after brief single stimulation (Arroyo et al., 2012; Bell et al., 2011; Ren et al., 2011).

The particular importance of nicotinic excitation has also emerged from finding that ChI provide NR dependent disynaptic inibition of principal projection neurons – medium spiny sized neurons (MSN) - in vitro and decrease the background firing of MSN in vivo (Witten et al., 2010).

• Cholinesterases, molecular forms and their function

ChEs are serine hydrolases that preferentially catalyse the hydrolysis of choline esters. Higher vertebrates, including humans, possess two ChEs: AChE (AC 3.1.1.7) and BChE (EC 3.1.1.8) encoded by two distinct genes (Massoulié, 2002). BChE gene is thought to be a result of AChE gene duplication early in the vertebrate evolution (Pezzementi and Chatonnet, 2010; Pezzementi et al., 2011). Even though AChE and BChE are related enzymes and share high sequence similarity, they present differences in substrate specificity and sensitivity to inhibitors. The preferential substrate of AChE is ACh. BChE can also hydrolyse ACh, but it is more active on higher acyls (Whittaker, 2010).

* Function of ChE

Primary function of AChE is to hydrolyse ACh into Ch and acetic acid (Massoulié, 2002; Massoulié and Millard, 2009). AChE is one of the fastest acting enzymes known, with the rate of ACh hydrolysis approaching the theoretical limits of substrate diffusion (Quinn, 1987).

The active site of AChE, comprising the catalytic triad serine-histidine-glutamate, is located at the bottom of 20 Å deep narrow gorge, which is mostly lined with the rings of 14 conserved aromatic residues (Silman and Sussman, 2008; Sussman et al., 1991). Before ACh slides down to the active site it is trapped by the so-called peripheral anionic site located at the outer rim of the cavity, increasing the probability of ACh to proceed into the active site (Silman and Sussman, 2008). In comparison to AChE, BChE has replaced several aromatic residues lining the gorge of AChE by hydrophobic ones (Harel et al., 1992; Nicolet et al., 2003). Importantly, the replacement of two phenylalanines found in AChE by leucine and valine, which have smaller side chains, results in a larger acyl-binding pocket of BChE allowing for accommodation of substrates bulkier than ACh (Harel et al., 1992; Nicolet et al., 2003).

At NMJ, hydrolysis of ACh by AChE clearly serves to rapidly terminate the fast cholinergic transmission allowing for high frequency stimulating of muscle fibers (Chang, 1998; Massoulié and Millard, 2009). In contrast, the brain AChE has been suggested to control the ambient level of ACh, rather than to completely eliminate it (Descarries, 1998; Descarries et al., 1997).

In addition to hydrolysis of ACh, many other biological functions which appear to be independent of catalytic properties, have been attributed to AChE (Soreq and Seidman, 2001). AChE might play an important role in cell adhesion and neurite outgrowth (Grifman et al., 1998; Johnson and Moore, 2004; Sharma et al., 2001; Whyte and Greenfield, 2003). AChE is expressed also in osteoblasts, where it might contribute to the metabolism of bone tissue (Genever et al., 1999). A growing body of evidence also suggests an important role of AChE in the process of apoptosis (Zhang and Greenberg, 2012).

While the function of AChE is well established, the role of BChE remains rather puzzling. BChE is present in almost all tissues and is especially abundant in the liver, serum, intestine and lung (Li et al., 2000; Masson and Lockridge, 2010). It is suggested that BChE serve as backup for AChE and as a scavenger of natural or man-made AChE inhibitors. The high expression of BChE in tissues of the first contact with external compounds (Jbilo et al., 1994) and BChE ability to hydrolyse broad range of esters such as cocaine (Sun et al., 2001), heroin (Lockridge et al., 1980), succinylcholine (Lockridge, 1990) and acetylsalicylic acid (Masson et al., 1998) further suggest an important role of BChE in detoxication.

The direct contribution of BChE in regulation of cholinergic signaling remains, however, an unresolved issue. Under some circumstances, such as genetic deletion of AChE in mice (AChE KO), BChE participate on ACh clearance as evidenced by the sensitivity of ACh ambient level in Hipp to inhibition of BChE (Naik et al., 2009). However, in AChE heterozygote (AChE Het) mice

with 40% reduction of AChE activity, inhibition of BChE has no impact on brain ACh levels, thus questioning the physiologically relevant contribution of BChE to ACh breakdown (Mohr et al., 2013).

Moreover, the naturally existing mutations in the human BChE gene triggering the partial or complete absence of BChE activity do not cause any health problems (Lockridge and Masson, 2000; Manoharan et al., 2006). Similarly the mice with absence of BChE activity (BChE KO) are healthy and do not suffer from such modification of their genome (Duysen et al., 2009). The deficit in BChE is first revealed when organism is challenged with drugs metabolized by BChE, such as cocaine and succinylcholine. The absence of BChE leads to increased toxicity of cocaine and to prolongation of the action of succinylcholine which was used as peripheral myorelaxans during short anaesthesia (Duysen et al., 2008; Li et al., 2008a; Lockridge, 1990).

* Diversity of ChE molecular forms

Even though both ChE are encoded by a single gene in vertebrates, they represent a family of diverse molecular forms (Massoulié, 2002; Massoulié et al., 2005) (Fig. 6).

The polymorphism of AChE arises at the genetic, post-transcriptional and post-translational levels (Massoulié, 2002; Meshorer and Soreq, 2006). The well-established diversity of AChE originates from alternative splicing at the 3' end of primary mRNA, giving a rise to 3 AChE protein variants that share a common catalytic domain but differ in their C terminal peptides (Li et al., 1993; Massoulié, 2002). The nature of the C terminal peptide dictates AChE post-translational processing, oligomerization and mode of attachment to the cell surface. Based on the specific characteristics, the three AChE variants are named R (read-through), H (hydrophobic or hematopoietic) and T (tailed) (Massoulié, 2002; Massoulié et al., 1993).

The absence of splicing in the 3' region following the last exon encoding the catalytic domain - exon 4 - generates R variant of AChE. The AChE R variant produces AChE protein that remains monomeric and is soluble (Soreq and Seidman, 2001). Even though AChE R represents a minor form of AChE under physiological conditions (Perrier et al., 2005), it is induced by AChE inhibition and physical stress (Kaufer et al., 1998; Meshorer et al., 2002).

Joining exon 4 with exon 5 produces H variant of AChE (hydrophobic or hematopoetic). The AChE H variant generates dimers linked by disulfide bond and anchored to the membrane by glycosylphosphatidylinositol anchor (GPI) (Coussen et al., 2001). The C terminal peptide of AChE H comprises a hydrophobic C-terminal region, which constitutes the signal for cleavage and GPI addition and one or two cysteines that are involved in dimerization by forming intercaternary disulfide bonds (Coussen et al., 2001; Morel et al., 2001). AChE H is mainly expressed in hematopoietic cells, where it is possibly involved in elimination of any ACh from the bloodstream (Massoulié, 2002).

Joining exon 4 with exon 6 produces AChE T transcripts (Guerra et al., 2008; Luo et al., 1998). The AChE T protein gives rise to a broad range of molecular forms including homoligomers: monomers, dimers, tetramers (Bon and Massoulié, 1997; Duval et al., 1992a), as well as hetero-oligomeric associations of AChE tetramers with anchoring proteins ColQ and PRiMA (Krejci et al., 1991, 1997; Perrier et al., 2002).

Furthermore, a distinct variant S (snake) has been described in Elapidae snakes. S variant is soluble and is concentrated in snake venom. However, the role of such variant is unclear. Its relation to venom toxicity has not been proved (Cousin et al., 1996, 1998).

As opposed to AChE, BChE exists solely as a T variant and the diversity of BChE molecular forms arises from homo- and hetero-oligomerization (Darvesh et al., 2003; Massoulié, 2002).

In addition to the alternative splicing in the 3' end of primary AChE mRNA, the alternate promoter usage and first exons further add to the diversity of AChE gene products (Meshorer and Soreq, 2006; Meshorer et al., 2004).

At least 5 and 4 alternative first exons have been described for mice and humans respectively. The combination of alternative 3' end splicings and the alternate first exons can thus theoretically yield 15 and 9 alternatively spliced isoforms of AChE in mice and humans respectively (Meshorer and Soreq, 2006; Meshorer et al., 2004). Even though the most of alternative first exons are non-coding, at least one of them has a potential to generate an extended AChE protein at its N- terminus. Such extension is predicted to prevent the cleavage of the N-terminal signal peptide and to generate N-terminal transmembrane domain, thus allowing to anchor AChE in the cell membrane independently of C-terminal peptide and accessory proteins ColQ and PRiMA (Meshorer and Soreq, 2006; Meshorer et al., 2004). Evidence indicates that the N-terminal extended AChE protein is present in human blood cells and possibly also in the brain (Meshorer et al., 2004).

- ***Properties of AChE T and its C terminal peptide***

AChE T is the principal variant of AChE present in CNS and in muscles where it is concentrated at NMJ (Dobbertin et al., 2009; Feng et al., 1999; Legay et al., 1995; Perrier et al., 2002).

T variant is characterized by the presence of C terminal peptide (t peptide) consisting of 40 amino acid residues in case of AChE and 41 in case of BChE. The primary structure comprises seven conserved aromatic amino acid residues, including three evenly spaced tryptophans and a cystein at position 4 from the C end (Massoulié, 2002; Massoulié et al., 1993). T peptide is organized as an alpha helix, in which aromatic residues are clustered to produce a hydrophobic region (Bon et al., 2004; Dvir et al., 2004).

T peptide confers to AChE T specific properties. First, it allows its oligomerization. Expression of T variant in cell cultures gives rise to a broad range of molecular forms: monomers,

dimers, tetramers, as well as unstable hexamers (Bon and Massoulié, 1997; Duval et al., 1992a). The absence of t peptide restricts the AChE production solely to monomeric species (Duval et al., 1992a).

Second, t peptide is responsible for the production of heteromeric associations of AChE with structural proteins ColQ, PRiMA and proline rich sequences of lamellipodin and other proteins (Biberoglu et al., 2012, 2013; Bon and Massoulié, 1997; Bon et al., 1997; Li et al., 2008c; Simon et al., 1998).

T peptide also serves as a signal of degradation. Part of the newly-synthesized AChE subunits undergo degradation via ERAD mechanism (endoplasmic reticulum-associated degradation) (Belbeoc'h et al., 2003). This property depends on the presence of aromatic amino acid residues and the hetero-oligomerization can prevent the degradation (Belbeoc'h et al., 2003) In addition, t peptide serves as a retention signal for the newly produced subunits to stay in the endoplasmic reticulum (ER) and association with structural partners (Belbeoc'h et al., 2004; Dobbertin et al., 2009).

Moreover, an evidence indicates that peptide derived from the T peptide is bioactive (Greenfield, 2005).

- ***The associations of AChE T with anchoring partners***

The association of AChE T subunits with anchoring partners is crucial for the placement of AChE on the sites of its action, particularly at NMJ and in CNS. Two distinct anchoring proteins have been described: ColQ and PRiMA (Krejci et al., 1991, 1997; Perrier et al., 2002). The association of AChE T subunits with anchoring proteins is mediated by the interaction of four t peptides called tryptophan amphiphilic tetramerization (WAT) domain (Simon et al., 1998) with proline rich attachment domain (PRAD) (Bon et al., 1997) located in the N-terminus of anchoring partners (Krejci et al., 1997; Perrier et al., 2002).

In fact, the T peptide behaves as an independent interaction domain (Simon et al., 1998). T peptide alone, without catalytic domain, or attached to foreign proteins such as alkaline phosphatase or green fluorescent protein, is able to interact with PRAD domain to produce tetrameric assemblies and target them to membrane surface (Simon et al., 1998) when PRAD is associated with GPI anchor (Duval et al., 1992b). Conversely, the PRAD domain alone or an artificial polyproline motif is able to organize tetramers of AChE T subunits (Bon and Massoulié, 1997; Noureddine et al., 2007).

The crystal structure of the synthetic WAT/PRAD complex has revealed that four parallel WAT domains organized as amphiphilic α helices form a left-handed superhelix around a central antiparallel oriented left-handed PRAD helix. The aromatic residues of t peptide are oriented towards the interior of formed cylinder and tryptophans make close contact with proline cycles (Dvir et al., 2004).

The production of homotetramers and PRAD-linked tetramers depends on the presence of aromatic residues in t peptides, particulary the central ones (Belbeoc'h et al., 2004). The intercaternary disulfide bonds between cystein at the position 4 from the end of t peptide and cysteines near the PRAD of anchoring proteins add to the stability of complex, but are not essential for its generation (Belbeoc'h et al., 2004; Bon et al., 1997; Noureddine et al., 2007; Simon et al., 1998). In contrast, the presence of an intercaternary disulfide bond appears to be required for dimerization (Belbeoc'h et al., 2004; Velan et al., 1991).

Although the associations of ChE subunits with anchoring partners is based on the same principle, distinct differences have been identified, such as production of different portion of heavy dimers (dimers disulfide-linked to anchoring structure) (Noureddine et al., 2008).

Recent evidence demonstrates that tetramers of BChE present in plasma also incorporate a proline rich peptides (Biberoglu et al., 2012; Li et al., 2008c). The origin of proline rich peptides is heterogeneous and several protein candidates that might serve as protein precursors have been identified. Importantly none of identified polyproline peptides has its origin in ColQ or PRiMA protein (Biberoglu et al., 2012). A very recent work identifies the incorporation of polyproline peptides of various lengths also in case of AChE tetramers present in fetal bovine plasma (Biberoglu et al., 2013). Similarly to BChE tetramers several precursor proteins have been identified, none of which is ColQ or PRiMA (Biberoglu et al., 2013).

AChE anchored by collagenic tail ColQ

Heteromeric complexes of AChE or BChE with ColQ are called asymmetric forms of AChE (A). ColQ is a three-helical collagen structure in which each strand of collagen is able to carry one tetramer of AChE or BChE. Depending on the number of tetramers, three asymmetric forms are recognized: A4, A8 and A12 (Dvir et al., 2004; Krejci et al., 1997; Massoulié and Millard, 2009). cDNA of ColQ was cloned for the first time from Torpedo (Krejci et al., 1991), later from rodents (Krejci et al., 1997) and humans (Donger et al., 1998; Ohno et al., 1998). The primary structure comprises a signal peptide, PRAD domain, collagen domain and C-terminal domain (Krejci et al., 1997).

Assymetric forms of ChE represent the major form of ChE at NMJ (Bernard et al., 2011; Feng et al., 1999). The ColQ anchor thethers AChE to the basal lamina of NMJ (Massoulié and Millard, 2009; McMahan et al., 1978). In addition to basal lamina, part of asymmetric forms is present also at the nerve endings of motoneurons (Bernard et al., 2011). However, the motoneuron AChE asymmetric forms are not produced by the motoneurons, but originate from the muscle cell. The mechanisms of transsynaptic anchoring of AChE by ColQ remain to be elucidated (Bernard et al., 2011).

The mutations in the gene encoding for ColQ cause a deficit of AChE activity at NMJ which is clinically manifested as myasthenic syndrome (Donger et al., 1998; Mihaylova et al., 2008; Ohno et al., 1998).

AChE anchored by transmembrane domain PRiMA

In the brain, the main form of ChE is AChE, while BChE constitutes the minor part of the total ChE activity (Li et al., 2000; Tago et al., 1992). In the brain, ChE are present as tetramers attached to the plasma membrane by a hydrophobic anchor (Gennari et al., 1987; Inestrosa et al., 1987; Koelle et al., 1987; Navaratnam et al., 2000; Rotundo, 1984). The amount of anchored AChE tetramers increases along with the brain development (Inestrosa and Ruiz, 1985; Inestrosa et al., 1994; Xie et al., 2010a)

The presence of 20 kDA hydrophobic protein associated with AChE in the brain was described for the first time in the year 1987 (Gennari et al., 1987; Inestrosa et al., 1987). However, the molecular and genetic nature of this protein had remained unknown for years.

The anchoring protein of ChE in the brain was cloned and described several years later and was termed PRiMA (Perrier et al., 2002). The PRiMA gene has 5 exons, from which the first one is noncoding. The primary structure of PRiMA comprises N-terminal signal peptide, an extracellular domain containing the PRAD domain, 5 cysteines and putative N- and O- glycosylation sites, the transmembrane domain and the C-terminal cytoplasmic domain. The PRAD domain of PRiMA consists of two strings of prolines (4 and 10) separated by one leucine (Perrier et al., 2002). PRiMA is able to organize tetramers of AChE as well as BChE (Perrier et al., 2002). The association of PRiMA with AChE requires the presence of t peptide, but not the C terminal cystein (Perrier et al., 2002).

To date, two splicing variants of PRiMA have been identified in rodents and humans, PRiMA I and PRiMA II, which differ in the length of their cytoplasmic domain (Perrier et al., 2003). In both variants, the transmembrane segment is followed by common 7 amino acid residues, but downstream of this common peptite, PRiMA I contians 33 residues encoded by exon 5 while PRiMA II only 4 residues encoded by alternative exon 4b and exon 5 is non-coding in PRiMA II (Perrier et al., 2003).

Two variants of PRiMA have been identified also in chicken brain and muscles (Mok et al., 2009).

PRiMA I is the primary transcript in CNS and muscles, although both variants are capable of efficient production of heterocomplex (Mok et al., 2009; Perrier et al., 2003; Xie et al., 2007). The interaction of PRiMA with AChE subunits depends on proline rich motif, but not on cytoplasmic domain (Perrier et al., 2002).

Since both PRiMA and AChE are glycoproteins, the role of glycosylation on formation of physiologically active PRiMA-linked AChE tetramers (PRiMA AChE) has been studied using site directed mutations (Chan et al., 2012; Chen et al., 2011). While N-glycosylation of AChE appears to be dispensable for AChE hetero-oligomerization with PRiMA, the lack of N-glycosylation affects the proper folding of AChE to acquire the full enzymatic activity of AChE and prevents proceeding of AChE heterocomplex with PRiMA into the secretory pathway (Chen et al., 2011).

In contrast to AChE, the absence of N-glycosylation of PRiMA does not interfere with assembly of AChE with PRiMA, AChE enzymatic activity and proper trafficking of the heterocomplex (Chan et al., 2012).

Within the architecture of plasma membrane of neurons, important part of PRiMA-linked AChE is associated with membrane microdomains called membrane rafts. The association with membrane rafts increases in the course of CNS development, but the functional importance of such association has not been identified (Xie et al., 2010b).

PRiMA- or ColQ-linked ChE complexes are always composed of homodimers of either AChE or BChE. The existence of heterodimers has not yet been confirmed (Chen et al., 2010). However, the mixed PRiMA- linked tetramers composed of one dimer of AChE and one dimer of BChE have been found not only in vitro, but also in vivo in the brain of birds. Moreover, the abundance of PRiMA-linked AChE-BChE hybrids increases during chicken brain development (Chen et al., 2010). The presence of such tetramers suggests the functional role of BChE in the regulation of cholinergic transmission in birds (Chen et al., 2010). The ability of ColQ to accommodate hybrid AChE-BChE tetramers has also been indicated in chicken muscle (Tsim et al., 1988).

The solely anchoring of AChE by PRiMA in the brain is still being discussed. Some studies suggest that the anchoring of AChE via PRiMA is the hallmark only of cholinergic neurons (Henderson et al., 2010; Perrier et al., 2003). However, AChE is present also in noncholinergic neurons such as dopaminergic neurons (Bernard et al., 1995; Henderson and Greenfield, 1984). While in situ hybridization indicates co-localization of AChE and PRiMA mRNA in substantia nigra (SN) (Perrier et al., 2003), Henderson and co-workers failed to detect PRiMA by means of cytochemical methods in SN dopaminergic neurons, but not in cholinergic neurons of forebrain structures (Henderson et al., 2010). A comparative study of AChE and PRiMA mRNA expression further indicates that in some brain areas such as Hipp, mRNA of AChE is present, but not mRNA of PRiMA (Perrier et al., 2003).

In addition to CNS, PRiMA-linked AChE is also found in muscles, but represents the minor part of total ChE activity in muscles (Bernard et al., 2011; Tsim et al., 2010). First, it is present at varicosities of motoneurons and is being produced by these neurons. Second, it is expressed along the muscle, out of NMJ borders (Bernard et al., 2011). The precise role of PRiMA-linked AChE in the muscle is not known. However, it was shown that the amount of PRiMA AChE is regulated by muscle activity (Gisiger et al., 1994; Tsim et al., 2008; Xie et al., 2007).

- **Genetic models targeting cholinesterases**

Until late 90‘s the physiological importance of CHE was studied mainly by the means of pharmacology and toxicology. Although this approach has proved its significance, it also has some limitations. First it is the specificity of drugs and the diversity in their targets. Second it is the CHE tissue and molecular form selectivity. Even though some compounds show great specificity to either BChE or AChE, the selectivity towards particular molecular form of CHE or tissue specifity is missing.

To overcome this problem, genetic engineering has been employed to modulate AChE activity in vivo. Advances in genetics has allowed for suppressing the expression of particular protein or conversely to enhance it in order to explore its functions.

Giving an essential role of AChE in cholinergic transmission the generation of viable AChE KO mouse with a complete absence of AChE protein (Xie et al., 1999) came as a big surprise. In the same year a knockout mouse for ColQ anchor was prepared (Feng et al., 1999). Subsequently Palmer Taylor‘s laboratory prepared a broad range of mutants with absence of either exon 5 or 6 and also with absence of both exons (Camp et al., 2005). In 2008 a mouse with a short deletion in intron 1 was created (Camp et al., 2008). The laboratory of Oksana Lokrigde continued in their efforts and produced a BChE KO mouse (Li et al., 2006). Finally the second anchor - PRiMA - was targeted in 2009 (Dobbertin et al., 2009) (Fig. 7). On the other hand a mouse lines with over-expression of particular AChE variant, including AChE T, AChE R or catalytically inactive AChE T have been also prepared (Beeri et al., 1995; Sternfeld et al., 1998).

Subsequent studies of these mutants have provided valuable new insights on ChE physiological properties. While some findings were expectable, some of them surprised.

* ACHE KO mice: allele with a deletion of catalytic domain

- *General phenotype of AChE KO mice*

AChE KO mice were prepared by the deletion of exons 2 to 5 of the AChE gene, encoding the catalytic domain, through homologous recombination in embryonic stem cells (Xie et al., 1999). Even though AChE KO mice are viable, they show a strongly compromised phenotype, postnatal developmental delay and need special handling to survive until adulthood (Duysen et al., 2002a; Xie et al., 2000). Early weaning and hand feeding by high-caloric diet such as Ensure®, higher ambient temperature and frequent bedding replacement to prevent Helicobacter infection can effectively increase the survival rate (Duysen et al., 2002a, 2002b; Sun et al., 2007). AChE KO mice do not breed and the colony has to be maintained by breeding of heterozygotes (Het) (Duysen et al., 2002a). At birth, AChE KO mice are indistinguishable from their WT littermates through visual inspection (Xie et al., 2000). However, within few days a characteristic phenotype becomes

visible and AChE KO mice start to be clearly recognized (Duysen et al., 2002a; Xie et al., 2000).

The phenotype of AChE KO mice comprises smaller size, lower weight, pinpoint pupils, abnormal gait and posture, absence of grip strength, muscle weakness, tremor which is apparent when AChE KO move, reduced pain perception, supersensitivity to stress and death from seizures (Duysen et al., 2002a; Xie et al., 2000). AChE KO show also delays in temperature regulation (day 22 vs. 15), in righting reflex (day 18 vs 12), in descent of testes (week 7-8 vs. 4), in estrous (week 15-16 vs. 6-7). AChE KO mice prefer to stay together in a group, lack aggresive behavior and do not use remote places for defecation and urination (Duysen et al., 2002a). AChE KO mice present impaired formation of inner retina, resulting in degeneration of all photoreceptors in adult and behavioral observation indicates that AChE KO mice never can see (Bytyqi et al., 2004).

Contrary to AChE KO mice, AChE Het mice which have 60-75% of AChE activity of WT mice and ACh levels elevated by 56% in Hipp do not show any visible signs of impairment or altered survival rate (Duysen et al., 2002a; Espallergues et al., 2010; Mohr et al., 2013). Despite significant reduction in AChE activity and increased ACh levels in brain, AChE Het mice perform as WT mice in several behavioral tasks addressing locomotion, exploration, anxiety and cognitive functions (Espallergues et al., 2010; Mohr et al., 2013).

- ***Central adaptation to the complete absence of AChE***

The central cholinergic system

Despite the absence of AChE, AChE KO mice establish central cholinergic pathways as indicated by the density and distribution pattern of cholinergic perikarya, axons and terminals (Mesulam et al., 2002). In addition the pattern of M1 positive neurons, that are mostly cholinoceptive is also unchanged (Mesulam et al., 2002) .

As predicted, the absence of AChE leads to the dramatic increase in ACh content in the brain. In hippocampus of AChE KO mice the ambient ACh level is 60fold elevated in comparison to WT mice, as measured by in vivo microdialysis (Hartmann et al., 2007). Infusion of tetradotoxin, which blocks voltage-dependent sodium channels and thus neuronal activity, into hippocampus of AChE KO mice reduces ACh level to 10% of baseline, indicating that cholinergic neurons are active in AChE KO mice and the excess of ACh has origin in neuronal activity (Hartmann et al., 2007).

In such situation MR respond to the excess of ACh in neurochemical environment by downregulation and redistribution from the cell surface (Bernard et al., 2003; Decossas et al., 2003; Li et al., 2003; Volpicelli-Daley et al., 2003a). The density of MR in plasma membranes derived from the whole brains is reduced by 50% in AChE KO mice as revealed by direct radioligand binding of 3H-QNB, which labels all subtypes of MR (Li et al., 2003). Western blot analysis of protein extracts from forebrains with MR subtype specific antibodies demonstrates that M1, M2

and M4 are reduced approximately by 50% (Li et al., 2003). Similarly, in Hipp and Cx of AChE KO mice, M1, M2 and M4 are reduced by 50-80% (Volpicelli-Daley et al., 2003b).

Detailed analysis of cellular and subcellular distribution of M2 in forebrain structures including Str, Cx and Hipp demonstrates that M2 are regulated at the level of receptor trafficking (Bernard et al., 2003). In AChE KO mice, M2 are almost absent at the plasma membrane, but accumulate in ER and Golgi apparatus (GA), the sites of receptor synthesis and maturation. In addition, the portion of M2 associated with lysosomes is markedly increased in AChE KO mice, indicating that a significant part of newly synthesized M2 are directly targeted to degradation (Bernard et al., 2003).

The decrease availability of MR on plasma membrane is not, however, a general rule and is neuron segment specific (Decossas et al., 2003). Contrary to plasma membrane of cell bodies and proximal dendrites, the presynaptic terminals of cholinergic neurons of NBM projecting to the frontal Cx show increased density of M2 receptors (Decossas et al., 2003).

M2 receptors serve as autoreceptors regulating ACh release (Zhang et al., 2002) and their functional state in terms of autoregulation of ACh release has been tested in vivo using microdialysis (Hartmann et al., 2008). Application of MR antagonist scopolamine (SCO) to perfusion fluid increases the detected amount of ACh both in WT and AChE KO mice, but in AChE KO mice the rise of ACh is modest (Hartmann et al., 2008). In WT mice, SCO infusion rises ACh level to 500 % of baseline, however in AChE KO mice the ACh level increases only to 160% of baseline suggesting that presynaptic autoreceptors in AChE KO mice are functional to some extent (Hartmann et al., 2008).

In line with the reduced availability of M1 in Hipp and Cx of AChE KO mice, treatment of AChE KO mice with oxotremorine (OXO), an MR agonist failed to stimulate ERK signaling cascade (Volpicelli-Daley et al., 2003b), which is known to be mediated by M1 (Berkeley et al., 2001; Hamilton and Nathanson, 2001). At the same dose, OXO effectively enhanced activation of ERK in WT mice (Volpicelli-Daley et al., 2003b).

The altered MR availability is also evident from behavioral responses to application of different cholinomimetics. Among other effects, OXO decreases the core body temperature, an effect mediated significantly by M2 (Gomeza et al., 1999b). Application of OXO at dose that triggers almost 12 degrees drop in temperature in WT mice has no effect on body temperature in AChE KO mice (Li et al., 2003). AChE KO mice are also resistant to pilocarpine (PIL) induced seizures (Li et al., 2003) by activation of M1 (Hamilton et al., 1997). On the other hand, AChE KO mice show increased response to SCO, which induces hyperlocomotion in rodents (Volpicelli-Daley et al., 2003a).

As opposed to MR, β2 NR protein level determined by western analysis is unchanged in AChE KO mice (Volpicelli-Daley et al., 2003a). However, the lack of change in density of NRs might be due to a limited specificity of antibodies (Moser et al., 2007).

ACh is synthetized within presynaptic terminals from its precursors Ch and acetyl-CoA by ChAT and is then concentrated in vesicles by VAChT. The activity of ChAT in Str of AChE KO mice do not differ from WT mice. Similarly, the protein level of VAChT in Str of AChE KO mice is unchanged, as determined by western analysis. In contrast, HACU and protein level of ChT is significantly increased in AChE KO mice. In striatum of AChE KO mice, the protein level of ChT is increased by 60% and HACU measured in Hipp of AChE KO mice is 2fold higher than in WT mice (Hartmann et al., 2008; Volpicelli-Daley et al., 2003a).

AChE Het mice with 30-40% reduction of AChE activity and ACh levels in Hipp elevated by 56% (Mohr et al., 2013) have MR density reduced by 25%, as measured by means of radioligand binding (Li et al., 2003). The altered MR abundance in AChE Het mice is indicated also by intermediate response to cholinomimetics (Li et al., 2003). The behavioural analysis of AChE Het suggests that the brain of AChE Het mice is well adapted to partial lack of AChE (Espallergues et al., 2010; Li et al., 2003; Mohr et al., 2013).

- ***The peripheral adaptations***

Vegetative nervous system

AChE KO mice have impaired thermoregulation by the day 22 of postnatal development (Duysen et al., 2002a) and increase in ambient temperature effectively prolongs the survival of AChE KO mice (Sun et al., 2007). Evidence indicates that the deficit in thermoregulation do not reside in the brain, but arises from decreased cholinergic signaling at sympathetic ganglia (SG). NR currents in acutely isolated SG neurons are reduced by 40% in AChE KO mice. The reduction of NR currents is not associated with change in properties of NRs and likely originates from the reduced density of NRs as a result of prolonged MR and NRs stimulation. Consistent with such assumption, treatment of AChE KO mice with methyl-atropine - MR antagonist - together with ivermectin - potentiator of NRs - can rescue the hypothermia of AChE KO mice at postnatal day 15 (Sun et al., 2007).

Respiration

Even though AChE KO mice are born alive and breath, they show altered respiration. Detailed analysis of AChE KO mice using whole-body plethysmography shows that AChE KO mice presents increased tidal volume (+89%), mean respiratory flow (+270%) and overall ventilation (+70%), while the breathing frequency is unchanged. AChE KO mice also display altered responses to hypercapnia and hypoxia (Boudinot et al., 2004).

In vitro, the basal respiratory burst frequency of respiratory motor neurons in AChE KO mice is not different from WT mice (Chatonnet et al., 2003). However, the respiratory motor neurons of AChE KO mice are resistant and less responsive to tonic discharge activity induced by cholinergic drugs and increase of respiratory frequency. These findings suggest an effective

adaptation of central mechanisms to the excess of ACh, likely due to the down-regulation of ChR responses to the elevated ACh levels (Chatonnet et al., 2003).

The lung tissue is under influence of cholinergic and adrenergic system, implying that both systems could be affected in AChE KO mice. Indeed, AChE KO mice do not show only reduction of MR density in lungs, due to the putative excess of ACh in lung tissue, but also reduction in α1 and β adrenoceptors density, further supporting the complex response to the absence of AChE (Myslivecek et al., 2007).

Neuromuscular junction and muscle

At NMJ, AChE rapidly clears ACh to prevent repetitive binding to NRs and failure of tetanic muscle stimulation. NMJs of AChE KO mice show strong remodelling and are characterized by smaller surface area, fragmented nerve terminals, irregular and shallow postjunctional folds, overall decrease in number of postjunctional folds, postjunctional membrane areas without innervation, Schwann cells penetrating into the synaptic cleft and over 50% downregulation of NRs (Adler et al., 2004, 2011; Girard et al., 2005). Since the morphology of normal NMJ, where the nerve terminal covers the whole synaptic cleft imposes limits on diffusion of ACh out from the synaptic cleft, the morphological traits of NMJ of AChE KO mice might serve to promote the alternative routes for ACh escape (Adler et al., 2004, 2011). In addition, the escape of ACh from synaptic cleft might be supported by reduced density of NRs (Adler et al., 2004), which under normal conditions repetitively bind ACh and thus retards its escape from NMJ by diffusion (Katz and Miledi, 1973).

In spite of the absence of AChE, NMJs of AChE KO mice are able to mediate muscle contraction and the compensatory mechanisms are highly effective, albeit within a limited range (Adler et al., 2004, 2011; Girard et al., 2005). Unexpectedly, the twitch tension elicited by a single nerve stimulation is markedly potentiated in AChE KO mice and characterized by slower rise and decay. Interstingly, over a limited range of frequencies (70-100Hz) AChE KO mice can maintain the tetanic tensions. However, lower or higher frequencies result in tetanic fade (Adler et al., 2004, 2011; Girard et al., 2005). In contrast to AChE KO mice, the acute inhibition of AChE has much more severe impact on tetanic tensions, resulting in a more profound and frequency-dependent reduction of tetanic tensions and inability to sustain nerve-evoked tetanic tensions with frequencies higher than 40Hz (Adler et al., 2004; Girard et al., 2005). The evoked endplate potentials (EPPs) in AChE KO mice exhibit a prolonged decay as compared to WT mice. In AChE KO mice, the repetitive nerve stimulation at frequencies higher than 20Hz results in the marked decline of successive EPP peak-amplitudes and prominent residual sustained depolarization of postsynaptic membrane (Adler et al., 2011; Minic et al., 2003).

In AChE KO mice, miniature endplate potentials (MEPPs) have the same amplitude but much longer decay time and occur at lower frequencies (Adler et al., 2011; Girard et al., 2007). Even though the prolonged decay of MEPPs and EPPs indicate the increased duration of ACh action on postsynaptic receptors, the prolongation of MEPPs is less marked than in case of acute

AChE inhibition (Adler et al., 2011). In addition, in normal muscles in which AChE is acutely inhibited, MEPPs have increased amplitudes (Adler et al., 2011).

Differences between acute AChE inhibition and AChE KO mice suggest greater accumulation of ACh in synaptic cleft of NMJ with acutely inhibited AChE than in AChE KO mice (Adler et al., 2004, 2011).

In addition to AChE, NMJ possess similar amount of BChE activity suggesting that BChE might participate on ACh hydrolysis (Blondet et al., 2010; Minic et al., 2003). However, in vitro studies of hemidiaphragm preparations of AChE KO and WT mice suggest that BChE is not involved in limiting the duration of ACh action on postsynaptic receptors, but participates in presynaptic modulation of ACh release process (Minic et al., 2003). Inhibition of BChE in AChE KO or WT mice decreases evoked quantal release, but does not affect the time course of MEPPs and EPPs (Minic et al., 2003). Even though it seems unlikely that BChE regulates the duration of ACh action on postsynaptic NRs, inhibition of BChE in AChE KO mice intensifies the tetanic fade at frequencies higher than 70 Hz, while not having noticeable effect on WT mice (Adler et al., 2004; Girard et al., 2005). The intensified tetanic fade following BChE inhibition in AChE KO mice is likely related to the presynaptic modulatory role of BChE on evoked transmitter release and in AChE KO mice, BChE might serve as protection of nerve terminals from the excess of ACh (Girard et al., 2005).

Overall it can be suggested that both synaptic remodelling, decreased density of NRs and BChE presence help AChE KO mice to maintain muscle function, albeit over a limited range (Adler et al., 2004, 2011; Girard et al., 2005).

In addition to impaired neuromuscular functioning, the muscles of AChE KO mice appear to present cellular and molecular changes (Vignaud et al., 2008a, 2008b). In vitro studies of soleus muscle demonstrate that the maximal tetanic force is reduced and the maximal velocity of shortening is increased in AChE KO mice, indicating that muscles of AChE KO mice are weaker and faster (Vignaud et al., 2008a, 2008b). In contrast, twitch properties and fatigue resistance are not altered in AChE KO mice. The number of muscle fibers do not differ between AChE KO and WT mice. However, the relative amount of slow myosin heavy chains (MHC-1) in muscle homogenates and the portion of muscle fibres expressing MHC-1 is decreased in AChE KO mice (Vignaud et al., 2008a).

Based on a recent work it seems that the muscle adaptation is very complex (Lin et al., 2010). Applying microarray analysis on total muscle RNA Lin et al. found that from 28853 genes tested, 303 genes were more then 2fold up- or down-regulated, including genes related to lipid metabolism and muscle contraction (Lin et al., 2010).

- ***A role of BChE in cholinergic transmission of AChE KO mice***

While AChE KO mice are devoid of AChE, they still possess BChE, which can also

hydrolyze ACh and is present in all tissues including brain, muscles, lung and blood (Blondet et al., 2010; Li et al., 2000). The level of BChE activity and its ditribution pattern in AChE KO mice is not altered and its presence might be central to the survival of AChE KO mice (Blondet et al., 2010; Chatonnet et al., 2003; Li et al., 2000; Mesulam et al., 2002).

12 day-old AChE KO mice are supersensitive to peripheral injection of BChE inhibitor bambuterol (Xie et al., 2000). While WT littermates do not show any sign of toxicity following bambuterol injection, AChE KO mice are dead within 10 min. The supersensitivity of AChE KO mice thus strongly suggests that BChE activity is central in the survival of AChE KO mice (Xie et al., 2000). Similarly, Chatonnet and co-workers showed that peripheral injection of bambuterol is lethal to neonate as well as to adult AChE KO mice (Chatonnet et al., 2003). Bambuterol at doses which decrease BChE activity only in the periphery and not in the brain, induce in AChE KO mice apnea and death. These findings indicate that the peripheral BChE has a particular role in the survival of AChE KO mice (Chatonnet et al., 2003). The respiratory failure due to the inhibition of BChE in the priphery is also supported by observations in vitro. Inhibition of BChE in isolated brainstem do not affect the central respiratory generator or output motorneurons (Chatonnet et al., 2003).

BChE is also present in the brain, albeit constitutes only minor part of total ChE activity (Li et al., 2000). However, BChE inhibition by BChE inhibitors delivered through the microdialysis probe results in up to 5fold elevation of ACh levels in Hipp of AChE KO mice. In contrast to AChE KO mice, inhibition of central BChE does not change ACh levels in WT mice. These results strongly suggest that, in the absence of AChE, BChE participates on clearence of ACh in the brain (Hartmann et al., 2007; Naik et al., 2009).

Considering the consequences of central and peripheral inhibition of BChE it is reasonable to suggest that BChE plays an important, if not the most important, role in surviving of AChE KO mice.

* BChE KO mice: allele with a deletion of the catalytic domain

BChE KO mice were generated in an effort to shed more light on the function of BChE, which remains largely elusive (Duysen et al., 2009; Li et al., 2006). Humans with a partial or complete absence of BChE are healthy (Manoharan et al., 2007). It was hoped that BChE KO mice would more approach the physiological function of BChE (Duysen et al., 2009; Li et al., 2006). BChE KO mice were generated by homologous recombination targeting part of exon 2, thus removing splice junction between intron 1 and exon 2, entire signal peptide including the translation start site, and the first 102 amino acids of mature BChE protein (Li et al., 2006).

Similar to humans, BChE KO mice are healthy and indistinguishable from WT mice (Duysen et al., 2009; Li et al., 2006, 2008a). BChE KO mice have the same rate of weight gaining, temperature, heart function, blood pressure, respiration and AChE activity. BChE KO mice do not

show delay in their development, acquire righting reflex at the same day as WT mice and are fertile (Li et al., 2008a). As expected, exposition to chemicals metabolized by BChE reveals absence of BChE. BChE KO mice are more prone to toxicity of cocaine and succinylcholine (Duysen et al., 2008; Li et al., 2008a). Morover, donepezil and huperizine A - selective inhibitors of AChE - are highly toxic to BChE KO mice, suggesting that when AChE is inhibited, BChE takes control over cholinergic transmission (Duysen et al., 2007). A dose of donepezil or huperizine A which elicits non-lethal cholinergic symptoms in WT mice, results in tonic convulsions and death in BChE KO mice (Duysen et al., 2007).

It is worth mentioning that the application of PIL triggers convulsions in BChE KO mice but not in WT mice (Li et al., 2008a). In addition, BChE KO mice do not recover from PIL induced hypothermia and eventually die or are moribund 24 hours postdosing. Toxicity of PIL appears to be not related to heart or respiratory system and might results from PIL-induced seizures. In contrast to increased toxicity of PIL, BChE KO mice are less sensitive to OXO. While BChE KO mice show similar OXO induced hypothermia and analgesia as WT mice, only WT mice experience severe body tremors. The altered responsiveness of BChE KO mice to MR drugs indicate that MR function is altered in BChE KO mice (Li et al., 2008a).

It has been also suggested that BChE has a role in fat metabolism. Interestingly, BChE KO mice fed a high fat diet became obese. However, neither increased food consumption nor decreased locomotor activity was observed (Li et al., 2008b). The precise mechanisms underlying this phenomenom remain to be described (Duysen et al., 2009).

Even though BChE KO mice have not come with the answer on the precise function of BChE, BChE KO mice already serve as a valuable tool for testing the toxicity of compounds metabolized by BChE, optimizing the routes for delivery of external BChE to protect from organophosphate poisoning (Duysen and Lockridge, 2008; Duysen et al., 2009; Johnson et al., 2009; Li et al., 2008a), for creation of excellent antibodies against BChE (Hrabovska et al., 2010a) and validate their specificities.

- **Genetic models with partial lack of AChE**

  * **AChE 1irr: allele with a deletion in intron 1**

A 250 bp sequence in the intron 1, identified to be crucial in AChE expression during early muscle differentiation, was deleted in AChE gene (Camp et al., 2005, 2008). The homozygote mice for this allele (AChE 1irr) are devoid of virtually all AChE in skeletal muscles. By contrast, AChE activity is preserved in brain and spinal cord. Unexpectedly the intron 1 regulatory region also controls the expression of AChE in platelets, but not in erythrocytes (Camp et al., 2008).

In some aspects AChE 1irr mice present phenotype similar to that of AChE KO mice (Boudinot et al., 2009; Camp et al., 2008). AChE i1rr mice show constant tremor, strong muscle weakness, decreased growth rate, smaller size and weight. Contrary to AChE KO mice, AChE 1irr mice are able to reproduce (Camp et al., 2005, 2008). Respiration of AChE 1irr mice is well maintained. However, AChE 1irr mice show blunted response to hypercapnia and hypoxia, possibly due to the muscle fatigue (Boudinot et al., 2009). Pharmacological inhibition of BChE by bambuterol - selective inhibitor of BChE, which does not pass through the blood-brain barrier -, while without effect in WT mice, in AChE 1irr mice, decreases tidal volume and body temperature (Boudinot et al., 2009). Even though BChE inhibition affects muscle contraction in AChE 1irr mice, presumably by blocking BChE regulating presynaptically release of ACh at NMJ (Girard et al., 2007; Minic et al., 2003), is not lethal to AChE 1irr mice. In contrast to AChE 1irr mice, AChE KO mice do not survive the same dose of bambuterol (Chatonnet et al., 2003). It has been suggested that survival of AChE 1irr mice following BChE inhibition might be due to the presence of AChE in the blood, that could hydrolyse ACh escaped from NMJs (Camp et al., 2005).

* AChE del E5: allele with the deletion of exon 5

Joining of exon 4 - the last exon encoding for common catalytic domain - with exon 5 generates AChE H subunits which produce AChE dimers attached via GPI anchor on the surface of blood cells (Massoulié et al., 2005). To selectively ablate AChE from hematopoietic cells, KO mice with deleted exon 5 (AChE delE5) were generated (Camp et al., 2005). Surprisingly, AChE activity in serum of AChE delE5 mice is reduced by 60%, although AChE del E5 mice are designed to lack only GPI anchored AChE forms. AChE del E5 mice have also modest reduction of AChE activity in brain and muscles (Camp et al., 2005, 2010).

* AChE del E6: allele with the deletion of exon 6

Joining of exon 4 with exon 6, generates the major species of AChE - AChE T variant - which interacts with PRAD of anchoring proteins ColQ and PRiMA and with polyproline peptides (Biberoglu et al., 2013; Massoulié et al., 2005; Noureddine et al., 2007). Deletion of exon 6 in mice (AChE delE6) was predicted to abolish the formation of tetramers and heterocomplex associations of AChE. Indeed, AChE activity in brain and muscle is reduced in AChE del E6 mice by 93% and 72%, respectively (Camp et al., 2005, 2010). Phenotype of AChE del E6 mice is similar to AChE 1irr mice. AChE delE6 mice are smaller than WT mice, live with constant tremor and show decreased growth rates. However, the overall phenotype of AChE del E6 is not as compromised as that of AChE KO mice and unlike AChE KO mice, AChE del E6 mice can reproduce (Camp et al., 2008).

* AChE del E5+6: allele with the deletion of exon 5 and 6

The deletion of exons 5 and 6 in AChE gene is predicted to restrict the diversity of AChE molecular forms to monomeric species (Camp et al., 2005).

Mice with deleted combination of exons 5 and 6 (AChE delE5+6), have very low levels of AChE in brain and muscles (Camp et al., 2005, 2010). The only form of AChE found in plasma and brain of AChE delE5+6 mice is nonamphiphilic soluble monomer which presumably corresponds to AChE R. Interestingly, AChE activity in serum of AChE del E5+6 mice is almost doubled (Camp et al., 2005, 2010).

The phenotype of AChE delE5+6 mice closely resembles that of AChE KO mice, but it is not as much compromised as in case of AChE KO mice (Boudinot et al., 2009; Camp et al., 2005). AChE delE5+6 mice display smaller size and lower weigth, decreased growth rates, muscle weakness, abnormal posture, involuntary motor movement, vocalization and lack of sexual reproduction (Dobbertin et al., 2009). Higher ambient temperature and liquid feeding can enhance the survival rate of AChE delE5+6 mice (Dobbertin et al., 2009). In contrast to AChE KO mice, AChE delE5+6 mice do not suffer from myoclonic seizures, present nociceptive tail pinch response and many AChE del E5+6 mice survive over 6 months even if not given special care (Dobbertin et al., 2009).

In striking contrast to AChE KO mice, AChE delE5+6 mice have well maintained respiration, albeit small differences can be observed (Boudinot et al., 2009). Responsiveness of AChE delE5+6 mice to bambuterol in terms of thermoregulation and respiration is similar to AChE 1irr mice, indicating that the absence of AChE in muscles underlie the toxicity of BChE inhibition in these strains. Similarly to AChE 1irr mice, BChE inhibition by bambuterol is not lethal to AChE delE5+6 mice even at much higher dose than the dose leading to death of AChE KO mice. The better resistance of AChE delE5+6 and AChE 1irr mice to toxic effects of BChE inhibitors suggests that the lethal effect of peripheral BChE inhibition in AChE KO mice is not caused solely by the lack of AChE at NMJs (Boudinot et al., 2009).

AChE delE5+6 mice have very low activity of AChE in brain, corresponding to 2-7% of WT activity (Camp et al., 2010; Dobbertin et al., 2009). As expected, PRiMA-linked tetramers are absent and only minute amount of nonamphiphilic monomer, likely AChE R, can be found in Str of AChE del E5+6 mice. The cellular and subcellular analysis of the distribution of remaining AChE activity in Str of AChE delE5+6 mice demonstrate that AChE is only detectable in cell bodies of ChI and is absent from plasma membrane, the principal localization of AChE in WT mice. Within cell bodies of ChI, AChE is associated mostly with ER and to a lower extent with GA and nuclear membrane (Dobbertin et al., 2009).

In AChE delE5+6 mice, M2 are redistributed from the plasma membrane and are trapped in the cell bodies (Dobbertin et al., 2009). Such redistribution of MR and other GPCR has been demonstrated many times to result from prolonged overstimulation of receptors by exogenous or

endogenous ligands (Bernard et al., 2006).

In muscles of AChE delE5+6 mice, AChE activity is reduced by 68% and at NMJs, no AChE activity is detectable by histochemical techniques (Camp et al., 2005; Girard et al., 2006). The absence of AChE at NMJs is also indicated by prolonged decay of MEPPs. Longer decays of MEPPs, reflecting the prolonged action of ACh on postsynaptic NRs, suggest that AChE R cannot replace heteromeric AChE in the synaptic cleft (Girard et al., 2006). At morphological level, the absence of AChE results in synaptic remodeling of mature NMJs in AChE del E5+6 mice (Girard et al., 2006).

- **Genetic models targeting the anchoring of CHE**

* ColQ KO : allele with deletion of the PRAD domain

The major form of AChE at NMJs is the asymmetric form of AChE in which 1, 2, or 3 tetramers of AChE T are associated with rod-shaped collagenic tail – ColQ (Bernard et al., 2011). Mutations in the ColQ gene in humans resulting in AChE deficiency at NMJs cause myasthenic syndrome (Mihaylova et al., 2008). Thus, it was of interest to generate a ColQ-deficient mouse model (ColQ KO) and address the role of ColQ in ChE assembly and NMJ function. ColQ KO mice were generated by knocking out the exon encoding the PRAD domain, which is responsible for association of ColQ with ChE (Feng et al., 1999).

ColQ KO mice are devoid of asymmetric forms of both ChE - AChE and BChE - in muscles and ColQ expressing tissues such as heart (Feng et al., 1999). ColQ KO mice are born alive and initially are indistinguishable from WT littermates. However, within few days ColQ KO mice start to show tremor when moving and this sign is kept during the whole life. Moreover, ColQ KO mice are charaterized by smaller size, decreased growth rates and muscle weakness. ColQ KO mice are able to feed themselves and remain active. However, the survival of ColQ KO mice is limited. Half of the mutants die within the period of weaning, two-thirds of mutants die in the subsequent few weeks and only 10-20% survive to adulthood (Feng et al., 1999).

The NMJ of ColQ KO mice is virtually devoid of AChE (Feng et al., 1999), but a residual AChE activity can be detected by histochemistry when a sufficient time (3 hours instead of 30 min) is given to AChE to generate substrate for visualization (Bernard et al., 2011). The residual AChE activity corresponds to PRiMA-linked tetramers produced by motor neurons and localized to pre-terminal and terminal regions of motor neurons (Bernard et al., 2011).

MEPPs measured from muscle fibers of ColQ KO mice have longer decay times, indicating prolonged action of ACh on postsynaptic NRs (Feng et al., 1999).

In addition to residual AChE activity, NMJs of ColQ KO mice retain part of BChE activity

that appears to be associated with nerve terminal Schwann cells and/or nerve terminals. Because BChE inhibition does not change the decay of MEPPs, the remaining BChE activity seems to be not involved in limiting the action of ACh on postsynaptic membrane (Feng et al., 1999).

The morphological structure of NMJs in ColQ KO mice is abnormal. In 20 days old ColQ KO mice, 40% of NMJs resemble the typical pretzel-like structure of NMJs found in WT mice, albeit are smaller. 20% of NMJ retain immature geometry characteristic of 1 week old WT mice and 40% of NMJs appear to be frangmented. In many NMJs, the subsynaptic cytoplasm shows signs of necrosis and some nerve terminlas are enwrapped by Schwann cells. However, in 6 months old mice, only few synapses appear to be necrotic and many are well developed and more than one-half of terminals is partially or completely enwrapped by Shwann cell processes (Feng et al., 1999).

* PRiMA KO : allele with deletion of the PRAD domain

PRiMA KO mice were generated to study the anchoring mechanisms of CHE selectively in the brain and to elaborate the physiological importance of PRiMA anchor. PRiMA KO mice were created by deletion, of PRAD domain of PRiMA by homologous recombination (Dobbertin et al., 2009). This pilot study brought valuable informations regarding the anchoring of AChE in the brain and the function of PRiMA.

AChE activity in Str of PRiMA KO mice is reduced to 2-3% of the AChE activity of WT mice (Dobbertin et al., 2009). As expected, the principal form of AChE in brain - PRiMA-linked AChE tetramer (Perrier et al., 2002) - is absent in PRiMA KO mice. The residual AChE corresponds to nonamphiphilic tetramer, amphiphilic monomer and dimer (Dobbertin et al., 2009).

Cellular and subcellular distribution of residual AChE in PRiMA KO mice demonstrate that PRiMA is a limiting factor in the anchoring of AChE in brain (Dobbertin et al., 2009). In Str of WT mice, the principal source of AChE are ChI. At cellular level, AChE is found at the plasma membrane of cell bodies, axons and varicosities of ChI (Dobbertin et al., 2009). In the absence of PRiMA, AChE is no more directed to the plasma membrane of ChI and remains trapped inside the cell bodies. Neither biochemical nor histological techniques did reveal any AChE either at the plasma membrane of ChI or in their close environment. These findings show that AChE can be anchored into the plasma membrane of neurons only by its interaction with PRiMA (Dobbertin et al., 2009).

Unexpectedly, PRiMA absence also interfere with early processing of AChE into the secretory pathway (Dobbertin et al., 2009). In heterologous expression systems, when AChE T is expressed alone without ColQ or PRiMA, AChE monomers and homo-oligomers appear to be efficiently secreted into the medium (Bon and Massoulié, 1997). However, in vivo in PRiMA KO mice, AChE subunits remain retained in ER and are not processed to Golgi appartus (Dobbertin et al., 2009). The retention is partially rescued by deletion of WAT domain in double KO mice (AChE del E5+6 and PRiMA KO), indicating that WAT domain contains a strong retention signal

in tissues in vivo (Dobbertin et al., 2009).

Contrary to AChE protein level, the level of AChE mRNA do not change in PRiMA KO mice, indicating that PRiMA absence do not affect the transcription of AChE and that the lack of AChE protein does not originate in decreased mRNA production (Dobbertin et al., 2009).

In the brain, ACh can be also hydrolysed by BChE (Mesulam et al., 2002). The control of ACh levels in the brain by BChE is apparent in AChE KO mice (Hartmann et al., 2007). In contrast to AChE, which is of neuronal origin, BChE is mainly of glial origin (Mesulam et al., 2002). At light microscopic level, histochemical staining of BChE in PRiMA KO mice is markedly reduced and appears to be restricted to cell bodies (Dobbertin et al., 2009). These findings suggest that, similarly to AChE, the anchoring of BChE in the brain depends on PRiMA anchor (Dobbertin et al., 2009).

Giving an essential role of AChE in spatial and temporal control of ACh levels in the brain and implication of cholinergic system in a broad range of functions, it was a surprise that PRiMA KO mice are born alive and do not show any changes of their phenotype visible to the naked eye (Dobbertin et al., 2009). PRiMA KO mice do not differ from WT mice in their body size and weight, survival rates, temperature, fertility and sexual behavior. PRiMA KO mice do not show any obvious alterations in body posture and locomotion. Pain response, geotaxis and rearing activity is similar to WT mice (Dobbertin et al., 2009). Despite the lack of AChE and BChE in the brain, respiration of PRiMA KO mice is not changed (Boudinot et al., 2009). The sensitivity of PRiMA KO mice to bambuterol - BChE inhibitor - is comparable to WT mice (Boudinot E et al 2009).

The phenotype of PRiMA KO mice (Dobbertin et al., 2009) strongly contrasts to that of AChE KO mice (Duysen et al., 2002a) and to ones expected.

• HYPOTHESES AND AIMS

AChE KO mice, in which AChE is absent in all tissues, have immediately apparent handicaps and suffer from the absence of AChE. Unexpectedly, PRiMA KO mice which lack the principal form of AChE in the CNS are indistinguishable from WT mice. The obvious difference between the phenotype of AChE KO and PRiMA KO mice thus might suggest that the severe handicaps of AChE KO mice mainly result from the absence of AChE outside the CNS and/or the central cholinergic sytem in PRiMA KO mice is less affected than in AChE KO mice.

The aim of the thesis is to explore the behavioral and biochemical consequences of the absence of PRiMA in PRiMA KO mice.

• METHODS

• Drugs

(±)-Butaclamol hydrochloride, (±)-vesamicol hydrochloride, (-)-scopolamine hydrochloride, acetyl coenzyme A sodium salt, apomorphine hydrochloride, atropine sulfate, hemicholinium-3, choline chloride, kainic acid monohydrate, L-glutamic acid, naloxone hydrochloride dehydrate, nicotine hydrogen tartrate, oxotremorine sesquifumarate, SR-95531, acetylthiocholine, butyrylthiocholine, tetra(monoisopropyl)pyrophosphortetramide (iso-OMPA), 1,5-bis(4-allyldimethylammoniumphenyl) pentan-3-one dibromide (BW284C51) were purchased from Sigma-Aldrich (Sigma-Aldrich Co, St. Louis, MO, USA). AMPA-a-[5methyl-3H]) (45.8 Ci/mmol), hemicholinium-3 diacetate salt [methyl-^{3}H] (125.4 Ci/mmol), Choline chloride[methyl-^{3}H] (85 Ci/mmol), kainic acid [vinylidene-^{3}H](49.9 Ci/mmol), Muscimol [methylene-^{3}H(N)] (35.6 Ci/mmol), pirenzepine [N-methyl-^{3}H] (83.4 Ci/mmol), Vesamicol L-[piperidinyl-3,4-^{3}H] (46.8 Ci/mmol) were from American Radiolabeled Chemicals (ARC, Inc.). Acetyl Coenzyme A [acetyl-^{3}H] (6 Ci/mmol), AF-DX 384 [2,3-dipropylamino-^{3}H] (106.5 Ci/mmol), CGP 39653 [propyl-2,3-^{3}H] (50 Ci/mmol), quinuclidinyl benzilate L-[benzilic-4,4'-^{3}H] (46 Ci/mmol), SCH 23390 [N-methyl-^{3}H] (85 Ci/mmol), [^{125}I]-Epibatidine (2200 Ci/mmol), [^{125}I]-Iodosulpride (2200 Ci/mmol), [^{125}I]-Tyr54-α-bungarotoxin (2200 Ci/mmol) were from Perkin Elmer (Perkin Elmer Inc., USA).

• Mice

Experiments were performed on four strains of mice: WT, mice nullizygous for PRiMA (PRiMA KO), mice nullizygous for ColQ (ColQ KO), mice nullizygous for AChE exons 5 and 6 (AChEdelE5+6). Genotypes were determined by PCR with primers described elsewhere (Dobbertin et al., 2009), before and after the experiments. The mice used for experiments were two to six months old, except for developmental studies, for which we used mice of various ages (embryonal day 18.5, just after the birth, 9-, 30-, 120-, and 425-day-old). The genetic background of the mice used was a mixture equivalent to that for an F3 mating of B6D2 strain. All experiments were performed in accordance with the regulations of the French Agriculture and Forestry Ministry (Veterinary Service Department of the Prefecture de Police, Paris, France). The mice were born at an animal facility in Paris and were then transported for rearing to Prague or Pilsen (Czech Republic) where they were allowed to acclimatize for at least 14 days. Animals were treated in accordance with the legislation in force in the Czech Republic and the EU, and the experimental protocol was approved by the Committee for the Protection of Experimental Animals of the 1st Medical Faculty, Charles University, Prague. The animals were maintained under controlled environmental conditions (12/12 light/dark cycle, 22±1°C, light on at 6 a.m.). Food and water were available ad

libitum. Female mice and their WT counterparts (weighing 20-25g, 11-13 weeks old) were used in the study. Microdialysis experiments, in particular, were carried out in accordance with the guidelines of the Regierungspräsidium Darmstadt, Germany.

• Behavioral tests

Behavioral tests were performed over a period of 25 days: open-field tests for 2 days, gait examination (CatWalk), 3 days without testing, rotarod and suspension wire tests for 3 days, spatial navigation in the Morris water maze (MWM) for 10 days, the probe trial in MWM on 11th day and visible-platform acquisition training in MWM for 5 days.

* Open-field test

The mice were placed in the middle of a square arena, the open field (40×40 cm, wall height 40 cm) and allowed to move freely for 5 min. The distance covered and the time spent in the central zone (central square equivalent to 9/25 of the total area) were evaluated. The test was repeated on the next day to assess habituation. The movement of the animal was recorded and evaluated with the EthoVision 3.0 tracking system (Noldus Information Technology, Wageningen, The Netherlands).

* Gait examination

The gait of the animal was studied with the automated overground locomotion gait analysis system CatWalk (Noldus Information Technology, Wageningen, The Netherlands) (Hamers et al., 2006). The mice were placed in a corridor (8 cm wide, 115 cm long) and allowed to walk freely. We recorded at least 20 sequences, through the visualized central part of the corridor (60 cm long), in which the animal walked in a straight line without interruption. Five of the tracks in which the mouse passed through the entire field without interruption or tracks containing at least five fluently consequential complete step cycles were analyzed for each mouse. We then averaged the values for the tracks analyzed for each individual animal. The following parameters were evaluated: walking speed (in cm/s), time between initial and maximal contact of the paw (in s), paw angle (angle in degrees between the long axis of the paw and the axis of the walking trajectory), stride length (in mm), stand (duration of the standing phase, in s), swing (duration of the swing phase, in s), swing speed (in m/s), base of support (distance in mm between the limb pairs in a girdle), print position (distance between a fore and a hind paw print in one step cycle, for right and left paws, separately), regularity index (% of regular step patterns, in healthy – fully coordinated – animals its value is 100%), support (combination of paws simultaneously in contact with the walkway as a % of walking time). Time between initial and maximal paw contact, paw angle, stride length, stand, swing and swing speed values were averaged for the left and right paw of the same girdle.

* Rotarod test and horizontal bar test

For the rotarod test, the mice were placed on a rotarod cylinder (diameter: 4 cm, constant rotation speed: 12 turns/min), with their heads facing away from the direction of rotation. For the horizontal bar test, the animal was suspended by its two forepaws in the middle of a horizontal wire (30 cm long, 1 mm in diameter) held taut between two wooden columns 55 cm above a table covered with a soft pillow. The time until the mice fell (fall latency) was measured. If the mouse reached a maximal latency of 120 s, the trial was stopped and the mouse was removed from the apparatus. Both tests were repeated four times per day, at 15-minute intervals, on three days. Mean fall latencies were calculated for each day.

* Morris water maze

Spatial orientation was investigated in the Morris water maze (Morris, 1984), in a circular pool (100 cm in diameter, water depth: 35 cm, height of the wall above the water level: 20 cm, water temperature: 25-26ºC) made of white plastic. A circular platform (8 cm in diameter) made of transparent Plexiglass was placed in the middle of the imaginary south-east quadrant. The platform was hidden 0.5 cm beneath the water surface. Four trials per day were performed, with starting points at imaginary cardinal points in the following order: north-south-west-east. If the mouse did not reach the platform within 60 s, it was guided to the platform. The mouse was left on the platform for 30 s after each trial. There was an interval of 20 minutes between trials. The experiment was repeated every day for 10 days. The EthoVision 3.0 (Noldus Information Technology bv, Wageningen, The Netherlands) automatic tracking system was used to detect mouse movement. Escape latency, distance moved, and swimming speed were evaluated. The ratio between escape latency and the ratio between the trajectory length on the last and the first day were also calculated to assess the change of these parameters during the course of the experiment. The probe trial was performed on the day after the last Morris water maze trial. The mice were released into the maze at the north starting position and left to swim in the maze without the platform for 60 s. We determined the amount of time spent in the south-east quadrant. The visible-platform acquisition training in MWM was performed following the probe trial. The hidden platform in south-east quadrant was visualized by a red flag and mice were trained as in the first 10 days. Escape latency, distance moved, and swimming speed were evaluated.

• Biochemical analysis

* High-affinity choline uptake

Freshly dissected brain regions were homogenized by three 10-second pulses with an Ultra-Turrax homogenizer (IKA-Werke, GmbH & Co.KG, Staufen, Germany), in 15 volumes of cold

0.32 M sucrose. Homogenates were centrifuged at 4°C for 10 min at 1000×g (Hettich Micro 22R, Andreas Hettich GmbH & Co. KG, Tuttlingen, Germany). The supernatant was then centrifuged at 4°C for 20 min at 20,000×g. The supernatant was discarded and the pellet was resuspended in 30 volumes of cold 0.32 M sucrose.

HACU was determined as previously described (Kristofiková et al., 2006). We added 100 µl of synaptosomal suspension to 800 µl of Krebs-Ringer-HEPES-glucose buffer (128 mM NaCl, 5 mM KCl, 2.7 mM CaCl2, 1.2 mM MgSO4, 5 mM glucose and 10 mM HEPES, pH 7.4) and incubated the mixture for 4 min at 37°C in a water bath. Uptake was initiated by adding 100 µl of [^{3}H]-choline in Krebs-Ringer-HEPES-glucose buffer (final dilution 10 nM) and was allowed to continue for 4 min at 37°C. Incubation was terminated by adding 4 ml of ice-cold Krebs-Ringer-HEPES-glucose buffer supplemented with 1 µM hemicholinium-3 and filtering rapidly through GF/B glass fiber filters in the Brandel cell harvester (Brandel, Inc., Gaithersburg, MD, USA). The filters were washed twice with 5ml of ice-cold Krebs-Ringer-HEPES-glucose buffer, allowed to dry at RT. Dried filters were transferred to scintillation vials and 10 ml of scintillation cocktail was added. The radioactivity associated with filters was measured by Beckman liquid scintillation counter (Beckamn Coulter, Inc., CA, USA). HACU was calculated as the difference in [^{3}H]-choline uptake between incubations with and without 1 µM hemicholinium-3. Samples were run in duplicate. Protein content was assessed in a commercially available bicinchoninic acid protein assay according to the manufacturers instructions (Pierce® BCA Protein Assay Kit, Thermo Fisher scientific, Inc., MA, USA).

* Choline acetyltransferase assay

Choline acetyltransferase activity was assessed by a modified version of Fonnum‘s method (Berrard et al., 1995; Fonnum, 1969), as previously described (Machová et al., 2008). Dissected brain regions were homogenized by three 10-second pulses with an Ultra-Turrax homogenizer (IKA-Werke, GmbH & Co.KG, Staufen, Germany), in 500 µl of assay buffer (10 mM sodium phosphate buffer, 200 mM NaCl, 0.2 % Triton X-100, pH 7.4). We then mixed 10 µl of a 1:5 dilution of homogenate with 40 µl of assay buffer supplemented with (final concentrations) 0.2 mM physostigmine, 2 mM choline and a mixture of 170 µM labeled and unlabeled acetylCoA (final specific radioactivity of about 200 dpm/pmol) in a standard 1.5 ml eppendorf tube and incubated the mixture for 15 min at 37°C. The reaction was stopped by adding 400 µl of ice-cold 10 mM sodium phosphate buffer and subsequently 400 µl of tetraphenylboron dissolved in butyronitrile (10 mg/ml). After being shaken gently for 4 min, the tubes were centrifuged at 3000×g at 4ºC for 4 min to promote the separation of the aqueous and organic phases. 200 µl of the upper organic layer was removed for scintillation counting. All samples were processed in duplicate. For the negative control the parallel incubations and extractions were performed without tissue sample. The activity was expressed as nmol of formed ACh per mg protein in 15 min. The amount of generated ACh was calculated from measured dpm values using specific radioactivity of [^{3}H]-acetyl-CoA.

* Acetylcholinesterase and butyrylcholinesterase activity

Activity of AChE and BChE was determined by Ellman's colorimetric method modified for a 96-well microtiter plate reader (Tecan Sunrise, Tecan Group Ltd, Männedorf, Switzerland)) similarly as previously described (Mrvova et al., 2012). The activity of AChE was assayed with 0.75 mM acetylthiocholine and 0.5 mM 5,5-dithiobis(2-nitrobenzoic acid) (DTNB) in 5 mM HEPES buffer pH 7.5. The total assay volume was 200 µl. The whole brains were homogenized with Ultra Turrax homogenizer (IKA-Werke, GmbH & Co.KG, Staufen, Germany) by 3 pulses of 10 seconds in 15 volumes of cold 0.32 M sucrose. The homogenates were centrifugated at 4˚C for 10 min at 1000×g (Hettich Micro 22R, Andreas Hettich GmbH & Co. KG, Tuttlingen, Germany) to remove cell debris and nuclear fraction. The supernatant was removed and centrifugated for 55 min at 17 000×g to obtain membrane preparation. Supernatant was discarded and the pellet was washed once with cold 50 mM Na/K phosphate buffer ph 7.4, suspended in the same buffer and directly used assays. 10 µg of membrane preparation was preincubated first with DTNB to saturate free sulfhydryl groups and with iso-OMPA (final concentration 0.1 mM) to block BChE activity during 30 min. The activity was measured at 412 nm. BChE activity was assayed as described for AChE except that butyrylthiocholine was used as a substrate and AChE activity was blocked with BW284C51 (final concentration 5 µM). The amount of reaction product was calculated according to the Beer-Lambert law, equation (1).

(1) $A = \varepsilon bc$

where A is absorbance, b is path length in centimeters (cm), c is concentration in moles/liter (M) and ε is molar extinction coeficient in ($M^{-1}cm^{-1}$).

• Radioligand binding

* Radioligand binding assays in membrane preparation

Mice were killed by decapitation. Their brains were immediately removed and dissected in a petri dish placed on ice into Str, Hipp and Cx. The standard weight of both striata, hippocampi and left and right cortices were approximately 26, 22, 75 mg respectively. Dissected brain regions were transfered into eppendorf tubes, flash frozen in the liquid nitrogen and stored at – 80 °C until use.

Pooled individual regions from four or five mice or whole brains were homogenized in glass tubes inserted in to the crushed ice with Ultra-Turrax homogenizer (IKA-Werke, GmbH & Co.KG, Staufen, Germany) by three 10-s pulses in 15 volumes of cold 0.32 M sucrose. The homogenisator was always washed in the buffer between the samples and the homogenates were kept on ice before their processing in centrifuge (Hettich Micro 22R, Andreas Hettich GmbH &

Co. KG, Tuttlingen, Germany). The plasma membrane preparation was prepared as previously described (Li et al., 2003). The homogenates were centrifugated at 4˚C for 10 min at 1000×g to remove cell debris and nuclear fraction. The supernatant was removed and centrifugated at 4˚C for 55 min at 17 000×g to obtain membrane preparation. Supernatant was discarded and the pellet was washed once with cold 50 mM sodium/potassium phosphate buffer pH 7.4, suspended in the same buffer and directly used for binding assay. The protein content was determined in a bicinchoninic acid protein assay according to the manufacturers instructions (Pierce® BCA Protein Assay Kit, Thermo Fisher scientific, Inc., MA, USA).

Total MR was labeled by a slightly modified version of published protocol (Yamamura and Snyder, 1974). 40 µl of plasma membranes were incubated in dublicates in 50 mM potassium phosphate buffer (pH 7,4) in the presence of various concentrations of [^{3}H]-QNB (30 – 1800 pM) in a total volume of 1 ml, for 1.5 h at RT. The nonspecific binding was determined by parallel incubations in the presence of 10 µM atropine sulfate. The reaction was stopped by adding of 3 ml of ice-cold potassium phosphate buffer and immediate vacuum filtration through GF/B glass fiber filters in the Brandel cell harvester (Brandel, Inc., Gaithersburg, MD, USA). Filters were washed 3 times with 3 ml of ice-cold potassium phosphate buffer, to remove the unbound radioligand, and were allowed to dry at RT overnight. Dried filters were transferred to scintillation vials and 10 ml of scintillation cocktail was added. The radioactivity associated with filters was measured by Beckman liquid scintillation counter (Beckamn Coulter, Inc., CA, USA). The specific binding corresponding to radioligand bound to receptors was calculated as the difference in binding in reaction mixtures with and without atropine. Specific binding values were converted into fmol per mg protein by the specific radioactivity constant which represents dpm value per fmol of the parituclar batch of radioligand. To determine dissociation constants (KD) and maximum binding sites (Bmax) data were fit to the equation (2) using non-linear regression (Graphpad Prism, San Diego, USA).

$$B = ([Bmax][L])/([KD]+[L]) \quad (2)$$

where B is the specific binding per mg of protein measured at various concentrations of [^{3}H]-QNB, Bmax is the total amount of receptors per mg of protein, L is concentration of free radioligand, and KD is the dissociation constant.

* Tissue preparation for autoradiography experiments

Mice were killed by cervical dislocation and decapitation. Brains were rapidly removed from the scull, frozen in isopenthane at -30˚C and stored at -80˚C until use. Alternatively brains were put on the piece of parafilm and placed on powdered dry ice in a closed polystyrene box. Before cryosectioning, brains were transferred from -80˚C to -20˚C for 3 h. Coronal brain secions 16 µM thick were cut on a cryostat (Leica CM3050S, Leica Microsystems, Wetzlar, Germany) at -20 ˚C, thaw mounted on Superfrost® Plus glass slides (Carl Roth GmbH & Co. KG, Karlsruhe, Germany) and stored in Rotilabo® storage boxes (Carl Roth GmbH & Co. KG, Karlsruhe,

Germany) at -80˚C until use. The brains were attached to the specimen holder by tissue glue matrix Tissue OCT (Labonord, Templemars, France). For each brain region, four sections were collected on each slide, while each section was 160 µM apart from the previous one to assure the homogenity of samples. For each autoradiography, 6 PRiMA KO and 6 WT mice were analysed.

* General procedure for autoradiography experiments

Each autoradiography procedure consisted of preincubation to remove endogenous ligands, incubation of tissue sections in incubation medium comprising the particular radioligand and from washing tissue sections to remove unbound radioligand from tissue. Sections were processed in plastic mailers fitted to 24-slides holder (Tissue-Tek®, Sakura Finetek). For non-specific binding, sections were processed in a Coplin staining dish for 10 slides (Carl Roth GmbH & Co. KG, Karlsruhe, Germany). Before each autoradiographic assay sections were allowed to thaw and dry for 20 min at RT. Following the washing period slides were immediately placed upright in the drain rack (DrainrackTM Jr., Electron Microscopy Sciences, Hatfield, PA, USA) with tissue sections on the top and dried by gentle stream of cold air.

* Autoradiography of muscarinic receptors

MR were determined as previously described (Wolff et al., 2008). Dried sections were preincubated for 30 min in 50 mM sodium/potassium phosphate buffer (pH 7.4) at RT. Following preincubation sections were transferred into fresh 50 mM sodium/potassium phosphate buffer containing 2 nM [^{3}H]-QNB and incubated for 2 hours at RT. Non-specific binding was assessed in the presence of 10 µM atropine sulfate. Sections were then washed two times for 5 min each in ice-cold buffer and dipped for 2 s in ice-cold water. For labeling of M1 and M2 sections were processed as described for [^{3}H]-QNB except that 5 nM [^{3}H]- pirenzepine and 2 nM [^{3}H]-AFDX384 were used, respectively. Dry sections were apposed to tritium sensitive Fuji BAS imaging plates (GE Healthcare Europe GmbH, Freiburg, Germany) in Kodak Biomax autoradiography cassettes (Carestream Health, Inc., Rochester, NY, USA).

* Autoradiography of β_2 subunit containing nicotinic receptors

Labeling of β2 subunit of NRs was done as previously published (Perry and Kellar, 1995). Following three 5 min preincubations in Tris-ions buffer (50 mM Tris-HCl buffer pH 7.4 containing 120 mM NaCl, 5 mM KCl, 2 mM CaCl2, 1 mM MgCl2) sections were incubated in the fresh Tris-ions buffer with 0.4 nM [^{125}I]-epibatidine for 40 min at RT. Non-specific binding was determined in the presence of 300 µM nicotine. After the incubation, sections were washed twice for 5 min each in ice-cold Tris-ions buffer and rinsed in ice-cold water for 2 s. Dried sections were exposed to Biomax MR films (Carestream Health, Inc., Rochester, NY, USA) in Kodak Biomax

autoradiography cassettes (Carestream Health, Inc., Rochester, NY, USA).

* Autoradiograpphy of α_7 nicotinic receptors

Labeling of α7 NRs was performed according to published protocol (Spurden et al., 1997). Sections were preincubated for 30 min in 50 mM Tris-HCl buffer supplemented with 0.1% bovine serum albumin, pH = 7.4. Sections were then incubated in the fresh buffer containing 0.5 nM [^{125}I]-α-bungarotoxin for 2 hours at RT. For non-specific labeling 1 mM nicotine was included in the reaction mixture. Sections were washed four times for 10 min each in ice-cold 50 mM Tris-HCl buffer, pH = 7.4, rinsed in ice-cold water for 2 s and dried. Dried sections were exposed to Biomax MR films (Carestream Health, Inc., Rochester, NY, USA) in Kodak Biomax autoradiography cassettes (Carestream Health, Inc., Rochester, NY, USA).

* Autoradiography of D_1 dopaminergic receptors

The relative density of D1 receptors was examined according to Fernagut et al. (2003) (Fernagut et al., 2003). Following preincubation in Tris-ions buffer (50 mM Tris-HCl, containing 120 mM NaCl, 5 mM KCl, 2 mM CaCl2, 1 mM MgCl2, pH 7.4) for 20 min at RT, sections were incubated in fresh Tris-ions buffer in the presence of 3 nM [^{3}H]-SCH23390 for 90 min at RT. To define the non-specific binding of [^{3}H]-SCH23390, sections were incubated in the presence of 10 µM butaclamol. Sections were then rinsed four times in ice-cold Tris-ions buffer for 5 min each, quickly rinsed in ice-cold water and dried. Dry sections were apposed to tritium sensitive Fuji BAS imaging plates (GE Healthcare Europe GmbH, Freiburg, Germany) in Kodak Biomax autoradiography cassettes (Carestream Health, Inc., Rochester, NY, USA).

* Autoradiography of D_2 receptors

D2 receptor autoradiography was done as described previously (Martres et al., 1985). We pre-incubated brain sections three times for 5 min each at RT in Tris-ions buffer buffer (50 mM Tris-HCl buffer pH 7.4 containing 120 mM NaCl, 5 mM KCl, 2 mM CaCl2, 1 mM MgCl2) supplemented with 0.1 % bovine serum albumin and 0.57 mM ascorbic acid. Sections were then incubated for 60 min at RT in the fresh buffer containing 0.2 nM [^{125}I]-iodosulpride. Non-specific binding was dermined in the presence of 10 µM apomorphine. The stock solution of apomorphine was freshly prepared in 5 mM ascorbic acid. Sections were then rinsed 4 times in ice-cold Tris ions buffer for 5 min each, quickly rinsed in ice-cold water and dried. Dried sections were exposed to Biomax MR films (Carestream Health, Inc., Rochester, NY, USA) in Kodak Biomax autoradiography cassettes (Carestream Health, Inc., Rochester, NY, USA).

* Autoradiography of vesicular acytylcholine transporter

Autoradiographic labeling of VAChT was performed essentialy as previously described (Albin et al., 1994). Sections were pre-incubated in phosphate-buffered saline containing EDTA (137 mM NaCl, 3 mM KCl, 8 mM Na2HPO4, 1.5 mM KH2PO4, 1 mM EDTA, pH 7.4) for 5 min at RT. Sections were then incubated in the fresh buffer with 20 nM [^{3}H]-vesamicol for 60 min at RT. Non-specific binding was determined in the presence of 100 µM unlabelled vesamicol. After incubation sections were washed two times for 2 min each in ice-cold buffer and rapidly dipped in ice-cold water. Dry sections were apposed to tritium sensitive Fuji BAS imaging plates in Kodak Biomax autoradiographic cassettes.

* Autoradiography of high-affinity choline transporter

ChT was labeled according to previously published protocol (Araki et al., 2000) with slight modifications. Sections were preincubated for 5 min at RT in 50mM Gly-Gly buffer containing 200 mM NaCl, pH adjusted with 1M NaOH to 7.8. Sections were then incubated in the fresh buffer containing 10 nM [^{3}H]-hemicholinium-3 without or with an excess of unlabelled hemicholinium-3 (10µM) to determine total and non-specific binding sites respectively. Following incubation sections were rinsed twice for 2 min each in ice-cold buffer and rinsed in ice-cold water for 2 s. Dry sections were apposed to tritium sensitive Fuji BAS imaging plates (GE Healthcare Europe GmbH, Freiburg, Germany) in Kodak Biomax autoradiography cassettes (Carestream Health, Inc., Rochester, NY, USA).

* Autoradiography of kainate receptors

Autoradiographic labeling of kainate receptors was done as previously described (Ayata et al., 1997). Following preincubation three times for 15 min each at RT in 50 mM Tris-acetate buffer, pH 7.4 sections were incubated in fresh Tris-acetate buffer in the presence of 12 nM [^{3}H]-kainate. The incubation lasted for 45 min at 4˚C. Non-specific binding was determined in the presence of 1 µM unlabelled kainate. Sections were then washed three times for 10 s each in ice-cold buffer, rapidly dipped in ice-cold water, dried and exposed to tritium sensitive Fuji BAS imaging plates (GE Healthcare Europe GmbH, Freiburg, Germany) in Kodak Biomax autoradiography cassettes (Carestream Health, Inc., Rochester, NY, USA).

* Autoradiography of NMDA receptors

Autoradiographic procedure for labeling of NMDA receptors was adopted from Ayata et al. (1997). Sections were preincubated three times for 15 min each in 50 mM TRIS HCl buffer, pH 7.4 and then incubated in the same buffer in the presence of 5 nM [^{3}H]-CGP-39653 for 60 min at RT. Non-specific binding was determined in the presence of 100 µM glutamate. Following

incubation sections were washed four times for 15 s each in ice-cold buffer, dipped in ice-cold water, dried and exposed to tritium sensitive Fuji BAS imaging plates (GE Healthcare Europe GmbH, Freiburg, Germany) in Kodak Biomax autoradiography cassettes (Carestream Health, Inc., Rochester, NY, USA).

* Autoradiography of AMPA receptors

Autoradiographic procedure for labeling of AMPA receptors was adopted from Ayata et al. (1997). Following preincubation three times for 15 min each at RT in 50 mM Tris-acetate buffer containing 100 mM KSCN and 2.5 mM CaCl2, pH 7.3 sections were incubated for 45 min at 4˚C in fresh buffer containing 9 nM [^{3}H]-AMPA. For non-specific binding 1 mM glutamate was added to the incubation mixture. Slides were washed three times for 10 s each in ice-cold buffer, rapidly dipped in ice-cold water and dried. Dried section were exposed to tritium sensitive Fuji BAS imaging plates (GE Healthcare Europe GmbH, Freiburg, Germany) in Kodak Biomax autoradiographic cassettes (Carestream Health, Inc., Rochester, NY, USA).

* Autoradiography of $GABA_A$ receptors

GABAA receptors were labeled according to previously published protocol (Dean et al., 1999). Sections were preincubated three times for 5 min each at 4˚C in 50 mM Tris-citrate buffer, pH 7.1 and subsequently incubated for 60 min at 4˚C in fresh buffer containing 10 nM [^{3}H]-muscimol. Non-specific binding was assessed in the presence of 10-5M SR-95531. Following 1 min wash in ice-cold buffer, sections were rapidly in-out dipped in ice-cold water and dried. Dried section were exposed to tritium sensitive Fuji BAS imaging plates (GE Healthcare Europe GmbH, Freiburg, Germany) in Kodak Biomax autoradiographic cassettes (Carestream Health, Inc., Rochester, NY, USA).

* Quantification of receptor density

To assure the linearity of the signal, autoradiographic standards (GE Healthcare Europe GmbH, Freiburg, Germany; American Radiolabeled Chemicals, Inc., St. Louis, MO, USA) were exposed along with the samples to the screens and films. The films were developed in Kodak X-ray GBX developer (VWR International, LLC, Radnor, PA, USA) for 5 min, rinsed in water, fixed in Kodak X-ray GBX fixer (VWR International, LLC, Radnor, PA, USA) for 5 min and rinsed in water for 10 min. The film autoradiograms were scanned and the densitometry was done with PC based analytical software, MCID analysis software (InterFocus GmbH, Mering, Germany). Imaging plates were processed in Typhoon FLA 7000 biomolecular imager (GE Healthcare Europe GmbH, Freiburg, Germany) or Fuji Bioimaging Analyzer BAS-5000 (FUJIFILM corporation, Tokio, Japan) and digitized images analysed with MCID analysis software. Measurements were taken and averaged from four sections for each animal and brain region.

* Pharmacological studies

Pilocarpine was dissolved in the physiological saline and injected itraperitonealy to the mice in the dose 200 mg/kg. Mice were observed for generation of tonic clonic seizures for 1 hour following drug application. The fresh stock solution of pilocarpine was prepared prior to each experiment (Li et al., 2003). We measured behavioral responses to drug application with a telemetry system (Respironics, USA). The transponders (E-Mitter, G2-HR) were implanted in the peritoneal cavity of mice under anesthesia induced either by injection of a xylazine/tiletamine/zolazepam mixture (Zoletil® 100, Ronetar® 2% 5:1, diluted 1:10, 3.2 ml/kg), or with isofluorane. Mice were allowed to recover from surgery for one week before their use in experiments. Temperature and activity measurements were acquired directly from the transponders by receivers connected in series and to a single port of a PC.

On the day of the experiment, cages with individual mice were placed over the corresponding receivers for at least three hours before drug application. Mice of various genotypes received subcutaneous or intraperitoneal injections of oxotremorine (0.2 mg/kg), scopolamine (0.05 mg/kg or 0.5 mg/kg) or donepezil (2 mg/kg or 10 mg/kg) dissolved in physiological saline or vehicle. Data were collected every 60 seconds for three hours before the injection and then for another 20 hours after the injection. VitalView and GraphPad were used for data analysis. The hypothermic effect of oxotremorine injection was evaluated by calculating the minimal temperature over a period of 10 minutes and the duration of hypothermia (the period for which temperature was below 34°C).

* Statistical analysis

Most of the data from behavioral tests were not normally distributed (checked with the Kolmogorov-Smirnov test). We used Mann-Whitney tests for comparisons of PRiMA KO and WT mice. To assess the change of parameters between two measurements in one group of mice we used the Wilcoxon matched pairs test. In all cases, $p<0.05$ was considered to indicate statistical significance. For developmental studies, the statistical differences among groups were determined by two-way analysis of variance (ANOVA): for multiple comparisons an adjusted t-test modified SNK (Student-Newman-Keuls) correction was used. Otherwise, we used Student's t test and significance was defined as $p<0.05$. Values are expressed as means±SEM.

• RESULTS

• Nearly unchanged behavioral phenotype of PRiMA KO mice

As opposed to AChE KO mice, PRiMA KO mice are indistinguishable from WT mice through visual inspection. We have never observed a trait that could distinguish PRiMA KO mice from WT mice during housing or handling of mice. In particular, the seizures commonly observed in AChE KO mice due to the discomforts, have never been noticed in PRiMA KO mice. Therefore, we explored the possible changes in behavior of PRiMA KO mice by subjecting mice to a battery of behavioral tests, focusing on motor evaluations and spatial learning.

* PRiMA KO and WT mice have similar locomotor activity in the open-field

We examined spontaneous locomotor activity of PRiMA KO and WT mice at the exploratory and habituated phases in the open-field test. The general locomotor activity of PRiMA KO mice did not differ from WT mice neither at the novel environment (day1) nor at the familiar environment (day2) (Fig. 8). The time spent in the center which reflects the level of anxiety was not different between PRiMA KO and WT mice at both phases of open-field test (Fig. 8).

* Static and dynamic parameters of the gait are nearly unchanged in PRiMA KO mice

AChE KO mice display abnormal posture and gait. We analyzed in detail the static and dynamic parameters of the gait in PRiMA KO and WT mice by automated gait analysis system. Individual evaluated gait parameters are shown and compared between PRiMA KO and WT mice in table 1. PRiMA KO mice showed significantly longer time between the initial and maximal contact of the fore paws, longer swing duration of both fore and hind paws, lower swing speed of both fore and hind paws and shorter distance between fore and hind paw print position (significant only for right paws).

In contrast to AChE KO mice (Duysen et al., 2002a), the gait of PRiMA KO mice is largely intact, albeit slight differences can be observed when detailed analysis is applied.

* Reduced motor skill performance but intact motor skill learning in PRiMA KO mice

We performed a rotarod test and hanging wire test to examine whether absence of PRiMA

affects the ability to acquire motor skill performance and learning.

In the rotarod test, WT mice reached significantly longer fall latencies than PRiMA KO mice on the first day (p=0.0079) (Fig. 9). During next two days both WT and PRiMA KO mice showed marked increase of latencies (day 1 vs. day 3 – WT: p=0.0156; KO: p=0.002). The mean increase of the latencies (D3/D1) was 8.14 ± 2.43 in PRiMA KO mice while in WT mice it was only 2.03 ± 0.47 and the difference was statistically significant (p=0.0247). Therefore on the second and third day PRiMA KO mice reached similar latencies as WT mice.

In the hanging wire test, WT mice reached significantly longer fall latencies than PRiMA KO mice on the first (p=0.003) and third day (p=0.0373) (Fig. 9). PRiMA KO mice showed significant increase of latencies (day 1 vs. day 3, p=0.0488) but not WT mice (day 1 vs. day 3, p=0.0977). The mean increase of the latencies (D3/D1) was 2.49 ± 0.68 in PRiMA KO mice and in WT mice it was only 2.15 ± 0.43 The difference in mean increase of the latencies was statistically insignificant (p=0.9025). Therefore on the third day, PRiMA KO mice reached shorter latencies than WT mice.

These results indicate that the motor performance of PRiMA KO mice is impaired by absence of PRiMA. However the ability to acquire motor skill learning appears to be higher (rotarod) or intact (hanging wire test) in PRiMA KO mice.

* Intact spatial learning ability in PRiMA KO mice

In MWM, both PRiMA KO and WT mice showed learning ability. The escape latencies and trajectory lengths shortened during the course of the experiment in both WT and PRiMA KO mice (day 1 (D1) vs. day 10 (D10) – WT latency: p=0.0039, WT trajectory: p=0.0039, KO latency: p=0.0098, KO trajectory: p=0.00998).

There were no significant differences in escape latencies and trajectory length between PRiMA KO and WT mice (Fig. 10). On the first day of the water maze test, WT mice showed slightly higher swimming speed than PRiMA KO mice (p=0.0373) (Fig. 10). The ratio between escape latency on D10 and D1 of MWM test was 0.53 ± 0.11 in PRiMA KO mice and 0.38 ± 0.08 in WT mice. For trajectory length, the ratio was 0.54 ± 0.12 in PRiMA KO mice and 0.34 ± 0.07 in WT mice. The differences between PRiMA KO and WT mice were statistically insignificant.

In the probe trial, mean time spent in the maze quadrant in which the platform was originally localized was 25.34 s ± 1.94 s in PRiMA KO mice and 29.56 s ± 1.78 s in WT mice. Mean distance to the platform center was 33.07 cm ± 2.02 cm in PRiMA KO mice and 29.55 cm ± 1.35 cm in WT mice. The differences between PRiMA KO and WT mice in the probe trial were statistically insignificant. In the visible-platform acquisition training, escape latencies, trajectory length and swimming spees of PRiMA KO mice was comaprable to WT mice (Fig. 10).

* Increased ACh levels in striatum of PRiMA KO and AChE del E5+6 mice

In vivo microdialysis revealed that striatal ACh levels are 200-300 times increased in PRiMA KO and AChE del E5+6 mice in comparison to WT mice (Fig. 11) Detailed methodological approach and estimated concentrations of ACh in perfusate taken from Str of PRiMA KO, AChE delE5+6 and WT mice are provided in Suppl. 1.

* Altered muscarinic receptors in PRiMA KO and AChE del E5+6 mice

In vitro and in vivo data have firmly demonstrated that the excess of endogenous neuromediators or prolonged stimulation by exogenous ligands results in reduced abundance and availability of MR and other GPCR. Therefore, we examined the response of MR to the excess of ACh in PRiMA KO and AChE del E5+6 mice by means of the radioligand binding assays. We also tested the functional state of MR in PRiMA KO and WT mice by measuring the physiological responses to the different MR ligands.

- *PRiMA KO mice have markedly reduced muscarinic binding sites in striatal, cortical and hippocampal plasma membrane preparations*

In the first step, we examined the density of total MR binding sites in membrane preparations derived from Str, Hipp and Cx by direct labeling of MR with MR antagonist [^{3}H]-QNB, which labels all five MR subtypes. In a series of saturation bindings we determined the maximal [^{3}H]-QNB binding sites (Bmax) and affinity of [^{3}H]-QNB to MRs (dissociation constant, Kd). In all three brain regions examined, Bmax was significantly reduced in PRiMA KO mice. The specific [^{3}H]-QNB binding sites in PRiMA KO mice were reduced by 48% in Hipp, by 52% in Str and by 39% in Cx. There was no statistically significant difference in Kd for [^{3}H]-QNB binding between PRiMA KO and WT mice in all three brain areas tested. The representative saturation binding curves of [^{3}H]-QNB binding in Str, Hipp and Cx of PRiMA KO and WT mice are shown in Fig. 12. Because the dissociation constants for [^{3}H]-QNB do not differ between PRiMA KO and WT mice, we can conclude that the decreases in [^{3}H]-QNB binding sites in PRiMA KO mice reflect the decreased densities of total MR and not the change in affinity of MR to [^{3}H]-QNB. For details of binding data see Suppl. 1.

- *Reduction of muscarinic binding sites throughout the whole brain in PRiMA KO mice*

To map adaptation of MR in a more detail we performed autoradiography in coronal brain sections with [^{3}H]-QNB. In addition, we labeled adjacent coronal brain section with [^{3}H]-NMS, which is an another MR antagonist with high affinity to all MR subtypes. Typical autoradiograms and quantitated data of [^{3}H]-QNB binding in coronal brain sections in PRiMA KO and WT mice

are presented in figure 13 and table 2. The non-specific binding was barely visible. The relative quantity of [^{3}H]-QNB binding sites in PRiMA KO mice was significantly reduced in comparison to WT mice in all brain regions analyzed. Consistent with [^{3}H]-QNB labeling, the relative density of [^{3}H]-NMS binding sites was also reduced in PRiMA KO mice when compared to WT mice. Typical autoradiograms and quantitated data of [^{3}H]-NMS binding in coronal brain sections of PRiMA KO and WT mice are presented in figure 14 and table 3. The non-specific binding was barely visible. The relative density of [^{3}H]-NMS binding sites was not different from the relative density of [^{3}H]-QNB binding sites both in PRiMA KO and WT mice.

- ***Enhanced scopolamine-induced locomotor activity***

SCO is a nonselective MR antagonist which induces hyperlocomotion in rodents. AChE KO mice are more sensitive to SCO-induced locomotion at a dose 0.05 mg/kg, presumably due to the reduced functional levels of MR, but not at a dose 0.5 mg/kg (Volpicelli-Daley et al., 2003a). We recorded the locomotor activity in PRiMA KO and WT mice in the open-field conditions following SCO injection at two doses (0.05 and 0.5 mg/kg, i.p.). At both doses, PRiMA KO mice were much more active than WT mice (Fig. 15). Following i.p. injection of SCO at a dose 0.05 mg/kg the locomotor activity of WT mice was not statistically different from saline injection. By contrast, the locomotor activity of PRiMA KO mice was enhanced by 198% when compared to saline injection. At a dose 0.5 mg/kg SCO enhanced locomotor activity both in PRiMA KO and WT mice in comparison to saline injection. While in WT mice the locomotor activity was increased only by 116%, in PRiMA KO mice it was increased by 514%. For more detailed data see Suppl. 1.

- ***Decreased oxotremorine-induced hypothermia***

OXO is a centrally acting, nonselective MR agonist that among other effects induces in normal mice hypothermia in a dose dependent manner. In both PRiMA KO and WT mice, subcutaneous injection of OXO at a dose 0.2 mg/kg induced hypothermia. However, the hypothermia in PRiMA KO mice was markedly reduced when compared to WT mice (Fig. 16). For more detailed data see Suppl. 1.

- ***Resistance to pilocarpine-induced epileptic seizures***

PIL is a nonselective MR agonist that at high doses induces epileptic-like seizures in rodents via activation of M1. PRiMA KO (n=18) and WT (n=18) mice received single i.p. injection of PIL at a dose 200 mg/kg and were observed for generalized tonic-clonic seizures for 60 min. 15 of the WT mice experienced seizures, whereas only 4 of the PRiMA KO mice experienced seizures. In contrast to WT mice which survived the treatment, albeit remained moribund, all PRiMA KO mice which developed generalized seizures died during the seizures.

- ***Unusual responsiveness to atropine***

In the brain of AChE KO mice, MR are almost absent on the plasma membrane - the major site of MR distribution in WT mice - and are trapped inside the cell bodies of neurons as revealed by immunoflourescence (Volpicelli-Daley et al., 2003a, 2003b). When AChE KO mice were injected 3 times during 90 min with atropine (ATR), a nonselective MR antagonist which passes through the blood-brain-barrier, MR immunoreactivity redistributed from intracellular compartments to the plasma membrane (Volpicelli-Daley et al., 2003a, 2003b). However, the behavioural responses to ATR treatment have not been described in a more detail. In PRiMA KO mice, MR are reduced and redistributed similarly to that of AChE KO mice (Dobbertin et al., 2009). Therefore, we examined behavioural responses of PRiMA KO and WT mice to the repeated injection of ATR at a dose and time interval similar to those used in AChE KO mice. For this experiment, PRiMA KO and WT mice were endowed with telemetric probes which measure simultaneously temperature, gross motor activity and heart rate.

As opposed to SCO, ATR has very low potency to enhance spontaneous locomotion in rodents (Sipos et al., 1999). The overall locomotor activity of saline treated WT mice (WT-sal) was 1065±195 and the activity of WT mice treated with ATR (WT-ATR) at a dose 6 mg/kg was 1401±250, but the difference was statistically insignificant. In contrast to WT mice, PRiMA KO mice showed strong locomotor response to injections of ATR (Fig. 17). While the locomotor activity of saline treated PRiMA KO mice was 890±117, the activity of ATR injected PRiMA KO mice was 3702±405 (Fig. 17). PRiMA KO displayed also different responses to ATR injections in terms of core body temperature. In WT mice, ATR had no significant effects on core body temperature (Fig. 17). However, PRiMA KO mice responded to the second ATR injection by rapid decline of core body temperature, which continued following the third ATR injection (Fig. 17).

WT and PRiMA KO mice also appeared to have different responsivenes to ATR in terms of heart rate (HR). In WT mice, each ATR injection was followed by temporal increase of HR, albeit not statistically significant (Fig. 17). In PRiMA KO mice, the response to the first injection of ATR resembled that of WT mice. Interestingly, the second and third ATR injections had any noticable effect on HR (Fig. 17). Future studies on larger mice groups are required to verify significance of ATR effect on HR.

- ***Reduction of MR binding sites throughout the whole brain both in PRiMA KO and AChE delE5+6 mice***

Both PRiMA KO and AChE delE5+6 mice have high levels of ACh, vastly exceeding levels of ACh in WT mice. Therefore, we explored the adaptation of MR also in AChE del E5+6 mice. The relative density of total MR was determined by autoradiography with [^{3}H]-QNB. To compare the relative densities of central MR in WT, PRiMA KO and AChE delE5+6 mice, we processed the brain sections of all three mouse strains simultaneously. In addition to [^{3}H]-QNB, we labeled MR in coronal brain sections with [^{3}H]-pirenzepine and [^{3}H]-AFDX384, which are commonly used to

determine the density of M1 and M2, respectively. The specific binding of the three radioligands in AChE delE5+6 mice was significantly reduced when compared to WT mice in all brain areas tested (Fig. 18, 19, 20), tables 4-6.. The reduction of the relative MR densities in AChE del E5+6 was comparable to that of PRiMA KO mice (Fig. 18, 19, 20), tables 4-6..

* Slight changes to nicotic receptors in PRiMA KO mice

We explored the possible adaptation of NRs to the absence of PRiMA and excess of ACh (Fig. 11) by assessing the relative density of β2 and α7 NR subunits in the brain of PRiMA KO and WT mice and by analyzing the functional responses of NR at the motoneuron-Renshaw cell synapse.

We performed β2 and α7 NR subunit autoradiography in coronal brain sections from PRiMA KO and WT mice. β2 and α7 NR subunits were labeled with [^{125}I]-epibatidine (Fig. 21) and [^{125}I]-α-bungarotoxin (Fig. 22), respectively. As opposed to dramatic reduction of MR, the relative density of β2 and α7 NR subunits was slightly altered. The relative densities of [^{125}I]-epibatidine specific binding sites in PRiMA KO mice were significantly reduced by 7% - 20% in the majority of brain regions examined (table 7). By contrast, the relative densities of [^{125}I]-α-bungarotoxin specific binding sites were similar in PRiMA KO and WT mice in most brain regions tested, with the exception of CA1 field of Hipp, where the binding was significantly reduced by 19% (table 8).

Despite the absence of AChE and excess of ACh, NRs at the motoneuron-Renshaw cell synapse are functional and mediate the fast synaptic responses (Fig. 23). For precise description of functional analysis of NRs see Suppl. 1.

* Lack of changes in presynaptic cholinergic markers

In the brain of AChE KO mice, the activity of ChAT - ACh synthesizing enzyme - and protein expression of VAChT, which concentrates ACh into the vesicles are unchanged (Volpicelli-Daley et al., 2003a). However, the activity and protein expression of ChT, which supplies Ch for ACh synthesis, are up-regulated (Hartmann et al., 2008; Volpicelli-Daley et al., 2003a). We examined possible changes in the activity of ChAT and ChT as well as the relative density of ChT and VAChT in different brain regions in PRiMA KO mice.

- *Unchanged activity and abundance of ChT*

We measured the uptake of [^{3}H]- choline (HACU) in synaptosomal preparations from Str, Hipp and Cx of PRiMA KO and WT mice. The activity of ChT was similar in PRiMA KO and WT mice in all three brain regions tested (Fig. 24). HACU was expressed as uptake of [^{3}H]- choline (fmol) by one mg synaptosomal protein in 1 min. In striatal synaptosomes, the mean HACU ± SEM was determined as 276.6±27.8 in PRiMA KO (n=15) and 244.3±14.3 in WT mice (n=15).

In hippocampal synaptosomes, HACU was determined as 85.3±5.5 in PRiMA KO (n=15) and 88.2±5.4 in WT mice (n=15). In cortical synaptosomes, HACU was determined as 53.8±3.7 in PRiMA KO (n=15) and 54.0±3.1 in WT mice (n=15). The differences between genotypes were statistically insignificant.

We determined the relative density of ChT in PRiMA KO and WT mice by autoradiography with [^{3}H]-hemicholinium-3. Representative autoradiograms and densitometry analysis of [^{3}H]-hemicholinium-3 binding in coronal brains sections are shown in Fig. 25 and table 9. The density of specific binding sites of [^{3}H]-hemicholinium-3 was similar in PRiMA KO and WT mice in all brain areas tested.

- ***Unchanged activity of ChAT***

We assessed the activity of ChAT in striatal, cortical and hippocampal homogenates from PRiMA KO and WT mice by radioassay with the substrate [^{3}H]-acetyl-CoA. In all brain regions tested, the activity of ChAT in PRiMA KO was comparable to WT mice (Fig, 26). ChAT activity was expressed as amount of newly formed ACh (nmol) by one mg protein of homogenate in 15 min. In striatal homogenates, the mean ChAT activity ± SEM was determined as 49.6±3.2 in PRiMA KO (n=8) and 55.8±4.4 in WT mice (n=8). In hippocampal homogenates, ChAT activity was 16.5±0.6 in PRiMA KO (n=8) and 18.0±0.6 in WT mice (n=8). In cortical homogenates, ChAT activity was 14.4±0.7 in PRiMA KO (n=8) and 15.4±0.3 in WT mice (n=8). The differences between PRiMA KO and WT mice were statistically insignificant.

- ***Unchaged density of VAChT***

We determined the abundance of VAChT in various brain regions of PRiMA KO and WT mice by means of autoradiography with [^{3}H]-vesamicol. Representative autoradiograms [^{3}H]-vesamicol in coronal brain sections are shown in Fig 27. and densitometry analysis is presented in table 10. The relative density of [^{3}H]-vesamicol specific binding in PRiMA KO mice was not significantly different from WT mice in all brain areas examined.

* Unchanged abundance of noncholinergic receptors in PRiMA KO mice

The central cholinergic pathways are widespread and target virtually all brain areas. ACh has been shown to modulate and interact with different neurotranmsitter systems including GABAergic, glutamatergic and dopaminergic. Therefore, we explored the possiblity that adaptation of brain of PRiMA KO mice also could recruit other receptor systems, not only cholinergic receptors. We determined the relative abundance of glutamatergic- AMPA, Kainate and NMDA receptors, GABAA receptors and dopaminergic- D1 and D2 receptors by autoradiography with respective radioligands.

- ***Autoradiography of glutamatergic receptors***

We determined the relative density of NMDA, AMPA and Kainate receptors in PRiMA KO and WT mice by autoragiography with [^{3}H]-CGP-39653, [^{3}H]-AMPA and [^{3}H]-kainate respectively.

- ***[^{3}H]CGP-39653 autoradiography***

Representative autoradiograms and densitometry analysis of [^{3}H]-CGP39653 binding in coronal brain sections of PRiMA KO and WT mice are shown in fig. 28 and table 11. The density and autoradiographic distribution of [^{3}H]-CGP-39653 binding sites was similar as previously reported (Ayata et al., 1997; Standley, 1999). [^{3}H]-CGP-39653 binding sites in PRiMA KO mice were not statistically different from WT mice in any brain region analyzed.

- ***[^{3}H]AMPA autoradiography***

Representative autoradiograms and densitometry analysis of [^{3}H]-AMPA binding in coronal brain sections of PRiMA KO and WT mice are shown in fig. 29 and table 12. The relative density and autoradiographic distribution of [^{3}H]-AMPA binding sites was similar as previously reported (Ayata et al., 1997; Boer et al., 2010). [^{3}H]-AMPA binding sites in PRiMA KO mice were not statistically different from WT mice in any brain region analyzed.

- ***[^{3}H]kainate autoradiography***

Representative autoradiograms and densitometry analysis of [^{3}H]-kainate binding in coronal brain sections of PRiMA KO and WT mice are shown in fig. 30 and table 13. The relative density and autoradiographic distribution of [^{3}H]-kainate specific binding sites was similar as previously reported (Ayata et al., 1997; Boer et al., 2010). [3H]-kainate binding sites in PRiMA KO mice were not statistically different from WT mice in any brain region analyzed.

- ***Autoradiography of GABAA receptors***

We determined the relative density of GABAA receptors in PRiMA KO and WT mice by autoradiography in coronal brain sections with [^{3}H]-muscimol. The relative density and autoradiographic distribution of [^{3}H]-muscimol specific binding sites was similar as reported previously (An et al., 2004). Representative autoradiograms and densitometry analysis of [^{3}H]-muscimol binding in coronal brain sections of PRiMA KO and WT mice are shown in fig. 31 and table 14. There were no significant differences in the relative density of [^{3}H]-muscimol specific binding sites between PRiMA KO and WT mice in analyzed brain areas.

- ***Autoradiography of dopaminergic receptors***

We examined the relative density of D1 and D2 dopaminergic receptors in dopamine rich areas of PRiMA KO and WT mice by autoradiography with [^{3}H]-SCH-23390 and [^{125}I]-iodosulpride, respectively. Typical image scans of total [^{3}H]-SCH-23390 and [^{125}I]-iodosulpride binding to the coronal brain sections of PRiMA KO and WT mice are presented in fig. 32 and fig. 33. The quantitated data of [^{3}H]-SCH-23390 specific binding are shown in table 15. The densitometry analysis of [^{125}I]-iodosulpride specific binding is presented in table 16. The relative density of specific binding sites of both radioligands did not differ between the two genotypes.

* Developmental regulation of MR abudance and ChE activity in PRiMA KO and WT mice

Our biochemical analysis focused on the key proteins involved in cholinergic transmission. In addition, we explored the possible alteration of noncholinergic receptors. The most obvious adaptation that we identified concerns MR. Therefore, we next addressed the ontogenetic development of MR abundance in PRiMA KO and WT mice. For this purpose we determined the density of total MR in plasma membranes derived from whole brains of PRiMA KO and WT mice at different ages –embryonic day 18.5 (E18.5), day of birth (P0) and postnatal days 9, 30, 120 and 425 (P9, P30, P120, P425) . In parallel we determined activity of AChE and BChE.

- ***Lack of ontogenic increase of AChE activity in the brain of PRiMA KO mice***

The AChE activity in PRiMA KO mice was reduced by 49% on embryonal day 18.5, albeit the difference was not statistically significant. From P0, AChE activity was significantly higher in WT than in PRiMA KO mice in which the activity remained unchanged from E18.5 till P425 (Fig. 34). On P425, AChE activity in PRiMA KO mice was reduced by 96% in comparison to WT mice. In WT mice, AChE activity rapidly increased till P30. Further increase of AChE activity in WT mice, albeit less marked, was measurable between P30 and P120. On P425 AChE activity in WT mice did not differ from P120 indicating that after P120 AChE activity remains stable.

- ***Postnatal reduction of BChE activity in the brain of PRiMA KO mice***

In WT mice, BChE activity decreased (Fig. 34) from E18.5 to P9 and then increased steeply until P120 and remained unchanged thereafter. By contrast, in PRiMA KO mice, BChE activity showed decline until P30 when it was reduced by 58% when compared to WT mice. On P120 and P425, BChE activity in PRiMA KO mice was not significantly different from P30, but represented less then 30% of BChE activity in WT mice.

- ***Postnatal reduction of the density of MR in the brain of PRiMA KO mice***

The ontogeneic development of the total number of MR binding sites (Fig. 35) copied the development of AChE activity (Fig. 34) and the gradual increase in the density of MR was similar as described previously (Zhu et al., 1996). In WT mice, density of MR increased steeply up to P30 and then less dramatically up to P120. In PRiMA KO mice, the ontogenic increase of MR density was similar to WT mice. However, the maximal density of MR was reached on P30. Despite the similar pattern of age-related increase in density of MR in PRiMA KO and WT mice, the abundance of MR in PRiMA KO mice was significatnly lower on P9, P30, P120 and P425. In PRiMA KO mice, the density of total MR binding sites in plasma membranes prepared from whole brains was reduced by 12% on P0, by 18% on P9, by 42% on P30, by 49% on P120 and by 49% on P425. Except for P0, the differences between PRiMA KO and WT mice were statistically significant.

* PRiMA KO mice are sensitive to donepezil-induced hypothermia

Among other effects, AChE inhibitors can induce hypothermia in WT mice, which is considered to result form the inhibition of AChE in the brain (Clement, 1993; Dronfield et al., 2000). Donepezil, a selective AChE inhibitor, induces hypothermic responses in WT mice, but not in AChE KO mice. We explored the site of donepezil-induced hypothermia by comparing the hypothermic responses in WT mice with mice strains with particular deficits of AChE (PRiMA KO, AChE del E5+6, ColQ KO mice). Unexpectedly, in PRiMA KO mice , donepezil at a dose 2 and 10 mg/kg induced hypothermic responses comparable to that seen in WT mice. By contrast, ColQ KO mice showed faster recovery from, and AChE del E5+6 mice were partially resistant to, hypothermia induced by donepezil at a dose 10 mg/kg (Fig. 36). The altered responsivennes of ColQ KO and AChE del E5+6 mice to donepezil-induced hypothermia became obvious at a dose 2 mg/kg. While in PRiMA KO and WT mice, donepezil at a dose 2 mg/kg induced similar hypothermia, in ColQ KO and AChE del E5+6 mice, injection of donepezil did not affect the core body temperature (Fig. 36). Detailed data are provided in Supl. 1.

• DISCUSSION

• Behaviour

As was previously reported by Dobbertin et al. PRiMA KO mice do not show any apparent phenotypical difference. (Dobbertin et al., 2009). Here we addressed the question if a more detailed analysis would reveal significant behavioural impairments in PRiMA KO mice. For this purpose, we subjected PRiMA KO mice to a battery of behavioural tests to examine their spontaneous locomotor activity, gait, motor skill learning, and spatial reference memory. We selected behavioural tests based on the previous reports showing alteration caused by the compromised cholinergic signaling in at least one of the examined behavioural parameters (Beeri et al., 1995; de Castro et al., 2009b; Conner et al., 2003; Duysen et al., 2002a; Erb et al., 2001; Gomeza et al., 1999a; Kitabatake et al., 2003; Miyakawa et al., 2001).

We explored the spontaneous locomotor activity of PRiMA KO mice using an open field conditions in two consecutive days to distinguish the exploratory and habituated activity. The increased spontaneous locomotion was noticed, for instance, in AChE Tg mice (Beeri et al., 1995), following cholinergic cell ablation in striatum (Kitabatake et al., 2003), or in mice devoid of M1 (Miyakawa et al., 2001) or M4 (Gomeza et al., 1999a). The increased locomotor activity is also commonly observed following aplication of MR antagonists (Shapovalova et al., 2005; Sipos et al., 1999). In addition, the strong involvement of cholinergic signaling in locomotion is indicated by recent findings that different mice strains with distinct deficit of VAChT in central cholinergic neurons are hyperactive (Martins-Silva et al., 2011; Martyn et al., 2012). Our working hypothesis was that the excess of ACh might results in an overall change in spontaneous locomotion of PRiMA KO mice. Surprisingly, PRiMA KO mice showed the same locomotor activity as WT mice, both at the exploratory and habituated phases of testing, indicating that they have acquired sufficient adaptation to the central deficit of AChE.

A large body of evidence suggest that cholinergic system plays an important role in the spatial reference learning (Deiana et al., 2011). Among the genetic models targeting cholinergic system, strong deficits in spatial reference learning examined with MWM is observed in two strains - AChE Tg mice (Beeri et al., 1995) and mice with selective lack of VAChT in basal forebrain cholinergic neurons (VAChT KOBF) (Martyn et al., 2012). In contrast to AChE Tg and VAChT KOBF mice, we did not observe significant differences in spatial learning with MWM between WT and PRiMA KO mice. Similarly to PRiMA KO mice, AChE Het mice with 25-35% reduction of AChE activity also do not show alteration in MWM performance (Espallergues et al., 2010). Here we extend this finding by demonstrating that the major deficit of AChE in the brain is compatible with normal (or intact) spatial learning.

AChE KO mice show abnormal posture and gait (Duysen et al., 2002a). Whether this

phenotype arises solely from muscle impairment or reflect deficits both in the periphery and CNS could not be concluded. Our detailed analysis of the gait revealed only a minor difference in two parameters among many analysed. Even though the slight changes in swing and swing speed might suggest some slowness of PRiMA KO mice, the overall speed was not significantly different between PRiMA KO and WT mice. The gait analysis indicates that PRiMA KO mice do not possess any obvious impairment in gait. Hence, these results strongly support conclusion that the gait phenotype of AChE KO mice originate mostly, if not exclusively, from the lack of AChE in the periphery.

It has been indicated that cholinergic system is important to motor skill learning (de Castro et al., 2009b; Conner et al., 2003). We examined motor skill learning in mice trained on rotarod for 3 consecutive days. Surprisingly, on the first day PRiMA KO mice were poor performers, but in the consecutive two days they strongly improved their skills and performed as good as WT mice. The preserved ability of motor learning suggests that the complex plasticity of neuronal circuits associated with improvement of task performance (Costa et al., 2004) and likely mediated by synaptic plasticity (Dang et al., 2006), are well preserved in PRiMA KO mice. Similarly, when we subjected PRiMA KO mice to suspension wire, the initial failing in performance the on the first day of training was markedly decreased on the second day. Although the third day an additional improvent was not observed, it has to be noted that this test is also dependent on power of muscles. PRiMA-linked AChE is present also in muscles where it is distributed along the muscle in extrajunctional regions and only minor part of AChE at NMJ corresponds to motor neuron-derived PRiMA-linked AChE (Bernard et al., 2011). Interestingly, the level of PRiMA-linked AChE in muscles appears to be regulated by training (Gisiger et al., 1994). Yet, the function of PRiMA-linked AChE and relevance of changes in its amount is not clear.

The planning, selection and learning of the most appropraite motor programs associated with motor skill learning has been attributed to a considerable extent to basal ganglia circuits (Doyon et al., 2009; Groenewegen, 2003; Charlesworth et al., 2012). Thus, in the context of motor functions of basal ganglia our results might suggest that basal ganglia circuits are intact at least in respect to motor skill learning. Furthermore, our results suggest that PRiMA KO possibly entered the training endowed with motor programs distinct from WT. Whether the absence of PRiMA in muscles or motor neurons is the cause of suggested difference in mature motor programs is unknown and deserves further investigation.

- **PRiMA KO presents an excess of ACh in striatum**

The biochemical and ultrastructural data have indicated that the principal consequence of PRiMA absence is the failure of targeting AChE on the surface of the neurons and axons (Dobbertin et al., 2009). On the other hand , the lack of any obvious phenotypical alteration (Dobbertin et al., 2009), absence of seizures typical for AChE KO (Duysen et al., 2002a), and the great perfomance

of PRiMA KO in several behavioural tests could raise doubts whether any excess of ACh is present in PRiMA KO. To directly resolve this issue, we performed microdialysis in the striatum of freely moving animals and quantified the amount of ACh in dialysates collected over 15 min period. The estimated concentrations of ACh in dialysates and extracellular space are 200-300 times higher in PRiMA KO and AChE del E5+6 than in WT In AChE KO, the 60-100 fold increase of ACh level was measured in hippocampus (Hartmann et al., 2007, 2008). Thus, our results imply that AChE is largely excluded from the spatial and temporal control of released ACh. In AChE KO mice, the excessive ACh levels are moderated by BChE despite the activity of BChE in the brain is very low in comparison to the AChE activity (Li et al., 2000) and BChE has less favourable glial localization (Mesulam et al., 2002). In AChE KO mice, 60fold increase of ACh levels is further fivefold elevated by infusion of BChE inhibitor bambuterol through microdialysis probe. Consistent with histochemical findings, showing retention of BChE inside cells in PRiMA KO mice, infusion of bambuterol does not change ACh levels in PRiMA KO (Mohr, unpulished data). Surprisingly, both PRiMA KO and AChE del E5+6 are sensitive to AChE inhibition resulting in further fourfold elevation of ACh (Mohr, unpulished data). The origin of AChE hydrolyzing ACh in PRiMA KO and AChE del E +6 mice is not known.

The measurement of ACh levels using the standard microdialysis is considered to reflect the ambient level of ACh in the extracellular space which is an equilibrium between its release and clearance (Descarries, 1998; Descarries et al., 1997). The fluctuations of ambient level over the baseline in a local neuronal environment is thus commonly believed to mediate cholinergic effects on for istance attention and arouasal states. However, such hypothesis has been recently challenged (Parikh et al., 2007).

The limitation of standard microdialysis is that the sample collection requires longer time over a scale of several minutes, thus limiting the temporal resolution. To overcome temporal limits of standard microdialysis, a more sensitive approach to measure the changes in ACh level, based on electrochemical detection of Ch derived from hydrolysis of newly released ACh, has been employed (Parikh et al., 2007). Parikh et al. followed the changes in Ch level in medial prefrontal Cx of rats performing the cue detection task. The successfull cue detection was associated with transient increase of Ch on the scale of seconds, while the missed cues were not (Parikh et al., 2007). One can thus hypothesize that commonly measured ambient levels of ACh in basal conditions or associated with certain behaviours are derived from cholinergic transients on the scale of seconds or even faster transients reflecting the firing activity of cholinergic neurons. The question that emerges from the study of Parikh and co-workers is whether our results from microdialysis reflect the “ambient level” of ACh to which the neuronal environment is continuosly exposed (Descarries, 1998; Descarries et al., 1997) or they indicate much stronger cholinergic transients, i.e. the increased average of ups and downs of cholinergic signals. If the latter were true, the brain might buffer ACh transients also by other mechanisms, not only by its direct hydrolysis in the immediate vicinity of the release sites, either forming synapses or not. Alternatively, the residual activity of AChE in PRiMA KO mice and preserved BChE activity in AChE KO could be sufficient

to drive ACh concentration gradients and facilitate its removal from release sites by diffusion. Then, the localization of AChE or BChE is likely not the limiting factor. According to proposed hypothesis, we can conclude that the concentration of ACh in dialysate samples is remarkably higher in PRiMA KO and AChE del E5+6 mice than in WT mice, but not exclude that cholinergic transients on the scale of seconds or even faster still do occur. Finally, the behaviour and phenotype of PRiMA KO mice appear to be more consistent with preserved cholinergic signaling (Sarter et al., 2009), albeit exaggerated, than hypothesis that the brain of PRiMA KO and AChE del E5+6 mice is permanently "soaked" in ACh (Descarries, 1998).

- **The adaptation of cholinergic system to the excess of ACh**

Our microdialysis experiments indicated that the neuronal environment in the striatum, and likely also in other brain areas with cholinergic innervation, is exposed to the excess of ACh. Surprisingly, PRiMA KO mice performed as WT mice in a variety of behavioural tests, suggesting efficient mechanisms of adaptation to the deficit of AChE. To unravel potential compensatory mechanisms we focused on proteins involved in ACh synthesis and storage as well as on ChR.

* The lack of changes in preterminal markers of cholinergic neurons

Neither the protein level nor the activity of ChT were changed in PRiMA KO mice. Likewise, ChAT activity and expression level of VAChT in striatum, cortex and hippocampus of PRiMA KO mice did not differ from WT mice. Similarly to PRiMA KO mice, no alteration in ChAT activity and protein level of VAChT have been reported for AChE KO mice (Volpicelli-Daley et al., 2003a). In contrast, however, AChE KO mice present 60% increase in total ChT level in striatum (Volpicelli-Daley et al., 2003a) and 136% increase in hippocampal HACU (Hartmann et al., 2008). At least two possibilities can be consider according to previously published data to explain the upregulation of CHT in AChE KO. One possibility, as suggested by Volpicelli-Daley and co-workers is that ChT is constitutively upregulated as a response to reduced metabolism of ACh into Ch and acetic acid (Volpicelli-Daley et al., 2003a). Another possibility to consider is that the upregulation of ChT and HACU reflects more vigorous activity of cholinergic neurons in AChE KO.

Elevation of ACh level in hippocampus of AChE KO is accompained by a 65% reduction of free Ch in the extacellular fluid (ECF) (Hartmann et al., 2008). Under normal conditions, when AChE activity is preserved, at least 40% of Ch derived from cleavage of ACh is reused in synthesis of ACh (Parikh and Sarter, 2006) and even the high cholinergic activity does not lead to the decrease in ECF Ch (Parikh et al., 2007, 2013). In fact, the cholinergic activity is reported by second based transient increases of Ch levels (Parikh et al., 2007, 2013). The possibility that in AChE KO Ch levels are reduced by deficits in ACh cleavage is supported by findings, that blocking HACU or silencing neuronal activity with infusion of hemicholinium-3 and tetrodotoxin at recording sites,

respectively, while having only minor effects on Ch level in WT mice, dramatically increase Ch level in AChE KO mice, approaching the WT basal Ch levels (Hartmann et al., 2007, 2008). Despite the fact that PRiMA KO and AChE KO mice have similar major AChE deficiencies in the brain, resulting in an excess of ACh, neither total ChT nor HACU are changed in PRiMA KO mice. Ch levels in PRiMA KO mice are reduced by 20%, but the reduction is not statistically significant (Mohr, unpulished data).Thus, our findings indicate that the lack of ACh hydrolysis is not by itself the cause of ChT and HACU upregulation in AChE KO mice.

Evidence suggest, that the density of ChT in plasma membrane and the mediated choline uptake correlate with cholinergic activity (Apparsundaram et al., 2005; Ferguson et al., 2003; Parikh et al., 2013; Simon and Kuhar, 1975). Since several kinds of behaviouraly salient stimuli can increase cholinergic activity (Acquas et al., 1996) and one of the prominent behavioural sign of AChE KO mice is their susceptibility to stress (Duysen et al., 2002a) it might be hypothesized that the cholinergic system was more excited shortly before the mice were sacrified (Apparsundaram et al., 2005). On the other hand the up-regulation of total ChT level could indicate a more persistent increase of cholinergic activity. ChT heterozygotes which have a 50% reduction in total ChT level are not able to increase ChT actvity above baseline levels and fail to release the same amounts of ACh as WT mice, indicating that total amount of ChT imposes limits on cholinergic activity (Parikh et al., 2013). Conversly, it can be suggested that increase in total reserve of ChT might be compensatory mechanism to higher demands on cholinergic activity. Similar to AChE KO mice, ChT level and HACU is up-regulated in AChE Tg mice. The total level of ChT as measured by autoradiography with 3H hemicholinium-3 is elevated by 100% in striatum and HACU measured in striatum and hippocampus is increased by 58% and 73%, respectively. Evidence suggest that ChT and HACU up-regulation has origin in increased cholinergic activity (Erb et al., 2001). AChE Tg mice have twofold higher AChE activity in hippocampal synaptosomes, but the basal ACh efflux in freely moving animals do not differ from control mice (Erb et al., 2001). However, under halothan anesthesia, previously elevated HACU in AChE Tg mice decreases almost to WT values and ACh efflux is reduced by 50% in comparison with WT values, indicating that in basal conditions the cholinergic activity in AChE Tg mice is higher and likely serves to compensate for accelerated ACh breakdown due to the increased AChE activity (Erb et al., 2001).

Even though it can not be at the moment completely excluded that the higher cholinergic activity maintains the homeostasis of cholinergic signaling in AChE KO mice, our results do not support such hypothesis. As PRiMA KO mice do not up-regulate ChT it is more likely that the severe peripheral deficits of AChE KO mice or the lack of AChE both in CNS and periphery trigger more vigorous activity of brain cholinergic system. Interestingly, AChE Het mice with 40% reduction of AChE activity and ACh levels increased only by 56% and Ch levels reduced by 24% as measured by microdialysis in hippocampus also show up-regulation of hippocampal HACU by 58% (Mohr et al., 2013). Our findings of unchanged ChT level and HACU in PRiMA KO mice together with findings in AChE KO and Het mice suggest that reduction or absence of AChE in the brain is not as important as AChE defcit in the periphery or in whole organism in terms of ChT

regulation. To test such hypothesis it will be intersting in the future to examine ChT regulation in ColQ KO mice and AChE i1rr mice as a model of peripheral deficit of AChE and in AChE del E5+6 mice as a model of AChE deficit in whole organism.

* PRiMA KO mice have similar adaptation of cholinergic receptors as AChE KO mice

Acute or chronic overstimulation of MR by exogenous cholinomimetics or by excess of endogenously released ACh due to the inhibition of AChE results in decreased density of MR at the plasma membrane (Bernard et al., 1998, 1999; Liste et al., 2002). In contrast to MR, NRs undergo upregulation following prolonged inhibition of AChE (Reid and Sabbagh, 2008). The increased densities of NR has been observed also in AChE Tg (Svedberg et al., 2002).

In the first experiments, we determined the binding properties of MR in plasma membranes prepared from Str, Hipp and Cx. The labeling of MR by [^{3}H]-QNB, which is a nonselective MR antagonist and labels all five MR subtypes was markedly reduced in all three regions examined. The affinity of MR to [^{3}H]-QNB did not differ between genotypes, suggesting that the decreased labeling was not the result of affinity changes to QNB but results from decreased density of MR.

To provide a more detailed map of MR adaptation, we performed autoradiography with [^{3}H]-QNB, [^{3}H]-AFDX-384 and [^{3}H]-pirenzepine. In a good agreement with results obtained on plasma membranes MR were found to be downregulated throughout the whole brain, with decreases ranging from 20 to 60 % both in PRiMA KO and AChE del E5+6 mice. [^{3}H]-AFDX-384 and [^{3}H]-pirenzepine are often used to label M2 and M1 receptors, respectively (Tien et al., 2004; Wolff et al., 2008). However, both ligands have been shown to have high affinity also for M4 (Dörje et al., 1991; Miller et al., 1991; Moriya et al., 1999).

The lack of more selective ligands precluded us to map the adaptation of particular MR by means of autoradiography, but our results indicate that M1, M2 and possibly M4 copy the general pattern of adaptation observed with [^{3}H]-QNB. Similar to our observations, profound alteration of MR density has been reported for AChE KO (Li et al., 2003; Volpicelli-Daley et al., 2003a, 2003b).

To further explore the adaptation of MR also in terms of functional state, we challenged PRiMA KO and WT mice with three MR cholinergic drugs: SCO, a nonselective antagonist, PIL a non-selective partial agonist and oxotremorine OXO a nonselective agonist. We anticipated that the decreased density of MR would be reflected by altered responsivenes to these drugs. In general, the decrease in density of receptors results in enhanced sensitivity to antagonists and conversely to reduced sensitivity to agonists (Li et al., 2003).

Among other effects, SCO is known to enhance the locomotor activity (Sipos et al., 1999), PIL at higher doses induces epileptic-like seizures (Curia et al., 2008) and OXO exert strong hypothermic effect (Lomax and Jenden, 1966; Sun et al., 2007).

Consistent with our expectation, PRiMA KO showed strongly altered responses to all cholinergic drugs. PRiMA KO are more resistant to OXO induced hypothermia and PIL induced seizures and more sensitive to SCO induced locomotion. It has been shown previously that PIL induced seizures are absent in M1 KO (Hamilton et al., 1997) and the hypothermic response of OXO at lower doses is absent and at higher doses is markedly reduced in M2 KO. The decreased responses of PRiMA to pilocarpine and OXO are thus consistent with the autoradiography results suggesting decreased availability of M1 and M2 receptors. The significant reponsivenes of PRiMA KO mice to PIL and OXO, albeit altered, further suggests that a portion of M1 (Hamilton et al., 1997) and possibly also M2 (Gomeza et al., 1999b) might be functional in PRiMA KO mice.

The question that raises from pharmacological and biochemical data is whether the signaling at the remaining MR can be still effective in governing the neuronal circuits. Even though a complex approach has to be employed to address this question, the intact locomotion of PRiMA KO, as distinct from M1 and M4 KO (Gerber et al., 2001; Gomeza et al., 1999a; Miyakawa et al., 2001) suggest that the muscarinic signaling is possibly well balanced. In addition, M1 receptors has been suggested to be present at high receptor reserve, and occupation of just 15% of M1 receptors may provide sufficient signaling (Porter et al., 2002), a value lower than the most pronouced decrease of 3H pirenzepine binding in PRiMA KO.

Despite it is well-known that among many MR antagonists, SCO has the strongest effect on locomotion, the underlying mechanisms are not well definied. Several lines of evidence indicate that the important site of SCO effects on locomotion are mesopontine cholinergic neurons projecting to dopaminergic cells in SN and VTA (Chapman et al., 1997; Laviolette et al., 2000; Mathur et al., 1997). By blocking inhibitory autoreceptors in LTD and PPT, scopolamine might promote the cholinergic excitation of midbrain dopaminergic neurons, resulting in enhanced release of dopamine in striatum (Chapman et al., 1997; Laviolette et al., 2000; Mathur et al., 1997). The enhanced activation of dopaminergic neurons in VTA and SN by cholinergic input can be than mediated by NR, M5 and possibly also NMDA receptors (Cachope et al., 2012; Higley et al., 2011; Ren et al., 2011), which mediate distinct phases of prolonged dopamine release in dorsal striatum and nucleus accumbens following electrical stimulation of PPT and LTD respectively (Forster and Blaha, 2000, 2003; Forster et al., 2002). Another site of SCO action could be the striatum, since direct infusion of MR antagonists into the striatum results in a similar behavioural activity as following i.p. SCO administration (Shapovalova et al., 2005). The relative contribution of particular MR has not been sufficently answered, even with the use of MR KO mice. M1 KO mice have the same responsivennes to SCO (Anagnostaras et al., 2003) and M5 KO mice have enhanced response to SCO (Chintoh et al., 2003; Steidl and Yeomans, 2009). The enhanced response to SCO in M5 KO mice, has been explained however in two ways. One possiblity is that M5 in midbrain dopaminergic cells inhibit SCO response (Chintoh et al., 2003), the other suggests that in the absence of M5, the cholinergic inputs in VTA inhibit locomotion (Steidl and Yeomans, 2009). The studies of anticataleptic effects of SCO on the catalapsy induced by D2 antagosits in M4 KO mice have brought contradictory results. While one group reports that in M4 KO mice the

anticataleptic effect of M4 is lost (Karasawa et al., 2003), the other did not observe alteration in anticataleptic potency of SCO in M4 KO mice (Fink-Jensen et al., 2011).

It is therefore difficult to draw the explanation of a such strong effect of SCO in PRiMA KO, and it is likely that this effect reflects adaptation of more than one MR subtype and possibly involves also other systems such as dopaminergic.

Our microdialysis experiments indicated that the ambient concentration of ACh in the striatum of PRiMA KO mice reached 3 μM, a value consistent with the observation of sustained NR activation in the spinal cord (Lamotte d'Incamps et al., 2012). These high extracellular ACh concentrations exceed the EC50 of MR (Lazareno and Birdsall, 1993; Shirey et al., 2008), but not that of most NRs (Giniatullin et al., 2005; Moroni et al., 2006). It is therefore not surprising that the main adaptation of ACh receptors concerns MR.

- **The noncholinergic receptors are unchanged in PRiMA KO**

The synaptic integration in a local neuronal circuits is under influence of multiple neurotramsmitters (Kaneko et al., 2000; Watanabe et al., 1998) and interactions of ACh with other neurotransmitter systems including dopaminergic, GABAergic and glutamatergic has been shown at different levels implying possible changes also in noncholinergic receptors.

We were particulary interested in abundace of dopaminergic receptors, since the co-operations and interactions of cholinergic and dopaminergic signaling are well documented and considered central for proper function of Str (Aosaki et al., 2010; Bonsi et al., 2011; Kaneko et al., 2000; Surmeier and Graybiel, 2012). Str is the major input structure of basal ganglia (BG) circuits which support motor and cognitive functions (Bolam et al., 2000). The principal cells of Str are GABAergic projection medium sized spiny neurons (MSN) which give rise to so called direct, striatonigral and indirect, striatopallidal pathways of BG which promote and suppress the motor behaviour, respectively (Kravitz et al., 2010). MSN are driven by extrinsinc glutamatergic excitatory synaptic inputs, mostly from Cx and thalamus. The excitatory input and the final output of MSN is modulated directly or indirectly by multiple other inputs, including extrinsic dopaminergic and intrinsinc cholinergic and GABAergic inputs (Kreitzer and Malenka, 2008; Lovinger, 2010). While the dopaminergic input originate from midbrain dopaminergic neurons, the only source of ACh in Str are tonically active cholinergic interneurons (ChI) (Gerfen and Surmeier, 2011; Kawaguchi et al., 1995). Despite few in number, ChI generate a dense meshwork of cholinergic fibers, infiltrating the whole striatal neuropil (Contant et al., 1996). Moreover, among other brain structures Str shows the highest AChE activity, levels of ACh and density of MR (Hammond et al., 1994; Wolfe and Yasuda, 1995).

The selective ablation of ChI in Str is compensated by changes in the density of dopaminergic receptors (Kaneko et al., 2000). On the other hand, depletion of dopamine dysregulates autocontrol

of ChI (Ding et al., 2006). Synchronous activation in a population of ChI triggers the release of dopamine from dopaminergic neurons by activating presynaptic NRs (Cachope et al., 2012; Threlfell et al., 2012). Conversly, dopamine by activating D2 receptors slows the spontaneous pacemaking of ChI and decreases the release of ACh (DeBoer et al., 1996; Maurice et al., 2004; Yan et al., 1997). At postsynaptic site of striatonigral neurons M4 receptor inhibit, while D1 stimulate production of cAMP (Jeon et al., 2010), which is required for promoting responsiveness of striatonigral MSN to glutamatergic input (Surmeier et al., 2007). As opposed to striatonigral MSN, striatopalidal neurons are enriched in D2 receptors which decreases responsiveness to glutamatergic input (Surmeier et al., 2007), while M1 receptors although express in both types of MSN more potently promote glutamatergic input in striatopallidal MSN (Shen et al., 2007).

Despite several sites of ACh and dopamine interactions we did not observe changes in dopaminergic receptors density in striatum of PRiMA KO. In striking contrast AChE KO mice showed remarkable decrease in the density of dopaminergic receptors. D1-like are reduced to 5% of WT density and D2-like are almost undetectable, as revealed by radioligand binding, Suppl. 1 (Hrabovska et al., 2010b). This discrepancy between PRiMA KO and AChE KO mice might suggest that either the ACh/dopamine interactions are less affected in PRiMA KO mice due to the residual AChE activity regulating ACh levels (Mohr, unpublished data) or the changes observed in AChE KO mice are caused by the absence of AChE in whole organism. We also cannot exclude the influence of genetic background. While AChE KO mice with 129/sv genetic background can survive to adult, thus allowing for intense examination, congenic AChE KO mice with inbred C57 or outbred CD1 genetic backgroung all die during seizures before postnatal day 21 (Duysen and Lockridge, 2006).

Similar to DR, glutamatergic (AMPA, NMDA, kainate receptors) and GABAergic receptor density is not altered in PRiMA KO in any brain region examined. We can not, however, exclude that more detailed analysis such as evaluation of synaptic plasticity at glutamatergic synapses (Gu and Yakel, 2011; Martyn et al., 2012) would uncover significant changes between PRiMA KO and WT mice.

• The role of AChE in the CNS

Undoubtedly, the principal role of AChE in the CNS is hydrolysis of ACh. When there is a deficit of AChE activity, induced either by pharmacological inhibition or genetic manipulations, increases in ACh concentration are reliably measured by standard microdialysis (Hartmann et al., 2007; Scali et al., 2002). However, the spatial and temporal demands on ACh hydrolysis are less well definied, especially when one has to consider a compelling evidence suggesting the

volume transmission mode of ACh. It is commonly accepted that similarly to NMJ, AChE in the CNS functions to rapidly terminate the cholinergic transmission, yet substantial differences exist between the nature of ACh carried transmission at NMJ and in the CNS.

At NMJ, ACh mediate the fast synaptic transmission. ACh is released from a single axon terminal with multiple active zones over a large postsynaptic surface endowed with high density of NRs. AChE is highly concentrated at NMJ and present mainly postsynaptic location (Bernard et al., 2011). When AChE is blocked, ACh accumulates in the synaptic cleft and its removal by diffusion is limited by repetitive binding to NRs (Katz and Miledi, 1973). As a consequence, muscles cannot sustain high frequency stimulation and tetanic muscle contraction fails (Chang, 1998). At the motoneuron Renshaw synapse, the synaptic transmission can be triggered by the antidromic stimulation of the axon of the motoneurons. Different cholinergic receptors (α7 and α*β*) are activated during these stimulations (Lamotte d'Incamps and Ascher, 2008). In normal condition, the decay of a synaptic current observed after five stimulations is longer than after single stimulation. When AChE is inhibited, the amplitude of synaptic current is progressively decreased suggesting that NR are desensitized or internalized. A staedy state current is observed and indicates the persistent presence of ACh. The time constant of decay of the ultra-slow component extends to seconds. In PRiMA KO mice, the shape of the EPSC is similar to the WT mice after inhibition of AChE by neostigmine, and characterized by an ultra slow prolongation. The amplitude of the EPSCs is lower indicating an adaptation of PRiMA KO mice by the reduction of functional NRs at the synapse. Addition of external AChE eliminates the ultraslow compound without major change of the synaptic transmission. This slow compound is mediated by heteromeric nicotinic receptors (α*β*) (Lamotte d'Incamps et al., 2012). In addition to the slow current, a very fast current is generated by homomeric nAChR (α7). This receptor has a very fast desentization and after AChE inhibition the α7 current disappears. In contrast, in PRiMA KO mice the α7 currents are unchanged, suggesting adaptation of the mutant.

In addition to the synaptic transmission that seems quite similar in the presence or absence of AChE and depends mainly upon the intrinsic properties of the receptors, the major change is the ultra slow compound that represents certainly the spillover of ACh from the synaptic cleft. Indeed either when the cholinergic boutons are not in regard of postsynaptic differenciation or when the cholinergic boutons are engaged in a synapse ACh can diffuse (Lamotte d'Incamps et al., 2012).

The splillover of ACh from release sites is central to the hypothesis postulated by Descarries that in the brain, a substantial portion of ACh operates in a volume transmission mode (Descarries et al., 1997). The concept of the volume transmission mode of ACh is supported by several lines of evidence. This includes the often very low synaptic incidence of cholinergic boutons (Contant et al., 1996; Descarries et al., 2004; Umbriaco et al., 1995), spatial relationship of cholinergic receptors and ACh release sites (Duffy et al., 2009; Fabian-Fine et al., 2001; Jones and Wonnacott, 2004; Jones et al., 2001; Yamasaki et al., 2010) and the electrophysiologial data (Arroyo et al., 2012; Bell et al., 2011; Ren et al., 2011). The morphological distribution of AChE in the brain is also different from NMJ. While at NMJ AChE is mainly associated with postsynaptic surface (Bernard

et al., 2011), in the brain, the majority of AChE is found presynaptically at cholinergic varicosities, along the axons and at cell bodies of cholinergic neurons (Dobbertin et al., 2009; Klinar and Brzin, 1977). Taken together, these differences suggest that the demands on ACh hydrolysis by AChE might differ from those at NMJ.

What is then the role of ACh breakdown by AChE in the brain if not rapid termination of the cholinergic signaling as at NMJ? Several possibilities for AChE function in the brain has been tentatively suggested (Descarries, 1998; Descarries et al., 1997; Hatton and Yang, 2002; Surmeier and Graybiel, 2012).

Descarries has assumed that the immediate driving force of ACh elimination whether released from varicosities with or without synaptic speacilisation is diffusion (Descarries et al., 1997). The suggested role of AChE is to take the control over ACh in the subsequent phase when ACh is spreading in the extracellular space, thus preventing its accumulation in local environment and keeping its ambient concentration within physiological limits, the ambient level of ACh, rather than completely eliminate ACh (Descarries, 1998; Descarries et al., 1997).

The presynaptic location of AChE at cholinergic varicosities might indicate involvement of AChE in the control the spontaneous release of ACh. For instance, in the supraoptic nucleus, where the cholinergic transmission appears to be synaptic, inhibition of AChE increases the frequency and amplitude of the sponateous EPSPs, supporting the role of AChE in the control of spontaneous events (Hatton and Yang, 2002).

Another feature of the cholinergic system in the brain, that has to be taken in the account when considering to role of AChE, is the ultrastructural localisation of ACh receptors. MR as well as NRs often show locations not closely associated with ACh release sites, suggesting that ACh has to travel longer distances to reach them (Duffy et al., 2009; Hersch et al., 1994; Jones and Wonnacott, 2004; Lendvai and Vizi, 2008; Yamasaki et al., 2010). How then can ACh activate them, when there is AChE in the way? One can assume, that only ACh releases large enough to pass through AChE barrier can be successful to activate the remote receptors (Surmeier and Graybiel, 2012). With respect to such hypothesis, the role of AChE would be the control of the strenght of cholinergic signals, i.e how far and how much of ACh will be allowed to diffuses in the extracellular space. The strong support for such role of AChE, at least in some instances, has emerged from recent findings demonstrating that the synchrony of firing in a population of cholinergic neurons or the tetanic stimulation of cholinergic axonal terminals is required to generate cholinergic responses (Ren et al., 2011; Threlfell et al., 2012). On the oher hand, MR and NR responses to endogenously released ACh can be enhanced by the inhibition of AChE (Narushima et al., 2007; Wanaverbecq et al., 2007). That AChE might impose limits on strenght of cholinergic signaling is suggested also by studies in AChE Tg, indicating higher demands on cholinergic activity to overcome increased AChE activity (Erb et al., 2001).

Owing to the regional differences in the proterties of cholinergic system (synaptic incidence, localization and diversity of ChR, AChE density and distribution, synaptic vs. volume transmission

mode) it is likely not possible to generalize the role of AChE and all of above mentioned hypothesis could be valid, at least to some extent.

- **Central versus peripheral changes in cholinergic function**

PRiMA KO mice, AChE KO mice and AChE del E5+6 mice have exceptional high levels of ambient extracellular ACh in the brain. In all these mutants, the excess of ACh is accompanied by similar reduction of MR density. Despite these similarities, the behavior of PRiMA KO mice appears normal and PRiMA KO mice are indistinguishable from WT mice, whereas both AChE KO and AChE del E5+6 mice are easily identified by their smaller size, poor locomotor activity, high levels of fatigability and tremor (Boudinot et al., 2009; Camp et al., 2005; Duysen et al., 2002a). Notably, only AChE KO mice develop seizures in response to very slight changes to their environment (Dobbertin et al., 2009; Duysen et al., 2002a). PRiMA KO mice have a normal respiratory function (Boudinot et al., 2009), whereas AChE KO mice display several respiratory abnormalities similar to those observed after the administration of AChE inhibitors (Chatonnet et al., 2003). AChE del E5+6 mice are less strongly affected than AChE KO mice, but nonetheless have a clear pathologic phenotype (Boudinot et al., 2009; Camp et al., 2005; Dobbertin et al., 2009). BChE, the other cholinesterase, moderates the ACh level in AChE KO mouse brain (Hartmann et al., 2007)and may contribute to the survival mechanism in AChE KO mice. However, the respiration of AChE KO mice is blocked by a BChE inhibitor bambuterol that does not cross the blood brain barrier (Chatonnet et al., 2003), suggesting a toxic effect at the periphery but not in CNS. In PRiMA KO mice, histological staining of BChE activity at light microscopic level indicate that BChE is trapped inside glial cells. The strong support for the absence of BChE at its active sites is provided by our preliminary results of microdialysis. As opposed to AChE KO mice, perfusion of recording sites with BChE inhibitor does not change ACh levels (Mohr, unpublished observations).

The normal levels of ColQ-linked AChE at the NMJ in PRiMA KO mice may account for some of their differences from AChE KO and AChE delE5+6 mice, including, in particular, the lower levels of motor activity of AChE KO mice. However, the presence of AChE in muscle cannot account for the milder CNS defects or the marked effects of donepezil on core body temperature in PRiMA KO mice. PRiMA KO mice must therefore have a source of AChE other than the NMJ. The two most plausible and non-exclusive hypotheses are the presence of residual AChE activity in the CNS and a contribution of the autonomic nervous system AChE.

ACh levels in PRiMA KO mice remain responsive to AChE inhibitors, thus we cannot exclude that a small amount of residual AChE in PRiMA KO mouse CNS (Mohr, unpublished observations) has a disproportionately large effect, accounting for the absence in PRiMA KO mice of an increase in ChT density (Volpicelli-Daley et al., 2003a) and the low number of dopamine receptors in AChE KO mice Suppl. 2 (Hrabovska et al., 2010b). Further investigation of these

aspects is required. Nevertheless, the most plausible explanation for the differences between PRiMA KO mice on the one hand, and AChE KO mice and AChEdel5+6 on the other, is that ColQ-anchored AChE is present not only at the NMJ, but also in the cholinergic synapses of the autonomic nervous system (Koelle et al., 1987; Skau and Brimijoin, 1980). This hypothesis is supported by the effects of donepezil on PRiMA KO mice, which cannot be explained by residual central AChE. First, the residual activity of AChE appear to be same in PRiMA KO mice and AChE del E5+6 mice (Mohr, unpublished observations). Second, the effects of donepezil are much larger in PRiMA KO mice than those observed in AChE del E5+6 mice and ColQ KO mice. We thus propose that the major targets of donepezil in PRiMA KO mice are the cholinergic synapses of the PNS and, more generally, that the persistence of AChE at these synapses may at least partially account for the mild phenotype of PRiMA KO mice. Indeed, AChE KO mice are by far the most strongly affected, as they die within the first three weeks of development. Some of the defects in these mice may be accounted for by a loss of brown adipose tissue thermoregulation, which involves the autonomic nervous system (Sun et al., 2007). Many ColQ KO mice (50%) die in the same period (Feng et al., 1999) and are rescued effectively by increasing the rearing temperature or energy intake, as in AChE KO mice. These results suggest that, when interpreting the effects of AChE inhibitors, the inhibition of autonomic nervous system and NMJ AChE may be more important than the inhibition of central AChE, contrary to previous explicit assumptions (Duysen et al., 2002a, 2007) or implicit assumptions such as those underlying the search for new antidotes for treating AChE inhibitors induced poisoning, e.g. by targeting oximes into the CNS (Wagner et al., 2010).

• PERSPECTIVES

Important questions that deserve further investigations concern the fate of released ACh in PRiMA KO mice. In AChE KO mice, the extracellular levels of ACh are moderated by BChE, which is intact in AChE KO mice. By contrast, current experiments demonstarte that the excess of ACh in PRiMA KO mice is moderated by residual AChE activity, but not by BChE activity. However, the origin and molecular forms of AChE activity which hydrolyses ACh in the neurochemical environment is unknown and deserve detailed investigation. Ongoing research focuses on residual AChE activity in Hipp. When enough time is given AChE in PRiMA KO mice to generate sufficient amount of reaction product, the staining of AChE activity in Hipp is clearly observable. Interestingly, in contrast to staining of AChE in Str, where staining is clearly concentrated in the cell bodies of ChI, in Hipp, part of the staining is diffuse. Therefore, the secretion of a minor part of AChE and its origin in distinct brain areas/cell types cannot be excluded at the moment. It will be also interesting to explore the changes of ACh levels in PRiMA KO mice during distinct behavioural tasks. Current evidence demonstrates that ACh levels fluctuate on the scale of seconds when mice perform attention tasks. As already discussed, the limitation of standard microdialysis is its temporal resolution and ACh detection methods with high temporal resolution will certainly shed more light on cholinergic signaling in the brain of PRiMA KO mice.

• CONCLUSIONS

In this thesis we show that the lack of AChE in CNS when PRiMA and AChE cannot interact (PRiMA KO and AChE del E5+6 mice) causes similar excess of ACh and reduction in MR density in the brain. However, the phenotype and the sensitivity to donepezil - a specific AChE inhibitor - is different in PRiMA KO and AChE del E5+6 mice. While PRiMA KO mice are indistinguishable from WT mice for their behaviour and sensitivity to an ACHE inhibitor, AChE del E5+6 mice are resistant to AChE inhibition and their behaviour is severely altered. Consequently, the previously observed phenotype of AChE KO mice seems to result from the lack of AChE primarily in the periphery and not in the brain.

• FIGURES

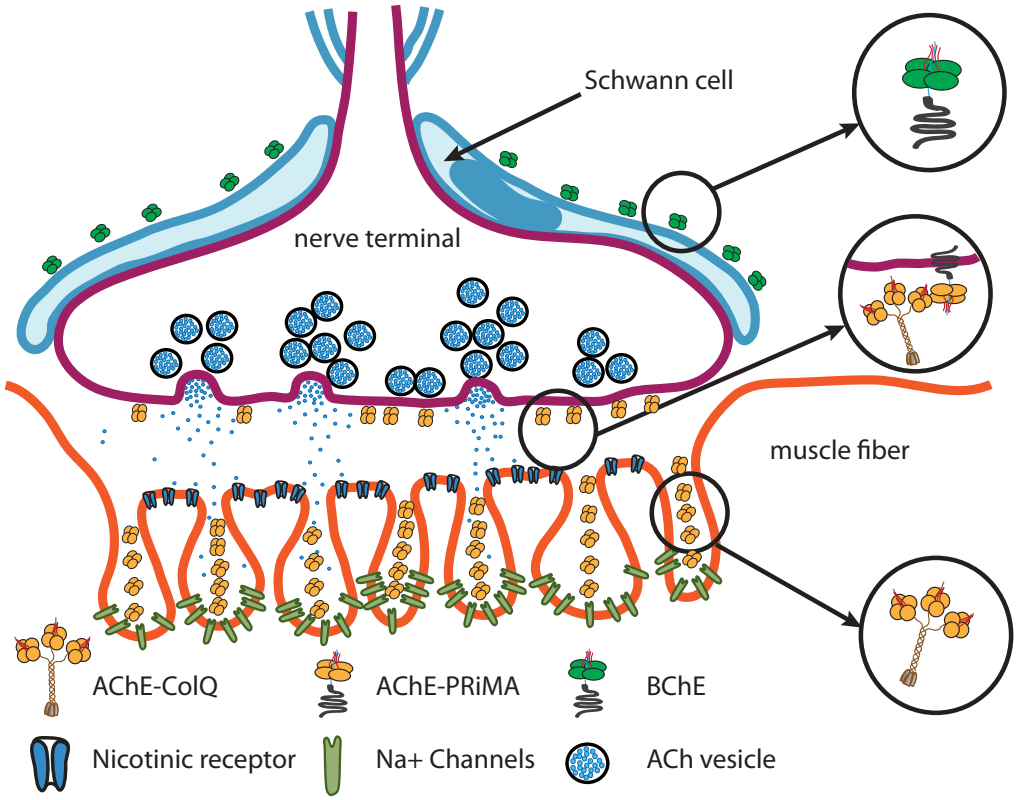

Fig. 1. Cartoon depiction of NMJ

NMJ represents a model of cholinergic synapse, where ACh mediates the fast synaptic transmission. The nerve terminal covers large surface area of postsynaptic muscle membrane and contains multiple active zones, where ACh is released. NRs are clustered at high density on the crests of postsynaptic membrane. AChE is present in the primary cleft along the nerve terminals where it is anchored by structural proteins ColQ and PRiMA and in the secondary folds, where it is anchored to the basal lamina by ColQ. Butyrylcholinesterase (BChE), a second cholinesterase is associated with Schwann cell enwraping the nerve terminal.

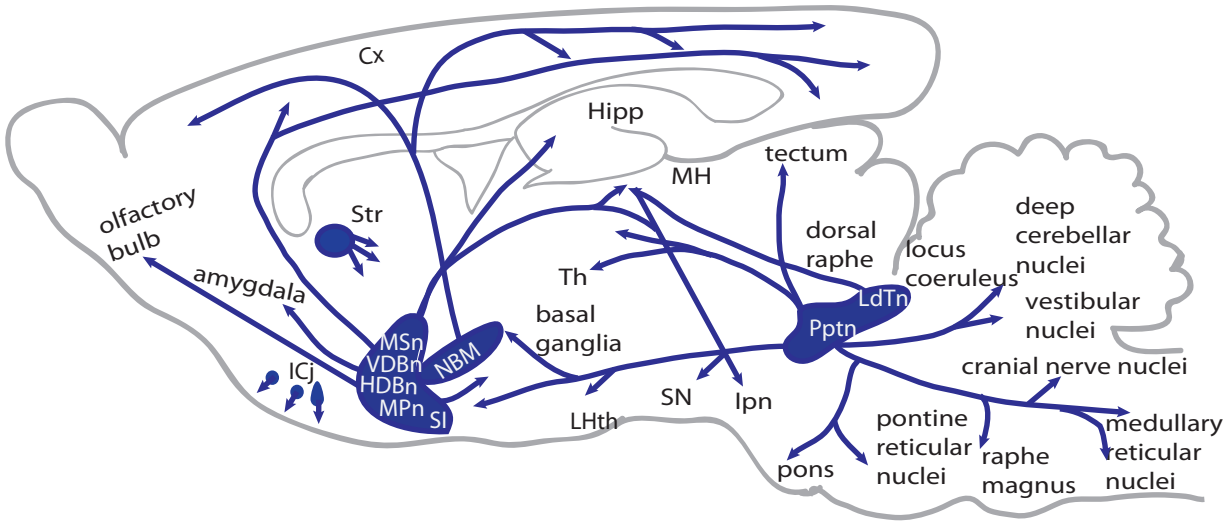

Fig. 2. Schematic representation of the location and projections of cholinergic neurons in the brain

Abbrevations: Cx, cortex; HDBn, horizontal diagonal band nucleus; Hipp, hippocampus; Icj, islands of Cajella; Ipn, interpenducular nucleus; LdTn, laterodorsal tegmental nucleus; LHth, lateral hypothalamus; NBM, nucleus basalis magnocellularis; MH, medial habenula; MPn, magnocellular preoptic nucleus; MSn, medial septum nucleus; Th, thalamus; Pptn, penduculopontine nucleus; SI, substantia inominata; SN, substantia nigra; Str, striatum; VDBn, vertical diagonal band nucleus. Adapted from Woolf and Butcher (2011).

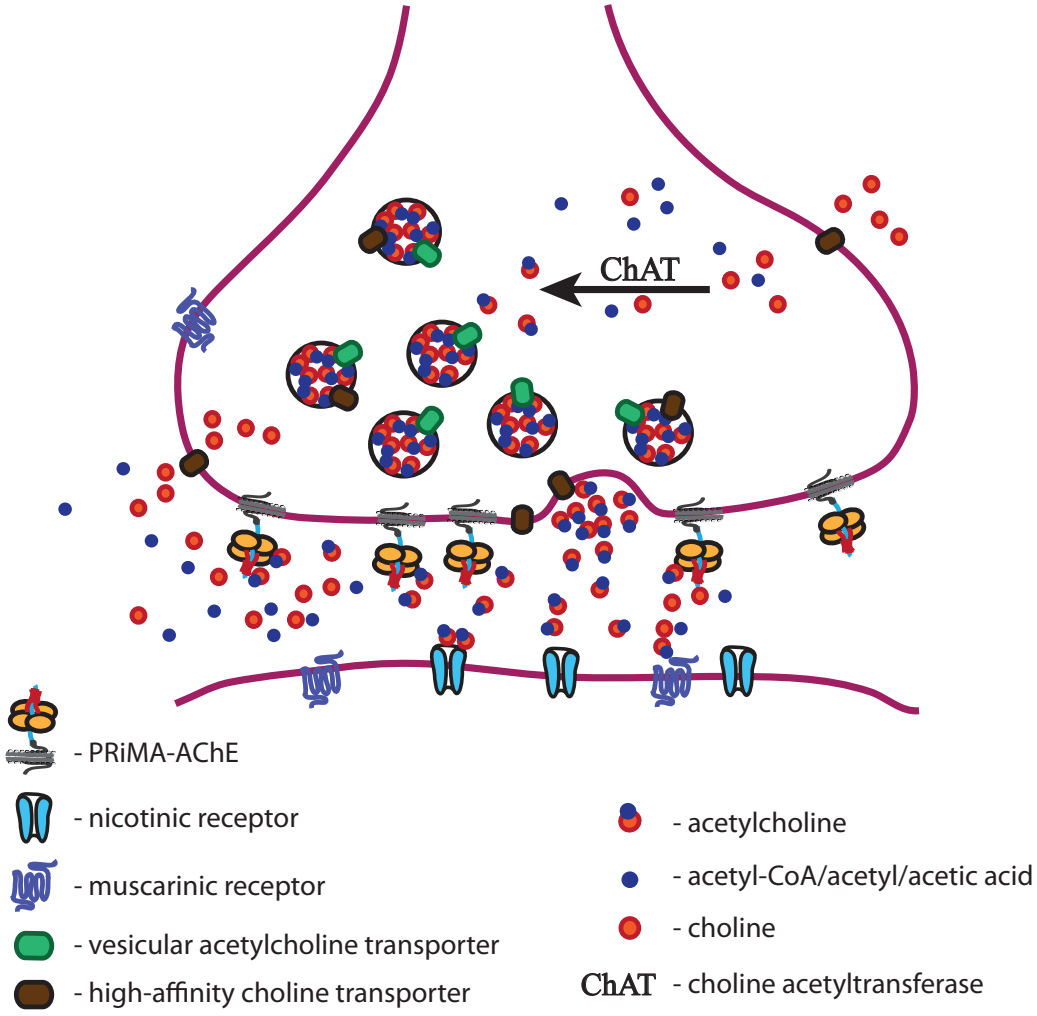

Fig. 3. The life cycle of ACh

In the cholinergic varicosities, ChAT catalyses the synthesis of ACh from choline and acetyl-coenzyme A. Acetyl-coenzyme A is derived from basal metabolism of cholinergic neurons and choline is supplied from the extracellular space by high-affinity choline transporter. The synthetized ACh is concentrated into the synaptic vesicles by vesicular ACh transporter. Action potentials trigger the release of ACh and ACh can bind to two classes of receptors: nicotinic and muscarinic receptors. In the extracellular space, ACh is primary hydrolysed by AChE, which is mainly associated with cholinergic neurons. Part of choline derived from ACh hydrolysis is captured by high-affinity choline transporter and reused in ACh synthesis.

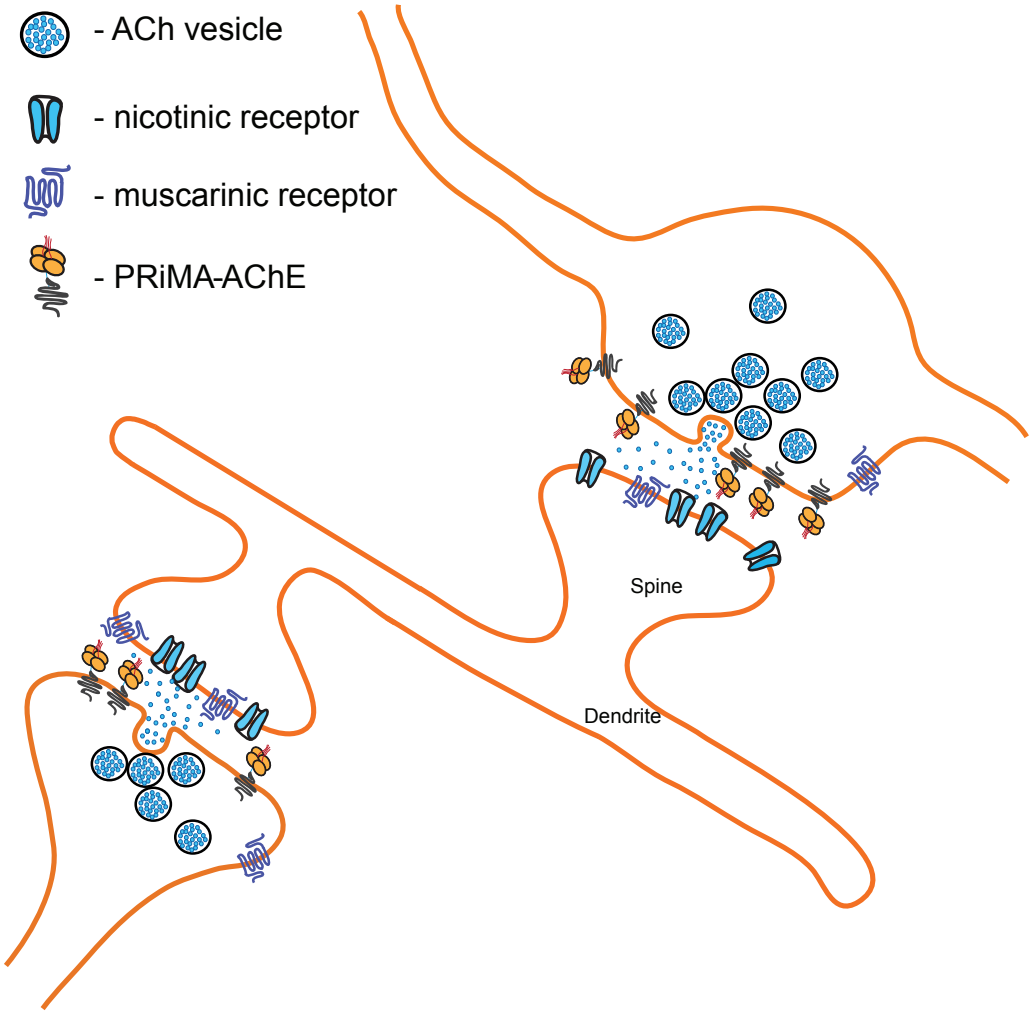

Fig. 4. Schematic representation of the synaptic transmission mode of cholinergic neurotransmission

In the synaptic or wired model of cholinergic neurotransmission, cholinergic varicosities form synaptic specialization with target cell. The released ACh operates within the borders of synapses and mediates the fast cholinergic transmission by activating NRs at postsynaptic membrane.

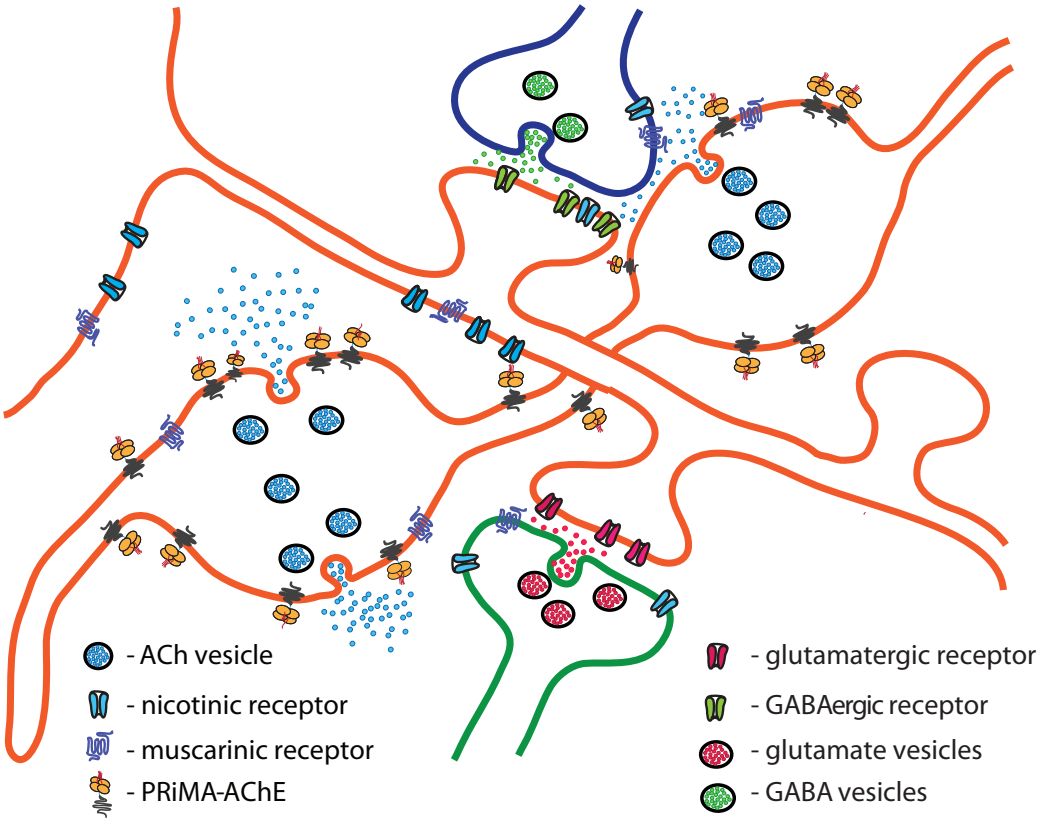

Fig. 5. Schematic representation of the volume transmission mode of cholinergic neurotransmission

In the volume model of cholinergic neurotransmission, cholinergic varicosities do not form synapses. The volume transmission assumes the spread of released ACh in the extracellular space and activation of non-synaptic cholinergic receptors on multiple target cells. As opposed to synaptic transmission, the volume transmission is characterized by long transmission delay.

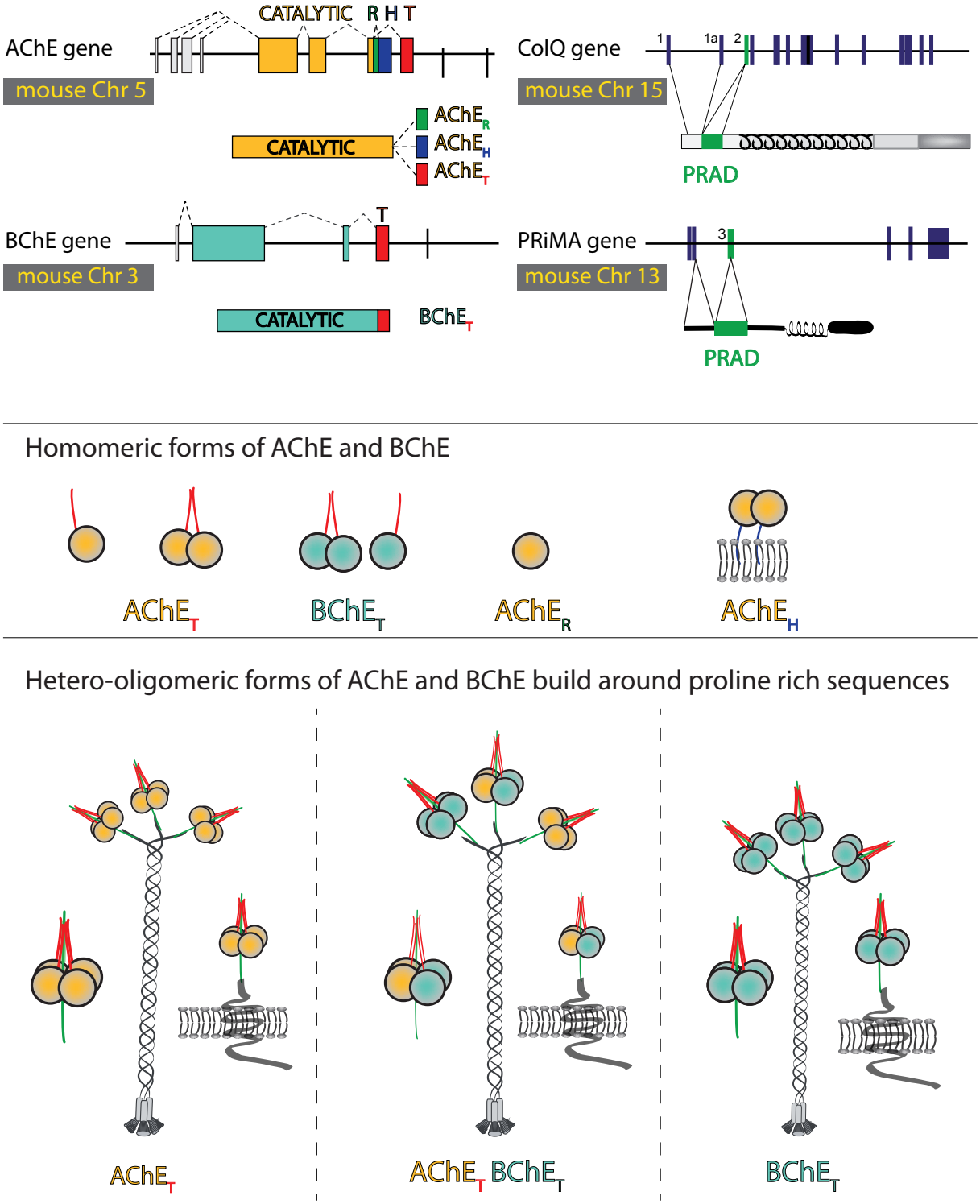

Fig. 6. Schematic representation of the gene structure, transcripts and molecular forms of mammalian AChE and BChE and gene structure and protein products of anchoring proteins ColQ and PRiMA

The molecular diversity of AChE arises from the alternative processing of the 3‘ end of primary mRNA, giving a rise to 3 AChE protein variants that have a common catalytic domain but possess distinct C terminal peptides – AChE R, AChE H and AChE T. The postranslational oligomerization and association of AChE T with structural proteins ColQ and PRiMA further add to the complexity of AChE molecular forms. Only subunits of type T exist for BChE.

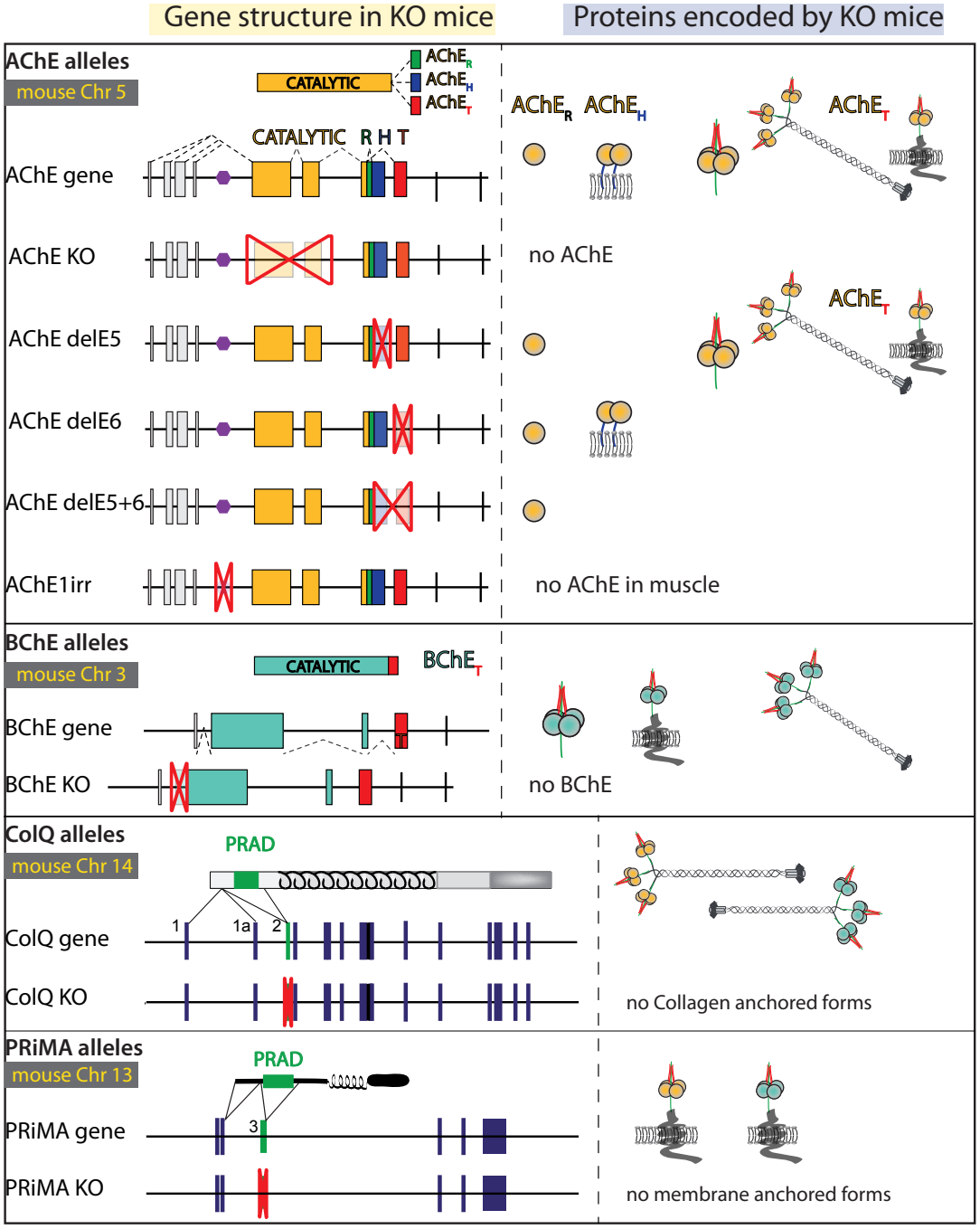

Fig. 7. Schematic representation of genetic strategy and protein products in ChE-deficient mouse strains

AChE gene generates 3 variants of AChE – AChE R, AChE H and AChE T. AChE R variant is monomeric and soluble. AChE H generates GPI-anchored dimers. The heteromeric associations of AChE T with structural proteins ColQ and PRiMA represent the principal form of AChE in muscles and brain, respectively. AChE KO mouse was generated by targeted deletion of the entire catalytic domain and has no AChE protein and activity. AChE delE5 mouse was produced by deletion of exon 5 and lacks AChE H variant. AChE delE6 mouse was created by deletion of exon 6 and lacks the principal AChE variant, AChE T. AChE delE+6 mouse has deleted exons 5 and 6 and can only produce AChE R variant. Deletion of part of exon 2 of BChE gene results in absence of BChE activity in BChE KO mouse. In AChE 1irr mouse, a 250 bp sequence in the intron 1 of AChE gene was deleted. AChE 1irr mouse has no AChE in skeletal muscles. PRiMA KO and ColQ KO mice were created by targeted deletion of the PRAD domain of PRiMA and ColQ genes, respectively.

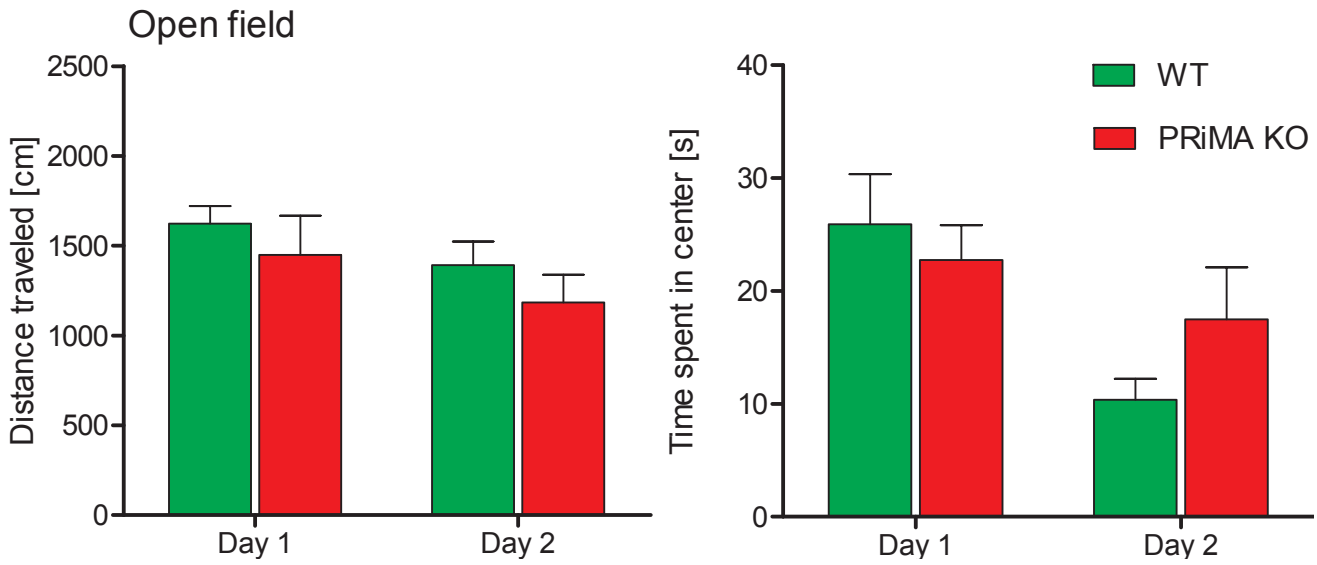

Fig. 8. Spontaneous locomotor activity and habituation of PRiMA KO and WT mice in open-field conditions

There was no significant difference between PRiMA KO and WT mice in spontaneous locomotor activity and time spent in the central zone of the open-field both at the exploratory and habituated phase of testing.

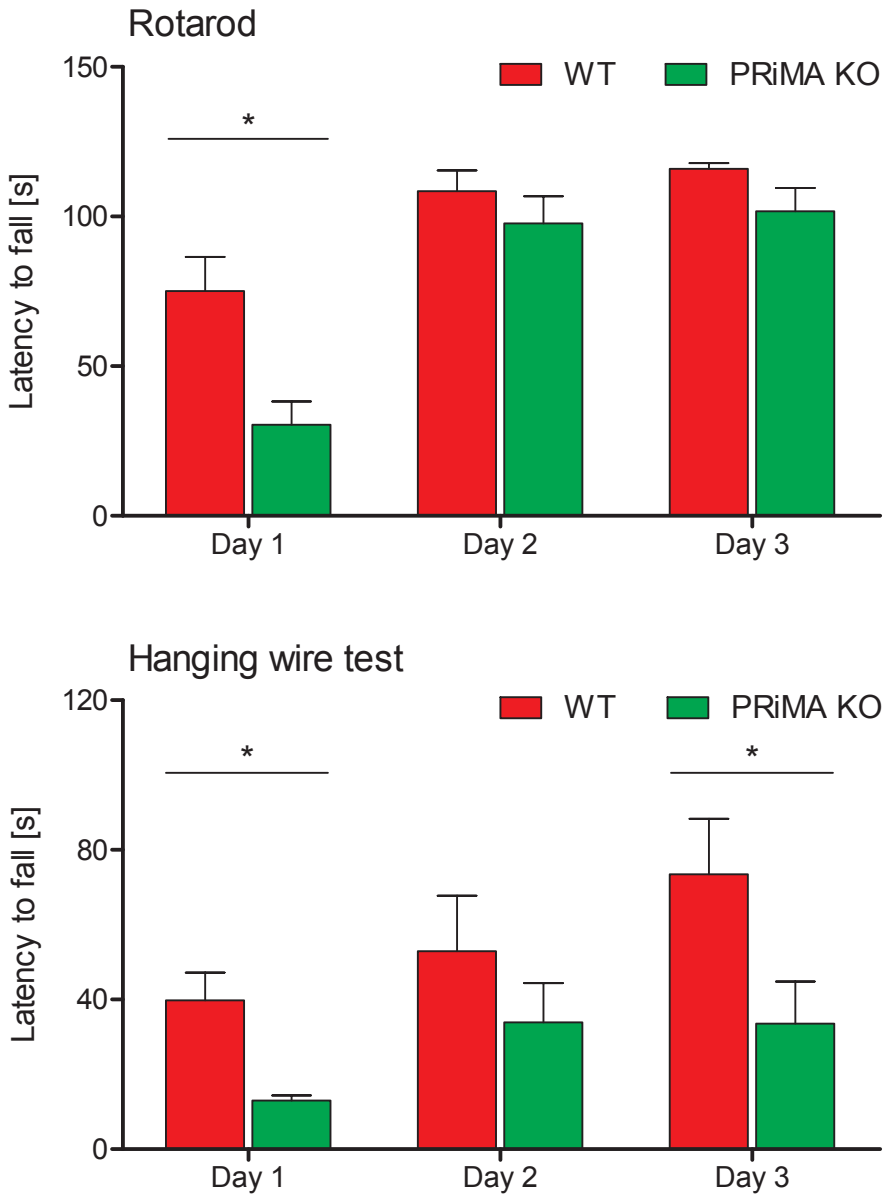

Fig. 9. Motor skill performance and learning in PRiMA KO mice.

While PRiMA KO mice showed worser motor performance both in rotarod and hanging wire test, the ability to acquire motor skill learning was higher (rotarod) or intact (hanging wire test) in PRiMA KO mice. Note the difference in motor performance between naive PRiMA KO and WT mice on the first day of training and dramatic improvement of motor performance of PRiMA KO mice on subsequent days.

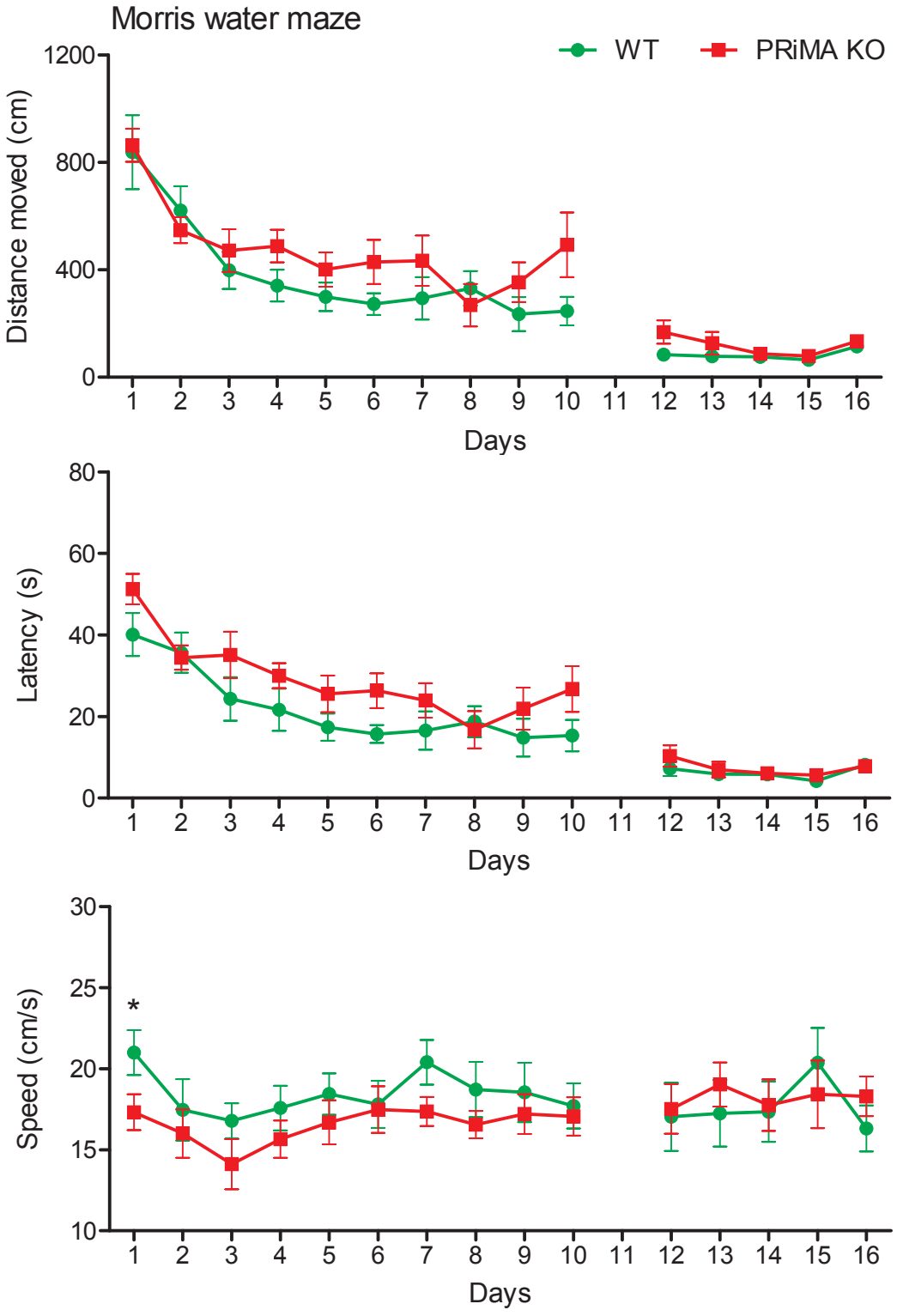

Fig. 10. Morris water maze.

First 10 days of MWM task, PRiMA KO and WT mice were trained to find the hidden platform in circular pool filled with water. We measured the time taken to reach the platform - escape latency - , total distance traveled and swimming speed. PRiMA KO showed spatial learning ability comparable to WT mice. Swimming speed of PRiMA KO mice was significantly lower on the 1st day of training in comparison to WT mice. On the 11th day we administered the probe trial. Following probe trial, we applied visible-platform acquisition training in MWM and measured escape latencies, distances moved, and swimming speeds. There were no significant differences between PRiMA KO and WT mice.

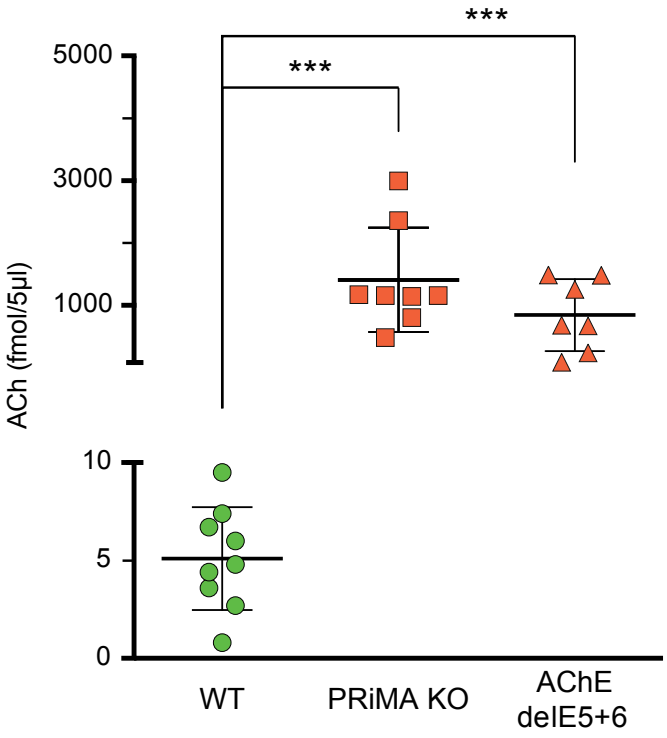

Fig. 11. Dramatic excess of ACh in striatum of PRiMA KO and AChE delE5+6 mice

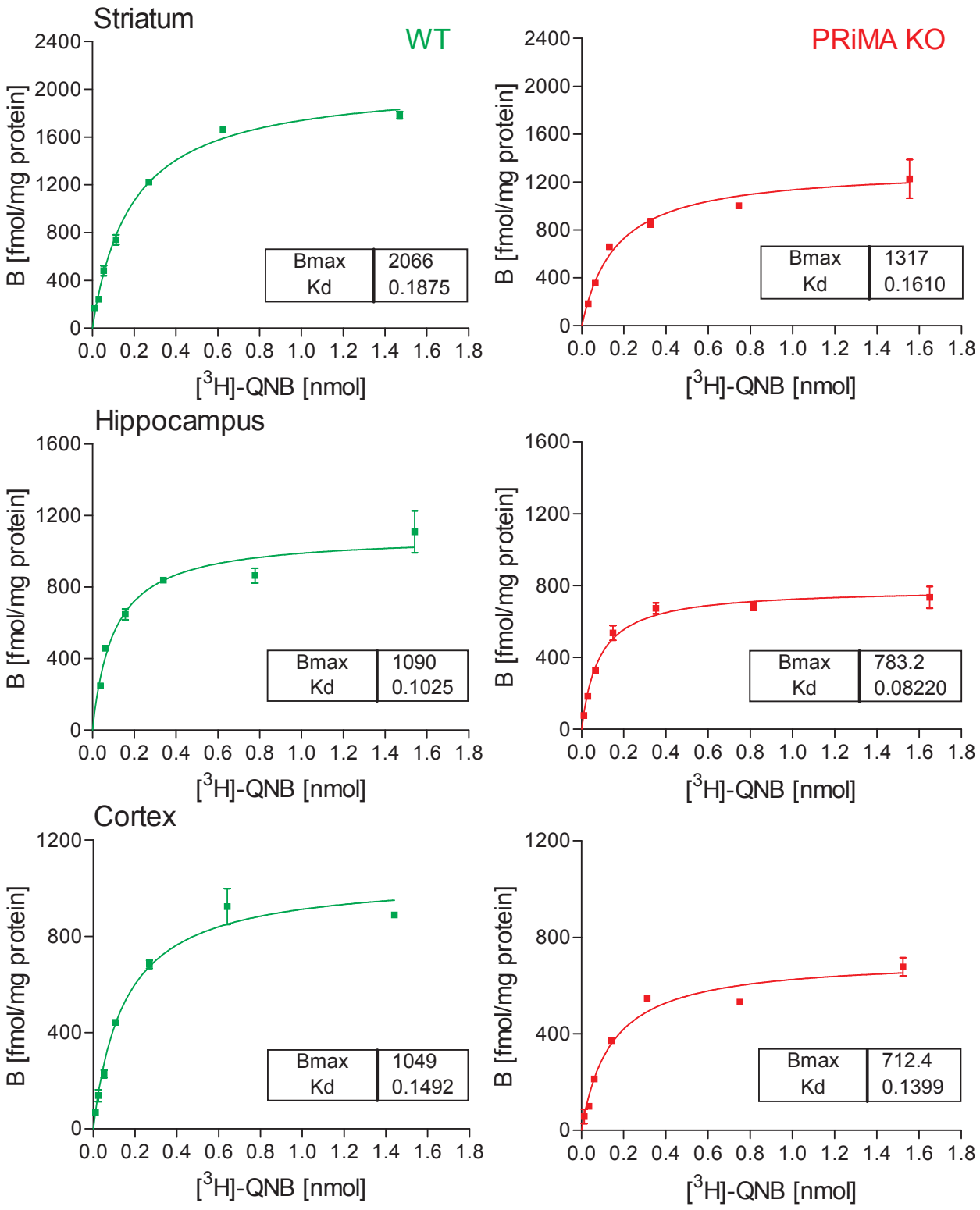

Fig. 12. Representative saturation binding curves of [^{3}H]-QNB binding in PRiMA KO and WT mice.

Titration of [^{3}H]-QNB binding to muscarinic receptors in plasma membranes from distinct brain regions was performed as described in Materials and methods. B is the specific binding per mg of protein measured at defined concentration of [^{3}H]-QNB, B_{max} is the total amount of receptors per mg of protein, L is concentration of free radioligand, and K_D is the dissociation constant. Free concentration of [^{3}H]-QNB is plotted on the X axis. Note the reduction of B_{max} in PRiMA KO mice in comparison to WT mice in all three brain regions. Affinity of muscarinic receptors to [^{3}H]-QNB - K_D - in PRiMA KO mice is comparable to WT mice.

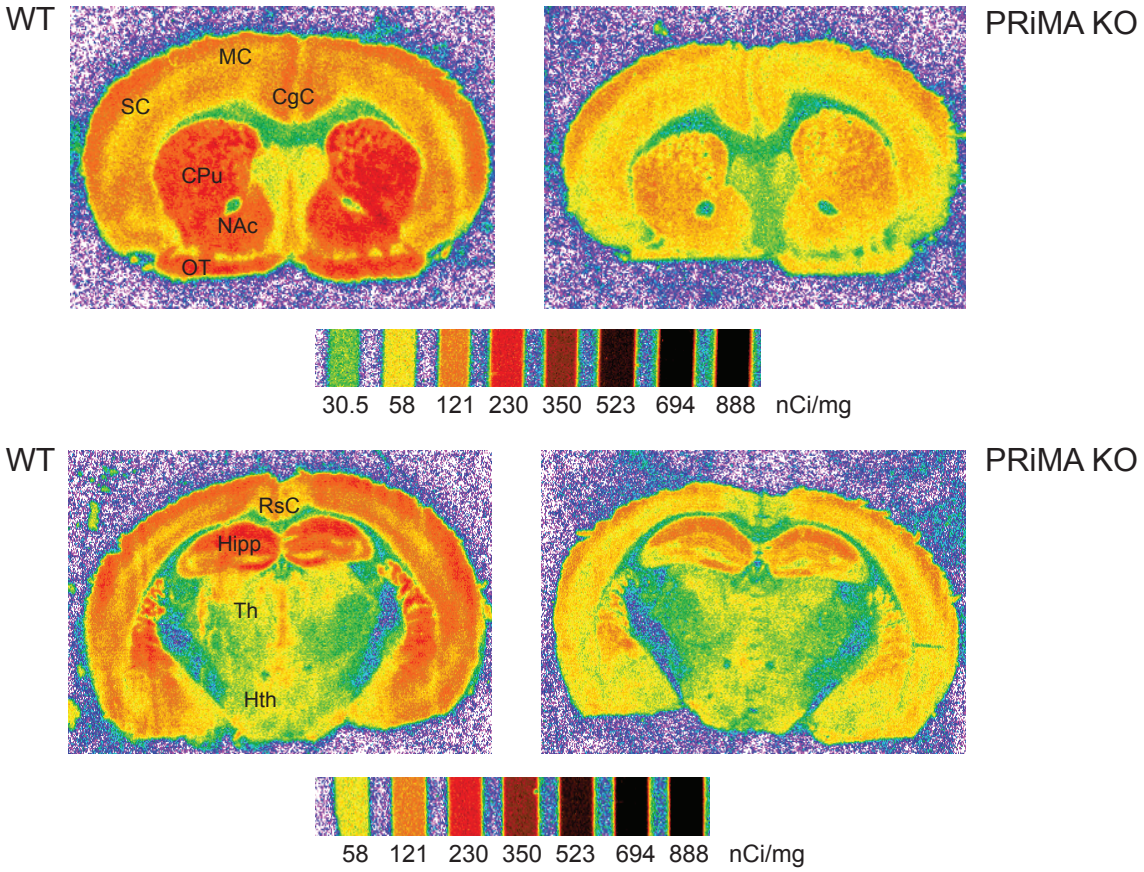

Fig. 13. Illustrative autoradiograms of QNB binding in coronal brain sections in PRiMA KO and WT mice.

[^{3}H]-QNB is a ligand that identifies the muscarinic receptor

MC, motor cortex; SC, somatosensory cortex; CgC, cingulatae cortex; RsC, retrosplenial cortex; OT, olfactory tubercle; CPu, caudate putamen; NAc, nucleus accumbens; Hipp, dorsal hippocampus; Th, thalamus; Hth, hypothalamus.

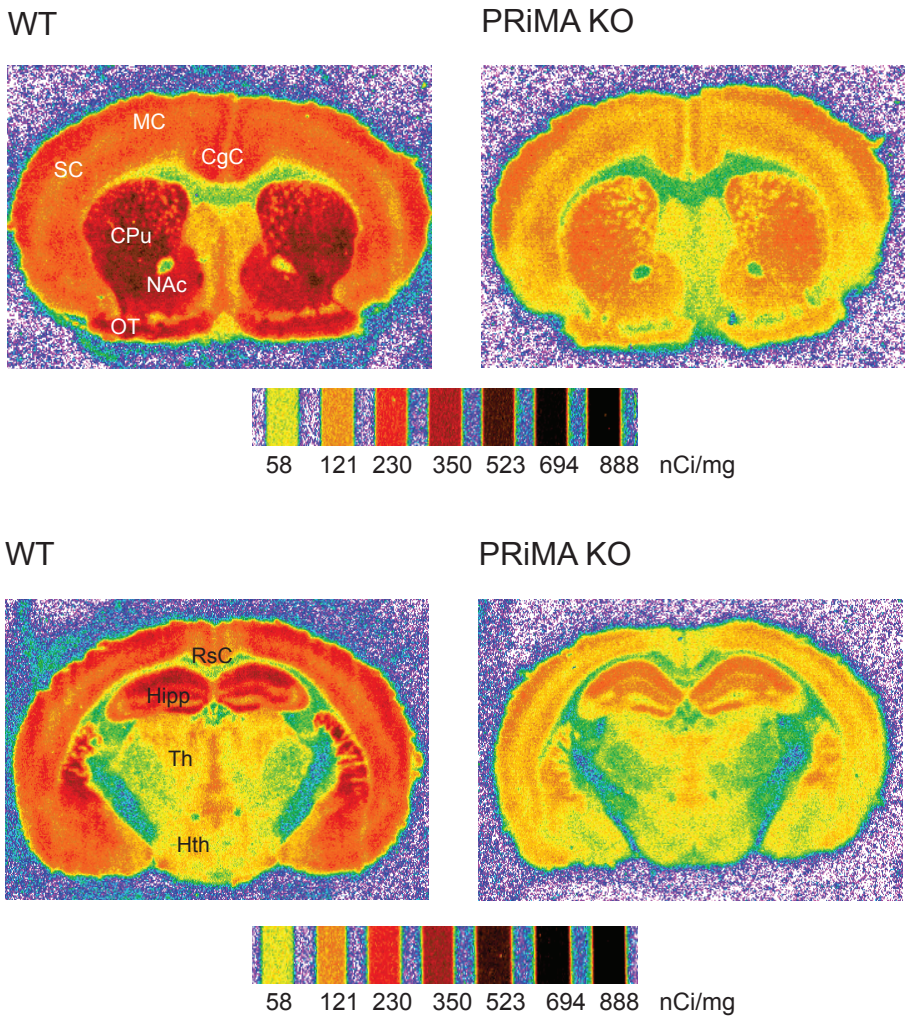

Fig. 14. Illustrative autoradiograms of [^{3}H]-NMS binding in coronal brain sections in PRiMA KO and WT mice.

MC, motor cortex; SC, somatosensory cortex; CgC, cingulatae cortex; RsC, retrosplenial cortex; OT, olfactory tubercle; CPu, caudate putamen; NAc, nucleus accumbens; Hipp, dorsal hippocampus; Th, thalamus; Hth, hypothalamus.

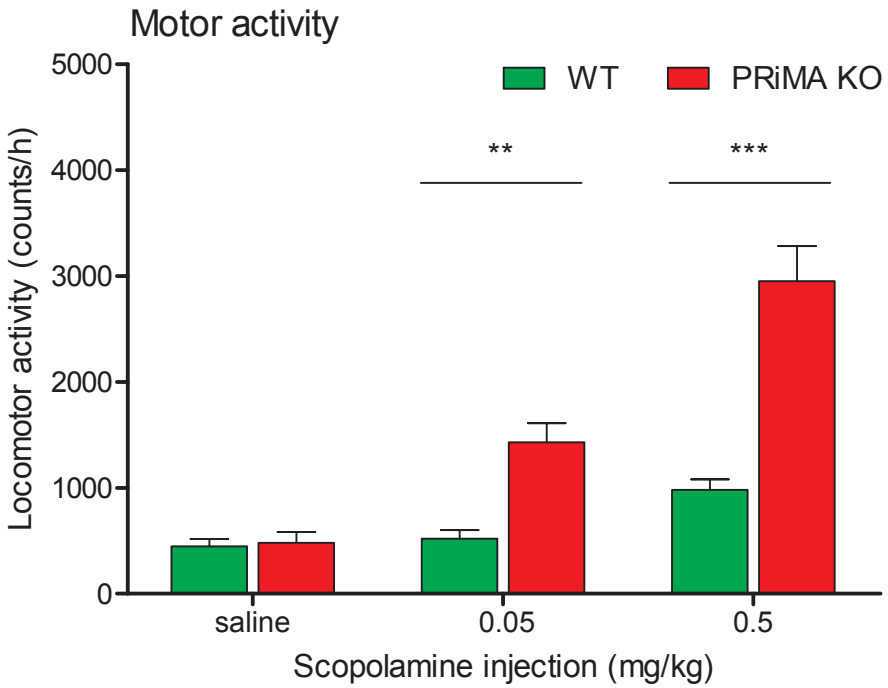

Fig. 15. PRiMA KO mice display enhanced sensitivity to scopolamine-induced motor activity.

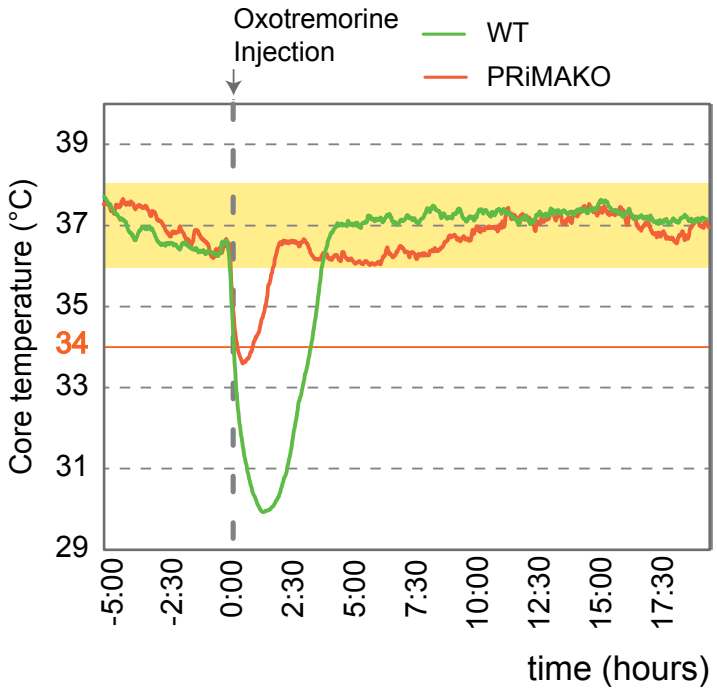

Fig. 16. PRiMA KO mice show decreased sensitivity to oxotremorine-induced hypothermia.

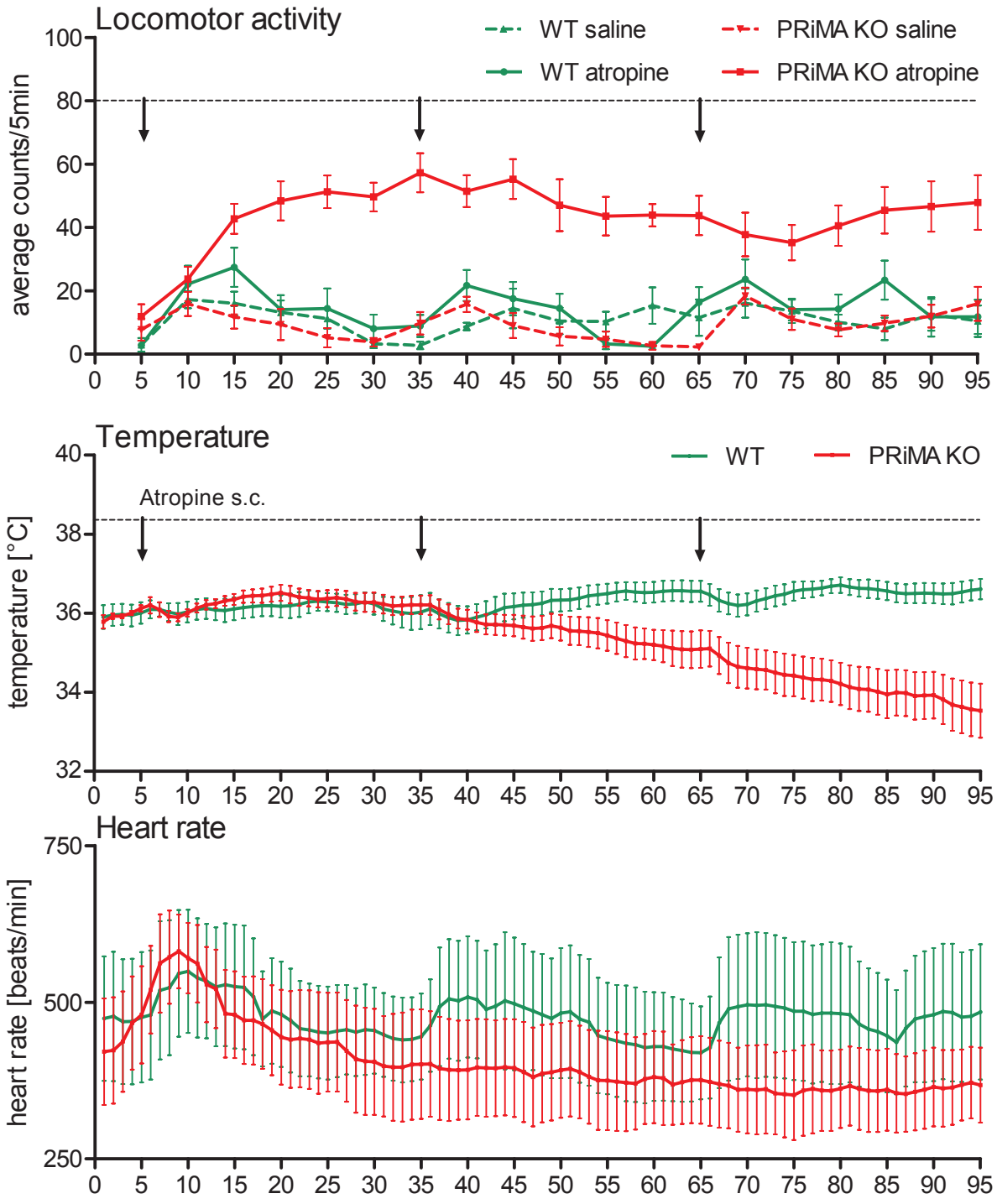

Fig. 17. Altered responsiveness of PRiMA KO mice to repeated ATR treatment.

The spontaneous locomotor activity of WT mice (n=6) given repeated s.c. injection of ATR at a dose 6 mg/kg every 30 min during 90 min was comparable to locomotor activity of saline treated WT mice (n=6). Unexpectedly, PRiMA KO mice (n=8) showed markedly increased spontaneous locomotor activity when compared to saline treated WT mice (n=6). While in WT mice (n=6), ATR treatment had no significant effect on core body temperature, in PRiMA KO mice (n=8), the second ATR injection resulted in rapid decline of core body temperature, which continued after and/or was intensified by the third ATR injection. In WT mice (n=4), every ATR injection resulted in temporal increase of HR, albeit not significant. By contrast, in PRiMA KO mice (n=4), only the first ATR injection resulted in insignificant increase of HR.

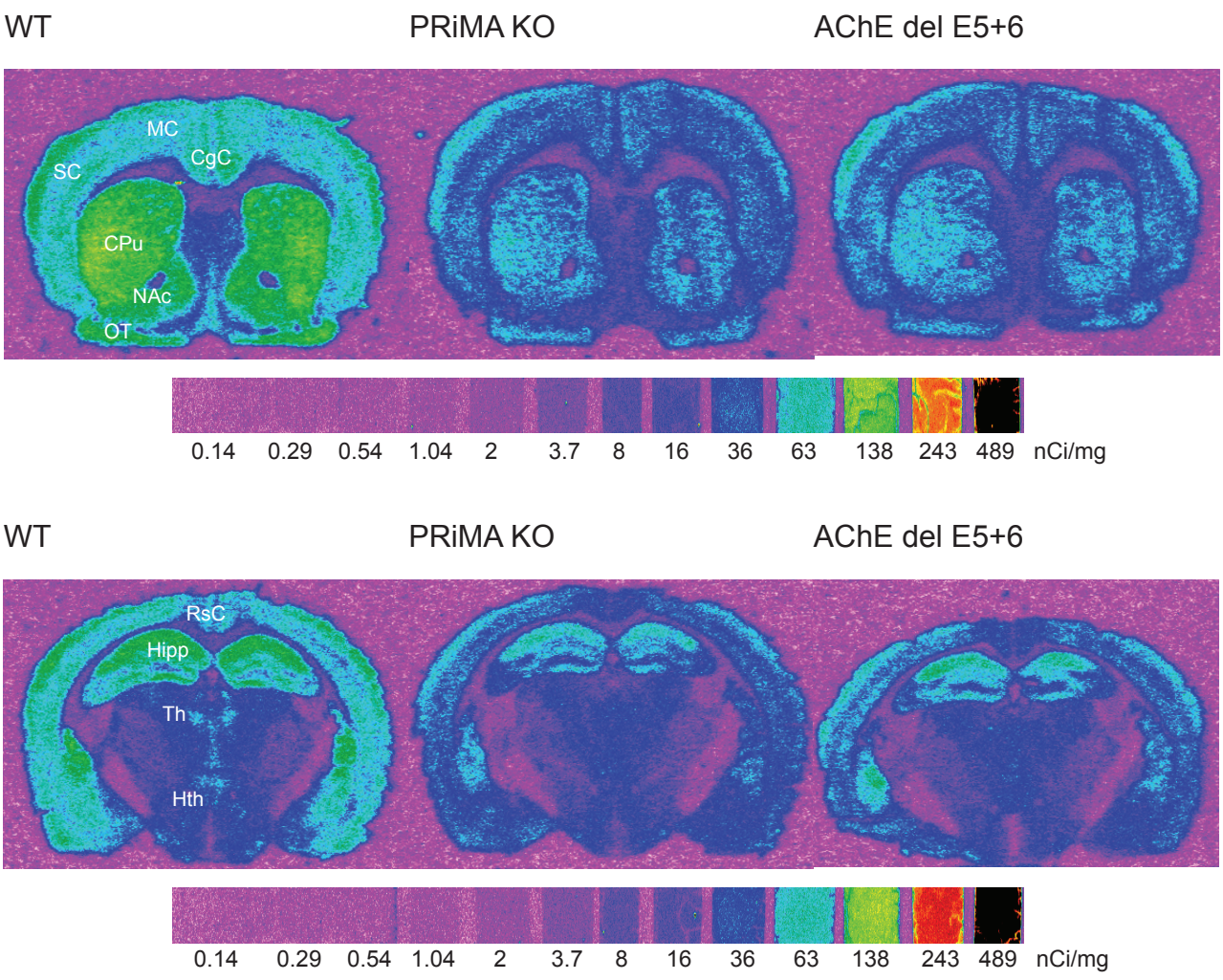

Fig. 18. Illustrative autoradiograms of [^{3}H]-QNB binding in coronal brain sections in PRiMA KO, AChE delE5+6 and WT mice.

MC, motor cortex; SC, somatosensory cortex; CgC, cingulatae cortex; RsC, retrosplenial cortex; OT, olfactory tubercle; CPu, caudate putamen; NAc, nucleus accumbens; Hipp, dorsal hippocampus; Th, thalamus; Hth, hypothalamus.

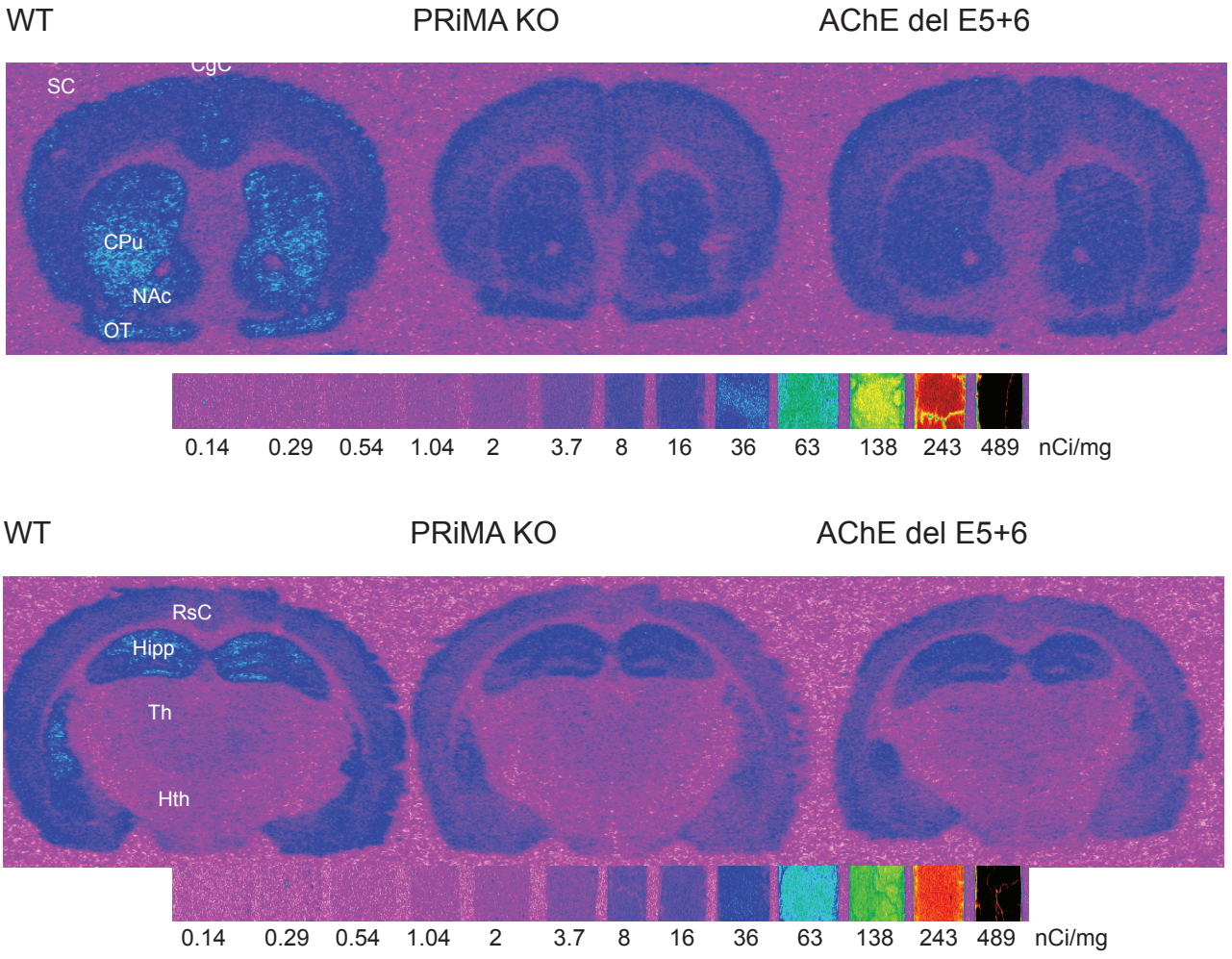

Fig. 19. Illustrative autoradiograms of [^{3}H]-pirenzepine binding in coronal brain sections in PRiMA KO, AChE delE5+6 and WT mice.

Note the barely visible labeling in Th and Hth, brain areas with few M_1. MC, motor cortex; SC, somatosensory cortex; CgC, cingulatae cortex; RsC, retrosplenial cortex; OT, olfactory tubercle; CPu, caudate putamen; NAc, nucleus accumbens; Hipp, dorsal hippocampus; Th, thalamus; Hth, hypothalamus.

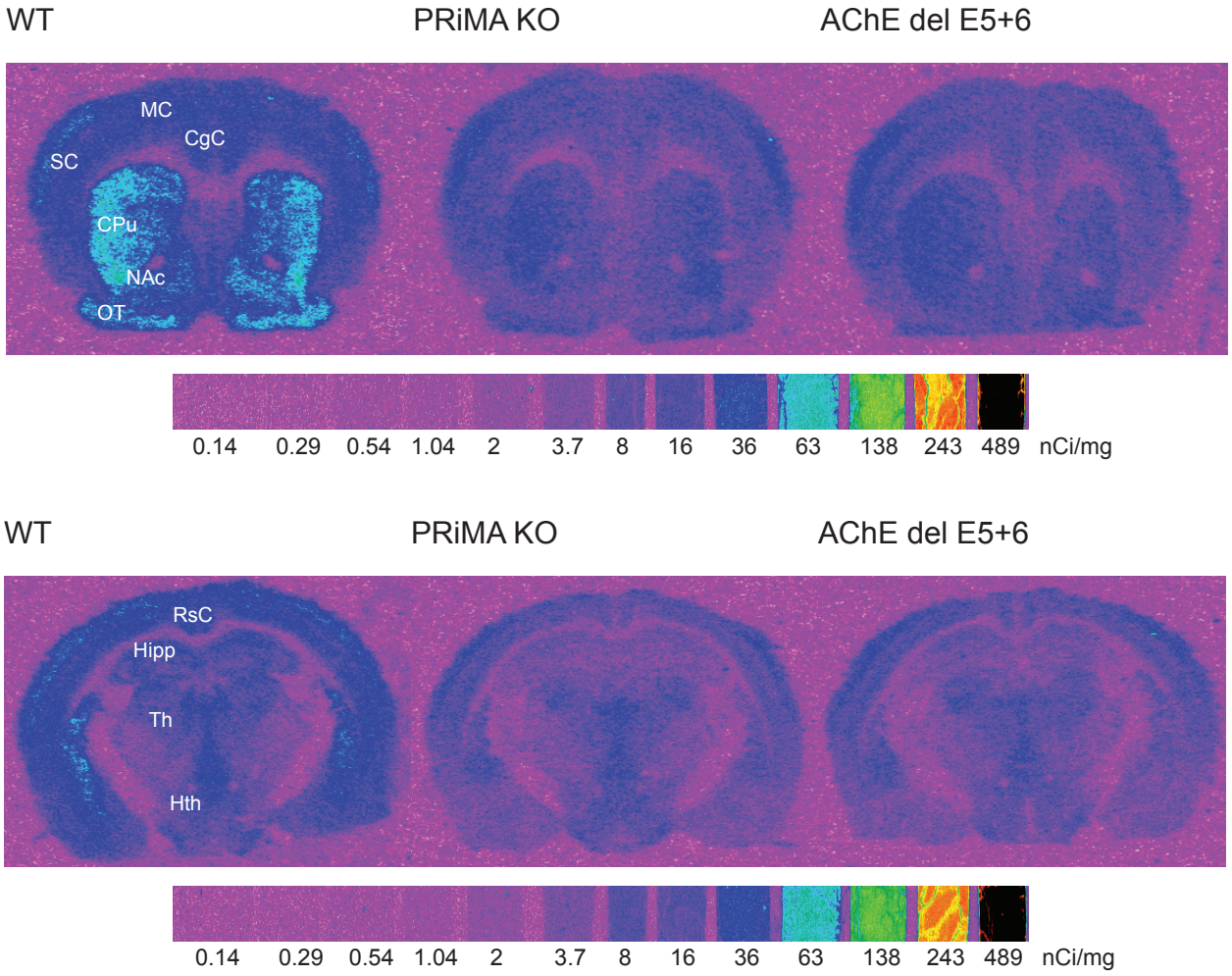

Fig. 20. Illustrative autoradiograms of [^{3}H]-AFDX-384 binding in coronal brain sections in PRiMA KO, AChE delE5+6 and WT mice.

MC, motor cortex; SC, somatosensory cortex; CgC, cingulatae cortex; RsC, retrosplenial cortex; OT, olfactory tubercle; CPu, caudate putamen; NAc, nucleus accumbens; Hipp, dorsal hippocampus; Th, thalamus; Hth, hypothalamus.

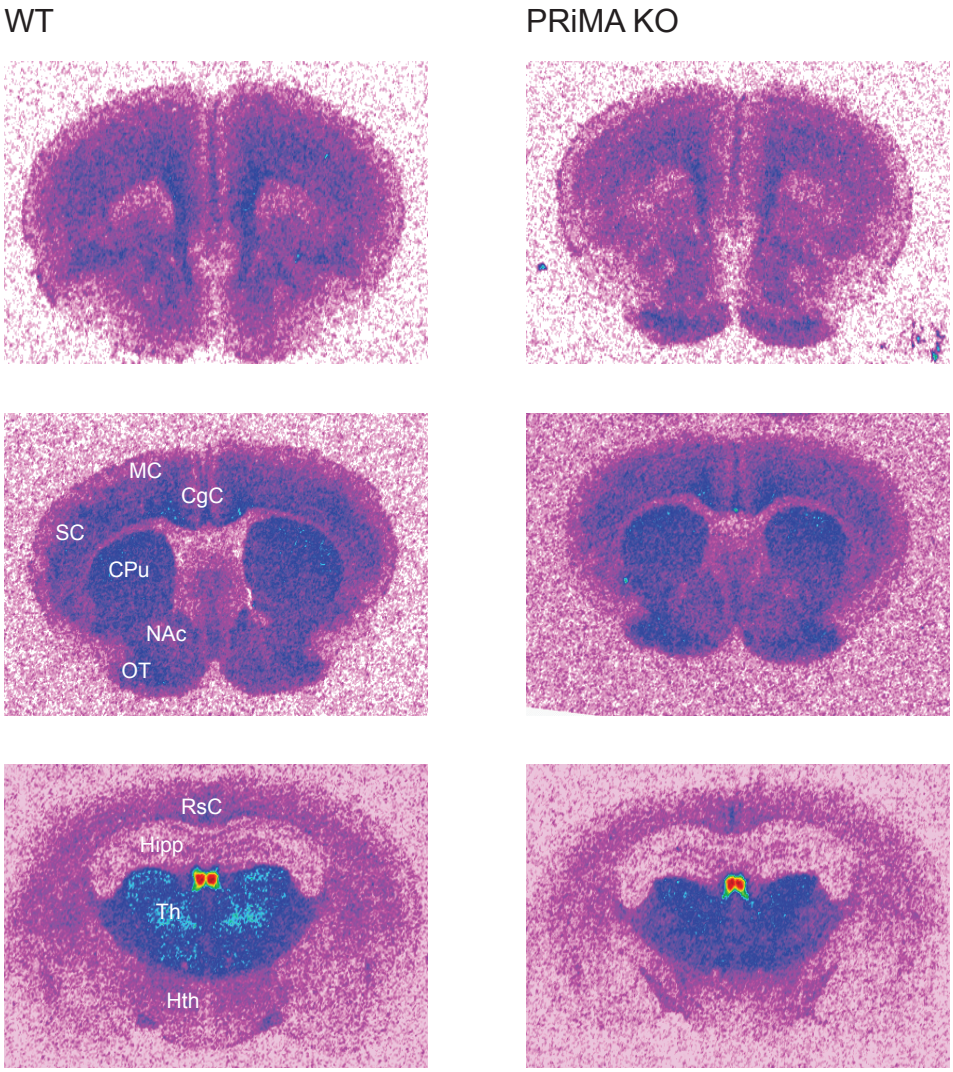

Fig. 21. Illustrative autoradiograms of [^{125}I]-epibatidine binding in coronal brain sections in PRiMA KO and WT mice.

PrlC, prelimbic cortex; MC, motor cortex; SC, somatosensory cortex; CgC, cingulatae cortex; RsC, retrosplenial cortex; OT, olfactory tubercle; CPu, caudate putamen; NAc, nucleus accumbens; Hipp, dorsal hippocampus; Th, thalamus; Hth, hypothalamus.

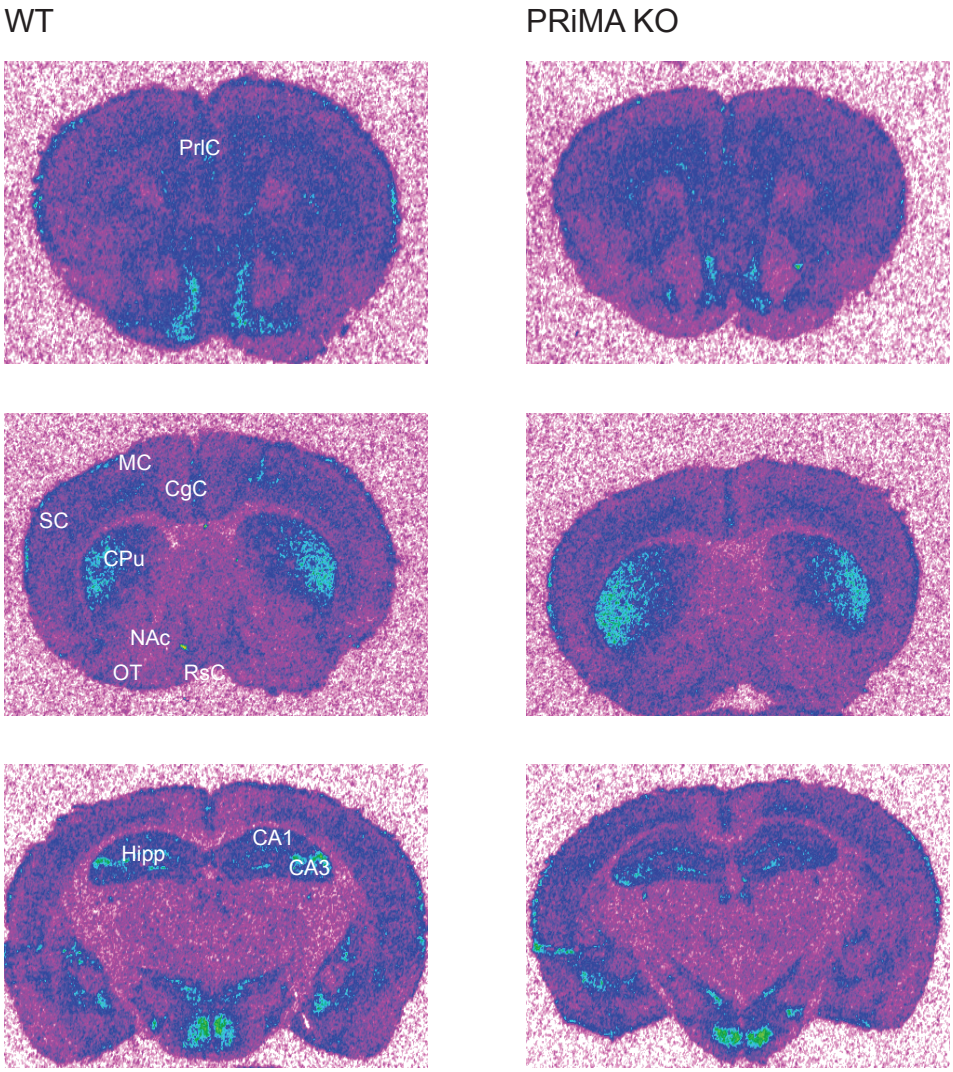

Fig. 22. Illustrative autoradiograms of [^{125}I]-α-bungarotoxin binding in coronal brain sections in PRiMA KO and WT mice.

PrlC, prelimbic cortex; MC, motor cortex; SC, somatosensory cortex; CgC, cingulatae cortex; RsC, retrosplenial cortex; OT, olfactory tubercle; CPu, caudate putamen; NAc, nucleus accumbens; Hipp, dorsal hippocampus; CA1; CA3, CA1, CA3 field of Hipp.

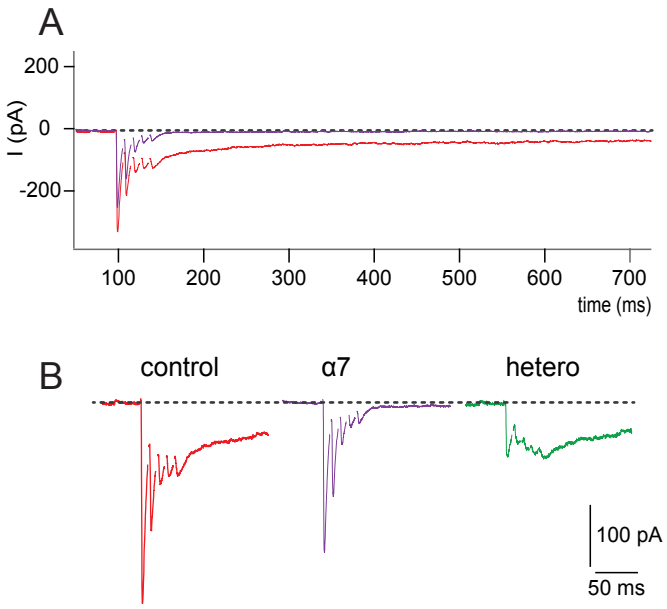

Fig. 23. Functional changes to synaptic transmission at the motoneuron-Renshaw cell synapse of PRiMA KO mice.

Recordings were obtained with spinal cord slices from P8 PRiMA KO mice. EPSCs were triggered by a train of 5 pulses applied to the ventral root at a frequency of 100 Hz in the presence of D-APV (50 µM) and NBQX (2 µM) to block glutamatergic currents. The membrane potential was held at -45 mV.

A The upper traces correspond to the control recording obtained before (red) and after (violet) the addition of 10 µM DHßE. DHßE eliminated both an early component and a very slowly decaying current. The current persisting after the addition of DHßE displayed rapid kinetics (rapid rise, rapid decay) and the repetition of the stimulus at 100 Hz induced a depression. This pattern is characteristic of α7 responses. The response persisting after the addition of DHßE was blocked by MLA (10 nM; not shown).

B The lower right trace (green, hetero) indicates the difference between control and DHßE and corresponds to the response of heteromeric nicotinic receptors. The ratio of the DHßE-sensitive and MLA-sensitive components was markedly different in the two examples, and such differences are also observed in WT mice.

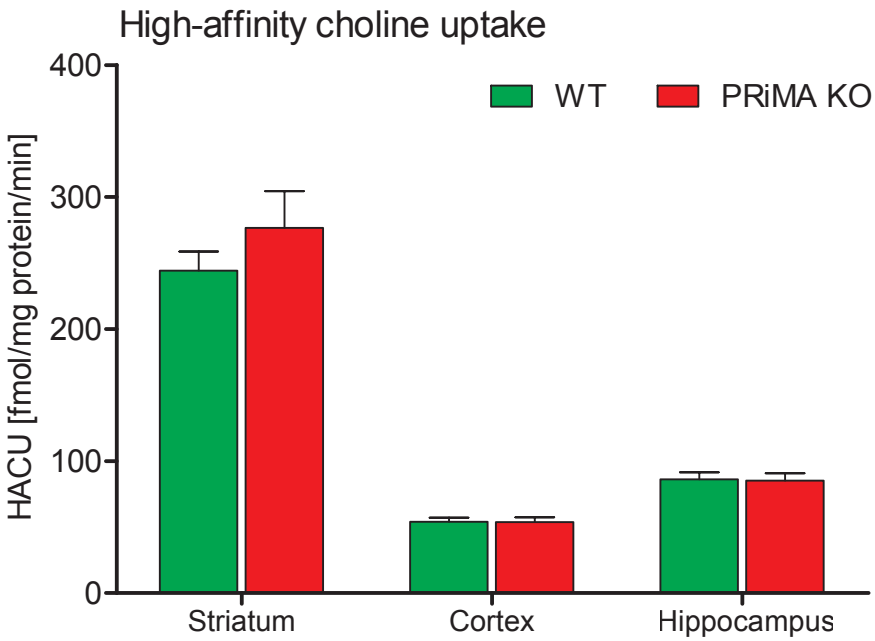

Fig. 24. [^{3}H]-choline uptake by high-affinity choline transporter (HACU) in synaptosomal preparations prepared from striatum, hippocampus and cortex of PRiMA KO and WT mice.

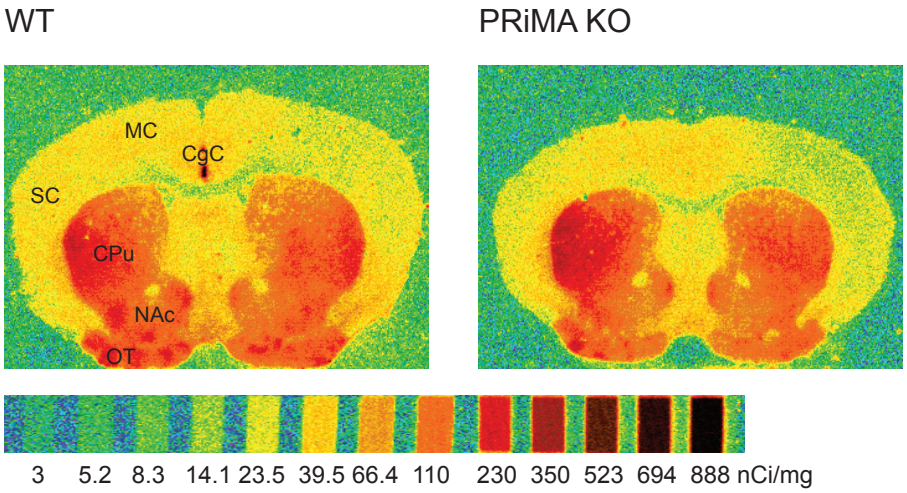

Fig. 25. Illustrative autoradiograms of [^{3}H]-hemicholinium-3 binding in coronal brain sections in PRiMA KO and WT mice.

MC, motor cortex; SC, somatosensory cortex; CgC, cingulatae cortex; OT, olfactory tubercle; CPu, caudate putamen; NAc, nucleus accumbens.

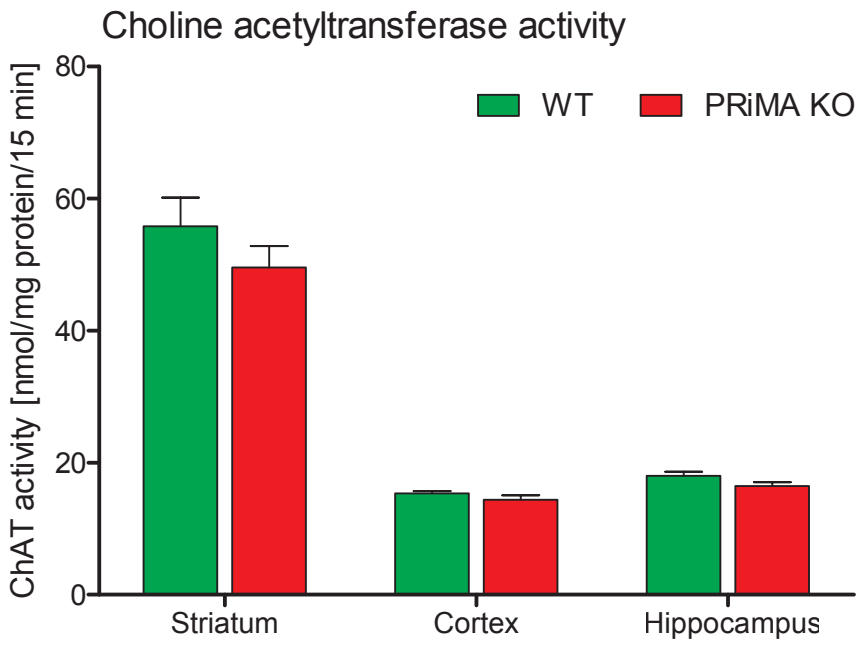

Fig. 26. Choline acetyltransferase activity in homogenates prepared from striatum, hippocampus and cortex of PRiMA KO and WT mice.

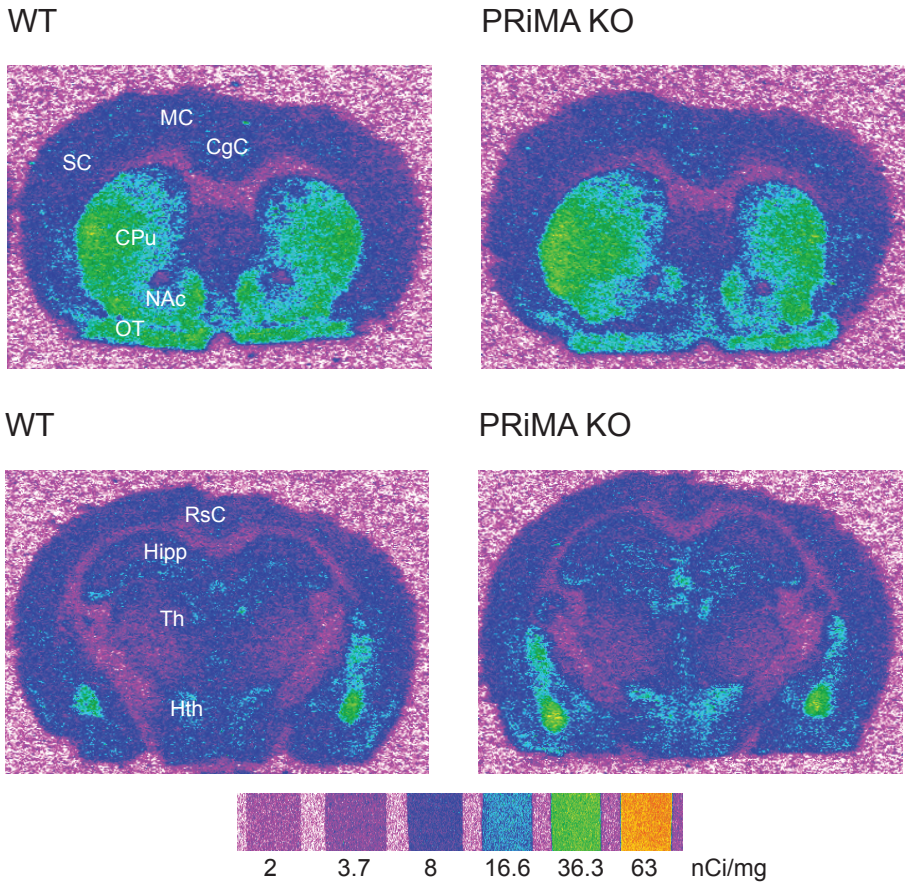

Fig. 27. Illustrative autoradiograms of [^{3}H]-vesamicol binding in coronal brain sections in PRiMA KO and WT mice.

MC, motor cortex; SC, somatosensory cortex; CgC, cingulatae cortex; RsC, retrosplenial cortex; OT, olfactory tubercle; CPu, caudate putamen; NAc, nucleus accumbens; Hipp, dorsal hippocampus; Th, thalamus; Hth, hypothalamus.

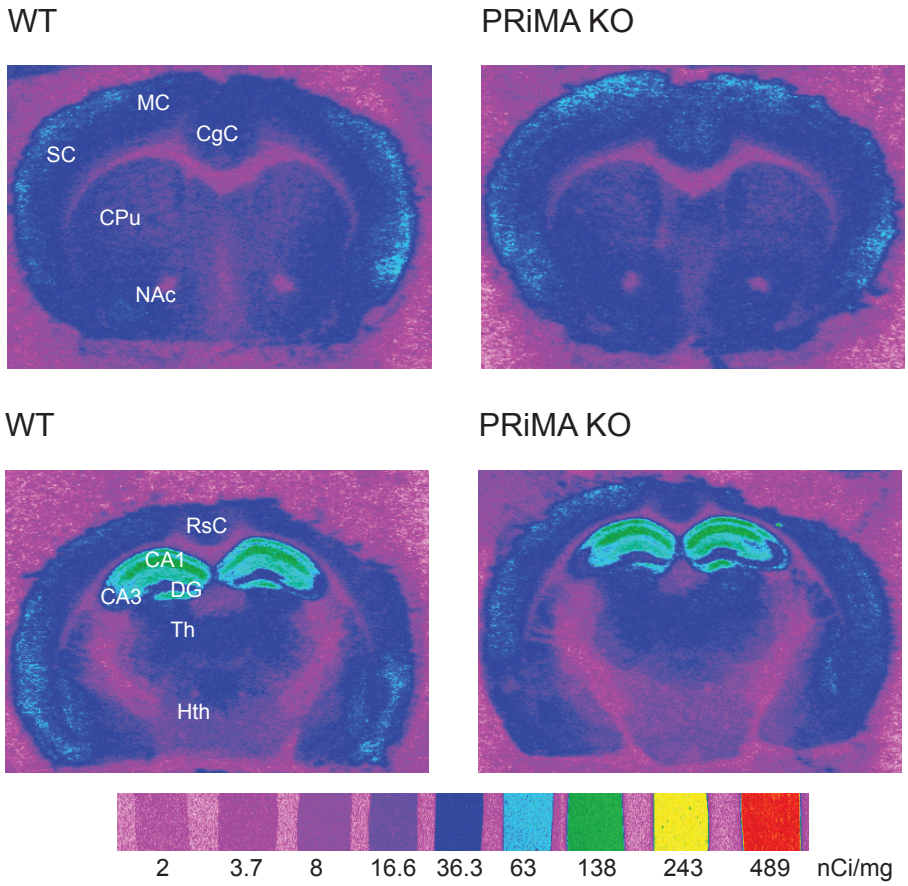

Fig. 28. Illustrative autoradiograms of [^{3}H]-CGP-39653 binding in coronal brain sections in PRiMA KO and WT mice.

MC, motor cortex; SC, somatosensory cortex; CgC, cingulatae cortex; RsC, retrosplenial cortex; CPu, caudate putamen; NAc, nucleus accumbens; Hipp, dorsal hippocampus; CA1; CA3, CA1, CA3 field of Hipp; DG, dentate gyrus; Th, thalamus; Hth, hypothalamus.

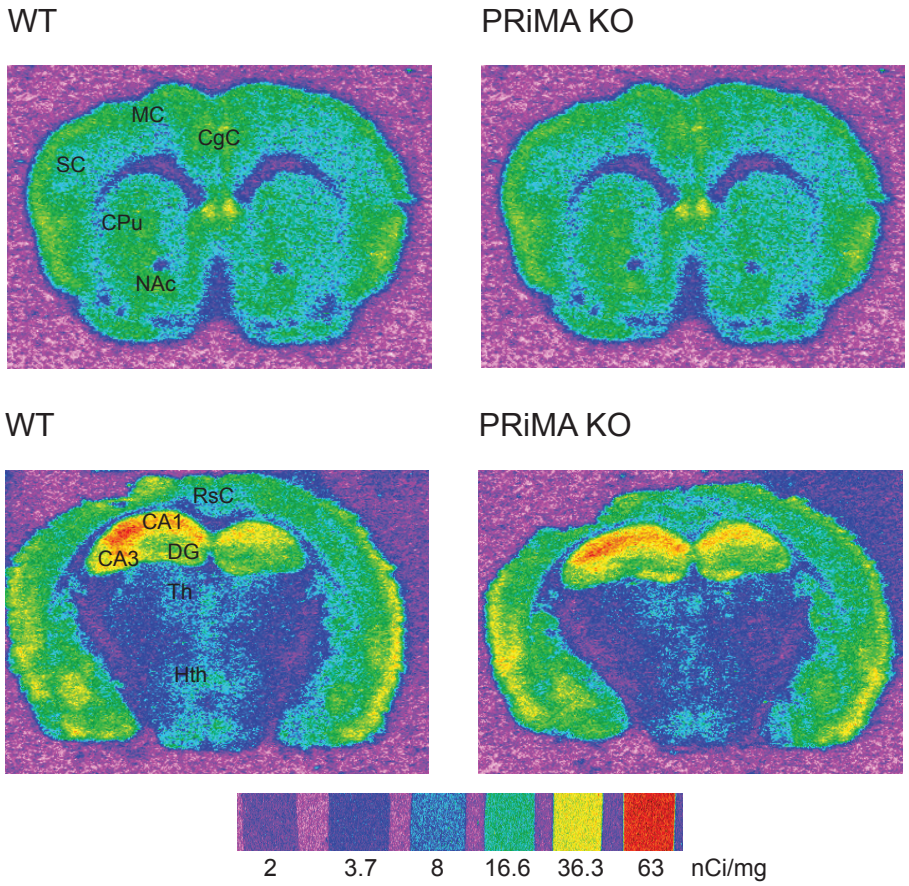

Fig. 29. Illustrative autoradiograms of [^{3}H]-AMPA binding in coronal brain sections in PRiMA KO and WT mice.

MC, motor cortex; SC, somatosensory cortex; CgC, cingulatae cortex; RsC, retrosplenial cortex; CPu, caudate putamen; NAc, nucleus accumbens; Hipp, dorsal hippocampus; CA1; CA3, CA1, CA3 field of Hipp; DG, dentate gyrus; Th, thalamus; Hth, hypothalamus.

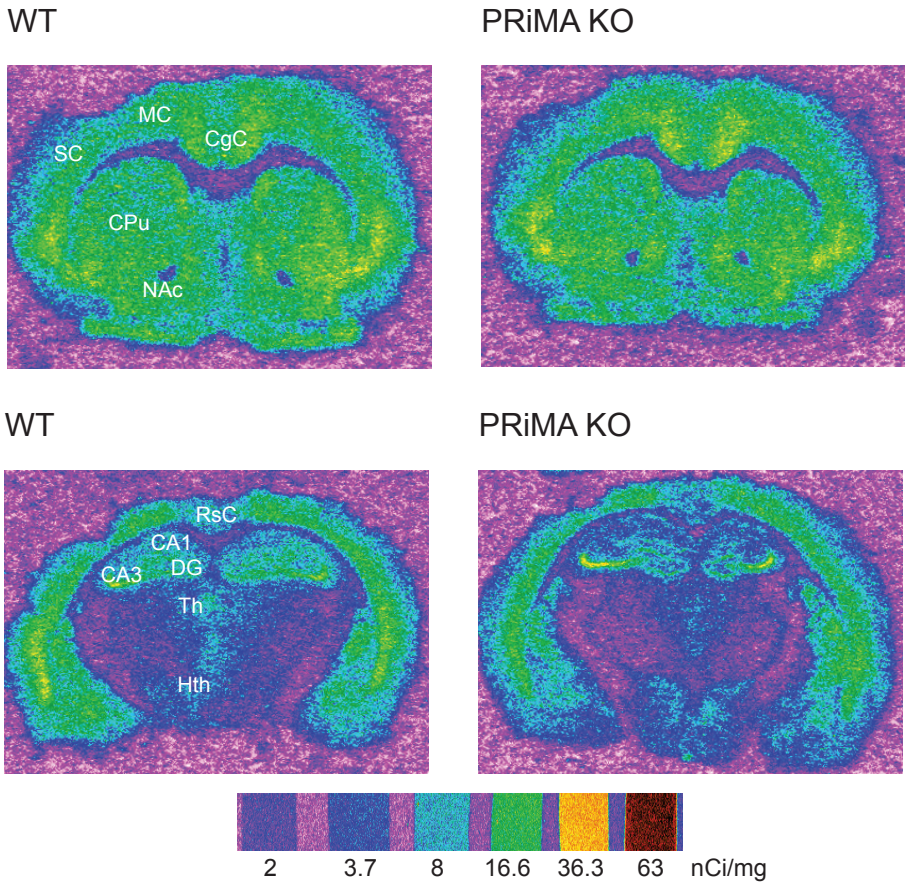

Fig. 30. Illustrative autoradiograms of [^{3}H]-kainate binding in coronal brain sections in PRiMA KO and WT mice.

MC, motor cortex; SC, somatosensory cortex; CgC, cingulatae cortex; RsC, retrosplenial cortex; CPu, caudate putamen; NAc, nucleus accumbens; Hipp, dorsal hippocampus; CA1; CA3, CA1, CA3 field of Hipp; DG, dentate gyrus; Th, thalamus; Hth, hypothalamus.

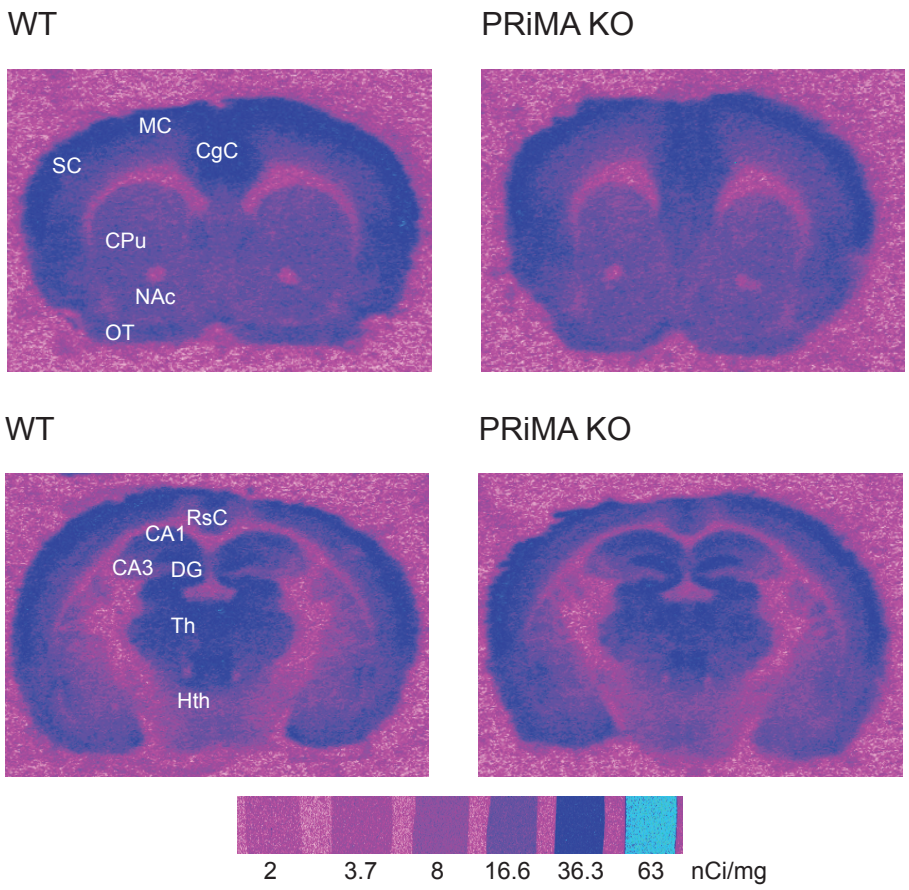

Fig. 31. Illustrative autoradiograms of [^{3}H]-muscimol binding in coronal brain sections in PRiMA KO and WT mice.

[^{3}H]-muscimol is a specific ligand to identify the $GABA_A$ receptor in brain section.

MC, motor cortex; SC, somatosensory cortex; CgC, cingulatae cortex; RsC, retrosplenial cortex; CPu, caudate putamen; NAc, nucleus accumbens; Hipp, dorsal hippocampus; CA1; CA3, CA1, CA3 field of Hipp; DG, dentate gyrus; Th, thalamus; Hth, hypothalamus.

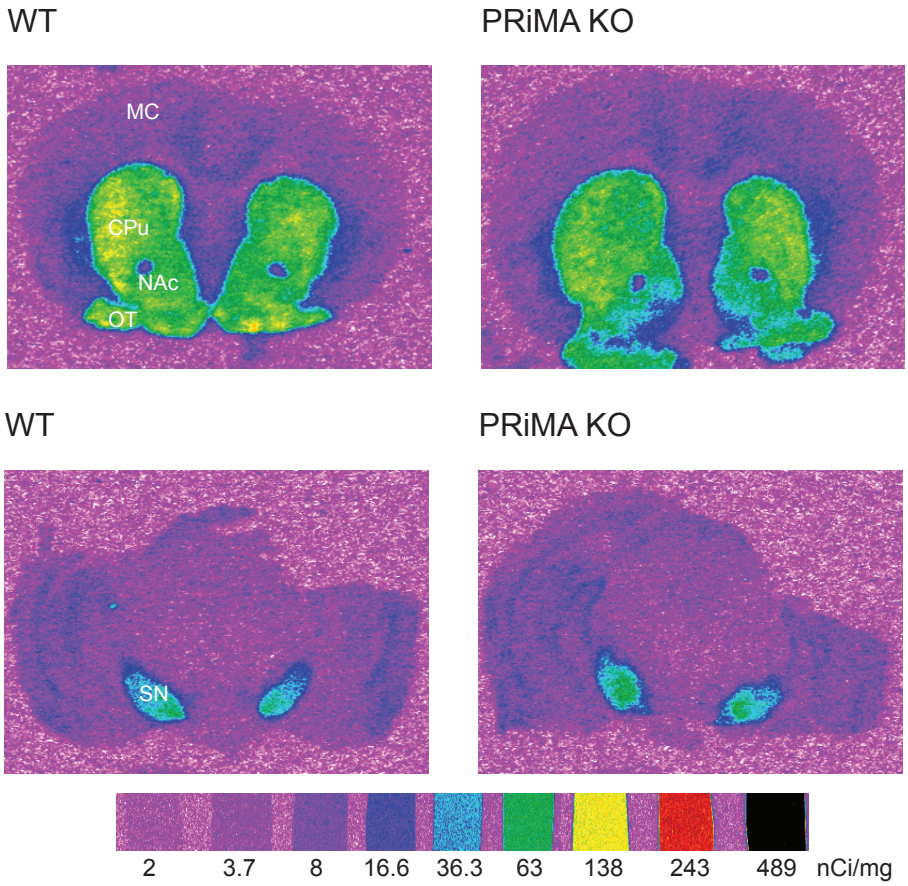

Fig. 32. Illustrative autoradiograms of [^{3}H]-SCH-23390 binding in coronal brain sections in PRiMA KO and WT mice.

MC, motor cortex; OT, olfactory tubercle; CPu, caudate putamen; NAc, nucleus accumbens; SN, substantia nigra.

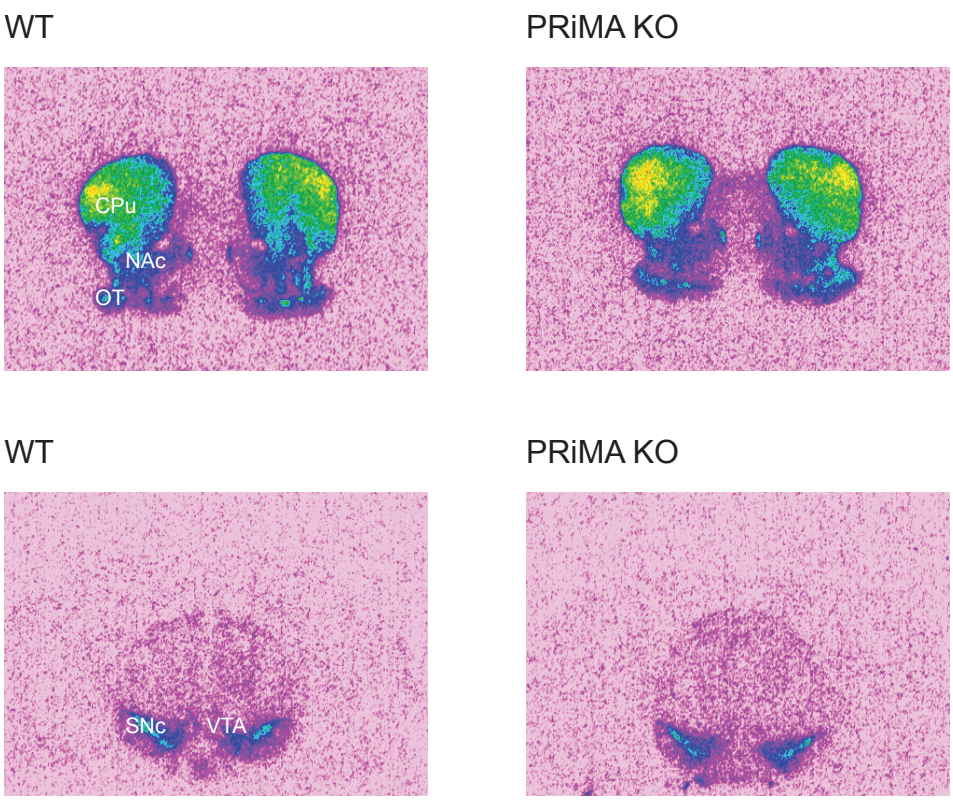

Fig. 33. Illustrative autoradiograms of [^{125}I]-iodosulpride binding in coronal brain sections in PRiMA KO and WT mice.

OT, olfactory tubercle; CPu, caudate putamen; NAc, nucleus accumbens; SNc, substantia nigra pars compacta; VTA, ventral tegmental area.

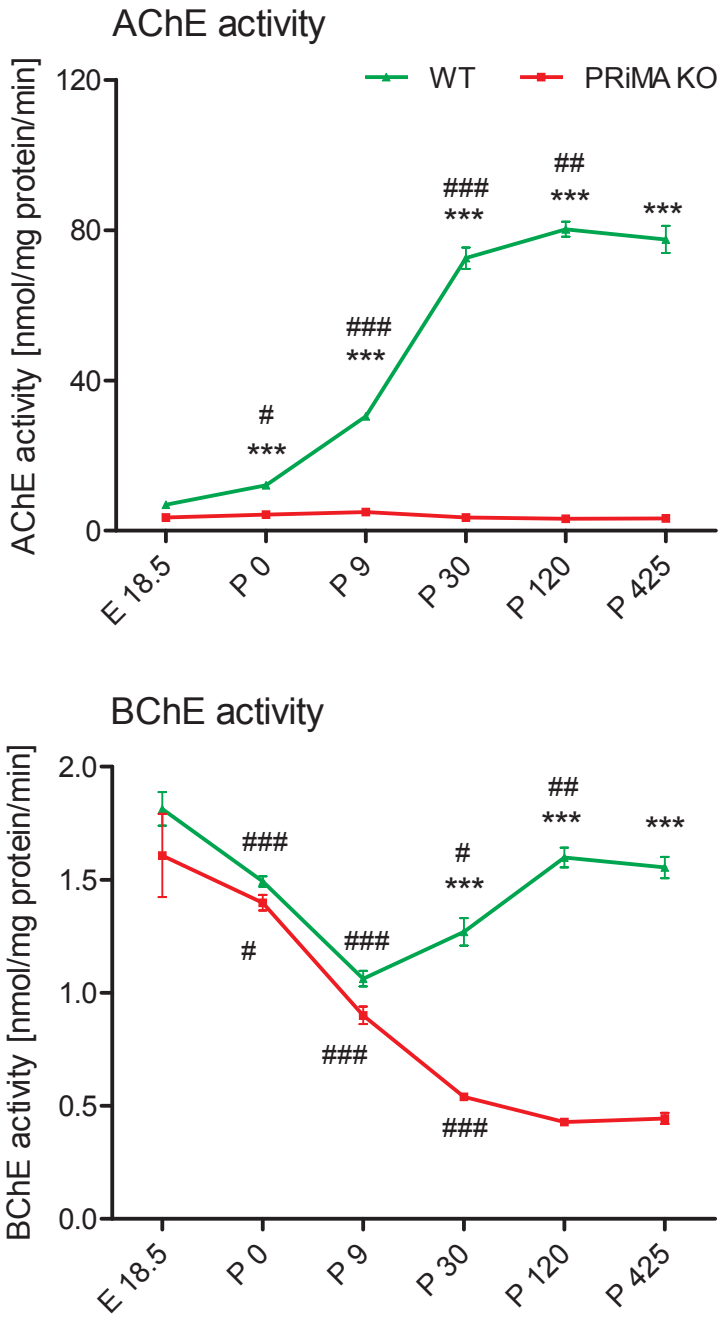

Fig. 34. Ontogenic development of AChE and BChE activity in the brain of PRiMA KO and WT mice.

Top: The ontogenic development of AChE activity in the brain of PRiMA KO and WT mice. **Bottom:** The ontogenci development of BChE activity in the brain of PRiMA KO and WT mice. Abbreviations: E18.5, embryonal day 18.5; P0, postnatal day 0; P9, postnatal day 9; P30, postnatal day 30; P120, postnatal day 120; P425, postnatal day 425. Three mice of each genotype were analysed. The statistical differences among groups were determined by two-way ANOVA: for multiple comparisons an adjusted t-test modified Student-Newman-Keuls correction was used. ***$p<0.001$, significant difference between PRiMA KO and WT mice. #$p<0.05$, ##$p<0.01$, ###$p<0.001$ significantly different from previous day of development.

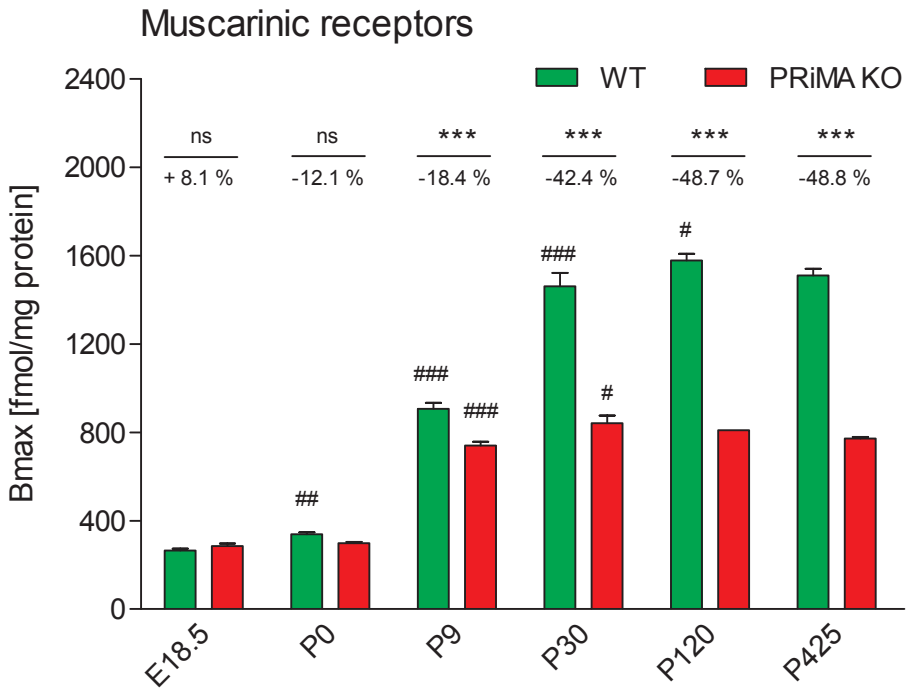

Fig. 35. Ontogenic development of the total density of MR in the brain of PRiMA KO and WT mice.

The ontogenic development of the total number of binding sites of MR (B_{max}) in the brain plasma membranes of PRiMA WT and PRiMA KO mice. The density of MR was determined by radioligand binding assay with [^{3}H]-QNB, a non-selective antagonist of MR. Abbreviations: E18.5, embryonal day 18.5 (n=9); P0, postnatal day 0 (n=9); P9, postnatal day 9 (n=8); P30, postnatal day 30 (n=5); P120, postnatal day 120 (n=3); P425, postnatal day 425 (n=4). The number of mice in each group and for each genotype is indicated in the parentheses. The statistical differences among groups were determined by two-way ANOVA: for multiple comparisons an adjusted t-test modified Student-Newman-Keuls correction was used. ns, not significant. ***p<0.001, significant difference between PRiMA KO and WT mice. #p<0.05, ##p<0.01, ###p<0.001 significantly different from previous day of development.

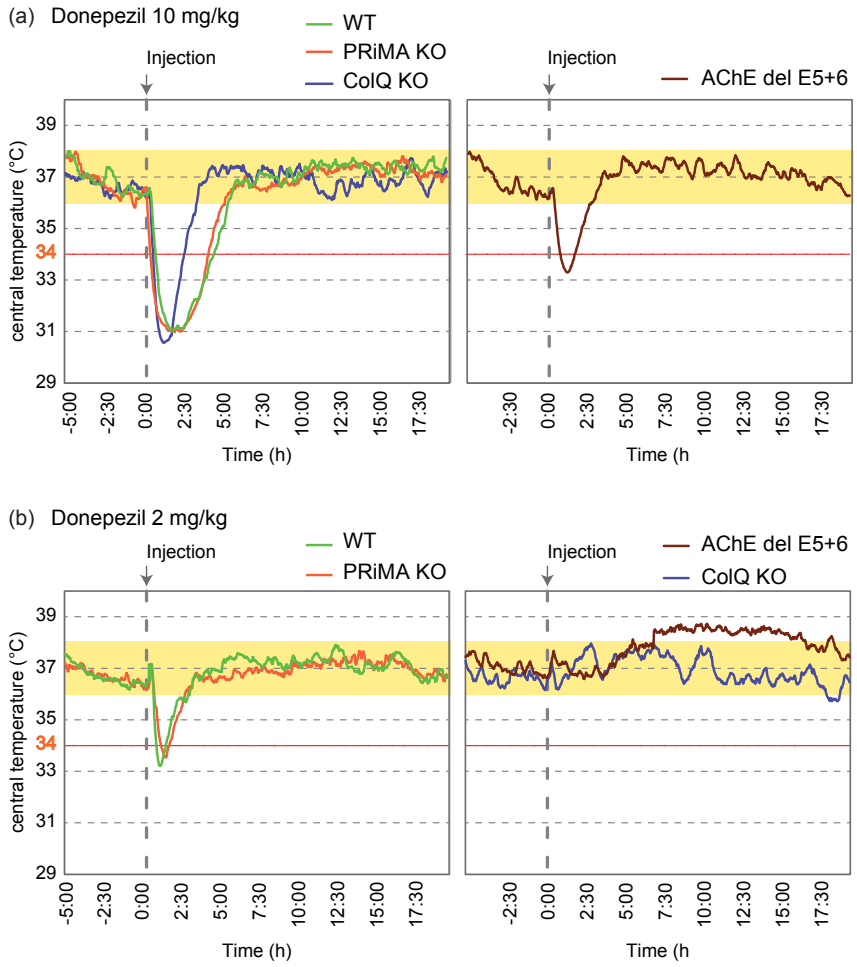

Fig. 36. Donepezil-induced hypothermic responses in mice strains with deficits in AChE activity.

(a) At a dose 2 mg/kg, donepezil-induced hypothermic responses in PRiMA KO mice are comparable to that seen in WT mice. At the same dose of donepezil, ColQ KO mice showed faster recovery from hypothermia and AChE del E5+6 were significantly resistant to donepezil-induced hypothermia. (b) At a dose 10 mg/kg, donepezil triggered similar hypothermia in PRiMA KO and WT mice. By contrast, in ColQ KO and AChE del E5+6 mice donepezil had no effect on core body temperature.

• TABLES

Table 1

Static and dynamic paramters of the gait of PRiMA KO and WT mice

			WT mice	PRiMA KO mice	p-level
walking speed (cm/s)			35.91 ± 3.51	28.37 ± 2.16	>0.05
regularity index (%)			99.79 ± 0.14	99.71 ± 0.15	>0.05
time between initial and maximal contact (s)		fore	$3.36\times10^{-2} \pm 3.08\times10^{-3}$	$4.3\times10^{-2} \pm 3.14\times10^{-3}$	0.0412
		hind	$3.57\times10^{-2} \pm 2.31\times10^{-3}$	$4.5\times10^{-2} \pm 5.92\times10^{-3}$	>0.05
paw angle (deg)		fore	17.86 ± 5.12	10.04 ± 2.29	>0.05
		hind	16.03 ± 3.31	21.79 ± 5.12	>0.05
stride length (mm)		fore	65.39 ± 3.21	62.89 ± 2.04	>0.05
		hind	65.00 ±3.28	63.21 ± 2.03	>0.05
stand duration (s)		fore	$1.05\times10^{-1} \pm 8.14\times10^{-3}$	$1.24\times10^{-1} \pm 9.07\times10^{-3}$	>0.05
		hind	$1.08\times10^{-1} \pm 8.19\times10^{-1}$	$1.29\times10^{-1} \pm 8.92\times10^{-3}$	>0.05
swing duration (s)		fore	$9.11\times10^{-2} \pm 3.42\times10^{-3}$	$1.13\times10^{-1} \pm 4.65\times10^{-3}$	0.0025
		hind	$8.56\times10^{-2} \pm 2.74\times10^{-3}$	$1.09\times10^{-1} \pm 4.73\times10^{-3}$	0.0037
swing speed (m/s)		fore	$7.51\times10^{-1} \pm 5.61\times10^{-2}$	$5.91\times10^{-1} \pm 3.51\times10^{-2}$	0.0338
		hind	$7.98\times10^{-1} \pm 5.86\times10^{-2}$	$6.17\times10^{-1} \pm 4.13\times10^{-2}$	0.0275
base of support (mm)		fore	$9.91 \pm 5.46\times10^{-1}$	$10.75 \pm 4.68\times10^{-1}$	>0.05
		hind	16.54 ± 1.07	$17.74 \pm 5.82\times10^{-1}$	>0.05
print position (mm)		right	$1.82 \pm 6.48\times10^{-1}$	$3.56\times10^{-2} \pm 4.34\times10^{-1}$	0.0338
		left	$1.54 \pm 5.96\times10^{-1}$	$4.07\times10^{-1} \pm 5.14\times10^{-1}$	>0.05
support (%)	zero		0 ± 0	0.5 ± 0.23	>0.05
	single		3.23 ± 1.5	5.16 ± 1.46	>0.05
	diagonal		75.35 ± 2.53	73.33 ± 2.09	>0.05
	lateral		1.15 ± 0.48	2.0 ± 0.39	>0.05
	girdle		0.99 ± 0.39	1.23 ± 0.32	>0.05
	three		16.34 ± 3.19	16.02 ± 2.9	>0.05
	four		2.94 ± 0.82	1.76 ± 0.63	>0.05

Table 2
Relative autoradiographic densities of [^{3}H]-QNB binding in coronal brain sections of WT and PRiMA KO mice

Brain region	Relative density		% variation
	WT	PRiMA KO	
MC	106.3 ± 2.3	65.4 ± 1.5	-38.5***
SC	106.7 ± 3.5	71.5 ± 2.1	-33.0***
CgC	118.3 ± 4.4	65.6 ± 2.0	-44.5***
RsC	93.8 ± 4.2	48.6 ± 1.5	-48.2***
VC	117.7 ± 4.1	74.0 ± 1.8	-37.1***
AC	113.8 ± 3.8	68.2 ± 1.4	-40.1***
OT	167.0 ± 6.0	63.0 ± 3.8	-62.3***
CPu	205.3 ± 7.0	83.7 ± 2.0	-59.2***
NAc	179.1 ± 8.2	76.5 ± 2.2	-57.3***
Hipp	141.0 ± 5.3	84.4 ± 2.6	-40.1***
Th	45.4 ± 2.1	35.0 ± 1.0	-22.9***
Hth	50.4 ± 1.3	39.2 ± 1.4	-22.2***

Values represent means ± SEM of specific radioligand binding from 6 mice in each group, expressed in units of apparent nCi/mg protein, as determined from densitometric analysis. MC, motor cortex; SC, somatosensory cortex; CgC, cingulatae cortex; RsC, retrosplenial cortex; VC, visual cortex; AC, auditory cortex; OT, olfactory tubercle; CPu, caudate putamen; NAc, nucleus accumbens; Hipp, dorsal hippocampus; Th, thalamus; Hth, hypothalamus. Statistical significance was evaluated with Student's t test. ***$p < 0.001$.

Table 3
Relative autoradiographic densities of [^{3}H]-NMS binding in coronal brain sections of WT and PRiMA KO mice

Brain region	Relative density		% variation
	WT	PRiMA KO	
MC	97.0 ± 2.5	59.3 ± 1.0	-38.9***
SC	92.1 ± 2.1	56.2 ± 1.8	-39.0***
CgC	111.0 ± 3.0	58.8 ± 0.7	-47.0***
RsC	75.6 ± 2.4	37.9 ± 1.0	-49.9***
VC	96.0 ± 2.6	56.5 ± 1.6	-41.1***
AC	94.1 ± 3.4	56.5 ± 1.4	-40.0***
OT	144.0 ± 4.7	50.8 ± 1.8	-64.7***
CPu	187.3 ± 5.0	71.2 ± 0.7	-62.0***
NAc	157.0 ± 4.0	58.8 ± 0.7	-62.5***
Hipp	111.8 ± 2.5	62.9 ± 1.3	-43.7***
Th	36.8 ± 0.7	29.0 ± 0.6	-21.2***
Hth	39.2 ± 0.6	30.6 ± 0.5	-21.9***

Values represent means ± SEM of specific radioligand binding from 6 mice in each group, expressed in units of apparent nCi/mg protein, as determined from densitometric analysis. MC, motor cortex; SC, somatosensory cortex; CgC, cingulatae cortex; RsC, retrosplenial cortex; VC, visual cortex; AC, auditory cortex; OT, olfactory tubercle; CPu, caudate putamen; NAc, nucleus accumbens; Hipp, dorsal hippocampus; Th, thalamus; Hth, hypothalamus. Statistical significance was evaluated with Student's t test. ***$p < 0.001$.

Table 4
Relative autoradiographic densities of [^{3}H]-QNB binding in coronal brain sections of WT, PRiMA KO and AChE del E5+6 mice

Brain region	Relative density			% variation	
	WT	PRiMA KO	AChE del E5+6	PRiMA KO	AChE del E5+6
MC	45.9 ± 1.4	29.3 ± 0.2	32.3 ± 0.8	-36.0***	-30.0***
SC	50.7 ± 1.3	30.2 ± 0.2	33.7 ± 0.9	-40.0***	-34.0***
OT	84.5 ± 3.2	31.2 ± 1.0	33.1 ± 0.2	-63.0***	-61.0***
CPu	82.3 ± 2.8	34.3 ± 1.2	36.4 ± 0.9	-58.0***	-56.0***
NAc	85.0 ± 0.6	31.3 ± 0.3	32.8 ± 1.3	-63.0***	-61.0***
Hipp	57.4 ± 0.6	36.4 ± 0.8	39.3 ± 1.4	-37.0***	-32.0***
Th	19.0 ± 0.7	15.8 ± 0.5	15.7 ± 0.6	-15.0**	-17.0**
Hth	20.4 ± 0.2	18.1 ± 0.3	17.6 ± 0.5	-12.0**	-14.0**

Values represent means ± SEM of specific radioligand binding from 6 mice in each group, expressed in units of apparent nCi/mg protein, as determined from densitometric analysis. MC, motor cortex; SC, somatosensory cortex; OT, olfactory tubercle; CPu, caudate putamen; NAc, nucleus accumbens; Hipp, dorsal hippocampus; Th, thalamus; Hth, hypothalamus. Statistical significance was evaluated with Student's t test. ***$p < 0.001$, **$p < 0.01$.

Table 5

Relative autoradiographic densities of [^{3}H]-pirenzepine binding in coronal brain sections of WT, PRiMA KO and AChE del E5+6 mice

Brain region	Relative density			% variation	
	WT	PRiMA KO	AChE del E5+6	PRiMA KO	AChE del E5+6
MC	12.6 ± 0.6	9.3 ± 0.1	9.1 ± 0.2	-26.0***	-28.0***
SC	12.1 ± 0.3	8.8 ± 0.3	8.9 ± 0.3	-27.0***	-26.0***
OT	21.8 ± 0.6	11.6 ± 0.5	11.1 ± 0.2	-47.0***	-49.0***
CPu	21.9 ± 0.6	11.8 ± 0.6	11.2 ± 0.4	-46.0***	-49.0***
NAc	23.0 ± 0.8	11.2 ± 0.2	11.7 ± 0.4	-51.0***	-49.0***
Hipp	24.7 ± 0.5	16.3 ± 0.4	17.3 ± 0.4	-34.0***	-30.0***

Values represent means ± SEM of specific radioligand binding from 6 mice in each group, expressed in units of apparent nCi/mg protein, as determined from densitometric analysis. MC, motor cortex; SC, somatosensory cortex; OT, olfactory tubercle; CPu, caudate putamen; NAc, nucleus accumbens; Hipp, dorsal hippocampus. Statistical significance was evaluated with Student's t test. ***$p < 0.001$.

Table 6
Relative autoradiographic densities of [^{3}H]-AFDX-384 binding in coronal brain sections of WT, PRiMA KO and AChE del E5+6 mice

Brain region	Relative density			% variation	
	WT	PRiMA KO	AChE del E5+6	PRiMA KO	AChE del E5+6
MC	16.7 ± 0.9	11.0 ± 0.3	11.2 ± 0.5	-34.0***	-33.0***
SC	20.4 ± 0.5	13.6 ± 0.8	13.2 ± 0.3	-33.0***	-35.0***
OT	33.0 ± 1.6	10.5 ± 0.5	8.3 ± 0.4	-68.0***	-75.0***
CPu	38.0 ± 1.3	13.2 ± 0.7	12.0 ± 0.5	-65.0***	-68.0***
NAc	32.5 ± 1.6	10.8 ± 0.9	9.3 ± 0.8	-67.0***	-71.0***
Hipp	12.3 ± 0.8	6.2 ± 0.2	7.1 ± 0.3	-50.0***	-42.0***
Th	11.3 ± 0.3	8.8 ± 0.3	9.0 ± 0.3	-23.0**	-20.0**
Hth	11.4 ± 0.3	9.7 ± 0.8	9.9 ± 0.3	-15.0**	-13.0**

Values represent means ± SEM of specific radioligand binding from 6 mice in each group, expressed in units of apparent nCi/mg protein, as determined from densitometric analysis. MC, motor cortex; SC, somatosensory cortex; OT, olfactory tubercle; CPu, caudate putamen; NAc, nucleus accumbens; Hipp, dorsal hippocampus; Th, thalamus; Hth, hypothalamus. Statistical significance was evaluated with Student's t test. ***$p < 0.001$, **$p < 0.01$.

Table 7
Relative autoradiographic densities of [^{125}I]-epibatidine binding in coronal brain sections of WT and PRiMA KO mice

Brain region	Relative density		% variation
	WT	PRiMA KO	
MC	93.5 ± 2.1	78.3 ± 2.2	-16.3***
SC	92.2 ± 3.3	75.0 ± 1.9	-18.7**
CgC	105.3 ± 1.7	88.2 ± 1.6	-16.2***
RsC	180.8 ± 5.5	149.9 ± 5.9	-17.1**
PrlC	93.3 ± 2.6	76.2 ± 2.5	-18.3***
OT	102.6 ± 2.6	101.3 ± 4.1	-1.3 ns
CPu	136.9 ± 2.4	127.3 ± 2.3	-7.0*
NAc	105.5 ± 2.9	88.3 ± 1.3	-16.3***
Th	436.3 ± 16.7	360.5 ± 8.9	-17.4**
Hth	96.1 ± 2.6	77.0 ± 2.0	-19.9***

Values represent means ± SEM of specific radioligand binding from 6 mice in each group, expressed in arbitrary units, as determined from densitometric analysis. MC, motor cortex; SC, somatosensory cortex; CgC, cingulatae cortex; RsC, retrosplenial cortex; PrlC, prelimbic cortex; OT, olfactory tubercle; CPu, caudate putamen; NAc, nucleus accumbens; Th, thalamus; Hth, hypothalamus. Statistical significance was evaluated with Student's t test. *$p < 0.05$,**$p < 0.01$, ***$p < 0.001$, ns (not significant).

Table 8
Relative autoradiographic densities of [^{125}I]-α-bungarotoxin binding in coronal brain sections of WT and PRiMA KO mice

Brain region	Relative density		% variation
	WT	PRiMA KO	
MC	79.1 ± 3.4	76.9 ± 2.4	-2.8 ns
SC	81.6 ± 3.2	77.7 ± 2.8	-4.8 ns
CgC	80.6 ± 2.4	78.8 ± 4.6	-2.2 ns
PrlC	88.8 ± 4.5	86.9 ± 4.1	-2.1 ns
OT	37.8 ± 2.7	46.3 ± 3.4	+22.5 ns
CPu	145.7 ± 11.5	152.1 ± 6.7	+4.4 ns
NAc	38.4 ± 2.2	42.1 ± 2.9	+9.6 ns
Hipp	114.0 ± 5.1	96.5 ± 4.8	-15.4*
CA1	96.0 ± 5.5	77.6 ± 4.2	-19.3*
CA3	133.2 ± 5.6	130.3 ± 4.7	-2.2 ns

Values represent means ± SEM of specific radioligand binding from 6 mice in each group, expressed in arbitrary units, as determined from densitometric analysis. MC, motor cortex; SC, somatosensory cortex; CgC, cingulatae cortex; PrlC, prelimbic cortex; OT, olfactory tubercle; CPu, caudate putamen; NAc, nucleus accumbens; Hipp, dorsal hippocampus; CA1; CA3, CA1, CA3 field of Hipp. Statistical significance was evaluated with Student's t test. *$p < 0.05$, ns (not significant).

Table 9
Relative autoradiographic densities of [^{3}H]-hemicholinium-3 binding in coronal brain sections of WT and PRiMA KO mice

Brain region	Relative density		% variation
	WT	PRiMA KO	
MC	16.9 ± 1.4	15.5 ± 0.6	-8.3 ns
SC	14.4 ± 1.2	13.5 ± 0.6	-6.3 ns
CgC	20.0 ± 1.7	15.3 ± 0.9	-23.5 ns
OT	99.9 ± 14.0	84.9 ± 5.9	-15.0 ns
CPu	87.4 ± 11.2	97.7 ± 9.7	+11.8 ns
NAc	85.8 ± 10.7	75.3 ± 4.3	-12.2 ns

Values represent means ± SEM of specific radioligand binding from 6 mice in each group, expressed in units of apparent nCi/mg protein, as determined from densitometric analysis. MC, motor cortex; SC, somatosensory cortex; CgC, cingulatae cortex; OT, olfactory tubercle; CPu, caudate putamen; NAc, nucleus accumbens. Statistical significance was evaluated with Student's t test. *$p < 0.05$, ns (not significant).

Table 10
Relative autoradiographic densities of [^{3}H]-vesamicol binding in coronal brain sections of WT and PRiMA KO mice

Brain region	Relative density		% variation
	WT	PRiMA KO	
MC	9.4 ± 0.3	9.9 ± 0.2	+5.3 ns
SC	8.1 ± 0.3	8.0 ± 0.4	-1.2 ns
CgC	10.1 ± 0.4	10.9 ± 1.1	+7.9 ns
RsC	8.9 ± 0.4	8.3 ± 0.6	-6.7 ns
OT	21.5 ± 1.1	21.1 ± 0.8	-1.9 ns
CPu	21.1 ± 0.7	21.5 ± 0.4	+1.9 ns
NAc	20.2 ± 1.0	19.2 ± 0.6	-5.0 ns
Hipp	9.5 ± 0.2	9.0 ± 0.3	-5.3 ns
Th	8.5 ± 0.4	7.8 ± 0.3	-8.2 ns
Hth	11.1 ± 0.3	10.8 ± 0.3	-2.7 ns

Values represent means ± SEM of specific radioligand binding from 6 mice in each group, expressed in units of apparent nCi/mg protein, as determined from densitometric analysis. MC, motor cortex; SC, somatosensory cortex; CgC, cingulatae cortex; RsC, retrosplenial cortex; OT, olfactory tubercle; CPu, caudate putamen; NAc, nucleus accumbens; Hipp, dorsal hippocampus; Th, thalamus; Hth, hypothalamus. Statistical significance was evaluated with Student's t test. *$p < 0.05$, ns (not significant).

Table 11
Relative autoradiographic densities of [^{3}H]-CGP-39653 binding in coronal brain sections of WT and PRiMA KO mice

Brain region	Relative density		% variation
	WT	PRiMA KO	
MC	30.9 ± 1.2	31.0 ± 1.6	0.0 ns
SC	30.0 ± 0.8	31.3 ± 0.8	+4.3 ns
CgC	35.7 ± 2.0	32.3 ± 1.6	-9.5 ns
RsC	22.3 ± 1.1	21.3 ± 1.1	-4.5 ns
CPu	17.8 ± 1.0	17.1 ± 1.1	-3.9 ns
NAc	22.6 ± 1.0	21.9 ± 1.3	-3.1 ns
Hipp	62.2 ± 3.9	60.9 ± 2.8	-2.1 ns
CA1	89.7 ± 2.0	89.1 ± 3.1	-0.7 ns
CA3	49.7 ± 2.4	50.0 ± 2.8	+0.6 ns
DG	58.6 ± 2.3	59.0 ± 2.3	+0.7 ns
Th	22.3 ± 0.6	22.5 ± 0.7	+0.9 ns
Hth	8.3 ± 0.8	8.2 ± 0.9	-1.2 ns

Values represent means ± SEM of specific radioligand binding from 6 mice in each group, expressed in units of apparent nCi/mg protein, as determined from densitometric analysis. MC, motor cortex; SC, somatosensory cortex; CgC, cingulatae cortex; RsC, retrosplenial cortex; CPu, caudate putamen; NAc, nucleus accumbens; Hipp, dorsal hippocampus; CA1; CA3 CA1, CA3 field of Hipp; DG, dentate gyrus; Th, thalamus; Hth, hypothalamus. Statistical significance was evaluated with Student's t test. *$p < 0.05$, ns (not significant).

Table 12
Relative autoradiographic densities of [^{3}H]-AMPA binding in coronal brain sections of WT and PRiMA KO mice

Brain region	Relative density		% variation
	WT	PRiMA KO	
MC	14.2 ± 0.5	14.2 ± 0.6	0.0 ns
SC	14.1 ± 0.7	14.2 ± 0.3	+0.7 ns
CgC	16.5 ± 0.7	15.1 ± 0.8	-8.5 ns
RsC	9.0 ± 0.4	8.9 ± 0.3	-1.1 ns
CPu	13.5 ± 0,4	13.0 ± 0.4	-3.7 ns
NAc	14.5 ± 2.6	15.0 ± 1.7	+3.5 ns
Hipp	28.2 ± 1.6	29.0 ± 1.1	+2.8 ns
CA1	35.7 ± 1.8	36.1 ± 1.4	+1.1 ns
CA3	24.6 ± 1.1	23.4 ± 0.7	-4.9 ns
DG	23.0 ± 1.7	24.4 ± 0.7	+6.1 ns
Th	3.7 ± 0.2	3.6 ± 0.2	-2.7 ns
Hth	5.0 ± 0.5	4.3 ± 0.5	-14.0 ns

Values represent means ± SEM of specific radioligand binding from 6 mice in each group, expressed in units of apparent nCi/mg protein, as determined from densitometric analysis. MC, motor cortex; SC, somatosensory cortex; CgC, cingulatae cortex; RsC, retrosplenial cortex; CPu, caudate putamen; NAc, nucleus accumbens; Hipp, dorsal hippocampus; CA1, CA3 CA1, CA3 field of Hipp; DG, dentate gyrus; Th, thalamus; Hth, hypothalamus. Statistical significance was evaluated with Student's t test. *$p < 0.05$, ns (not significant).

Table 13
Relative autoradiographic densities of [^{3}H]-kainate binding in coronal brain sections of WT and PRiMA KO mice

Brain region	Relative density		% variation
	WT	PRiMA KO	
MC	11.7 ± 0.5	12.2 ± 0.3	+4.3 ns
SC	10.5 ± 0.3	10.1 ± 0.3	-3.8 ns
CgC	14.9 ± 0.5	15.3 ± 0.6	+2.7 ns
RsC	6.5 ± 0.2	5.9 ± 0.1	-9.2 ns
CPu	13.7 ± 0.4	13.2 ± 0.3	-3.7 ns
NAc	15.9 ± 0.6	14.8 ± 0.6	-6.9 ns
Hipp	7.5 ± 0.2	6.8 ± 0.3	-9.3 ns
CA1	5.4 ± 0.3	5.0 ± 0.2	-7.4 ns
CA3	11.0 ± 0.	10.6 ± 0.6	-3.6 ns
DG	8.7 ± 0.4	7.8 ± 0.3	-10.4 ns
Th	2.9 ± 0.1	2.6 ± 0.1	-10.4 ns
Hth	6.6 ± 0.6	6.2 ± 0.2	-6.1 ns

Values represent means ± SEM of specific radioligand binding from 6 mice in each group, expressed in units of apparent nCi/mg protein, as determined from densitometric analysis. MC, motor cortex; SC, somatosensory cortex; CgC, cingulatae cortex; RsC, retrosplenial cortex; CPu, caudate putamen; NAc, nucleus accumbens; Hipp, dorsal hippocampus; CA1, CA3 CA1, CA3 field of Hipp; DG, dentate gyrus; Th, thalamus; Hth, hypothalamus. Statistical significance was evaluated with Student's t test. *$p < 0.05$, ns (not significant).

Table 14
Relative autoradiographic densities of [^{3}H]-muscimol binding in coronal brain sections of WT and PRiMA KO mice

Brain region	Relative density		% variation
	WT	PRiMA KO	
MC	23.5 ± 1.1	23.2 ± 0.6	-1.3 ns
SC	25.5 ± 0.9	25.1 ± 0.6	-1.6 ns
CgC	32.4 ± 1.3	30.6 ± 0.9	-5.6 ns
RsC	21.6 ± 1.1	20.9 ± 0.9	-3.2 ns
CPu	13.9 ± 0.6	13.5 ± 0.3	-2.9 ns
NAc	14.3 ± 0.4	14.4 ± 0.2	+0.7 ns
Hipp	22.9 ± 0.6	23.3 ± 0.6	+1.8 ns
CA1	28.7 ± 0.8	28.0 ± 1.4	-2.4 ns
CA3	11.6 ± 0.4	11.5 ± 0.4	-0.9 ns
DG	27.4 ± 0.7	28.4 ± 1.1	+3.7 ns
Th	28.6 ± 1.0	26.4 ± 0.5	-7.7 ns
Hth	10.7 ± 0.4	9.7 ± 0.2	-9.4 ns

Values represent means ± SEM of specific radioligand binding from 6 mice in each group, expressed in units of apparent nCi/mg protein, as determined from densitometric analysis. MC, motor cortex; SC, somatosensory cortex; CgC, cingulatae cortex; RsC, retrosplenial cortex; CPu, caudate putamen; NAc, nucleus accumbens; Hipp, dorsal hippocampus; CA1; CA3 CA1, CA3 field of Hipp; DG, dentate gyrus; Th, thalamus; Hth, hypothalamus. Statistical significance was evaluated with Student's t test. *$p < 0.05$, ns (not significant).

Table 15
Relative autoradiographic densities of [^{3}H]-SCH-23390 binding in coronal brain sections of WT and PRiMA KO mice

Brain region	Relative density		% variation
	WT	PRiMA KO	
MC	4.3 ± 0.1	4.9 ± 0.5	+14.0 ns
OT	78.7 ± 3.0	80.0 ± 2.5	+4.7 ns
CPu	101.9 ± 3.9	96.9 ± 3.1	-4.9 ns
NAc	74.3 ± 4.0	77.1 ± 4.7	+3.9 ns
SN	43.1 ± 0.6	44.3 ± 0.6	+2.8 ns

Values represent means ± SEM of specific radioligand binding from 6 mice in each group, expressed in units of apparent nCi/mg protein, as determined from densitometric analysis. MC, motor cortex; OT, olfactory tubercle; CPu, caudate putamen; NAc, nucleus accumbens; SN, substantia nigra. Statistical significance was evaluated with Student's t test. *$p < 0.05$, ns (not significant).

Table 16
Relative autoradiographic densities of [^{125}I]-iodosulpride binding in coronal brain sections of WT and PRiMA KO mice

Brain region	Relative density		% variation
	WT	PRiMA KO	
lGP	34.9 ± 2.7	33.9 ± 0.9	-3.0 ns
Hth	15.7 ± 0.2	16.6 ± 0.4	+5.6 ns
SNc	50.6 ± 7.9	50.8 ± 2.6	+0.5 ns
VTA	37.9 ± 1.4	37.0 ± 1.3	-0.6 ns
OT	94.2 ± 1.0	93.2 ± 4.0	-2.2 ns
CPu	231.2 ± 9.9	239.2 ± 7.1	+3.5 ns
Nac	100.7 ± 5.7	94.6 ± 2.8	-6.1 ns

Values represent means ± SEM of specific radioligand binding from 6 mice in each group, expressed in arbitrary units, as determined from densitometric analysis. lGP, lateral globulus pallidus; Hth, hypothalamus; SNc, substantia nigra pars compacta; VTA, ventral tegmental area; OT, olfactory tubercle; CPu, caudate putamen; NAc, nucleus accumbens. Statistical significance was evaluated with Student's t test. *$p < 0.05$, ns (not significant).

• REFERENCES

Acquas, E., Wilson, C., and Fibiger, H.C. (1996). Conditioned and unconditioned stimuli increase frontal cortical and hippocampal acetylcholine release: effects of novelty, habituation, and fear. J. Neurosci. *16*, 3089–3096.

Adler, M., Manley, H.A., Purcell, A.L., Deshpande, S.S., Hamilton, T.A., Kan, R.K., Oyler, G., Lockridge, O., Duysen, E.G., and Sheridan, R.E. (2004). Reduced acetylcholine receptor density, morphological remodeling, and butyrylcholinesterase activity can sustain muscle function in acetylcholinesterase knockout mice. Muscle Nerve *30*, 317–327.

Adler, M., Sweeney, R.E., Hamilton, T.A., Lockridge, O., Duysen, E.G., Purcell, A.L., and Deshpande, S.S. (2011). Role of acetylcholinesterase on the structure and function of cholinergic synapses: insights gained from studies on knockout mice. Cell. Mol. Neurobiol. *31*, 909–920.

Albin, R.L., Howland, M.M., Higgins, D.S., and Frey, K.A. (1994). Autoradiographic quantification of muscarinic cholinergic synaptic markers in bat, shrew, and rat brain. Neurochem. Res. *19*, 581–589.

Alkondon, M., Pereira, E.F., and Albuquerque, E.X. (1998). alpha-bungarotoxin- and methyllycaconitine-sensitive nicotinic receptors mediate fast synaptic transmission in interneurons of rat hippocampal slices. Brain Res. *810*, 257–263.

An, J.J., Bae, M.-H., Cho, S.R., Lee, S.-H., Choi, S.-H., Lee, B.H., Shin, H.-S., Kim, Y.N., Park, K.W., Borrelli, E., et al. (2004). Altered GABAergic neurotransmission in mice lacking dopamine D2 receptors. Mol. Cell. Neurosci. *25*, 732–741.

Anagnostaras, S.G., Maren, S., and Fanselow, M.S. (1995). Scopolamine selectively disrupts the acquisition of contextual fear conditioning in rats. Neurobiol Learn Mem *64*, 191–194.

Anagnostaras, S.G., Murphy, G.G., Hamilton, S.E., Mitchell, S.L., Rahnama, N.P., Nathanson, N.M., and Silva, A.J. (2003). Selective cognitive dysfunction in acetylcholine M1 muscarinic receptor mutant mice. Nat. Neurosci. *6*, 51–58.

Antonelli, T., Beani, L., Bianchi, C., Pedata, F., and Pepeu, G. (1981). Changes in synaptosomal high affinity choline uptake following electrical stimulation of guinea-pig cortical slices: effect of atropine and physostigmine. Br. J. Pharmacol. *74*, 525–531.

Aosaki, T., Miura, M., Suzuki, T., Nishimura, K., and Masuda, M. (2010). Acetylcholine-dopamine balance hypothesis in the striatum: an update. Geriatr Gerontol Int *10 Suppl 1*, S148–157.

Apparsundaram, S., Martinez, V., Parikh, V., Kozak, R., and Sarter, M. (2005). Increased capacity and density of choline transporters situated in synaptic membranes of the right medial prefrontal cortex of attentional task-performing rats. J. Neurosci. *25*, 3851–3856.

Araki, T., Tanji, H., Fujihara, K., Kato, H., Imai, Y., Mizugaki, M., and Itoyama, Y. (2000). Sequential changes of cholinergic and dopaminergic receptors in brains after 6-hydroxydopamine lesions of the medial forebrain bundle in rats. J Neural Transm *107*, 873–884.

Arroyo, S., Bennett, C., Aziz, D., Brown, S.P., and Hestrin, S. (2012). Prolonged disynaptic inhibition in the cortex mediated by slow, non-α7 nicotinic excitation of a specific subset of cortical interneurons. J. Neurosci. *32*, 3859–3864.

Ayata, C., Ayata, G., Hara, H., Matthews, R.T., Beal, M.F., Ferrante, R.J., Endres, M., Kim, A., Christie, R.H., Waeber, C., et al. (1997). Mechanisms of reduced striatal NMDA excitotoxicity in type I nitric oxide synthase knock-out mice. J. Neurosci. *17*, 6908–6917.

Azam, L., and McIntosh, J.M. (2006). Characterization of nicotinic acetylcholine receptors that modulate nicotine-evoked [3H]norepinephrine release from mouse hippocampal synaptosomes. Mol. Pharmacol. *70*, 967–976.

Aznavour, N., Watkins, K.C., and Descarries, L. (2005). Postnatal development of the cholinergic innervation in the dorsal hippocampus of rat: Quantitative light and electron microscopic

immunocytochemical study. J. Comp. Neurol. *486*, 61–75.

Baddick, C.G., and Marks, M.J. (2011). An autoradiographic survey of mouse brain nicotinic acetylcholine receptors defined by null mutants. Biochem. Pharmacol. *82*, 828–841.

Beeri, R., Andres, C., Lev-Lehman, E., Timberg, R., Huberman, T., Shani, M., and Soreq, H. (1995). Transgenic expression of human acetylcholinesterase induces progressive cognitive deterioration in mice. Curr. Biol. *5*, 1063–1071.

Belbeoc'h, S., Massoulié, J., and Bon, S. (2003). The C-terminal T peptide of acetylcholinesterase enhances degradation of unassembled active subunits through the ERAD pathway. EMBO J. *22*, 3536–3545.

Belbeoc'h, S., Falasca, C., Leroy, J., Ayon, A., Massoulié, J., and Bon, S. (2004). Elements of the C-terminal t peptide of acetylcholinesterase that determine amphiphilicity, homomeric and heteromeric associations, secretion and degradation. Eur. J. Biochem. *271*, 1476–1487.

Bell, K.A., Shim, H., Chen, C.-K., and McQuiston, A.R. (2011). Nicotinic excitatory postsynaptic potentials in hippocampal CA1 interneurons are predominantly mediated by nicotinic receptors that contain α4 and β2 subunits. Neuropharmacology *61*, 1379–1388.

Berkeley, J.L., Gomeza, J., Wess, J., Hamilton, S.E., Nathanson, N.M., and Levey, A.I. (2001). M1 muscarinic acetylcholine receptors activate extracellular signal-regulated kinase in CA1 pyramidal neurons in mouse hippocampal slices. Mol. Cell. Neurosci. *18*, 512–524.

Bernard, V., Legay, C., Massoulie, J., and Bloch, B. (1995). Anatomical analysis of the neurons expressing the acetylcholinesterase gene in the rat brain, with special reference to the striatum. Neuroscience *64*, 995–1005.

Bernard, V., Laribi, O., Levey, A.I., and Bloch, B. (1998). Subcellular redistribution of m2 muscarinic acetylcholine receptors in striatal interneurons in vivo after acute cholinergic stimulation. J. Neurosci. *18*, 10207–10218.

Bernard, V., Levey, A.I., and Bloch, B. (1999). Regulation of the subcellular distribution of m4 muscarinic acetylcholine receptors in striatal neurons in vivo by the cholinergic environment: evidence for regulation of cell surface receptors by endogenous and exogenous stimulation. J. Neurosci. *19*, 10237–10249.

Bernard, V., Brana, C., Liste, I., Lockridge, O., and Bloch, B. (2003). Dramatic depletion of cell surface m2 muscarinic receptor due to limited delivery from intracytoplasmic stores in neurons of acetylcholinesterase-deficient mice. Mol. Cell. Neurosci. *23*, 121–133.

Bernard, V., Décossas, M., Liste, I., and Bloch, B. (2006). Intraneuronal trafficking of G-protein-coupled receptors in vivo. Trends Neurosci. *29*, 140–147.

Bernard, V., Girard, E., Hrabovska, A., Camp, S., Taylor, P., Plaud, B., and Krejci, E. (2011). Distinct localization of collagen Q and PRiMA forms of acetylcholinesterase at the neuromuscular junction. Mol. Cell. Neurosci. *46*, 272–281.

Berrard, S., Varoqui, H., Cervini, R., Israël, M., Mallet, J., and Diebler, M.F. (1995). Coregulation of two embedded gene products, choline acetyltransferase and the vesicular acetylcholine transporter. J. Neurochem. *65*, 939–942.

Biberoglu, K., Schopfer, L.M., Tacal, O., and Lockridge, O. (2012). The proline-rich tetramerization peptides in equine serum butyrylcholinesterase. FEBS J. *279*, 3844–3858.

Biberoglu, K., Schopfer, L.M., Saxena, A., Tacal, O., and Lockridge, O. (2013). Polyproline tetramer organizing peptides in fetal bovine serum acetylcholinesterase. Biochim. Biophys. Acta *1834*, 745–753.

Blackmer, T., Larsen, E.C., Takahashi, M., Martin, T.F., Alford, S., and Hamm, H.E. (2001). G protein betagamma subunit-mediated presynaptic inhibition: regulation of exocytotic fusion downstream of Ca2+ entry. Science *292*, 293–297.

Blackmer, T., Larsen, E.C., Bartleson, C., Kowalchyk, J.A., Yoon, E.-J., Preininger, A.M., Alford, S., Hamm, H.E., and Martin, T.F.J. (2005). G protein betagamma directly regulates SNARE protein fusion

machinery for secretory granule exocytosis. Nat. Neurosci. *8*, 421–425.

Blondet, B., Carpentier, G., Ferry, A., Chatonnet, A., and Courty, J. (2010). Localization of butyrylcholinesterase at the neuromuscular junction of normal and acetylcholinesterase knockout mice. J. Histochem. Cytochem. *58*, 1075–1082.

Boer, S., Sanchez, D., Reinieren, I., van den Boom, T., Udawela, M., Scarr, E., Ganfornina, M.D., and Dean, B. (2010). Decreased kainate receptors in the hippocampus of apolipoprotein D knockout mice. Prog. Neuropsychopharmacol. Biol. Psychiatry *34*, 271–278.

Bolam, J.P., Hanley, J.J., Booth, P.A., and Bevan, M.D. (2000). Synaptic organisation of the basal ganglia. J. Anat. *196 (Pt 4)*, 527–542.

Bon, S., and Massoulié, J. (1997). Quaternary associations of acetylcholinesterase. I. Oligomeric associations of T subunits with and without the amino-terminal domain of the collagen tail. J. Biol. Chem. *272*, 3007–3015.

Bon, S., Coussen, F., and Massoulié, J. (1997). Quaternary associations of acetylcholinesterase. II. The polyproline attachment domain of the collagen tail. J. Biol. Chem. *272*, 3016–3021.

Bon, S., Dufourcq, J., Leroy, J., Cornut, I., and Massoulié, J. (2004). The C-terminal t peptide of acetylcholinesterase forms an alpha helix that supports homomeric and heteromeric interactions. Eur. J. Biochem. *271*, 33–47.

Bonsi, P., Martella, G., Cuomo, D., Platania, P., Sciamanna, G., Bernardi, G., Wess, J., and Pisani, A. (2008). Loss of muscarinic autoreceptor function impairs long-term depression but not long-term potentiation in the striatum. J. Neurosci. *28*, 6258–6263.

Bonsi, P., Cuomo, D., Martella, G., Madeo, G., Schirinzi, T., Puglisi, F., Ponterio, G., and Pisani, A. (2011). Centrality of striatal cholinergic transmission in Basal Ganglia function. Front Neuroanat *5*, 6.

Boudinot, E., Emery, M.J., Mouisel, E., Chatonnet, A., Champagnat, J., Escourrou, P., and Foutz, A.S. (2004). Increased ventilation and CO2 chemosensitivity in acetylcholinesterase knockout mice. Respir Physiol Neurobiol *140*, 231–241.

Boudinot, E., Bernard, V., Camp, S., Taylor, P., Champagnat, J., Krejci, E., and Foutz, A.S. (2009). Influence of differential expression of acetylcholinesterase in brain and muscle on respiration. Respir Physiol Neurobiol *165*, 40–48.

Brandon, E.P., Lin, W., D'Amour, K.A., Pizzo, D.P., Dominguez, B., Sugiura, Y., Thode, S., Ko, C.-P., Thal, L.J., Gage, F.H., et al. (2003). Aberrant patterning of neuromuscular synapses in choline acetyltransferase-deficient mice. J. Neurosci. *23*, 539–549.

Brown, D.A. (2010). Muscarinic acetylcholine receptors (mAChRs) in the nervous system: some functions and mechanisms. J. Mol. Neurosci. *41*, 340–346.

Buchanan, K.A., Petrovic, M.M., Chamberlain, S.E.L., Marrion, N.V., and Mellor, J.R. (2010). Facilitation of long-term potentiation by muscarinic M(1) receptors is mediated by inhibition of SK channels. Neuron *68*, 948–963.

Bushnell, P.J. (1987). Effects of scopolamine on locomotor activity and metabolic rate in mice. Pharmacol. Biochem. Behav. *26*, 195–198.

Bytyqi, A.H., Lockridge, O., Duysen, E., Wang, Y., Wolfrum, U., and Layer, P.G. (2004). Impaired formation of the inner retina in an AChE knockout mouse results in degeneration of all photoreceptors. Eur. J. Neurosci. *20*, 2953–2962.

Cachope, R., Mateo, Y., Mathur, B.N., Irving, J., Wang, H.-L., Morales, M., Lovinger, D.M., and Cheer, J.F. (2012). Selective activation of cholinergic interneurons enhances accumbal phasic dopamine release: setting the tone for reward processing. Cell Rep *2*, 33–41.

Calabresi, P., Centonze, D., Pisani, A., Sancesario, G., North, R.A., and Bernardi, G. (1998). Muscarinic IPSPs in rat striatal cholinergic interneurones. J. Physiol. (Lond.) *510 (Pt 2)*, 421–427.

Calabresi, P., Centonze, D., Gubellini, P., Pisani, A., and Bernardi, G. (2000). Acetylcholine-mediated

modulation of striatal function. Trends Neurosci. *23*, 120–126.

Camp, S., Zhang, L., Marquez, M., de la Torre, B., Long, J.M., Bucht, G., and Taylor, P. (2005). Acetylcholinesterase (AChE) gene modification in transgenic animals: functional consequences of selected exon and regulatory region deletion. Chem. Biol. Interact. *157-158*, 79–86.

Camp, S., De Jaco, A., Zhang, L., Marquez, M., De la Torre, B., and Taylor, P. (2008). Acetylcholinesterase expression in muscle is specifically controlled by a promoter-selective enhancesome in the first intron. J. Neurosci. *28*, 2459–2470.

Camp, S., Zhang, L., Krejci, E., Dobbertin, A., Bernard, V., Girard, E., Duysen, E.G., Lockridge, O., De Jaco, A., and Taylor, P. (2010). Contributions of selective knockout studies to understanding cholinesterase disposition and function. Chem. Biol. Interact. *187*, 72–77.

Carr, D.B., and Surmeier, D.J. (2007). M1 muscarinic receptor modulation of Kir2 channels enhances temporal summation of excitatory synaptic potentials in prefrontal cortex pyramidal neurons. J. Neurophysiol. *97*, 3432–3438.

De Castro, B.M., De Jaeger, X., Martins-Silva, C., Lima, R.D.F., Amaral, E., Menezes, C., Lima, P., Neves, C.M.L., Pires, R.G., Gould, T.W., et al. (2009a). The vesicular acetylcholine transporter is required for neuromuscular development and function. Mol. Cell. Biol. *29*, 5238–5250.

De Castro, B.M., Pereira, G.S., Magalhães, V., Rossato, J.I., De Jaeger, X., Martins-Silva, C., Leles, B., Lima, P., Gomez, M.V., Gainetdinov, R.R., et al. (2009b). Reduced expression of the vesicular acetylcholine transporter causes learning deficits in mice. Genes Brain Behav. *8*, 23–35.

Caulfield, M.P., and Birdsall, N.J. (1998). International Union of Pharmacology. XVII. Classification of muscarinic acetylcholine receptors. Pharmacol. Rev. *50*, 279–290.

Clement, J.G. (1993). Pharmacological nature of soman-induced hypothermia in mice. Pharmacol. Biochem. Behav. *44*, 689–702.

Coleman, C.G., Lydic, R., and Baghdoyan, H.A. (2004). M2 muscarinic receptors in pontine reticular formation of C57BL/6J mouse contribute to rapid eye movement sleep generation. Neuroscience *126*, 821–830.

Collier, B., and Katz, H.S. (1974). Acetylcholine synthesis from recaptured choline by a sympathetic ganglion. J. Physiol. (Lond.) *238*, 639–655.

Conner, J.M., Culberson, A., Packowski, C., Chiba, A.A., and Tuszynski, M.H. (2003). Lesions of the Basal forebrain cholinergic system impair task acquisition and abolish cortical plasticity associated with motor skill learning. Neuron *38*, 819–829.

Consonni, S., Leone, S., Becchetti, A., and Amadeo, A. (2009). Developmental and neurochemical features of cholinergic neurons in the murine cerebral cortex. BMC Neurosci *10*, 18.

Contant, C., Umbriaco, D., Garcia, S., Watkins, K.C., and Descarries, L. (1996). Ultrastructural characterization of the acetylcholine innervation in adult rat neostriatum. Neuroscience *71*, 937–947.

Costa, R.M., Cohen, D., and Nicolelis, M.A.L. (2004). Differential corticostriatal plasticity during fast and slow motor skill learning in mice. Curr. Biol. *14*, 1124–1134.

Cousin, X., Créminon, C., Grassi, J., Méflah, K., Cornu, G., Saliou, B., Bon, S., Massoulié, J., and Bon, C. (1996). Acetylcholinesterase from Bungarus venom: a monomeric species. FEBS Lett. *387*, 196–200.

Cousin, X., Bon, S., Massoulié, J., and Bon, C. (1998). Identification of a novel type of alternatively spliced exon from the acetylcholinesterase gene of Bungarus fasciatus. Molecular forms of acetylcholinesterase in the snake liver and muscle. J. Biol. Chem. *273*, 9812–9820.

Coussen, F., Ayon, A., Le Goff, A., Leroy, J., Massoulié, J., and Bon, S. (2001). Addition of a glycophosphatidylinositol to acetylcholinesterase. Processing, degradation, and secretion. J. Biol. Chem. *276*, 27881–27892.

Crespo, J.A., Sturm, K., Saria, A., and Zernig, G. (2006). Activation of muscarinic and nicotinic

acetylcholine receptors in the nucleus accumbens core is necessary for the acquisition of drug reinforcement. J. Neurosci. *26*, 6004–6010.

Csaba, Z., Krejci, E., and Bernard, V. (2013). Postsynaptic muscarinic m2 receptors at cholinergic and glutamatergic synapses of mouse brainstem motoneurons. J. Comp. Neurol. *521*, 2008–2024.

Curia, G., Longo, D., Biagini, G., Jones, R.S.G., and Avoli, M. (2008). The pilocarpine model of temporal lobe epilepsy. J. Neurosci. Methods *172*, 143–157.

Dajas-Bailador, F., and Wonnacott, S. (2004). Nicotinic acetylcholine receptors and the regulation of neuronal signalling. Trends Pharmacol. Sci. *25*, 317–324.

Dang, M.T., Yokoi, F., Yin, H.H., Lovinger, D.M., Wang, Y., and Li, Y. (2006). Disrupted motor learning and long-term synaptic plasticity in mice lacking NMDAR1 in the striatum. Proc. Natl. Acad. Sci. U.S.A. *103*, 15254–15259.

Dani, J.A., and Bertrand, D. (2007). Nicotinic acetylcholine receptors and nicotinic cholinergic mechanisms of the central nervous system. Annu. Rev. Pharmacol. Toxicol. *47*, 699–729.

Darvesh, S., Hopkins, D.A., and Geula, C. (2003). Neurobiology of butyrylcholinesterase. Nat. Rev. Neurosci. *4*, 131–138.

Dean, B., Hussain, T., Hayes, W., Scarr, E., Kitsoulis, S., Hill, C., Opeskin, K., and Copolov, D.L. (1999). Changes in serotonin2A and GABA(A) receptors in schizophrenia: studies on the human dorsolateral prefrontal cortex. J. Neurochem. *72*, 1593–1599.

DeBoer, P., Heeringa, M.J., and Abercrombie, E.D. (1996). Spontaneous release of acetylcholine in striatum is preferentially regulated by inhibitory dopamine D2 receptors. Eur. J. Pharmacol. *317*, 257–262.

Decossas, M., Bloch, B., and Bernard, V. (2003). Trafficking of the muscarinic m2 autoreceptor in cholinergic basalocortical neurons in vivo: differential regulation of plasma membrane receptor availability and intraneuronal localization in acetylcholinesterase-deficient and -inhibited mice. J. Comp. Neurol. *462*, 302–314.

Deiana, S., Platt, B., and Riedel, G. (2011). The cholinergic system and spatial learning. Behav. Brain Res. *221*, 389–411.

Dencker, D., Thomsen, M., Wörtwein, G., Weikop, P., Cui, Y., Jeon, J., Wess, J., and Fink-Jensen, A. (2012). Muscarinic Acetylcholine Receptor Subtypes as Potential Drug Targets for the Treatment of Schizophrenia, Drug Abuse and Parkinson's Disease. ACS Chemical Neuroscience *3*, 80–89.

Descarries, L. (1998). The hypothesis of an ambient level of acetylcholine in the central nervous system. J. Physiol. Paris *92*, 215–220.

Descarries, L., Gisiger, V., and Steriade, M. (1997). Diffuse transmission by acetylcholine in the CNS. Prog. Neurobiol. *53*, 603–625.

Descarries, L., Mechawar, N., Aznavour, N., and Watkins, K.C. (2004). Structural determinants of the roles of acetylcholine in cerebral cortex. Prog. Brain Res. *145*, 45–58.

Dickinson, J.A., Kew, J.N.C., and Wonnacott, S. (2008). Presynaptic alpha 7- and beta 2-containing nicotinic acetylcholine receptors modulate excitatory amino acid release from rat prefrontal cortex nerve terminals via distinct cellular mechanisms. Mol. Pharmacol. *74*, 348–359.

Ding, J., Guzman, J.N., Tkatch, T., Chen, S., Goldberg, J.A., Ebert, P.J., Levitt, P., Wilson, C.J., Hamm, H.E., and Surmeier, D.J. (2006). RGS4-dependent attenuation of M4 autoreceptor function in striatal cholinergic interneurons following dopamine depletion. Nat. Neurosci. *9*, 832–842.

Dobbertin, A., Hrabovska, A., Dembele, K., Camp, S., Taylor, P., Krejci, E., and Bernard, V. (2009). Targeting of acetylcholinesterase in neurons in vivo: a dual processing function for the proline-rich membrane anchor subunit and the attachment domain on the catalytic subunit. J. Neurosci. *29*, 4519–4530.

Dolezal, V., and Tucek, S. (1999). Calcium channels involved in the inhibition of acetylcholine release by presynaptic muscarinic receptors in rat striatum. Br. J. Pharmacol. *127*, 1627–1632.

Dolezal, V., and Wecker, L. (1990). Muscarinic receptor blockade increases basal acetylcholine release from striatal slices. J. Pharmacol. Exp. Ther. *252*, 739–743.

Donger, C., Krejci, E., Serradell, A.P., Eymard, B., Bon, S., Nicole, S., Chateau, D., Gary, F., Fardeau, M., Massoulié, J., et al. (1998). Mutation in the human acetylcholinesterase-associated collagen gene, COLQ, is responsible for congenital myasthenic syndrome with end-plate acetylcholinesterase deficiency (Type Ic). Am. J. Hum. Genet. *63*, 967–975.

Dörje, F., Wess, J., Lambrecht, G., Tacke, R., Mutschler, E., and Brann, M.R. (1991). Antagonist binding profiles of five cloned human muscarinic receptor subtypes. J. Pharmacol. Exp. Ther. *256*, 727–733.

Doyon, J., Bellec, P., Amsel, R., Penhune, V., Monchi, O., Carrier, J., Lehéricy, S., and Benali, H. (2009). Contributions of the basal ganglia and functionally related brain structures to motor learning. Behav. Brain Res. *199*, 61–75.

Dronfield, S., Egan, K., Marsden, C.A., and Green, A.R. (2000). Comparison of donepezil-, tacrine-, rivastigmine- and metrifonate-induced central and peripheral cholinergically mediated responses in the rat. J. Psychopharmacol. (Oxford) *14*, 275–279.

Duffy, A.M., Zhou, P., Milner, T.A., and Pickel, V.M. (2009). Spatial and intracellular relationships between the alpha7 nicotinic acetylcholine receptor and the vesicular acetylcholine transporter in the prefrontal cortex of rat and mouse. Neuroscience *161*, 1091–1103.

Duval, N., Massoulié, J., and Bon, S. (1992a). H and T subunits of acetylcholinesterase from Torpedo, expressed in COS cells, generate all types of globular forms. J. Cell Biol. *118*, 641–653.

Duval, N., Krejci, E., Grassi, J., Coussen, F., Massoulié, J., and Bon, S. (1992b). Molecular architecture of acetylcholinesterase collagen-tailed forms; construction of a glycolipid-tailed tetramer. EMBO J. *11*, 3255–3261.

Duysen, E.G., and Lockridge, O. (2006). Phenotype comparison of three acetylcholinesterase knockout strains. J. Mol. Neurosci. *30*, 91–92.

Duysen, E.G., and Lockridge, O. (2008). Whole body and tissue imaging of the butyrylcholinesterase knockout mouse injected with near infrared dye labeled butyrylcholinesterase. Chem. Biol. Interact. *175*, 119–124.

Duysen, E.G., Stribley, J.A., Fry, D.L., Hinrichs, S.H., and Lockridge, O. (2002a). Rescue of the acetylcholinesterase knockout mouse by feeding a liquid diet; phenotype of the adult acetylcholinesterase deficient mouse. Brain Res. Dev. Brain Res. *137*, 43–54.

Duysen, E.G., Fry, D.L., and Lockridge, O. (2002b). Early weaning and culling eradicated Helicobacter hepaticus from an acetylcholinesterase knockout 129S6/SvEvTac mouse colony. Comp. Med. *52*, 461–466.

Duysen, E.G., Li, B., Darvesh, S., and Lockridge, O. (2007). Sensitivity of butyrylcholinesterase knockout mice to (--)-huperzine A and donepezil suggests humans with butyrylcholinesterase deficiency may not tolerate these Alzheimer's disease drugs and indicates butyrylcholinesterase function in neurotransmission. Toxicology *233*, 60–69.

Duysen, E.G., Li, B., Carlson, M., Li, Y.-F., Wieseler, S., Hinrichs, S.H., and Lockridge, O. (2008). Increased hepatotoxicity and cardiac fibrosis in cocaine-treated butyrylcholinesterase knockout mice. Basic Clin. Pharmacol. Toxicol. *103*, 514–521.

Duysen, E.G., Li, B., and Lockridge, O. (2009). The butyrylcholinesterase knockout mouse a research tool in the study of drug sensitivity, bio-distribution, obesity and Alzheimer's disease. Expert Opin Drug Metab Toxicol *5*, 523–528.

Dvir, H., Harel, M., Bon, S., Liu, W.-Q., Vidal, M., Garbay, C., Sussman, J.L., Massoulié, J., and Silman, I. (2004). The synaptic acetylcholinesterase tetramer assembles around a polyproline II helix. EMBO J. *23*, 4394–4405.

Erb, C., Troost, J., Kopf, S., Schmitt, U., Löffelholz, K., Soreq, H., and Klein, J. (2001). Compensatory mechanisms enhance hippocampal acetylcholine release in transgenic mice expressing human acetylcholinesterase. J. Neurochem. *77*, 638–646.

Espallergues, J., Galvan, L., Sabatier, F., Rana-Poussine, V., Maurice, T., and Chatonnet, A. (2010). Behavioral phenotyping of heterozygous acetylcholinesterase knockout (AChE+/-) mice showed no memory enhancement but hyposensitivity to amnesic drugs. Behav. Brain Res. *206*, 263–273.

Fabian-Fine, R., Skehel, P., Errington, M.L., Davies, H.A., Sher, E., Stewart, M.G., and Fine, A. (2001). Ultrastructural distribution of the alpha7 nicotinic acetylcholine receptor subunit in rat hippocampus. J. Neurosci. *21*, 7993–8003.

Fagerlund, M.J., and Eriksson, L.I. (2009). Current concepts in neuromuscular transmission. Br J Anaesth *103*, 108–114.

Felder, C.C. (1995). Muscarinic acetylcholine receptors: signal transduction through multiple effectors. FASEB J. *9*, 619–625.

Feng, G., Krejci, E., Molgo, J., Cunningham, J.M., Massoulié, J., and Sanes, J.R. (1999). Genetic analysis of collagen Q: roles in acetylcholinesterase and butyrylcholinesterase assembly and in synaptic structure and function. J. Cell Biol. *144*, 1349–1360.

Ferguson, S.M., Savchenko, V., Apparsundaram, S., Zwick, M., Wright, J., Heilman, C.J., Yi, H., Levey, A.I., and Blakely, R.D. (2003). Vesicular localization and activity-dependent trafficking of presynaptic choline transporters. J. Neurosci. *23*, 9697–9709.

Ferguson, S.M., Bazalakova, M., Savchenko, V., Tapia, J.C., Wright, J., and Blakely, R.D. (2004). Lethal impairment of cholinergic neurotransmission in hemicholinium-3-sensitive choline transporter knockout mice. Proc. Natl. Acad. Sci. U.S.A. *101*, 8762–8767.

Fernagut, P.-O., Chalon, S., Diguet, E., Guilloteau, D., Tison, F., and Jaber, M. (2003). Motor behaviour deficits and their histopathological and functional correlates in the nigrostriatal system of dopamine transporter knockout mice. Neuroscience *116*, 1123–1130.

Fernández de Sevilla, D., Núñez, A., Borde, M., Malinow, R., and Buño, W. (2008). Cholinergic-mediated IP3-receptor activation induces long-lasting synaptic enhancement in CA1 pyramidal neurons. J. Neurosci. *28*, 1469–1478.

Fink-Jensen, A., Schmidt, L.S., Dencker, D., Schülein, C., Wess, J., Wörtwein, G., and Woldbye, D.P.D. (2011). Antipsychotic-induced catalepsy is attenuated in mice lacking the M4 muscarinic acetylcholine receptor. Eur. J. Pharmacol. *656*, 39–44.

Fisahn, A., Yamada, M., Duttaroy, A., Gan, J.-W., Deng, C.-X., McBain, C.J., and Wess, J. (2002). Muscarinic induction of hippocampal gamma oscillations requires coupling of the M1 receptor to two mixed cation currents. Neuron *33*, 615–624.

Fonnum, F. (1969). Radiochemical micro assays for the determination of choline acetyltransferase and acetylcholinesterase activities. Biochem. J. *115*, 465–472.

Forster, G.L., and Blaha, C.D. (2000). Laterodorsal tegmental stimulation elicits dopamine efflux in the rat nucleus accumbens by activation of acetylcholine and glutamate receptors in the ventral tegmental area. Eur. J. Neurosci. *12*, 3596–3604.

Forster, G.L., and Blaha, C.D. (2003). Pedunculopontine tegmental stimulation evokes striatal dopamine efflux by activation of acetylcholine and glutamate receptors in the midbrain and pons of the rat. Eur. J. Neurosci. *17*, 751–762.

Forster, G.L., Yeomans, J.S., Takeuchi, J., and Blaha, C.D. (2002). M5 muscarinic receptors are required for prolonged accumbal dopamine release after electrical stimulation of the pons in mice. J. Neurosci. *22*, RC190.

Frazier, C.J., Buhler, A.V., Weiner, J.L., and Dunwiddie, T.V. (1998). Synaptic potentials mediated via alpha-bungarotoxin-sensitive nicotinic acetylcholine receptors in rat hippocampal interneurons. J. Neurosci. *18*, 8228–8235.

Frotscher, M., Vida, I., and Bender, R. (2000). Evidence for the existence of non-GABAergic, cholinergic interneurons in the rodent hippocampus. Neuroscience *96*, 27–31.

Ge, S., and Dani, J.A. (2005). Nicotinic acetylcholine receptors at glutamate synapses facilitate long-

term depression or potentiation. J. Neurosci. *25*, 6084–6091.

Genever, P.G., Birch, M.A., Brown, E., and Skerry, T.M. (1999). Osteoblast-derived acetylcholinesterase: a novel mediator of cell-matrix interactions in bone? Bone *24*, 297–303.

Gennari, K., Brunner, J., and Brodbeck, U. (1987). Tetrameric detergent-soluble acetylcholinesterase from human caudate nucleus: subunit composition and number of active sites. J. Neurochem. *49*, 12–18.

Gerber, D.J., Sotnikova, T.D., Gainetdinov, R.R., Huang, S.Y., Caron, M.G., and Tonegawa, S. (2001). Hyperactivity, elevated dopaminergic transmission, and response to amphetamine in M1 muscarinic acetylcholine receptor-deficient mice. Proc. Natl. Acad. Sci. U.S.A. *98*, 15312–15317.

Gerfen, C.R., and Surmeier, D.J. (2011). Modulation of striatal projection systems by dopamine. Annu. Rev. Neurosci. *34*, 441–466.

Gibbins, I.L., and Morris, J.L. (2006). Structure of peripheral synapses: autonomic ganglia. Cell Tissue Res. *326*, 205–220.

Giniatullin, R., Nistri, A., and Yakel, J.L. (2005). Desensitization of nicotinic ACh receptors: shaping cholinergic signaling. Trends Neurosci. *28*, 371–378.

Girard, E., Barbier, J., Chatonnet, A., Krejci, E., and Molgó, J. (2005). Synaptic remodeling at the skeletal neuromuscular junction of acetylcholinesterase knockout mice and its physiological relevance. Chem. Biol. Interact. *157-158*, 87–96.

Girard, E., Bernard, V., Camp, S., Taylor, P., Krejci, E., and Molgó, J. (2006). Remodeling of the neuromuscular junction in mice with deleted exons 5 and 6 of acetylcholinesterase. J. Mol. Neurosci. *30*, 99–100.

Girard, E., Bernard, V., Minic, J., Chatonnet, A., Krejci, E., and Molgó, J. (2007). Butyrylcholinesterase and the control of synaptic responses in acetylcholinesterase knockout mice. Life Sci. *80*, 2380–2385.

Gisiger, V., Bélisle, M., and Gardiner, P.F. (1994). Acetylcholinesterase adaptation to voluntary wheel running is proportional to the volume of activity in fast, but not slow, rat hindlimb muscles. Eur. J. Neurosci. *6*, 673–680.

Gkogkas, C., Sonenberg, N., and Costa-Mattioli, M. (2010). Translational control mechanisms in long-lasting synaptic plasticity and memory. J. Biol. Chem. *285*, 31913–31917.

Gomeza, J., Zhang, L., Kostenis, E., Felder, C., Bymaster, F., Brodkin, J., Shannon, H., Xia, B., Deng, C., and Wess, J. (1999a). Enhancement of D1 dopamine receptor-mediated locomotor stimulation in M(4) muscarinic acetylcholine receptor knockout mice. Proc. Natl. Acad. Sci. U.S.A. *96*, 10483–10488.

Gomeza, J., Shannon, H., Kostenis, E., Felder, C., Zhang, L., Brodkin, J., Grinberg, A., Sheng, H., and Wess, J. (1999b). Pronounced pharmacologic deficits in M2 muscarinic acetylcholine receptor knockout mice. Proc. Natl. Acad. Sci. U.S.A. *96*, 1692–1697.

Gotti, C., and Clementi, F. (2004). Neuronal nicotinic receptors: from structure to pathology. Prog. Neurobiol. *74*, 363–396.

Gotti, C., Clementi, F., Fornari, A., Gaimarri, A., Guiducci, S., Manfredi, I., Moretti, M., Pedrazzi, P., Pucci, L., and Zoli, M. (2009). Structural and functional diversity of native brain neuronal nicotinic receptors. Biochem. Pharmacol. *78*, 703–711.

Grady, S.R., Meinerz, N.M., Cao, J., Reynolds, A.M., Picciotto, M.R., Changeux, J.P., McIntosh, J.M., Marks, M.J., and Collins, A.C. (2001). Nicotinic agonists stimulate acetylcholine release from mouse interpeduncular nucleus: a function mediated by a different nAChR than dopamine release from striatum. J. Neurochem. *76*, 258–268.

Grady, S.R., Salminen, O., Laverty, D.C., Whiteaker, P., McIntosh, J.M., Collins, A.C., and Marks, M.J. (2007). The subtypes of nicotinic acetylcholine receptors on dopaminergic terminals of mouse striatum. Biochem. Pharmacol. *74*, 1235–1246.

Grady, S.R., Salminen, O., McIntosh, J.M., Marks, M.J., and Collins, A.C. (2010). Mouse striatal dopamine nerve terminals express alpha4alpha5beta2 and two stoichiometric forms of alpha4beta2*-

nicotinic acetylcholine receptors. J. Mol. Neurosci. *40*, 91–95.

Gray, R., Rajan, A.S., Radcliffe, K.A., Yakehiro, M., and Dani, J.A. (1996). Hippocampal synaptic transmission enhanced by low concentrations of nicotine. Nature *383*, 713–716.

Greenfield, S. (2005). A peptide derived from acetylcholinesterase is a pivotal signalling molecule in neurodegeneration. Chem. Biol. Interact. *157-158*, 211–218.

Grifman, M., Galyam, N., Seidman, S., and Soreq, H. (1998). Functional redundancy of acetylcholinesterase and neuroligin in mammalian neuritogenesis. Proc. Natl. Acad. Sci. U.S.A. *95*, 13935–13940.

Groenewegen, H.J. (2003). The basal ganglia and motor control. Neural Plast. *10*, 107–120.

Grybko, M.J., Hahm, E.-T., Perrine, W., Parnes, J.A., Chick, W.S., Sharma, G., Finger, T.E., and Vijayaraghavan, S. (2011). A transgenic mouse model reveals fast nicotinic transmission in hippocampal pyramidal neurons. Eur. J. Neurosci. *33*, 1786–1798.

Gu, Z., and Yakel, J.L. (2011). Timing-dependent septal cholinergic induction of dynamic hippocampal synaptic plasticity. Neuron *71*, 155–165.

Guerra, M., Dobbertin, A., and Legay, C. (2008). Identification of cis-acting elements involved in acetylcholinesterase RNA alternative splicing. Mol. Cell. Neurosci. *38*, 1–14.

Gulledge, A.T., Bucci, D.J., Zhang, S.S., Matsui, M., and Yeh, H.H. (2009). M1 receptors mediate cholinergic modulation of excitability in neocortical pyramidal neurons. J. Neurosci. *29*, 9888–9902.

Guyenet, P., Lefresne, P., Rossier, J., Beaujouan, J.C., and Glowinski, J. (1973). Inhibition by hemicholinium-3 of (14C)acetylcholine synthesis and (3H)choline high-affinity uptake in rat striatal synaptosomes. Mol. Pharmacol. *9*, 630–639.

Hamers, F.P.T., Koopmans, G.C., and Joosten, E.A.J. (2006). CatWalk-assisted gait analysis in the assessment of spinal cord injury. J. Neurotrauma *23*, 537–548.

Hamilton, S.E., and Nathanson, N.M. (2001). The M1 receptor is required for muscarinic activation of mitogen-activated protein (MAP) kinase in murine cerebral cortical neurons. J. Biol. Chem. *276*, 15850–15853.

Hamilton, S.E., Loose, M.D., Qi, M., Levey, A.I., Hille, B., McKnight, G.S., Idzerda, R.L., and Nathanson, N.M. (1997). Disruption of the m1 receptor gene ablates muscarinic receptor-dependent M current regulation and seizure activity in mice. Proc. Natl. Acad. Sci. U.S.A. *94*, 13311–13316.

Hammond, P., Rao, R., Koenigsberger, C., and Brimijoin, S. (1994). Regional variation in expression of acetylcholinesterase mRNA in adult rat brain analyzed by in situ hybridization. Proc. Natl. Acad. Sci. U.S.A. *91*, 10933–10937.

Harel, M., Sussman, J.L., Krejci, E., Bon, S., Chanal, P., Massoulié, J., and Silman, I. (1992). Conversion of acetylcholinesterase to butyrylcholinesterase: modeling and mutagenesis. Proc. Natl. Acad. Sci. U.S.A. *89*, 10827–10831.

Hartmann, J., Kiewert, C., Duysen, E.G., Lockridge, O., Greig, N.H., and Klein, J. (2007). Excessive hippocampal acetylcholine levels in acetylcholinesterase-deficient mice are moderated by butyrylcholinesterase activity. J. Neurochem. *100*, 1421–1429.

Hartmann, J., Kiewert, C., Duysen, E.G., Lockridge, O., and Klein, J. (2008). Choline availability and acetylcholine synthesis in the hippocampus of acetylcholinesterase-deficient mice. Neurochem. Int. *52*, 972–978.

Hatton, G.I., and Yang, Q.Z. (2002). Synaptic potentials mediated by alpha 7 nicotinic acetylcholine receptors in supraoptic nucleus. J. Neurosci. *22*, 29–37.

Hefft, S., Hulo, S., Bertrand, D., and Muller, D. (1999). Synaptic transmission at nicotinic acetylcholine receptors in rat hippocampal organotypic cultures and slices. J. Physiol. (Lond.) *515 (Pt 3)*, 769–776.

Henderson, Z., and Greenfield, S.A. (1984). Ultrastructural localization of acetylcholinesterase in

substantia nigra: a comparison between rat and guinea pig. J. Comp. Neurol. *230*, 278–286.

Henderson, Z., Matto, N., John, D., Nalivaeva, N.N., and Turner, A.J. (2010). Co-localization of PRiMA with acetylcholinesterase in cholinergic neurons of rat brain: an immunocytochemical study. Brain Res. *1344*, 34–42.

Hersch, S.M., Gutekunst, C.A., Rees, H.D., Heilman, C.J., and Levey, A.I. (1994). Distribution of m1-m4 muscarinic receptor proteins in the rat striatum: light and electron microscopic immunocytochemistry using subtype-specific antibodies. J. Neurosci. *14*, 3351–3363.

Higley, M.J., Gittis, A.H., Oldenburg, I.A., Balthasar, N., Seal, R.P., Edwards, R.H., Lowell, B.B., Kreitzer, A.C., and Sabatini, B.L. (2011). Cholinergic interneurons mediate fast VGluT3-dependent glutamatergic transmission in the striatum. PLoS ONE *6*, e19155.

Holmstrand, E.C., Asafu-Adjei, J., Sampson, A.R., Blakely, R.D., and Sesack, S.R. (2010). Ultrastructural localization of high-affinity choline transporter in the rat anteroventral thalamus and ventral tegmental area: differences in axon morphology and transporter distribution. J. Comp. Neurol. *518*, 1908–1924.

Hrabovska, A., Bernard, V., and Krejci, E. (2010a). A novel system for the efficient generation of antibodies following immunization of unique knockout mouse strains. PLoS ONE *5*, e12892.

Hrabovska, A., Farar, V., Bernard, V., Duysen, E.G., Brabec, J., Lockridge, O., and Myslivecek, J. (2010b). Drastic decrease in dopamine receptor levels in the striatum of acetylcholinesterase knock-out mouse. Chem. Biol. Interact. *183*, 194–201.

Chan, W.K.B., Chen, V.P., Luk, W.K.W., Choi, R.C.Y., and Tsim, K.W.K. (2012). N-linked glycosylation of proline-rich membrane anchor (PRiMA) is not required for assembly and trafficking of globular tetrameric acetylcholinesterase. Neurosci. Lett. *523*, 71–75.

Chang, C.C. (1998). Neuromuscular toxicity of anticholinesterase agents. J Toxicol Sci *23 Suppl 2*, 117–121.

Chapman, C.A., Yeomans, J.S., Blaha, C.D., and Blackburn, J.R. (1997). Increased striatal dopamine efflux follows scopolamine administered systemically or to the tegmental pedunculopontine nucleus. Neuroscience *76*, 177–186.

Charlesworth, J.D., Warren, T.L., and Brainard, M.S. (2012). Covert skill learning in a cortical-basal ganglia circuit. Nature *486*, 251–255.

Chatonnet, F., Boudinot, E., Chatonnet, A., Taysse, L., Daulon, S., Champagnat, J., and Foutz, A.S. (2003). Respiratory survival mechanisms in acetylcholinesterase knockout mouse. Eur. J. Neurosci. *18*, 1419–1427.

Chen, K.C., Baxter, M.G., and Rodefer, J.S. (2004). Central blockade of muscarinic cholinergic receptors disrupts affective and attentional set-shifting. Eur. J. Neurosci. *20*, 1081–1088.

Chen, V.P., Xie, H.Q., Chan, W.K.B., Leung, K.W., Chan, G.K.L., Choi, R.C.Y., Bon, S., Massoulié, J., and Tsim, K.W.K. (2010). The PRiMA-linked cholinesterase tetramers are assembled from homodimers: hybrid molecules composed of acetylcholinesterase and butyrylcholinesterase dimers are up-regulated during development of chicken brain. J. Biol. Chem. *285*, 27265–27278.

Chen, V.P., Choi, R.C.Y., Chan, W.K.B., Leung, K.W., Guo, A.J.Y., Chan, G.K.L., Luk, W.K.W., and Tsim, K.W.K. (2011). The assembly of proline-rich membrane anchor (PRiMA)-linked acetylcholinesterase enzyme: glycosylation is required for enzymatic activity but not for oligomerization. J. Biol. Chem. *286*, 32948–32961.

Chintoh, A., Fulton, J., Koziel, N., Aziz, M., Sud, M., and Yeomans, J.S. (2003). Role of cholinergic receptors in locomotion induced by scopolamine and oxotremorine-M. Pharmacol. Biochem. Behav. *76*, 53–61.

Ichikawa, T., Ajiki, K., Matsuura, J., and Misawa, H. (1997). Localization of two cholinergic markers, choline acetyltransferase and vesicular acetylcholine transporter in the central nervous system of the rat: in

situ hybridization histochemistry and immunohistochemistry. J. Chem. Neuroanat. *13*, 23–39.

Inestrosa, N.C., and Ruiz, G. (1985). Membrane-bound form of acetylcholinesterase activated during postnatal development of the rat somatosensory cortex. Dev. Neurosci. *7*, 120–132.

Inestrosa, N.C., Roberts, W.L., Marshall, T.L., and Rosenberry, T.L. (1987). Acetylcholinesterase from bovine caudate nucleus is attached to membranes by a novel subunit distinct from those of acetylcholinesterases in other tissues. J. Biol. Chem. *262*, 4441–4444.

Inestrosa, N.C., Moreno, R.D., and Fuentes, M.E. (1994). Monomeric amphiphilic forms of acetylcholinesterase appear early during brain development and may correspond to biosynthetic precursors of the amphiphilic G4 forms. Neurosci. Lett. *173*, 155–158.

Jbilo, O., Bartels, C.F., Chatonnet, A., Toutant, J.P., and Lockridge, O. (1994). Tissue distribution of human acetylcholinesterase and butyrylcholinesterase messenger RNA. Toxicon *32*, 1445–1457.

Jeon, J., Dencker, D., Wörtwein, G., Woldbye, D.P.D., Cui, Y., Davis, A.A., Levey, A.I., Schütz, G., Sager, T.N., Mørk, A., et al. (2010). A subpopulation of neuronal M4 muscarinic acetylcholine receptors plays a critical role in modulating dopamine-dependent behaviors. J. Neurosci. *30*, 2396–2405.

Ji, D., Lape, R., and Dani, J.A. (2001). Timing and location of nicotinic activity enhances or depresses hippocampal synaptic plasticity. Neuron *31*, 131–141.

Johnson, G., and Moore, S.W. (2004). Identification of a structural site on acetylcholinesterase that promotes neurite outgrowth and binds laminin-1 and collagen IV. Biochem. Biophys. Res. Commun. *319*, 448–455.

Johnson, N.D., Duysen, E.G., and Lockridge, O. (2009). Intrathecal delivery of fluorescent labeled butyrylcholinesterase to the brains of butyrylcholinesterase knock-out mice: visualization and quantification of enzyme distribution in the brain. Neurotoxicology *30*, 386–392.

Jones, I.W., and Wonnacott, S. (2004). Precise localization of alpha7 nicotinic acetylcholine receptors on glutamatergic axon terminals in the rat ventral tegmental area. J. Neurosci. *24*, 11244–11252.

Jones, I.W., Bolam, J.P., and Wonnacott, S. (2001). Presynaptic localisation of the nicotinic acetylcholine receptor beta2 subunit immunoreactivity in rat nigrostriatal dopaminergic neurones. J. Comp. Neurol. *439*, 235–247.

Kalappa, B.I., Feng, L., Kem, W.R., Gusev, A.G., and Uteshev, V.V. (2011). Mechanisms of facilitation of synaptic glutamate release by nicotinic agonists in the nucleus of the solitary tract. Am. J. Physiol., Cell Physiol. *301*, C347–361.

Kaneko, S., Hikida, T., Watanabe, D., Ichinose, H., Nagatsu, T., Kreitman, R.J., Pastan, I., and Nakanishi, S. (2000). Synaptic integration mediated by striatal cholinergic interneurons in basal ganglia function. Science *289*, 633–637.

Karasawa, H., Taketo, M.M., and Matsui, M. (2003). Loss of anti-cataleptic effect of scopolamine in mice lacking muscarinic acetylcholine receptor subtype 4. Eur. J. Pharmacol. *468*, 15–19.

Katz, B., and Miledi, R. (1973). The binding of acetylcholine to receptors and its removal from the synaptic cleft. J. Physiol. (Lond.) *231*, 549–574.

Kaufer, D., Friedman, A., Seidman, S., and Soreq, H. (1998). Acute stress facilitates long-lasting changes in cholinergic gene expression. Nature *393*, 373–377.

Kawaguchi, Y., Wilson, C.J., Augood, S.J., and Emson, P.C. (1995). Striatal interneurones: chemical, physiological and morphological characterization. Trends Neurosci. *18*, 527–535.

Kimura, F., and Baughman, R.W. (1997). Distinct muscarinic receptor subtypes suppress excitatory and inhibitory synaptic responses in cortical neurons. J. Neurophysiol. *77*, 709–716.

Kitabatake, Y., Hikida, T., Watanabe, D., Pastan, I., and Nakanishi, S. (2003). Impairment of reward-related learning by cholinergic cell ablation in the striatum. Proc. Natl. Acad. Sci. U.S.A. *100*, 7965–7970.

Klinar, B., and Brzin, M. (1977). Cytochemical localization of acetylcholinesterase in the rat striatum.

Acta Histochem. *59*, 223–231.

Koelle, G.B., Massoulié, J., Eugène, D., Melone, M.A., and Boulla, G. (1987). Distributions of molecular forms of acetylcholinesterase and butyrylcholinesterase in nervous tissue of the cat. Proc. Natl. Acad. Sci. U.S.A. *84*, 7749–7752.

Koós, T., and Tepper, J.M. (2002). Dual cholinergic control of fast-spiking interneurons in the neostriatum. J. Neurosci. *22*, 529–535.

Kravitz, A.V., Freeze, B.S., Parker, P.R.L., Kay, K., Thwin, M.T., Deisseroth, K., and Kreitzer, A.C. (2010). Regulation of parkinsonian motor behaviours by optogenetic control of basal ganglia circuitry. Nature *466*, 622–626.

Kreitzer, A.C., and Malenka, R.C. (2008). Striatal plasticity and basal ganglia circuit function. Neuron *60*, 543–554.

Krejci, E., Coussen, F., Duval, N., Chatel, J.M., Legay, C., Puype, M., Vandekerckhove, J., Cartaud, J., Bon, S., and Massoulié, J. (1991). Primary structure of a collagenic tail peptide of Torpedo acetylcholinesterase: co-expression with catalytic subunit induces the production of collagen-tailed forms in transfected cells. EMBO J. *10*, 1285–1293.

Krejci, E., Thomine, S., Boschetti, N., Legay, C., Sketelj, J., and Massoulié, J. (1997). The mammalian gene of acetylcholinesterase-associated collagen. J. Biol. Chem. *272*, 22840–22847.

Krishnaswamy, A., and Cooper, E. (2009). An activity-dependent retrograde signal induces the expression of the high-affinity choline transporter in cholinergic neurons. Neuron *61*, 272–286.

Kristofiková, Z., Rícný, J., Kozmiková, I., Rípová, D., Zach, P., and Klaschka, J. (2006). Sex-dependent actions of amyloid beta peptides on hippocampal choline carriers of postnatal rats. Neurochem. Res. *31*, 351–360.

Kulak, J.M., McIntosh, J.M., Yoshikami, D., and Olivera, B.M. (2001). Nicotine-evoked transmitter release from synaptosomes: functional association of specific presynaptic acetylcholine receptors and voltage-gated calcium channels. J. Neurochem. *77*, 1581–1589.

Kupchik, Y.M., Barchad-Avitzur, O., Wess, J., Ben-Chaim, Y., Parnas, I., and Parnas, H. (2011). A novel fast mechanism for GPCR-mediated signal transduction--control of neurotransmitter release. J. Cell Biol. *192*, 137–151.

Lamotte d'Incamps, B., and Ascher, P. (2008). Four excitatory postsynaptic ionotropic receptors coactivated at the motoneuron-Renshaw cell synapse. J. Neurosci. *28*, 14121–14131.

Lamotte d'Incamps, B., Krejci, E., and Ascher, P. (2012). Mechanisms shaping the slow nicotinic synaptic current at the motoneuron-renshaw cell synapse. J. Neurosci. *32*, 8413–8423.

Lanzafame, A.A., Christopoulos, A., and Mitchelson, F. (2003). Cellular signaling mechanisms for muscarinic acetylcholine receptors. Recept. Channels *9*, 241–260.

Laviolette, S.R., Priebe, R.P., and Yeomans, J.S. (2000). Role of the laterodorsal tegmental nucleus in scopolamine- and amphetamine-induced locomotion and stereotypy. Pharmacol. Biochem. Behav. *65*, 163–174.

Lazareno, S., and Birdsall, N.J. (1993). Pharmacological characterization of acetylcholine-stimulated [35S]-GTP gamma S binding mediated by human muscarinic m1-m4 receptors: antagonist studies. Br. J. Pharmacol. *109*, 1120–1127.

Legay, C., Huchet, M., Massoulié, J., and Changeux, J.P. (1995). Developmental regulation of acetylcholinesterase transcripts in the mouse diaphragm: alternative splicing and focalization. Eur. J. Neurosci. *7*, 1803–1809.

Léna, C., and Changeux, J.P. (1997). Role of Ca2+ ions in nicotinic facilitation of GABA release in mouse thalamus. J. Neurosci. *17*, 576–585.

Lendvai, B., and Vizi, E.S. (2008). Nonsynaptic chemical transmission through nicotinic acetylcholine

receptors. Physiol. Rev. *88*, 333–349.

Levey, A.I. (1996). Muscarinic acetylcholine receptor expression in memory circuits: implications for treatment of Alzheimer disease. Proc. Natl. Acad. Sci. U.S.A. *93*, 13541–13546.

Li, B., Stribley, J.A., Ticu, A., Xie, W., Schopfer, L.M., Hammond, P., Brimijoin, S., Hinrichs, S.H., and Lockridge, O. (2000). Abundant tissue butyrylcholinesterase and its possible function in the acetylcholinesterase knockout mouse. J. Neurochem. *75*, 1320–1331.

Li, B., Duysen, E.G., Volpicelli-Daley, L.A., Levey, A.I., and Lockridge, O. (2003). Regulation of muscarinic acetylcholine receptor function in acetylcholinesterase knockout mice. Pharmacol. Biochem. Behav. *74*, 977–986.

Li, B., Duysen, E.G., Saunders, T.L., and Lockridge, O. (2006). Production of the butyrylcholinesterase knockout mouse. J. Mol. Neurosci. *30*, 193–195.

Li, B., Duysen, E.G., Carlson, M., and Lockridge, O. (2008a). The butyrylcholinesterase knockout mouse as a model for human butyrylcholinesterase deficiency. J. Pharmacol. Exp. Ther. *324*, 1146–1154.

Li, B., Duysen, E.G., and Lockridge, O. (2008b). The butyrylcholinesterase knockout mouse is obese on a high-fat diet. Chem. Biol. Interact. *175*, 88–91.

Li, H., Schopfer, L.M., Masson, P., and Lockridge, O. (2008c). Lamellipodin proline rich peptides associated with native plasma butyrylcholinesterase tetramers. Biochem. J. *411*, 425–432.

Li, Y., Camp, S., and Taylor, P. (1993). Tissue-specific expression and alternative mRNA processing of the mammalian acetylcholinesterase gene. J. Biol. Chem. *268*, 5790–5797.

Lin, H.-Q., Choi, R., Chan, K.-L., Ip, D., Tsim, K.W.-K., and Wan, D.C.-C. (2010). Differential gene expression profiling on the muscle of acetylcholinesterase knockout mice: a preliminary analysis. Chem. Biol. Interact. *187*, 120–123.

Liste, I., Bernard, V., and Bloch, B. (2002). Acute and chronic acetylcholinesterase inhibition regulates in vivo the localization and abundance of muscarinic receptors m2 and m4 at the cell surface and in the cytoplasm of striatal neurons. Mol. Cell. Neurosci. *20*, 244–256.

Lockridge, O. (1990). Genetic variants of human serum cholinesterase influence metabolism of the muscle relaxant succinylcholine. Pharmacol. Ther. *47*, 35–60.

Lockridge, O., and Masson, P. (2000). Pesticides and susceptible populations: people with butyrylcholinesterase genetic variants may be at risk. Neurotoxicology *21*, 113–126.

Lockridge, O., Mottershaw-Jackson, N., Eckerson, H.W., and La Du, B.N. (1980). Hydrolysis of diacetylmorphine (heroin) by human serum cholinesterase. J. Pharmacol. Exp. Ther. *215*, 1–8.

Lomax, P., and Jenden, D.J. (1966). Hypothermia following systematic and intracerebral injection of oxotremorine in the rat. Int J Neuropharmacol *5*, 353–359.

Lovinger, D.M. (2010). Neurotransmitter roles in synaptic modulation, plasticity and learning in the dorsal striatum. Neuropharmacology *58*, 951–961.

Luo, Z.D., Camp, S., Mutero, A., and Taylor, P. (1998). Splicing of 5' introns dictates alternative splice selection of acetylcholinesterase pre-mRNA and specific expression during myogenesis. J. Biol. Chem. *273*, 28486–28495.

Lüscher, C., and Slesinger, P.A. (2010). Emerging roles for G protein-gated inwardly rectifying potassium (GIRK) channels in health and disease. Nat. Rev. Neurosci. *11*, 301–315.

Machová, E., Jakubík, J., Michal, P., Oksman, M., Iivonen, H., Tanila, H., and Dolezal, V. (2008). Impairment of muscarinic transmission in transgenic APPswe/PS1dE9 mice. Neurobiol. Aging *29*, 368–378.

Malenka, R.C., and Bear, M.F. (2004). LTP and LTD: an embarrassment of riches. Neuron *44*, 5–21.

Manoharan, I., Wieseler, S., Layer, P.G., Lockridge, O., and Boopathy, R. (2006). Naturally occurring mutation Leu307Pro of human butyrylcholinesterase in the Vysya community of India. Pharmacogenet.

Genomics *16*, 461–468.

Manoharan, I., Boopathy, R., Darvesh, S., and Lockridge, O. (2007). A medical health report on individuals with silent butyrylcholinesterase in the Vysya community of India. Clin. Chim. Acta *378*, 128–135.

Mark, G.P., Kinney, A.E., Grubb, M.C., Zhu, X., Finn, D.A., Mader, S.L., Berger, S.P., and Bechtholt, A.J. (2006). Injection of oxotremorine in nucleus accumbens shell reduces cocaine but not food self-administration in rats. Brain Res. *1123*, 51–59.

Marks, M.J., Laverty, D.S., Whiteaker, P., Salminen, O., Grady, S.R., McIntosh, J.M., and Collins, A.C. (2010). John Daly's compound, epibatidine, facilitates identification of nicotinic receptor subtypes. J. Mol. Neurosci. *40*, 96–104.

Martins-Silva, C., De Jaeger, X., Guzman, M.S., Lima, R.D.F., Santos, M.S., Kushmerick, C., Gomez, M.V., Caron, M.G., Prado, M.A.M., and Prado, V.F. (2011). Novel strains of mice deficient for the vesicular acetylcholine transporter: insights on transcriptional regulation and control of locomotor behavior. PLoS ONE *6*, e17611.

Martres, M.P., Sales, N., Bouthenet, M.L., and Schwartz, J.C. (1985). Localisation and pharmacological characterisation of D-2 dopamine receptors in rat cerebral neocortex and cerebellum using [125I] iodosulpride. Eur. J. Pharmacol. *118*, 211–219.

Martyn, A.C., De Jaeger, X., Magalhães, A.C., Kesarwani, R., Gonçalves, D.F., Raulic, S., Guzman, M.S., Jackson, M.F., Izquierdo, I., Macdonald, J.F., et al. (2012). Elimination of the vesicular acetylcholine transporter in the forebrain causes hyperactivity and deficits in spatial memory and long-term potentiation. Proc. Natl. Acad. Sci. U.S.A. *109*, 17651–17656.

Maskos, U. (2010). Role of endogenous acetylcholine in the control of the dopaminergic system via nicotinic receptors. J. Neurochem. *114*, 641–646.

Maskos, U., Molles, B.E., Pons, S., Besson, M., Guiard, B.P., Guilloux, J.-P., Evrard, A., Cazala, P., Cormier, A., Mameli-Engvall, M., et al. (2005). Nicotine reinforcement and cognition restored by targeted expression of nicotinic receptors. Nature *436*, 103–107.

Masson, P., and Lockridge, O. (2010). Butyrylcholinesterase for protection from organophosphorus poisons: catalytic complexities and hysteretic behavior. Arch. Biochem. Biophys. *494*, 107–120.

Masson, P., Froment, M.T., Fortier, P.L., Visicchio, J.E., Bartels, C.F., and Lockridge, O. (1998). Butyrylcholinesterase-catalysed hydrolysis of aspirin, a negatively charged ester, and aspirin-related neutral esters. Biochim. Biophys. Acta *1387*, 41–52.

Massoulié, J. (2002). The origin of the molecular diversity and functional anchoring of cholinesterases. Neurosignals *11*, 130–143.

Massoulié, J., and Millard, C.B. (2009). Cholinesterases and the basal lamina at vertebrate neuromuscular junctions. Curr Opin Pharmacol *9*, 316–325.

Massoulié, J., Pezzementi, L., Bon, S., Krejci, E., and Vallette, F.M. (1993). Molecular and cellular biology of cholinesterases. Prog. Neurobiol. *41*, 31–91.

Massoulié, J., Bon, S., Perrier, N., and Falasca, C. (2005). The C-terminal peptides of acetylcholinesterase: cellular trafficking, oligomerization and functional anchoring. Chem. Biol. Interact. *157-158*, 3–14.

Mathur, A., Shandarin, A., LaViolette, S.R., Parker, J., and Yeomans, J.S. (1997). Locomotion and stereotypy induced by scopolamine: contributions of muscarinic receptors near the pedunculopontine tegmental nucleus. Brain Res. *775*, 144–155.

Maurice, N., Mercer, J., Chan, C.S., Hernandez-Lopez, S., Held, J., Tkatch, T., and Surmeier, D.J. (2004). D2 dopamine receptor-mediated modulation of voltage-dependent Na+ channels reduces autonomous activity in striatal cholinergic interneurons. J. Neurosci. *24*, 10289–10301.

McCoy, P.A., and McMahon, L.L. (2007). Muscarinic receptor dependent long-term depression in rat visual cortex is PKC independent but requires ERK1/2 activation and protein synthesis. J. Neurophysiol.

98, 1862–1870.

McGehee, D.S., Heath, M.J., Gelber, S., Devay, P., and Role, L.W. (1995). Nicotine enhancement of fast excitatory synaptic transmission in CNS by presynaptic receptors. Science *269*, 1692–1696.

McMahan, U.J., Sanes, J.R., and Marshall, L.M. (1978). Cholinesterase is associated with the basal lamina at the neuromuscular junction. Nature *271*, 172–174.

Mechawar, N., Watkins, K.C., and Descarries, L. (2002). Ultrastructural features of the acetylcholine innervation in the developing parietal cortex of rat. J. Comp. Neurol. *443*, 250–258.

Meshorer, E., and Soreq, H. (2006). Virtues and woes of AChE alternative splicing in stress-related neuropathologies. Trends Neurosci. *29*, 216–224.

Meshorer, E., Erb, C., Gazit, R., Pavlovsky, L., Kaufer, D., Friedman, A., Glick, D., Ben-Arie, N., and Soreq, H. (2002). Alternative splicing and neuritic mRNA translocation under long-term neuronal hypersensitivity. Science *295*, 508–512.

Meshorer, E., Toiber, D., Zurel, D., Sahly, I., Dori, A., Cagnano, E., Schreiber, L., Grisaru, D., Tronche, F., and Soreq, H. (2004). Combinatorial complexity of 5' alternative acetylcholinesterase transcripts and protein products. J. Biol. Chem. *279*, 29740–29751.

Mesulam, M.M., Mufson, E.J., Wainer, B.H., and Levey, A.I. (1983). Central cholinergic pathways in the rat: an overview based on an alternative nomenclature (Ch1-Ch6). Neuroscience *10*, 1185–1201.

Mesulam, M.-M., Guillozet, A., Shaw, P., Levey, A., Duysen, E.G., and Lockridge, O. (2002). Acetylcholinesterase knockouts establish central cholinergic pathways and can use butyrylcholinesterase to hydrolyze acetylcholine. Neuroscience *110*, 627–639.

Mihaylova, V., Müller, J.S., Vilchez, J.J., Salih, M.A., Kabiraj, M.M., D'Amico, A., Bertini, E., Wölfle, J., Schreiner, F., Kurlemann, G., et al. (2008). Clinical and molecular genetic findings in COLQ-mutant congenital myasthenic syndromes. Brain *131*, 747–759.

Michel, V., Yuan, Z., Ramsubir, S., and Bakovic, M. (2006). Choline transport for phospholipid synthesis. Exp. Biol. Med. (Maywood) *231*, 490–504.

Miller, J.H., Gibson, V.A., and McKinney, M. (1991). Binding of [3H]AF-DX 384 to cloned and native muscarinic receptors. J. Pharmacol. Exp. Ther. *259*, 601–607.

Minic, J., Chatonnet, A., Krejci, E., and Molgó, J. (2003). Butyrylcholinesterase and acetylcholinesterase activity and quantal transmitter release at normal and acetylcholinesterase knockout mouse neuromuscular junctions. Br. J. Pharmacol. *138*, 177–187.

Mirza, N.R., and Stolerman, I.P. (2000). The role of nicotinic and muscarinic acetylcholine receptors in attention. Psychopharmacology (Berl.) *148*, 243–250.

Miyakawa, T., Yamada, M., Duttaroy, A., and Wess, J. (2001). Hyperactivity and intact hippocampus-dependent learning in mice lacking the M1 muscarinic acetylcholine receptor. J. Neurosci. *21*, 5239–5250.

Mohr, F., Zimmermann, M., and Klein, J. (2013). Mice heterozygous for AChE are more sensitive to AChE inhibitors but do not respond to BuChE inhibition. Neuropharmacology *67*, 37–45.

Mok, M.K.W., Leung, K.W., Xie, H.Q., Guo, A.J.Y., Chen, V.P., Zhu, J.T.T., Choi, R.C.Y., and Tsim, K.W.K. (2009). A new variant of proline-rich membrane anchor (PRiMA) of acetylcholinesterase in chicken: expression in different muscle fiber types. Neurosci. Lett. *461*, 202–206.

Morel, N., Leroy, J., Ayon, A., Massoulié, J., and Bon, S. (2001). Acetylcholinesterase H and T dimers are associated through the same contact. Mutations at this interface interfere with the C-terminal T peptide, inducing degradation rather than secretion. J. Biol. Chem. *276*, 37379–37389.

Moriya, H., Takagi, Y., Nakanishi, T., Hayashi, M., Tani, T., and Hirotsu, I. (1999). Affinity profiles of various muscarinic antagonists for cloned human muscarinic acetylcholine receptor (mAChR) subtypes and mAChRs in rat heart and submandibular gland. Life Sci. *64*, 2351–2358.

Moroni, M., Zwart, R., Sher, E., Cassels, B.K., and Bermudez, I. (2006). alpha4beta2 nicotinic receptors with high and low acetylcholine sensitivity: pharmacology, stoichiometry, and sensitivity to long-

term exposure to nicotine. Mol. Pharmacol. *70*, 755–768.

Morris, R. (1984). Developments of a water-maze procedure for studying spatial learning in the rat. J. Neurosci. Methods *11*, 47–60.

Moser, N., Mechawar, N., Jones, I., Gochberg-Sarver, A., Orr-Urtreger, A., Plomann, M., Salas, R., Molles, B., Marubio, L., Roth, U., et al. (2007). Evaluating the suitability of nicotinic acetylcholine receptor antibodies for standard immunodetection procedures. J. Neurochem. *102*, 479–492.

Mrvova, K., Obzerova, L., Girard, E., Krejci, E., and Hrabovska, A. (2012). Monoclonal antibodies to mouse butyrylcholinesterase. Chem. Biol. Interact.

Mrzljak, L., Pappy, M., Leranth, C., and Goldman-Rakic, P.S. (1995). Cholinergic synaptic circuitry in the macaque prefrontal cortex. J. Comp. Neurol. *357*, 603–617.

Mufson, E.J., Martin, T.L., Mash, D.C., Wainer, B.H., and Mesulam, M.M. (1986). Cholinergic projections from the parabigeminal nucleus (Ch8) to the superior colliculus in the mouse: a combined analysis of horseradish peroxidase transport and choline acetyltransferase immunohistochemistry. Brain Res. *370*, 144–148.

Murrin, L.C., and Kuhar, M.J. (1976). Activation of high-affinity choline uptake in vitro by depolarizing agents. Mol. Pharmacol. *12*, 1082–1090.

Myslivecek, J., Duysen, E.G., and Lockridge, O. (2007). Adaptation to excess acetylcholine by downregulation of adrenoceptors and muscarinic receptors in lungs of acetylcholinesterase knockout mice. Naunyn Schmiedebergs Arch. Pharmacol. *376*, 83–92.

Naik, R.S., Hartmann, J., Kiewert, C., Duysen, E.G., Lockridge, O., and Klein, J. (2009). Effects of rivastigmine and donepezil on brain acetylcholine levels in acetylcholinesterase-deficient mice. J Pharm Pharm Sci *12*, 79–85.

Nakata, K., Okuda, T., and Misawa, H. (2004). Ultrastructural localization of high-affinity choline transporter in the rat neuromuscular junction: enrichment on synaptic vesicles. Synapse *53*, 53–56.

Narushima, M., Uchigashima, M., Fukaya, M., Matsui, M., Manabe, T., Hashimoto, K., Watanabe, M., and Kano, M. (2007). Tonic enhancement of endocannabinoid-mediated retrograde suppression of inhibition by cholinergic interneuron activity in the striatum. J. Neurosci. *27*, 496–506.

Nathanson, N.M. (2000). A multiplicity of muscarinic mechanisms: enough signaling pathways to take your breath away. Proc. Natl. Acad. Sci. U.S.A. *97*, 6245–6247.

Navaratnam, D.S., Fernando, F.S., Priddle, J.D., Giles, K., Clegg, S.M., Pappin, D.J., Craig, I., and Smith, A.D. (2000). Hydrophobic protein that copurifies with human brain acetylcholinesterase: amino acid sequence, genomic organization, and chromosomal localization. J. Neurochem. *74*, 2146–2153.

Nicolet, Y., Lockridge, O., Masson, P., Fontecilla-Camps, J.C., and Nachon, F. (2003). Crystal structure of human butyrylcholinesterase and of its complexes with substrate and products. J. Biol. Chem. *278*, 41141–41147.

Noureddine, H., Schmitt, C., Liu, W., Garbay, C., Massoulié, J., and Bon, S. (2007). Assembly of acetylcholinesterase tetramers by peptidic motifs from the proline-rich membrane anchor, PRiMA: competition between degradation and secretion pathways of heteromeric complexes. J. Biol. Chem. *282*, 3487–3497.

Noureddine, H., Carvalho, S., Schmitt, C., Massoulié, J., and Bon, S. (2008). Acetylcholinesterase associates differently with its anchoring proteins ColQ and PRiMA. J. Biol. Chem. *283*, 20722–20732.

Le Novère, N., Corringer, P.-J., and Changeux, J.-P. (2002). The diversity of subunit composition in nAChRs: evolutionary origins, physiologic and pharmacologic consequences. J. Neurobiol. *53*, 447–456.

Oda, Y. (1999). Choline acetyltransferase: the structure, distribution and pathologic changes in the central nervous system. Pathol. Int. *49*, 921–937.

Ohno, K., Brengman, J., Tsujino, A., and Engel, A.G. (1998). Human endplate acetylcholinesterase deficiency caused by mutations in the collagen-like tail subunit (ColQ) of the asymmetric enzyme. Proc.

Natl. Acad. Sci. U.S.A. *95*, 9654–9659.

Ohno, M., Yamamoto, T., and Watanabe, S. (1994). Blockade of hippocampal M1 muscarinic receptors impairs working memory performance of rats. Brain Res. *650*, 260–266.

Oki, T., Takagi, Y., Inagaki, S., Taketo, M.M., Manabe, T., Matsui, M., and Yamada, S. (2005). Quantitative analysis of binding parameters of [3H]N-methylscopolamine in central nervous system of muscarinic acetylcholine receptor knockout mice. Brain Res. Mol. Brain Res. *133*, 6–11.

Parent, M., and Descarries, L. (2008). Acetylcholine innervation of the adult rat thalamus: distribution and ultrastructural features in dorsolateral geniculate, parafascicular, and reticular thalamic nuclei. J. Comp. Neurol. *511*, 678–691.

Parikh, V., and Sarter, M. (2006). Cortical choline transporter function measured in vivo using choline-sensitive microelectrodes: clearance of endogenous and exogenous choline and effects of removal of cholinergic terminals. J. Neurochem. *97*, 488–503.

Parikh, V., Kozak, R., Martinez, V., and Sarter, M. (2007). Prefrontal acetylcholine release controls cue detection on multiple timescales. Neuron *56*, 141–154.

Parikh, V., St Peters, M., Blakely, R.D., and Sarter, M. (2013). The presynaptic choline transporter imposes limits on sustained cortical acetylcholine release and attention. J. Neurosci. *33*, 2326–2337.

Pattij, T., Janssen, M.C.W., Loos, M., Smit, A.B., Schoffelmeer, A.N.M., and van Gaalen, M.M. (2007). Strain specificity and cholinergic modulation of visuospatial attention in three inbred mouse strains. Genes Brain Behav. *6*, 579–587.

Perrier, A.L., Massoulié, J., and Krejci, E. (2002). PRiMA: the membrane anchor of acetylcholinesterase in the brain. Neuron *33*, 275–285.

Perrier, N.A., Khérif, S., Perrier, A.L., Dumas, S., Mallet, J., and Massoulié, J. (2003). Expression of PRiMA in the mouse brain: membrane anchoring and accumulation of "tailed" acetylcholinesterase. Eur. J. Neurosci. *18*, 1837–1847.

Perrier, N.A., Salani, M., Falasca, C., Bon, S., Augusti-Tocco, G., and Massoulié, J. (2005). The readthrough variant of acetylcholinesterase remains very minor after heat shock, organophosphate inhibition and stress, in cell culture and in vivo. J. Neurochem. *94*, 629–638.

Perry, D.C., and Kellar, K.J. (1995). [3H]epibatidine labels nicotinic receptors in rat brain: an autoradiographic study. J. Pharmacol. Exp. Ther. *275*, 1030–1034.

Perry, M.L., Andrzejewski, M.E., Bushek, S.M., and Baldo, B.A. (2010). Intra-accumbens infusion of a muscarinic antagonist reduces food intake without altering the incentive properties of food-associated cues. Behav. Neurosci. *124*, 44–54.

Petrovic, M.M., Nowacki, J., Olivo, V., Tsaneva-Atanasova, K., Randall, A.D., and Mellor, J.R. (2012). Inhibition of post-synaptic Kv7/KCNQ/M channels facilitates long-term potentiation in the hippocampus. PLoS ONE *7*, e30402.

Pezzementi, L., and Chatonnet, A. (2010). Evolution of cholinesterases in the animal kingdom. Chem. Biol. Interact. *187*, 27–33.

Pezzementi, L., Nachon, F., and Chatonnet, A. (2011). Evolution of acetylcholinesterase and butyrylcholinesterase in the vertebrates: an atypical butyrylcholinesterase from the Medaka Oryzias latipes. PLoS ONE *6*, e17396.

Porter, A.C., Bymaster, F.P., DeLapp, N.W., Yamada, M., Wess, J., Hamilton, S.E., Nathanson, N.M., and Felder, C.C. (2002). M1 muscarinic receptor signaling in mouse hippocampus and cortex. Brain Res. *944*, 82–89.

Power, J.M., and Sah, P. (2002). Nuclear calcium signaling evoked by cholinergic stimulation in hippocampal CA1 pyramidal neurons. J. Neurosci. *22*, 3454–3462.

Prado, M.A.M., Reis, R.A.M., Prado, V.F., de Mello, M.C., Gomez, M.V., and de Mello, F.G. (2002).

Regulation of acetylcholine synthesis and storage. Neurochem. Int. *41*, 291–299.

Pratt, W.E., and Blackstone, K. (2009). Nucleus accumbens acetylcholine and food intake: decreased muscarinic tone reduces feeding but not food-seeking. Behav. Brain Res. *198*, 252–257.

Quinn, D. (1987). Acetylcholinesterase: enzyme structure, reaction dynamics, and virtual transition states. Chem. Rev. *87*, 955–979.

Quirion, R., Wilson, A., Rowe, W., Aubert, I., Richard, J., Doods, H., Parent, A., White, N., and Meaney, M.J. (1995). Facilitation of acetylcholine release and cognitive performance by an M(2)-muscarinic receptor antagonist in aged memory-impaired. J. Neurosci. *15*, 1455–1462.

Radcliffe, K.A., and Dani, J.A. (1998). Nicotinic stimulation produces multiple forms of increased glutamatergic synaptic transmission. J. Neurosci. *18*, 7075–7083.

Radcliffe, K.A., Fisher, J.L., Gray, R., and Dani, J.A. (1999). Nicotinic modulation of glutamate and GABA synaptic transmission of hippocampal neurons. Ann. N. Y. Acad. Sci. *868*, 591–610.

Rassadi, S., Krishnaswamy, A., Pié, B., McConnell, R., Jacob, M.H., and Cooper, E. (2005). A null mutation for the alpha3 nicotinic acetylcholine (ACh) receptor gene abolishes fast synaptic activity in sympathetic ganglia and reveals that ACh output from developing preganglionic terminals is regulated in an activity-dependent retrograde manner. J. Neurosci. *25*, 8555–8566.

Reid, R.T., and Sabbagh, M.N. (2008). Effects of cholinesterase inhibitors on rat nicotinic receptor levels in vivo and in vitro. J Neural Transm *115*, 1437–1444.

Ren, J., Qin, C., Hu, F., Tan, J., Qiu, L., Zhao, S., Feng, G., and Luo, M. (2011). Habenula "cholinergic" neurons co-release glutamate and acetylcholine and activate postsynaptic neurons via distinct transmission modes. Neuron *69*, 445–452.

Reuben, M., and Clarke, P.B. (2000). Nicotine-evoked [3H]5-hydroxytryptamine release from rat striatal synaptosomes. Neuropharmacology *39*, 290–299.

Rosenblum, K., Futter, M., Jones, M., Hulme, E.C., and Bliss, T.V. (2000). ERKI/II regulation by the muscarinic acetylcholine receptors in neurons. J. Neurosci. *20*, 977–985.

Rotundo, R.L. (1984). Purification and properties of the membrane-bound form of acetylcholinesterase from chicken brain. Evidence for two distinct polypeptide chains. J. Biol. Chem. *259*, 13186–13194.

Rouse, S.T., Hamilton, S.E., Potter, L.T., Nathanson, N.M., and Conn, P.J. (2000a). Muscarinic-induced modulation of potassium conductances is unchanged in mouse hippocampal pyramidal cells that lack functional M1 receptors. Neurosci. Lett. *278*, 61–64.

Rouse, S.T., Edmunds, S.M., Yi, H., Gilmor, M.L., and Levey, A.I. (2000b). Localization of M(2) muscarinic acetylcholine receptor protein in cholinergic and non-cholinergic terminals in rat hippocampus. Neurosci. Lett. *284*, 182–186.

Ruff, R.L. (2003). Neurophysiology of the neuromuscular junction: overview. Ann. N. Y. Acad. Sci. *998*, 1–10.

Sanford, L.D., Yang, L., Tang, X., Dong, E., Ross, R.J., and Morrison, A.R. (2006). Cholinergic regulation of the central nucleus of the amygdala in rats: effects of local microinjections of cholinomimetics and cholinergic antagonists on arousal and sleep. Neuroscience *141*, 2167–2176.

Sarter, M., Parikh, V., and Howe, W.M. (2009). Phasic acetylcholine release and the volume transmission hypothesis: time to move on. Nat. Rev. Neurosci. *10*, 383–390.

Satoh, K., Armstrong, D.M., and Fibiger, H.C. (1983). A comparison of the distribution of central cholinergic neurons as demonstrated by acetylcholinesterase pharmacohistochemistry and choline acetyltransferase immunohistochemistry. Brain Res. Bull. *11*, 693–720.

Scali, C., Casamenti, F., Bellucci, A., Costagli, C., Schmidt, B., and Pepeu, G. (2002). Effect of subchronic administration of metrifonate, rivastigmine and donepezil on brain acetylcholine in aged F344 rats. J Neural Transm *109*, 1067–1080.

Seeger, T., and Alzheimer, C. (2001). Muscarinic activation of inwardly rectifying K(+) conductance

reduces EPSPs in rat hippocampal CA1 pyramidal cells. J. Physiol. (Lond.) *535*, 383–396.

Seeger, T., Fedorova, I., Zheng, F., Miyakawa, T., Koustova, E., Gomeza, J., Basile, A.S., Alzheimer, C., and Wess, J. (2004). M2 muscarinic acetylcholine receptor knock-out mice show deficits in behavioral flexibility, working memory, and hippocampal plasticity. J. Neurosci. *24*, 10117–10127.

Shabani, S., Foster, R., Gubner, N., Phillips, T.J., and Mark, G.P. (2010). Muscarinic type 2 receptors in the lateral dorsal tegmental area modulate cocaine and food seeking behavior in rats. Neuroscience *170*, 559–569.

Shapovalova, K.B., Kamkina, Y.V., and Mysovskii, D.A. (2005). The effects of microinjection of the selective blocker of muscarinic M1 receptors pirenzepine into the neostriatum on the motor behavior of rats. Neurosci. Behav. Physiol. *35*, 589–594.

Sharma, G., and Vijayaraghavan, S. (2003). Modulation of presynaptic store calcium induces release of glutamate and postsynaptic firing. Neuron *38*, 929–939.

Sharma, G., Grybko, M., and Vijayaraghavan, S. (2008). Action potential-independent and nicotinic receptor-mediated concerted release of multiple quanta at hippocampal CA3-mossy fiber synapses. J. Neurosci. *28*, 2563–2575.

Sharma, K.V., Koenigsberger, C., Brimijoin, S., and Bigbee, J.W. (2001). Direct evidence for an adhesive function in the noncholinergic role of acetylcholinesterase in neurite outgrowth. J. Neurosci. Res. *63*, 165–175.

Shen, J., and Yakel, J.L. (2009). Nicotinic acetylcholine receptor-mediated calcium signaling in the nervous system. Acta Pharmacol. Sin. *30*, 673–680.

Shen, W., Hamilton, S.E., Nathanson, N.M., and Surmeier, D.J. (2005). Cholinergic suppression of KCNQ channel currents enhances excitability of striatal medium spiny neurons. J. Neurosci. *25*, 7449–7458.

Shen, W., Tian, X., Day, M., Ulrich, S., Tkatch, T., Nathanson, N.M., and Surmeier, D.J. (2007). Cholinergic modulation of Kir2 channels selectively elevates dendritic excitability in striatopallidal neurons. Nat. Neurosci. *10*, 1458–1466.

Shinoe, T., Matsui, M., Taketo, M.M., and Manabe, T. (2005). Modulation of synaptic plasticity by physiological activation of M1 muscarinic acetylcholine receptors in the mouse hippocampus. J. Neurosci. *25*, 11194–11200.

Shirey, J.K., Xiang, Z., Orton, D., Brady, A.E., Johnson, K.A., Williams, R., Ayala, J.E., Rodriguez, A.L., Wess, J., Weaver, D., et al. (2008). An allosteric potentiator of M4 mAChR modulates hippocampal synaptic transmission. Nat. Chem. Biol. *4*, 42–50.

Schmidt, L.S., Thomsen, M., Weikop, P., Dencker, D., Wess, J., Woldbye, D.P.D., Wortwein, G., and Fink-Jensen, A. (2011). Increased cocaine self-administration in M4 muscarinic acetylcholine receptor knockout mice. Psychopharmacology (Berl.) *216*, 367–378.

Silman, I., and Sussman, J.L. (2008). Acetylcholinesterase: how is structure related to function? Chem. Biol. Interact. *175*, 3–10.

Simon, J.R., and Kuhar, M.G. (1975). Impulse-flow regulation of high affinity choline uptake in brain cholinergic nerve terminals. Nature *255*, 162–163.

Simon, S., Krejci, E., and Massoulié, J. (1998). A four-to-one association between peptide motifs: four C-terminal domains from cholinesterase assemble with one proline-rich attachment domain (PRAD) in the secretory pathway. EMBO J. *17*, 6178–6187.

Sipos, M.L., Burchnell, V., and Galbicka, G. (1999). Dose-response curves and time-course effects of selected anticholinergics on locomotor activity in rats. Psychopharmacology (Berl.) *147*, 250–256.

Skau, K.A., and Brimijoin, S. (1980). Multiple molecular forms of acetylcholinesterase in rat vagus nerve, smooth muscle, and heart. J. Neurochem. *35*, 1151–1154.

Slutsky, I., Wess, J., Gomeza, J., Dudel, J., Parnas, I., and Parnas, H. (2003). Use of knockout mice reveals involvement of M2-muscarinic receptors in control of the kinetics of acetylcholine release. J.

Neurophysiol. *89*, 1954–1967.

Smiley, J.F., Morrell, F., and Mesulam, M.M. (1997). Cholinergic synapses in human cerebral cortex: an ultrastructural study in serial sections. Exp. Neurol. *144*, 361–368.

Soreq, H., and Seidman, S. (2001). Acetylcholinesterase--new roles for an old actor. Nat. Rev. Neurosci. *2*, 294–302.

Spurden, D.P., Court, J.A., Lloyd, S., Oakley, A., Perry, R., Pearson, C., Pullen, R.G., and Perry, E.K. (1997). Nicotinic receptor distribution in the human thalamus: autoradiographical localization of [3H] nicotine and [125I] alpha-bungarotoxin binding. J. Chem. Neuroanat. *13*, 105–113.

Standley, C.A. (1999). N-methyl-D-aspartate receptor binding is altered and seizure potential reduced in pregnant rats. Brain Res. *844*, 10–19.

Steidl, S., and Yeomans, J.S. (2009). M5 muscarinic receptor knockout mice show reduced morphine-induced locomotion but increased locomotion after cholinergic antagonism in the ventral tegmental area. J. Pharmacol. Exp. Ther. *328*, 263–275.

Sternfeld, M., Patrick, J.D., and Soreq, H. (1998). Position effect variegations and brain-specific silencing in transgenic mice overexpressing human acetylcholinesterase variants. J. Physiol. Paris *92*, 249–255.

Sun, J., and Kapur, J. (2012). M-type potassium channels modulate Schaffer collateral-CA1 glutamatergic synaptic transmission. J. Physiol. (Lond.) *590*, 3953–3964.

Sun, H., El Yazal, J., Lockridge, O., Schopfer, L.M., Brimijoin, S., and Pang, Y.P. (2001). Predicted Michaelis-Menten complexes of cocaine-butyrylcholinesterase. Engineering effective butyrylcholinesterase mutants for cocaine detoxication. J. Biol. Chem. *276*, 9330–9336.

Sun, M., Lee, C.J., and Shin, H.-S. (2007). Reduced nicotinic receptor function in sympathetic ganglia is responsible for the hypothermia in the acetylcholinesterase knockout mouse. J. Physiol. (Lond.) *578*, 751–764.

Surmeier, D.J., and Graybiel, A.M. (2012). A feud that wasn't: acetylcholine evokes dopamine release in the striatum. Neuron *75*, 1–3.

Surmeier, D.J., Ding, J., Day, M., Wang, Z., and Shen, W. (2007). D1 and D2 dopamine-receptor modulation of striatal glutamatergic signaling in striatal medium spiny neurons. Trends Neurosci. *30*, 228–235.

Sussman, J.L., Harel, M., Frolow, F., Oefner, C., Goldman, A., Toker, L., and Silman, I. (1991). Atomic structure of acetylcholinesterase from Torpedo californica: a prototypic acetylcholine-binding protein. Science *253*, 872–879.

Svedberg, M.M., Svensson, A.-L., Johnson, M., Lee, M., Cohen, O., Court, J., Soreq, H., Perry, E., and Nordberg, A. (2002). Upregulation of neuronal nicotinic receptor subunits alpha4, beta2, and alpha7 in transgenic mice overexpressing human acetylcholinesterase. J. Mol. Neurosci. *18*, 211–222.

Szutowicz, A., Tomaszewicz, M., and Bielarczyk, H. (1996). Disturbances of acetyl-CoA, energy and acetylcholine metabolism in some encephalopathies. Acta Neurobiol Exp (Wars) *56*, 323–339.

Tago, H., Maeda, T., McGeer, P.L., and Kimura, H. (1992). Butyrylcholinesterase-rich neurons in rat brain demonstrated by a sensitive histochemical method. J. Comp. Neurol. *325*, 301–312.

Threlfell, S., Lalic, T., Platt, N.J., Jennings, K.A., Deisseroth, K., and Cragg, S.J. (2012). Striatal dopamine release is triggered by synchronized activity in cholinergic interneurons. Neuron *75*, 58–64.

Tien, L.-T., Fan, L.-W., Sogawa, C., Ma, T., Loh, H.H., and Ho, I.-K. (2004). Changes in acetylcholinesterase activity and muscarinic receptor bindings in mu-opioid receptor knockout mice. Brain Res. Mol. Brain Res. *126*, 38–44.

Tsim, K.W., Randall, W.R., and Barnard, E.A. (1988). An asymmetric form of muscle acetylcholinesterase contains three subunit types and two enzymic activities in one molecule. Proc. Natl.

Acad. Sci. U.S.A. *85*, 1262–1266.

Tsim, K.W.K., Choi, R.C.Y., Xie, H.Q., Zhu, J.T.T., Leung, K.W., Lau, F.T.C., Chu, G.K.Y., Chen, V.P., Mok, M.K.W., Cheung, A.W.H., et al. (2008). Transcriptional control of different subunits of AChE in muscles: signals triggered by the motor nerve-derived factors. Chem. Biol. Interact. *175*, 58–63.

Tsim, K.W.K., Leung, K.W., Mok, K.W., Chen, V.P., Zhu, K.Y., Zhu, J.T.T., Guo, A.J.Y., Bi, C.W.C., Zheng, K.Y.Z., Lau, D.T.W., et al. (2010). Expression and Localization of PRiMA-linked globular form acetylcholinesterase in vertebrate neuromuscular junctions. J. Mol. Neurosci. *40*, 40–46.

Tucek, S. (1983). Acetylcoenzyme A and the synthesis of acetylcholine in neurones: review of recent progress. Gen. Physiol. Biophys. *2*, 313–324.

Turrini, P., Casu, M.A., Wong, T.P., De Koninck, Y., Ribeiro-da-Silva, A., and Cuello, A.C. (2001). Cholinergic nerve terminals establish classical synapses in the rat cerebral cortex: synaptic pattern and age-related atrophy. Neuroscience *105*, 277–285.

Tzavara, E.T., Bymaster, F.P., Felder, C.C., Wade, M., Gomeza, J., Wess, J., McKinzie, D.L., and Nomikos, G.G. (2003). Dysregulated hippocampal acetylcholine neurotransmission and impaired cognition in M2, M4 and M2/M4 muscarinic receptor knockout mice. Mol. Psychiatry *8*, 673–679.

Tzavara, E.T., Bymaster, F.P., Davis, R.J., Wade, M.R., Perry, K.W., Wess, J., McKinzie, D.L., Felder, C., and Nomikos, G.G. (2004). M4 muscarinic receptors regulate the dynamics of cholinergic and dopaminergic neurotransmission: relevance to the pathophysiology and treatment of related CNS pathologies. FASEB J. *18*, 1410–1412.

Umbriaco, D., Watkins, K.C., Descarries, L., Cozzari, C., and Hartman, B.K. (1994). Ultrastructural and morphometric features of the acetylcholine innervation in adult rat parietal cortex: an electron microscopic study in serial sections. J. Comp. Neurol. *348*, 351–373.

Umbriaco, D., Garcia, S., Beaulieu, C., and Descarries, L. (1995). Relational features of acetylcholine, noradrenaline, serotonin and GABA axon terminals in the stratum radiatum of adult rat hippocampus (CA1). Hippocampus *5*, 605–620.

Velan, B., Grosfeld, H., Kronman, C., Leitner, M., Gozes, Y., Lazar, A., Flashner, Y., Marcus, D., Cohen, S., and Shafferman, A. (1991). The effect of elimination of intersubunit disulfide bonds on the activity, assembly, and secretion of recombinant human acetylcholinesterase. Expression of acetylcholinesterase Cys-580----Ala mutant. J. Biol. Chem. *266*, 23977–23984.

Vignaud, A., Fougerousse, F., Mouisel, E., Guerchet, N., Hourde, C., Bacou, F., Butler-Browne, G.S., Chatonnet, A., and Ferry, A. (2008a). Genetic inactivation of acetylcholinesterase causes functional and structural impairment of mouse soleus muscles. Cell Tissue Res. *333*, 289–296.

Vignaud, A., Fougerousse, F., Mouisel, E., Bertrand, C., Bonafos, B., Molgo, J., Ferry, A., and Chatonnet, A. (2008b). Genetic ablation of acetylcholinesterase alters muscle function in mice. Chem. Biol. Interact. *175*, 129–130.

Villalobos, C., Foehring, R.C., Lee, J.C., and Andrade, R. (2011). Essential role for phosphatidylinositol 4,5-bisphosphate in the expression, regulation, and gating of the slow afterhyperpolarization current in the cerebral cortex. J. Neurosci. *31*, 18303–18312.

Volpicelli-Daley, L.A., Hrabovska, A., Duysen, E.G., Ferguson, S.M., Blakely, R.D., Lockridge, O., and Levey, A.I. (2003a). Altered striatal function and muscarinic cholinergic receptors in acetylcholinesterase knockout mice. Mol. Pharmacol. *64*, 1309–1316.

Volpicelli-Daley, L.A., Duysen, E.G., Lockridge, O., and Levey, A.I. (2003b). Altered hippocampal muscarinic receptors in acetylcholinesterase-deficient mice. Ann. Neurol. *53*, 788–796.

Wagner, S., Kufleitner, J., Zensi, A., Dadparvar, M., Wien, S., Bungert, J., Vogel, T., Worek, F., Kreuter, J., and von Briesen, H. (2010). Nanoparticulate transport of oximes over an in vitro blood-brain barrier model. PLoS ONE *5*, e14213.

Wanaverbecq, N., Semyanov, A., Pavlov, I., Walker, M.C., and Kullmann, D.M. (2007). Cholinergic axons modulate GABAergic signaling among hippocampal interneurons via postsynaptic alpha 7 nicotinic

receptors. J. Neurosci. *27*, 5683–5693.

Wang, Z., Kai, L., Day, M., Ronesi, J., Yin, H.H., Ding, J., Tkatch, T., Lovinger, D.M., and Surmeier, D.J. (2006). Dopaminergic control of corticostriatal long-term synaptic depression in medium spiny neurons is mediated by cholinergic interneurons. Neuron *50*, 443–452.

Watanabe, D., Inokawa, H., Hashimoto, K., Suzuki, N., Kano, M., Shigemoto, R., Hirano, T., Toyama, K., Kaneko, S., Yokoi, M., et al. (1998). Ablation of cerebellar Golgi cells disrupts synaptic integration involving GABA inhibition and NMDA receptor activation in motor coordination. Cell *95*, 17–27.

Wess, J. (1996). Molecular biology of muscarinic acetylcholine receptors. Crit Rev Neurobiol *10*, 69–99.

Wess, J., Eglen, R.M., and Gautam, D. (2007). Muscarinic acetylcholine receptors: mutant mice provide new insights for drug development. Nat Rev Drug Discov *6*, 721–733.

Whitlock, J.R., Heynen, A.J., Shuler, M.G., and Bear, M.F. (2006). Learning induces long-term potentiation in the hippocampus. Science *313*, 1093–1097.

Whittaker, V.P. (2010). How the cholinesterases got their modern names. Chem. Biol. Interact. *187*, 23–26.

Whyte, K.A., and Greenfield, S.A. (2003). Effects of acetylcholinesterase and butyrylcholinesterase on cell survival, neurite outgrowth, and voltage-dependent calcium currents of embryonic ventral mesencephalic neurons. Exp. Neurol. *184*, 496–509.

Witten, I.B., Lin, S.-C., Brodsky, M., Prakash, R., Diester, I., Anikeeva, P., Gradinaru, V., Ramakrishnan, C., and Deisseroth, K. (2010). Cholinergic interneurons control local circuit activity and cocaine conditioning. Science *330*, 1677–1681.

Wolfe, B.B., and Yasuda, R.P. (1995). Development of selective antisera for muscarinic cholinergic receptor subtypes. Ann. N. Y. Acad. Sci. *757*, 186–193.

Wolff, S.C., Hruska, Z., Nguyen, L., and Dohanich, G.P. (2008). Asymmetrical distributions of muscarinic receptor binding in the hippocampus of female rats. Eur. J. Pharmacol. *588*, 248–250.

Wonnacott, S. (1997). Presynaptic nicotinic ACh receptors. Trends Neurosci. *20*, 92–98.

Wonnacott, S., Barik, J., Dickinson, J., and Jones, I.W. (2006). Nicotinic receptors modulate transmitter cross talk in the CNS: nicotinic modulation of transmitters. J. Mol. Neurosci. *30*, 137–140.

Woolf, N.J., and Butcher, L.L. (1986). Cholinergic systems in the rat brain: III. Projections from the pontomesencephalic tegmentum to the thalamus, tectum, basal ganglia, and basal forebrain. Brain Res. Bull. *16*, 603–637.

Woolf, N.J., and Butcher, L.L. (1989). Cholinergic systems in the rat brain: IV. Descending projections of the pontomesencephalic tegmentum. Brain Res. Bull. *23*, 519–540.

Woolf, N.J., and Butcher, L.L. (2011). Cholinergic systems mediate action from movement to higher consciousness. Behav. Brain Res. *221*, 488–498.

Woolf, N.J., Eckenstein, F., and Butcher, L.L. (1984). Cholinergic systems in the rat brain: I. projections to the limbic telencephalon. Brain Res. Bull. *13*, 751–784.

Xie, H.Q., Choi, R.C.Y., Leung, K.W., Siow, N.L., Kong, L.W., Lau, F.T.C., Peng, H.B., and Tsim, K.W.K. (2007). Regulation of a transcript encoding the proline-rich membrane anchor of globular muscle acetylcholinesterase. The suppressive roles of myogenesis and innervating nerves. J. Biol. Chem. *282*, 11765–11775.

Xie, H.Q., Leung, K.W., Chen, V.P., Chan, G.K.L., Xu, S.L., Guo, A.J.Y., Zhu, K.Y., Zheng, K.Y.Z., Bi, C.W., Zhan, J.Y.X., et al. (2010a). PRiMA directs a restricted localization of tetrameric AChE at synapses. Chem. Biol. Interact. *187*, 78–83.

Xie, H.Q., Liang, D., Leung, K.W., Chen, V.P., Zhu, K.Y., Chan, W.K.B., Choi, R.C.Y., Massoulié, J., and Tsim, K.W.K. (2010b). Targeting acetylcholinesterase to membrane rafts: a function mediated by the

proline-rich membrane anchor (PRiMA) in neurons. J. Biol. Chem. *285*, 11537–11546.

Xie, W., Wilder, P.J., Stribley, J., Chatonnet, A., Rizzino, A., Taylor, P., Hinrichs, S.H., and Lockridge, O. (1999). Knockout of one acetylcholinesterase allele in the mouse. Chem. Biol. Interact. *119-120*, 289–299.

Xie, W., Stribley, J.A., Chatonnet, A., Wilder, P.J., Rizzino, A., McComb, R.D., Taylor, P., Hinrichs, S.H., and Lockridge, O. (2000). Postnatal developmental delay and supersensitivity to organophosphate in gene-targeted mice lacking acetylcholinesterase. J. Pharmacol. Exp. Ther. *293*, 896–902.

Yakel, J.L. (2012). Nicotinic ACh Receptors in the Hippocampus: Role in Excitability and Plasticity. Nicotine Tob. Res. *14*, 1249–1257.

Yamamura, H.I., and Snyder, S.H. (1972). Choline: high-affinity uptake by rat brain synaptosomes. Science *178*, 626–628.

Yamamura, H.I., and Snyder, S.H. (1974). Muscarinic cholinergic binding in rat brain. Proc. Natl. Acad. Sci. U.S.A. *71*, 1725–1729.

Yamasaki, M., Matsui, M., and Watanabe, M. (2010). Preferential localization of muscarinic M1 receptor on dendritic shaft and spine of cortical pyramidal cells and its anatomical evidence for volume transmission. J. Neurosci. *30*, 4408–4418.

Yan, Z., and Surmeier, D.J. (1996). Muscarinic (m2/m4) receptors reduce N- and P-type Ca2+ currents in rat neostriatal cholinergic interneurons through a fast, membrane-delimited, G-protein pathway. J. Neurosci. *16*, 2592–2604.

Yan, Z., Song, W.J., and Surmeier, J. (1997). D2 dopamine receptors reduce N-type Ca2+ currents in rat neostriatal cholinergic interneurons through a membrane-delimited, protein-kinase-C-insensitive pathway. J. Neurophysiol. *77*, 1003–1015.

Zappettini, S., Grilli, M., Salamone, A., Fedele, E., and Marchi, M. (2010). Pre-synaptic nicotinic receptors evoke endogenous glutamate and aspartate release from hippocampal synaptosomes by way of distinct coupling mechanisms. Br. J. Pharmacol. *161*, 1161–1171.

Zappettini, S., Grilli, M., Lagomarsino, F., Cavallero, A., Fedele, E., and Marchi, M. (2011). Presynaptic nicotinic α7 and non-α7 receptors stimulate endogenous GABA release from rat hippocampal synaptosomes through two mechanisms of action. PLoS ONE *6*, e16911.

Zhang, J., and Berg, D.K. (2007). Reversible inhibition of GABAA receptors by alpha7-containing nicotinic receptors on the vertebrate postsynaptic neurons. J. Physiol. (Lond.) *579*, 753–763.

Zhang, X.-J., and Greenberg, D.S. (2012). Acetylcholinesterase involvement in apoptosis. Front Mol Neurosci *5*, 40.

Zhang, W., Basile, A.S., Gomeza, J., Volpicelli, L.A., Levey, A.I., and Wess, J. (2002). Characterization of central inhibitory muscarinic autoreceptors by the use of muscarinic acetylcholine receptor knock-out mice. J. Neurosci. *22*, 1709–1717.

Zhu, J., Takita, M., Konishi, Y., Sudo, M., and Muramatsu, I. (1996). Chronic nicotine treatment delays the developmental increase in brain muscarinic receptors in rat neonate. Brain Res. *732*, 257–260.

• SUPPLEMENTS

1. Farar V., Mohr, F., Legrand M., Lamotte d'Incamps, B., Cendelin, J., Leroy, J., Abitbol, M., Bernard, V., Baud, F., Fournet, V., Houze, P., Klein, J., Plaud, B., Tuma, J., Zimmermann, M., Ascher, P., Hrabovska, A., Myslivecek, J., Krejci E.: Near complete adaptation of the PRiMA knockout to the lack of central acetylcholinesterase. J. Neurochem., 122, 1065–1080, 2012
2. Hrabovska A., Farar V., Li B., Bernard V., Duysen E.G., Brabec J., Lockridge O., Myslivecek J: Drastic decrease in dopamine receptor levels in the striatum of acetylcholinesterase knock-out mouse. Chemico-Biological Interactions. 183 (1), 194–201, 2010
3. Farar, V., Hrabovska, A., Krejci, E. and Myslivecek J: Developmental adaptation of central nervous system to extremely high acetylcholine levels.

* Supplement 1

JOURNAL OF NEUROCHEMISTRY | 2012 | 122 | 1065–1080 doi: 10.1111/j.1471-4159.2012.07856.x

ORIGINAL ARTICLE

Near-complete adaptation of the PRiMA knockout to the lack of central acetylcholinesterase

Vladimir Farar,*·† Franziska Mohr,‡ Marie Legrand,* Boris Lamotte d'Incamps,§ Jan Cendelin,¶ Jacqueline Leroy,* Marc Abitbol,* Veronique Bernard,** Frédéric Baud,†† Vincent Fournet,** Pascal Houze,‡‡ Jochen Klein,‡ Benoit Plaud,§§ Jan Tuma,¶ Martina Zimmermann,‡ Philippe Ascher,¶¶ Anna Hrabovska,*** Jaromir Myslivecek†·†††·[1] and Eric Krejci*

*Centre d'Etude de la Sensorimotricité, Université Paris Descartes, CNRS UMR 8194, Paris, France
†First Medical Faculty, Institute of Physiology, Charles University, Prague, Czech Republic
‡Pharmakologisches Institut für Naturwissenschaftler, Universität Frankfurt, Frankfurt, Germany
§Neurophysique et Physiologie, CNRS UMR 8119, Université Paris Descartes, Paris, France
¶Department of Pathophysiology, Faculty of Medicine, Charles University, Pilsen, Czech Republic
**INSERM UMRS 952, CNRS UMR 7224, Université Pierre et Marie Curie, Paris, France
††Groupe hospitalier Lariboisière-Saint Louis, Université Paris, Paris Diderot, Paris, France
‡‡Faculty of Pharmacy EA4463, C-TAC, Université Paris Descartes, Paris, France
§§Service d'anesthésie, réanimation chirurgicale, Université Paris-Est Créteil & Assistante Publique - Hôpitaux de Paris, GHU Henri Mondor, Créteil, France
¶¶Physiologie cérébrale, CNRS UMR 8118, Université Paris Descartes, Paris, France
***Department of Pharmacology and Toxicology, Faculty of Pharmacy, Comenius University, Bratislava, Slovakia
†††Laboratory of Physiology, Institute of Health Studies, Liberec, Czech Republic

Abstract

Acetylcholinesterase (AChE) rapidly hydrolyzes acetylcholine. At the neuromuscular junction, AChE is mainly anchored in the extracellular matrix by the collagen Q, whereas in the brain, AChE is tethered by the proline-rich membrane anchor (PRiMA). The AChE-deficient mice, in which AChE has been deleted from all tissues, have severe handicaps. Surprisingly, PRiMA KO mice in which AChE is mostly eliminated from the brain show very few deficits. We now report that most of the changes observed in the brain of AChE-deficient mice, and in particular the high levels of ambient extracellular acetylcholine and the massive decrease of muscarinic receptors, are also observed in the brain of PRiMA KO. However, the two groups of mutants differ in their responses to AChE inhibitors. Since PRiMA-KO mice and AChE-deficient mice have similar low AChE concentrations in the brain but differ in the AChE content of the peripheral nervous system, these results suggest that peripheral nervous system AChE is a major target of AChE inhibitors, and that its absence in AChE- deficient mice is the main cause of the slow development and vulnerability of these mice. At the level of the brain, the adaptation to the absence of AChE is nearly complete.

Keywords: acetylcholine, Alzheimer's disease, autonomous nervous system, cholinergic receptors, microdialysis, mouse genetics.
J. Neurochem. (2012) **122**, 1065–1080.

Received May 27, 2012; revised manuscript received June 24, 2012; accepted June 25, 2012.

Address correspondence and reprint request to Eric Krejci, CNRS UMR 8194, Centre d'Etude de la Sensorimotricité, Université Paris Descartes, Paris, France. E-mail: eric.krejci@parisdescartes.fr
[1]Co-supervisor of V. Farar.

Abbreviations used: AChE, acetylcholinesterase; BChE, butyrylcholinesterase; ChAT, choline acetyltransferase; ColQ, collagen Q; DHβE, dihydro-β-erythroidine; EPSCs, excitatory postsynaptic currents; hChT, high-affinity choline transporter; mAChRs, muscarinic receptors; nAChRs, nicotinic receptors; NMJ, neuromuscular junction; OT, olfactory tubercle; PRiMA, proline-rich membrane anchor.

© 2012 The Authors
Journal of Neurochemistry © 2012 International Society for Neurochemistry,

Acetylcholinesterase (AChE) is a well-known enzyme present at the neuromuscular junction (NMJ), in the brain and in the autonomic nervous system. The functions of AChE have long been deduced mostly from the effects of AChE inhibitors until the cloning of AChE (Schumacher *et al.* 1986) offered the possibility to construct AChE knockouts. Because high concentrations of AChE inhibitors given acutely are lethal (Taylor 1996), it came as a surprise that mice lacking AChE in both the central and the peripheral nervous system can adapt to the absence of AChE and survive. Nevertheless, this adaptation is clearly incomplete since in AChE-deficient mice the postnatal development is impaired and the animals which survive are severely handicaped. The first AChE-deficient mice analyzed were AChE-KO mice, in which the catalytic domain of AChE was deleted. These mice die soon after birth (Xie *et al.* 2000) if not given special care during postnatal development such as liquid diet (Duysen *et al.* 2002) or high ambient temperature (Sun *et al.* 2007) because of the infant thermoregulatory dysfunction. The animals which survive develop slowly and the adults have muscle weakness, body tremors, abnormal gait and posture, abnormal respiratory functions, and die prematurely from seizures (Duysen *et al.* 2002; Chatonnet *et al.* 2003; Boudinot *et al.* 2004). A second type of AChE-deficient mice has been constructed as AChEdelE5 + 6 mice, in which the two last exons of the AChE gene are deleted, which prevents the anchoring of AChE and transforms AChE in a soluble monomeric enzyme (Camp *et al.* 2005). Like the AChE-KO mice, these mice have a very low level of AChE activity in brain and muscle (Dobbertin *et al.* 2009; Camp *et al.* 2010), but a higher level in the serum (Camp *et al.* 2010). They are significantly smaller than their WT controls and show higher tidal volume, ventilation, and mean inspiratory flow than WT mice, even if the increases detected are lower than those observed in AChE-KO mice with comparable weights (Boudinot *et al.* 2009; Camp *et al.* 2010). In addition, the mice have a profound motor deficit (body tremors) likely as a result of the deficit in AChE at the NMJ (Camp *et al.* 2010).

A better understanding of the role of AChE was reached when it was finally demonstrated that AChE is anchored differently in the NMJ and the CNS. In the NMJ, most of the AChE is anchored in the subsynaptic domains of the basal lamina by collagen Q (ColQ) (Krejci *et al.* 1997; Bernard *et al.* 2011). By contrast, in the CNS, most of the AChE is tethered to the plasma membranes of neurons by a small transmembrane protein, proline-rich membrane anchor (PRiMA) (Perrier *et al.* 2002). The discovery that AChE has distinct anchors in the peripheral and central nervous systems paved the way to the strategy of creating novel KO mice in which AChE is deleted in specific regions or tissues of the body. The first such mutants were the ColQ KO mice, obtained by deleting the proline-rich sequence which links AChE to ColQ (Bon *et al.* 1997; Feng *et al.* 1999). These mice survive better than the AChE-deficient mice, have a slow development and also benefit from being raised at high ambient temperature. As expected, their adult phenotype concerns the neuromuscular system and reproduces the major features of human myasthenic syndrome (Mihaylova *et al.* 2008).

The comparison of the AChE-deficient mice and ColQ KO mice suggested that the seizures, the adult thermoregulation or the respiration are partly controlled by brain AChE. If this assumption were true, one could expect a strong phenotype in the PRiMA KO mice, in which similarly most of the central AChE was expected to be absent. It was therefore quite surprising to find that the PRiMA KO mice were indistinguishable from WT mice in terms of weight, body temperature, and ventilation (Boudinot *et al.* 2009) and more generally had a very mild behavioral phenotype, despite the fact that central AChE is mainly retained in the neurons and represents only 2% of the AChE content found in normal mice (Dobbertin *et al.* 2009).

Our experiments aimed at understanding this unexpected contrast between PRiMA KO and AChE-deficient mice. First we extended the initial description of the behavioral phenotype of the PRiMA KO mice and confirmed that it was indeed quite mild. We then compared the biochemical and physiological deficits of the PRiMA KO mice with that of the AChE-deficient mice and found major similarities: both mice have a very high level of extracellular acetylcholine (ACh) in the CNS, both have adapted to the excess ACh through a major decrease in the density of muscarinic receptors (mAChRs) and a slight decrease of nicotinic receptors (nAChRs), both strains of mice show an increased sensitivity to scopolamine. A few differences were observed, among which the most significant appeared to be the effects on thermoregulation of a specific AChE inhibitor, donepezil. WT mice respond to donepezil by a strong hypothermia, whereas AChE-deficient mice are resistant to donepezil. PRiMA KO mice have a strong hypothermic response to donepezil, resembling that of WT mice. This observation suggests that some of the strong perturbations of AChE-deficient mice (and, by extension, of mice intoxicated by AChE inhibitors) are actually the result of uncorrected deficits of AChE in the autonomic nervous system, whereas in all cases the CNS adapts very well to a long-lasting AChE inhibition.

Materials and methods

Mice

Experiments were performed on four strains of mice: WT, mice nullizygous for PRiMA (PRiMA KO), mice nullizygous for ColQ (ColQ KO), mice nullizygous for AChE exons 5 and 6 (AChEdel-E5+6). Genotypes were determined by PCR with primers described elsewhere (Dobbertin *et al.* 2009), before and after the experiments. The mice used for experiments were 2–6 months old, except for

© 2012 The Authors

electrophysiology experiments, for which we used 6–10 day-old mice. The genetic background of the mice used was a mixture equivalent to that for an F3 mating of B6D2 strain. All experiments were performed in accordance with the regulations of the French Agriculture and Forestry Ministry (Veterinary Service Department of the Prefecture de Police, Paris, France). The mice were born at an animal facility in Paris and were then transported for rearing to Prague or Pilsen (Czech Republic) where they were allowed to acclimatize for at least 14 days. Animals were treated in accordance with the legislation in force in the Czech Republic and the EU, and the experimental protocol was approved by the Committee for the Protection of Experimental Animals of the first Medical Faculty, Charles University, Prague. The animals were maintained under controlled environmental conditions (12/12 light/dark cycle, 22 ± 1°C, light on at 6 a.m.). Food and water were available *ad libitum*. Female mice and their WT counterparts (weighing 20–25 g, 11–13 weeks old) were used in the study. Microdialysis experiments, in particular, were carried out in accordance with the guidelines of the Regierungspräsidium Darmstadt, Germany.

Drugs

(±)-Butaclamol hydrochloride, (±)-vesamicol hydrochloride, (-)-scopolamine hydrochloride, acetyl coenzyme A sodium salt, apomorphine hydrochloride, atropine sulfate, hemicholinium-3, choline chloride, kainic acid monohydrate, L-glutamic acid, naloxone hydrochloride dehydrate, nicotine hydrogen tartrate, oxotremorine sesquifumarate and SR-95531 were purchased from Sigma-Aldrich Chemie, Saint-Quentin Fallavier, France. α-Amino-3-hydroxy-5-methylisoxazole-4-propionate (AMPA)-a-[5methyl-^{3}H]) (45.8 Ci/mmol), hemicholinium-3 diacetate salt [methyl-^{3}H] (125.4 Ci/mmol), choline chloride[methyl-^{3}H] (85 Ci/mmol), kainic acid [vinylidene-^{3}H](49.9 Ci/mmol), muscimol [methylene-^{3}H(N)] (35.6 Ci/mmol), pirenzepine [*N*-methyl-^{3}H] (83.4 Ci/mmol) and vesamicol L-[piperidinyl-3,4-^{3}H] (46.8 Ci/mmol) were obtained from American Radiolabeled Chemicals (ARC, Inc.). Acetyl coenzyme A [acetyl-^{3}H] (6 Ci/mmol), AF-DX 384 [2,3-dipropylamino-^{3}H] (106.5 Ci/mmol), CGP 39653 [propyl-2,3-^{3}H] (50 Ci/mmol), quinuclidinyl benzilate L-[benzilic-4,4′-^{3}H] (46 Ci/mmol), SCH 23390 [*N*-methyl-^{3}H] (85 Ci/mmol), [^{125}I]-epibatidine (2200 Ci/mmol), [^{125}I]-iodosulpride (2200 Ci/mmol) and [^{125}I]-Tyr54-α-bungarotoxin (2200 Ci/mmol) were obtained from PerkinElmer, Courtaboeuf, France.

Behavioral tests

Behavioral tests were performed over a period of 20 days: open-field tests for 2 days, gait examination, 3 days without testing, rotarod and suspension wire tests for 3 days, spatial navigation in the Morris water maze for 10 days and the probe trial in the Morris water maze on the last day.

Open-field test

The mice were placed in the middle of a square arena, the open field (40 × 40 cm, wall height 40 cm) and allowed to move freely for 5 min. The distance covered and the time spent in the central zone (central square equivalent to 9/25 of the total area) were evaluated. The test was repeated on the next day to assess habituation. The movement of the animal was recorded and evaluated with the EthoVision 3.0 tracking system (Noldus Information Technology, Wageningen, The Netherlands).

Gait examination

The gait of the animal was studied with the automated overground locomotion gait analysis system CatWalk (Noldus Information Technology) (Hamers *et al.* 2006). The mice were placed in a corridor (8 cm wide, 115 cm long) and allowed to walk freely. We recorded at least 20 sequences, through the visualized central part of the corridor (60 cm long), in which the animal walked in a straight line without interruption. Five of the tracks in which the mouse passed through the entire field without interruption or tracks containing at least five fluently consequential complete step cycles were analyzed for each mouse. We then averaged the values for the tracks analyzed for each individual animal. The following parameters were evaluated: walking speed (in cm/s), time between initial and maximal contact of the paw (in s), paw angle (angle in degrees between the long axis of the paw and the axis of the walking trajectory), stride length (in mm), stand (duration of the standing phase, in s), swing (duration of the swing phase, in s), swing speed (in m/s), base of support (distance in mm between the limb pairs in a girdle), print position (distance between a fore and a hind paw print in one step cycle, for right and left paws, separately), regularity index (% of regular step patterns), support (combination of paws simultaneously in contact with the walkway as a % of walking time). Time between initial and maximal paw contact, paw angle, stride length, stand, swing, and swing speed values were averaged for the left and right paw of the same girdle. For a description of the parameters see (Hamers *et al.* 2006).

Rotarod test

For the rotarod test, the mice were placed on a rotarod cylinder (diameter: 4 cm, constant rotation speed: 12 turns/min), with their heads facing away from the direction of rotation. For the horizontal bar test, the animal was suspended by its two forepaws in the middle of a horizontal wire (30 cm long, 1 mm in diameter) held taut between two wooden columns 55 cm above a table covered with a soft pillow. The time until the mice fell (fall latency) was measured. If the mouse reached a maximal latency of 120 s, the trial was stopped and the mouse was removed from the apparatus. Both tests were repeated four times per day, at 15-min intervals, on 3 days. Mean fall latencies were calculated for each day.

Morris water maze

Spatial orientation was investigated in the Morris water maze (Morris 1984), in a circular pool (100 cm in diameter, water depth: 35 cm, height of the wall above the water level: 20 cm, water temperature: 25–26°C) made of white plastic. A circular platform (8 cm in diameter) made of transparent Plexiglass was placed in the middle of the imaginary southeast quadrant. The platform was hidden 0.5 cm beneath the water surface. Four trials per day were performed, with starting points at imaginary cardinal points in the following order: north-south-west-east. If the mouse did not reach the platform within 60 s, it was guided to the platform. The mouse was left on the platform for 30 s after each trial. There was an interval of 20 min between trials. The experiment was repeated every day for 10 days. The EthoVision 3.0 (Noldus Information Technology) automatic tracking system was used to detect mouse movement. The probe trial was performed on the day after the last Morris water maze trial. The mice were released into the maze at the north starting position and left to swim in the maze

© 2012 The Authors

without the platform for 60 s. We determined the amount of time spent in the southeast quadrant.

Microdialysis experiments

On day one, mice were anesthetized with isoflurane (induction dose 4%; maintenance dose 2–2.5%) in a 20%/80% mixture of oxygen and nitrogen. Home-made, I-shaped, concentric microdialysis probes (Hartmann *et al.* 2007) with an exchange length of 2 mm were implanted into the striatum at the following coordinates (from bregma): AP: +0.5 mm; L: −2.2 mm; DV: −3.8 mm (Paxinos and Watson 2007). Microdialysis experiments were carried out after a 24 h recovery period. Specifically, on day 2, probes were perfused with artificial cerebrospinal fluid (aCSF: 147 mM NaCl, 4 mM KCl, 1.2 mM $CaCl_2$ and 1.2 mM $MgCl_2$) at a flow rate of 1 μL/min. Following 30 min of equilibration, samples were collected at 15-min intervals over a period of 90 min. Basal ACh levels were determined by averaging the values for the five samples collected. The mice were killed on day 3 and the location of the probe was checked.

Chemical analysis of microdialysates

Microdialysis samples were injected into an Eicom HTEC-500 microbore system coupled to a Shimadzu SIL-20AC autosampler. The buffer used consisted of 5 g $KHCO_3$, 400 mg sodium decanesulfonate and 50 mg EDTA in 1 L RotisolV® HPLC Gradient-Grade water (pH 8.3). We used a flow rate of 0.15 mL/min, and the retention time for ACh was 14.4 min. The limit of detection was 1–2 fmol of analyte per 5 μL injected.

High-affinity choline uptake

Freshly dissected brain regions were homogenized by three 10-s pulses with an Ultra-Turrax homogenizer, in 15 volumes of cold 0.32 M sucrose. Homogenates were centrifuged at 4°C for 10 min at 1000 *g*. The supernatant was then centrifuged at 4°C for 20 min at 20 000 *g*. The supernatant was discarded and the pellet was resuspended in cold 0.32 M sucrose.

High-affinity choline uptake was determined as previously described (Kristofiková *et al.* 2006). We added 100 μL of synaptosomal suspension to 800 μL of Krebs-Ringer-HEPES-glucose buffer (128 mM NaCl, 5 mM KCl, 2.7 mM $CaCl_2$, 1.2 mM $MgSO_4$, 5 mM glucose and 10 mM HEPES, pH 7.4) and incubated the mixture for 4 min at 37°C. Uptake was initiated by adding 100 μL of [^{3}H]-choline in Krebs-Ringer-HEPES-glucose buffer (final dilution 10 nM) and was allowed to continue for 4 min at 37°C. Incubation was terminated by adding 4 mL of ice-cold Krebs-Ringer-HEPES-glucose buffer supplemented with 1 μM hemicholinium-3 and filtering rapidly through GF/B glass fiber filters in the Brandel cell harvester. The filters were washed twice with ice-cold Krebs-Ringer-HEPES-glucose buffer, allowed to dry at 22°C and the radioactivity associated with filters was measured in a scintillation counter. High-affinity choline uptake was calculated as the difference in [^{3}H]-choline uptake between incubations with and without 1 μM hemicholinium-3. Samples were run in duplicate. Protein content was assessed in a bicinchoninic acid protein assay (Fisher Scientific, Illkirch, France).

Choline acetyltransferase assay

Choline acetyltransferase activity was assessed by a modified version of Fonnum's method (Fonnum 1969; Berrard *et al.* 1995), as previously described (Machová *et al.* 2008). Dissected brain regions were homogenized by three 10-s pulses with an Ultra-Turrax homogenizer, in 500 μl of assay buffer (10 mM sodium phosphate buffer, 200 mM NaCl, 0.2% Triton X-100, pH 7.4). We then mixed 10 μl of a 1 : 5 dilution of homogenate with 40 μL of assay buffer supplemented with (final concentrations) 0.2 mM physostigmine, 2 mM choline, and a mixture of 170 μM labeled and unlabeled acetylCoA (final specific radioactivity of about 200 dpm/pmol) and incubated the mixture for 15 min at 37°C. The reaction was stopped by adding 400 μL of ice-cold 10 mM sodium phosphate buffer and 400 μL of tetraphenylboron dissolved in butyronitrile (10 mg/mL). The tritiated ACh synthesized was extracted into the organic layer, of which 200 μL was removed for scintillation counting. All samples were processed in duplicate.

Tissue preparation for autoradiography experiments

Mice were killed by cervical dislocation and decapitation. Brains were rapidly removed, frozen in isopentane at −30°C, and stored at −80°C until use. Coronal brain sections 16 μm thick were cut on a cryostat at −20°C, thaw-mounted on Superfrost Plus glass slides, and stored in storage boxes at −80 until use. Before each autoradiographic assay, the sections were allowed to thaw and dry for 20 min at 22°C. The slides were processed as shown in the Table 1, according to the references: 1) (Wolff *et al.* 2008); 2) (Spurden *et al.* 1997); 3) (Perry and Kellar 1995); 4) (Fernagut *et al.* 2003); 5) (Martres *et al.* 1985); 6) (Ayata *et al.* 1997); 7) (Dean *et al.* 1999); 8) (Albin *et al.* 1994); 9) (Araki *et al.* 2000).

Radioligand binding assays with membrane preparations

Mice were killed by decapitation. Their brains were immediately removed and dissected on ice into striatum, hippocampus, and cortex. Dissected brain regions were flash frozen in liquid nitrogen and stored at – 80°C until use.

Pooled individual regions from four or five mice were homogenized by three 10-s pulses with an Ultra-Turrax homogenizer, in 15 volumes of cold 0.32 M sucrose. The homogenates were centrifuged at 4°C for 10 min at 1000 *g* to remove cell debris and the nuclear fraction. The supernatant was removed and centrifuged for 55 min at 17 000 *g* to obtain a membrane preparation. The supernatant was discarded and the pellet was washed once with cold sodium/potassium phosphate buffer pH 7.4, suspended in the same buffer and used directly for the binding assay. Protein content was determined in a bicinchoninic acid protein assay.

Total mAChR was labeled by a slightly modified version of a published protocol (Yamamura and Snyder 1974). We incubated 40 μL of plasma membranes, in duplicate, in 50 mM potassium phosphate buffer pH 7.4, in the presence of various concentrations of [^{3}H]-QNB (30 – 1800 pM) in a total volume of 1 mL, for 1.5 h at 22°C. Nonspecific binding was determined by parallel incubations in the presence of 10 μM atropine sulfate. The reaction was stopped by adding 3 mL of ice-cold phosphate buffer and immediately subjecting the mixture to vacuum filtration through GF/B glass fiber filters in the Brandel cell harvester. Filters were washed three times with 3 mL of ice-cold buffer, to remove the unbound radioligand, and were allowed to dry at 22°C overnight. Dried filters were transferred to scintillation vials and the scintillation cocktail was added. The radioactivity associated with the filters was measured using a Beckman liquid scintillation

© 2012 The Authors

Table 1 Incubation procedures for autoradiography experiments

Receptor	Radioligand	Nonspecific binding	Incubation	Incubation solution	Preincubation	Washing	Reference
MR	2 nM [^{3}H]-QNB	10 μM atropine	120 min, 22°C	50 mM Na/K PB, pH 7.4	2 × 30 min, 22°C	2 × 5 min	(1)
M1	5 nM [^{3}H]-pirenzepine	10 μM atropine	120 min, 22°C	50 mM Na/K PB, pH 7.4	2 × 30 min, 22°C	2 × 5 min	(1)
M2	2 nM [^{3}H]-AFDX 384	10 μM atropine	120 min, 22°C	50 mM Na/K PB, pH 7.4	2 × 30 min, 22°C	2 × 5 min	(1)
alpha7 NR	0.5 nM [^{125}I]-α-bungarotoxin	1 mM nicotine		50 mM TRIS-HCl, 0.1 % BSA, pH 7.4	1 × 30 min, 22°C	4 × 10 min	(2)
beta2 NR	0.4 nM [^{125}I]-epibatidine	300 μM nicotine	40 min, 22°C	50 mM TRIS-HCl, 120 mM NaCl, 5 mM KCl, 2 mM $CaCl_2$, 1 mM $MgCl_2$, pH 7.4	3 × 5 min, 22°C	2 × 5 min	(3)
D1	3 nM [^{3}H]-SCH 23390	10 μM butaclamol	90 min, 22°C	50 mM TRIS-HCl, 120 mM NaCl, 5 mM KCl, 2 mM $CaCl_2$, 1 mM $MgCl_2$, pH 7.4	1 × 20 min, 22°C	4 × 5 min	(4)
D2	0.2 nM [^{125}I]-iodosulpride	10 μM apomorphine	60 min, 22°C	50 mM TRIS-HCl, 120 mM NaCl, 5 mM KCl, 2 mM $CaCl_2$, 1 mM $MgCl_2$, 0.1 % BSA, 0.57 mM ascorbic acid, pH 7.4	3 × 5 min, 22°C	4 × 5 min	(5)
NMDA	5 nM [^{3}H]-CGP 39653	100 μM glutamate	60 min, 22°C	50 mM TRIS HCl, pH 7.4	3 × 15 min, 22°C	4 × 15 s	(6)
Kainate	12 nM [^{3}H]-kainate	1 μM kainate	45 min, 4°C	50 mM Tris-acetate, pH 7.4	3 × 15 min, 22°C	3 × 10 s	(6)
AMPA	9 nM [^{3}H]-AMPA	1 mM glutamate	45 min, 4°C	50 mM Tris-acetate, 100 mM KSCN, 2.5 mM $CaCl_2$, pH 7.3	3 × 15 min, 22°C	3 × 10 s	(6)
GABAA	10 nM [^{3}H]-muscimol	10 μM SR 95531	60 min, 4°C	50 mM Tris-citrate, pH 7.1	3 × 5 min, 4°C	1 × 1 min	(7)
vAChT	20 nM [3H]-vesamicol	100 μM vesamicol	60 min, 22°C	137 mM NaCl, 3 mMKCl, 8 mM Na2HPO4, 1.5 mM KH2PO4, 1 mM EDTA, pH 7.4	1 × 5 min, 22°C	2 × 2 min	(8)
hChT	10 nM [^{3}H]-hemicholinium-3	10 μM hemicholinium-3	120 min, 22°C	50mM Gly-Gly buffer, 200 mM NaCl, pH 7.8	1 × 5 min, 22°C	2 × 2 min	(9)

counter. The specific binding corresponding to radioligand bound to receptors was calculated as the difference in binding in reaction mixtures with and without atropine. Specific binding values were converted into fmol per mg protein. We determined dissociation constants (KD) and maximum binding sites (Bmax), we fitted equation (1) to the data by nonlinear regression (GraphPad Software Inc., San Diego, CA, USA).

$$B = ([Bmax][L])([KD] + [L]) \quad (1)$$

where B is the specific binding per mg of protein measured at various concentrations of QNB, Bmax is the total number of receptors per mg of protein, L is the concentration of free radioligand, and KD is the dissociation constant.

Quantification of receptor density

We ensured that the signal was linear, by exposing films to autoradiographic standards (GE Healthcare Europe GmbH, Velizy-Villacoublay, France) together with the samples, in the presence of screens. The autoradiographs obtained were scanned and subjected to densitometry analysis with MCID analysis software on a PC. Imaging plates were processed in a Typhoon fla 7000 biomolecular imager or a Fuji BAS-5000 Bioimaging Analyzer and digitized images were obtained, which were analyzed with MCID analysis software. We averaged the measurements for four sections for each animal and brain region.

Electrophysiology

The methods used have been described elsewhere (Lamotte d'Incamps and Ascher 2008; Lamotte d'Incamps *et al.* 2012). Briefly, slices of the lumbar cord were prepared from PRiMA KO mice (P5–P10). Renshaw cells were identified on the basis of their characteristic response to single ventral root stimulation (a train of action potentials) in the cell-attached mode. They were then voltage-clamped in the whole-cell configuration. The recording solution contained 125 mM Cs gluconate, 5 mM QX-314 Cl, 10 mM HEPES, 10 mM EGTA, 1 mM $CaCl_2$, 4 mM Mg-ATP, 0.4 mM Na_2GTP. The pH was adjusted to 7.3 with CsOH, and the osmolarity was adjusted to 285–295 mOsm. The slices used contained a ventral rootlet sufficiently long for mounting on a suction stimulation electrode with a tip size adapted to the diameter of the rootlet (40–170 μm). Stimulus intensity varied between 1 and 50 V; stimulus duration varied between 10 and 300 μs. We repeated five-pulse trains (internal frequency 100 Hz) at 10 s intervals. The glutamatergic components of the MN-RC response were suppressed by adding 2 μM NBQX (2,3-dioxo-6-nitro-1,2,3,4tetrahydrobenzo(f)quinoxaline-7-sulfonamide) to block the AMPA receptors and 50 μM D-APV (D(-)-2-amino-5-phosphonopentanoic acid) to block the NMDA receptors. NBQX and D-APV were purchased from Tocris Bioscience Distributor Network, Lille, France and Ascent (Abcam Biochemicals, Cambridge, UK). QX-314 chloride was obtained from Alomone Laboratories (EUROMEDEX, Souffelweyersheim, France). All the other chemicals were obtained from Sigma.

Telemetry for temperature recording

We measured behavioral responses to drug application using a telemetry system (Respironics, USA). The transponders (G2E-Mitter or G2-HR E-Mitter) were implanted in the peritoneal cavity of mice under anesthesia induced either by injection of a xylazine/

© 2012 The Authors

tiletamine/zolazepam mixture (Zoletil® 100, Ronetar® 2% 5 : 1, diluted 1 : 10, 3.2 mL/kg), or with isofluorane. Mice were allowed to recover from surgery for 1 week before their use in experiments. Temperature and activity measurements were acquired directly from the transponders by receivers connected in series and to a single port of a PC.

On the day of the experiment, cages with individual mice were placed over the corresponding receivers for at least 3 h before drug application. Mice of various genotypes received subcutaneous or intraperitoneal injections of oxotremorine (0.2 mg/kg), scopolamine (0.05 mg/kg or 0.5 mg/kg) or donepezil (2 mg/kg or 10 mg/kg) dissolved in physiological saline or vehicle. Data were collected every 60 s for 3 h before the injection and then for another 20 h after the injection.

VitalView and GraphPad were used for data analysis. The hypothermic effect of oxotremorine injection was evaluated by calculating the minimal temperature over a period of 10 min and the duration of hypothermia (the period for which temperature was below 34°C).

Statistical analysis

Most of the data from behavioral tests were not normally distributed (checked with the Kolmogorov–Smirnov test). We used Mann–Whitney tests for comparisons of PRiMA KO and wild-type mice. In all cases, $p < 0.05$ was considered to indicate statistical significance. Otherwise, we used Student's *t*-test and significance was presented as *** is $p < 0.001$, ** < 0.01 and * is $p < 0.05$. Values are expressed as means ± SEM.

Results

The subtle motor phenotype of PRiMA KO mice

We evaluated possible changes in behavior caused by the AChE deficit, by subjecting PRiMA KO mice to a series of motor evaluations. We measured their spontaneous activity in open-field situations in control conditions. We also evaluated their motor coordination in the rotarod test, the bare wire task and the CatWalk and assessed their spatial learning in the Morris water maze. A parallel evaluation of the motor phenotype of AChEdelE5 + 6 mice was not possible because, as noted by Camp (Camp *et al.* 2010), deletion of exon 6 produced animals which ''lived with constant tremors from birth, making it impossible to assess their capabilities with simple tests that required physical coordination''.

In open-field conditions, the basal motor activity of PRiMA KO mice (quantified by measuring the distance covered in 5 min) was identical to that of WT mice and there was no significant difference in the time spent in the central zone (Fig. 1a).

In the rotarod test, a significant difference in performance was observed between naive PRiMA KO mice and WT mice on the first day of exposure to the rotarod test (Fig. 1b). However, from the second day of rotarod testing onward, similar results were obtained for PRiMA KO mice and WT mice.

In the wire task, the mice were suspended from a wire by their forelimbs and the time until they fell was determined. The PRiMA KO mice fell from the wire more rapidly than their WT mice counterparts (mean fall latencies, in seconds ± SEM WT vs. KO, 39.8 ± 7.4 vs. 13.0 ± 1.4 (1st day), $p < 0.001$, 52.9 ± 14.8 vs. 33.9 ± 10.5 (2nd day), $p = 0.178$, 73.5 ± 14.8 vs. 33.6 ± 11.2 (3rd day), $p = 0.037$). Additional studies are required to determine the reasons for this difference.

In the CatWalk system, the swing associated with the walk of the PRiMA KO mice was slightly greater than that of WT mice (Fig. 1c left). As PRiMA KO and WT mice took the same amount of time to cover the entire distance, this difference may reflect a slightly slower limb displacement speed during walking (Fig. 1c, right).

Spatial learning and memory in mice have often been reported to improve after AChE inhibition (Pepeu and Giovannini 2010). We compared the performances of PRiMA KO mice and WT mice in the Morris water maze. We found no significant difference between these two strains of mice during a training procedure with a hidden platform (Fig. 1d) and during the trial itself, in which the platform was removed (mean time, in seconds, spent in the quadrant of the previously positioned platform: 29.6 ± 1.7 in WT mice vs. 25.3 ± 1.9 in PRiMA KO mice, $p = 0.236$).

In conclusion, there appear to be subtle differences between the motor phenotypes of PRiMA KO and WT mice.

High levels of ACh in the striatum of PRiMA KO mice

We previously showed (Dobbertin *et al.* 2009), by biochemical and morphological analyses, that AChE levels in in the striatum of PRiMA KO and AChEdelE5 + 6 mice are only 2% those measured in the wild type. Moreover, AChE enzyme can be detected in the endoplasmic reticulum of PRiMA KO mice and in intracellular compartments in AChEdelE5 + 6 mice by electron microscopy analysis (Dobbertin *et al.* 2009). We investigated the effect of an absence of AChE/PRiMA on ambient ACh concentration in the brain, by using microdialysis to determine extracellular ACh concentration in the striatum of the two mutants, as previously reported for AChE-KO mice (Hartmann *et al.* 2007). A microdialysis probe was inserted in the striatum. It was perfused with artificial cerebrospinal fluid. 24 h later, ACh concentrations in the artificial cerebrospinal fluid were 281 ± 167 nM for PRiMA KO mice and 168 ± 115 nM for AChEdelE5 + 6 mice (Fig. 2), values 200 – 300 times higher than the concentration measured in the WT mice (1 ± 0.5 nM). Mean probe recovery rates of 9.1% were recorded, indicating that the concentration of ACh in the extracellular space in the striatum was about 2 – 3 μM in both AChEdelE5 + 6 and PRiMA KO mice, but only about 10 nM in WT mice.

The high level of ACh in the striatum of the mutants (and probably in many other brain structures, see discus-

© 2012 The Authors

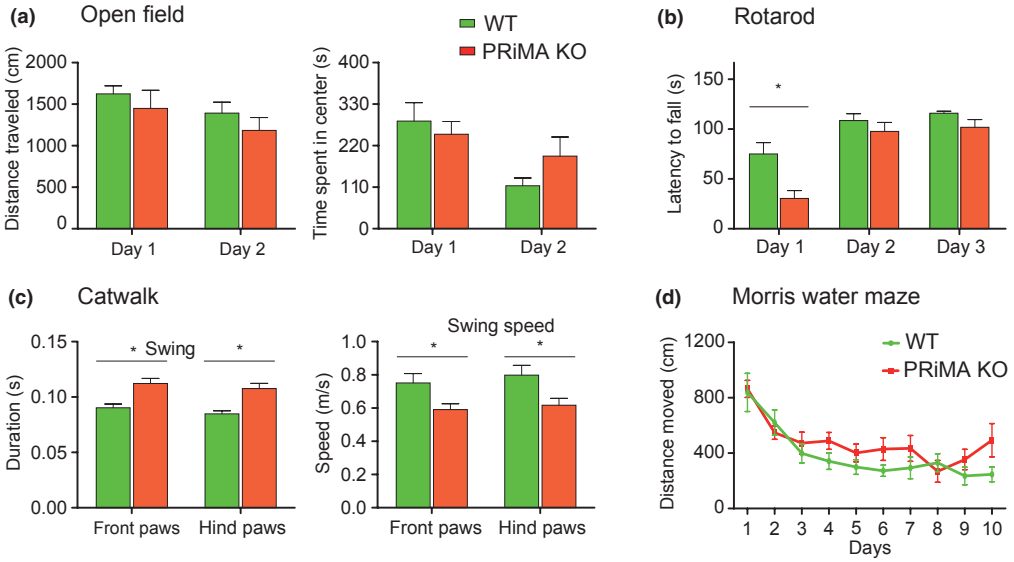

Fig. 1 Phenotype of PRiMA KO mice (a) Open-field activity: The mice were placed in the middle of the open field and the distance travelled (left) and the time spent in the center of the field (right) were measured over a period of 5 min. No significant difference was observed between the two groups during the trials on the first and second days. Locomotor activity was evaluated by telemetry (counts per hour). Before injection, activity levels were similar in the two groups (447 ± 69 (n = 5) and 481 ± 101 (n = 5), p = 0.78 for WT and PRiMA KO mice, respectively). (b) Rotarod test: The mice were placed on the rotarod cylinder, which was turning at a constant speed and we measured the time until the mouse fell off. The PRiMA KO naive mice fell sooner (30.4 ± 7.9 s (n = 5) than the WT mice (75.1 ± 11.4 s (n = 5), p = 0.007) on the first day. However, on the second and third days, the two groups performed similarly. (c) Gait examination in the CatWalk system: The system automatically recorded hind and front paw prints during displacements within the black chamber. Swing time (the time in seconds required for the movement of the limb from the back to the front) was the only parameter found to be moderately higher in PRiMA KO mice ($1.13\times10^{-1} \pm 4.65\times10^{-3}$, $1.09\times10^{-1} \pm 4.73\times10^{-3}$) than in WT mice ($9.11\times10^{-2} \pm 3.42\times10^{-3}$, $8.56\times10^{-2} \pm 2.74\times10^{-3}$), p = 0.0025 and p = 0.0037 for the fore and hind limbs, respectively. The calculated speed of this movement therefore appeared to be lower for the mutant mice than for the WT mice. (d) Morris water maze: We investigated spatial orientation and learning in the Morris water maze over a period of 10 days. We evaluated the distance covered to find the platform on each day. We observed no tremors or seizures, either at rest or during handling. Statistical significance was evaluated in Student's t-test. * is $p < 0.01$.

sion) might be expected to modify motor behavior, because activation of the striatal cholinergic system in WT mice is known to reduce motor activity, whereas mAChR inhibition is known to induce abnormal activity (Andersson *et al.* 2010). The absence of major motor disturbances suggests that the motor system has adapted to the high levels of ACh. We investigated this adaptation by quantifying the major proteins involved in cholinergic transmission in presynaptic terminals, and for mAChRs and nAChRs.

Lack of change in the presynaptic markers of cerebral ACh biosynthesis

The uptake of choline by the high-affinity choline transporter (hChT) is a controlled, limiting step in ACh synthesis. AChE-KO mice have been reported to have high levels of hChT (Volpicelli-Daley *et al.* 2003b; Hartmann *et al.* 2008). We collected purified synaptosomes from three different regions of the forebrain (striatum, cerebral cortex, and hippocampus) of PRiMA KO and WT mice. High-affinity choline uptake was similar in the three regions studied, in both strains of mice (Fig 3a). We then assessed the binding of [^{3}H]-hemicholinium-3, a specific ligand of hChT, throughout the forebrain. We found that the PRiMA KO and WT mice displayed very similar patterns of specific [^{3}H]-hemicholinium-3 binding (Fig. 3b). Thus, in contrast to what was found for AChE-KO mice (Volpicelli-Daley *et al.* 2003b; Hartmann *et al.* 2008), hChT levels are unchanged in PRiMA KO mice.

It has been shown in AChE-KO mice that the high level of ACh has no effect on choline acetyltransferase (ChAT) activity or on vesicular ACh transporter levels (Volpicelli-Daley *et al.* 2003b). We investigated ChAT enzymatic activity and the binding of [^{3}H]-vesamicol, a specific ligand of vesicular ACh transporter, in PRiMA KO and WT mice. We observed no difference in ChAT activity or in the binding of [^{3}H]-vesamicol to brain tissue sections, whatever part of the brain was considered (Fig 3c and d).

© 2012 The Authors

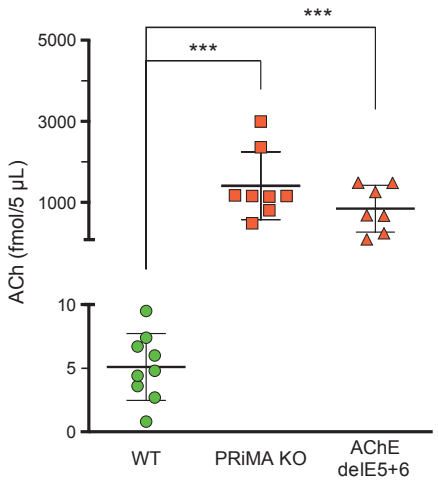

Fig. 2 Ambient ACh concentration in the striatum Extracellular ACh concentrations were determined by microdialysis of the mouse striatum. The basal ACh concentrations of PRiMA KO mice (1408 ± 836 fmol/5 µL, $n = 8$) and AChEdelE5+6 (844 ± 576 fmol/5 µL, $n = 7$) mice were significantly higher than those in WT mice (5.1 ± 2.6 fmol/5 µL, $n = 9$). The ACh concentrations of PRiMA KO and AChEdel5+6 mice were not significantly different. Individual data are presented as the means of five consecutive samples. Statistical significance was evaluated in Student's *t*-test (*** is $p < 0.001$).

Thus, despite the lower levels of extracellular ACh hydrolysis, no decrease in ACh synthesis was observed in any region of the brain in PRiMA KO mice.

Large decrease in mAChR expression and muscarinic responses

We investigated the muscarinic responses of PRiMA KO mice in three series of experiments: 1) we evaluated the binding of a series of ligands of mAChRs in various brain structures; 2) we analyzed the effects of an mAChR antagonist on motor behavior and 3) we measured the thermoregulatory responses induced by mAChR activation.

We initially used the non-selective mAChR ligand [^{3}H]-QNB for quantitative analysis of the distribution of mAChRs. Membrane preparations of PRiMA KO mice displayed binding affinities similar to those obtained for WT mice, but weaker labeling. Binding affinities (wild type (WT) versus PRiMA KO) were 114 ± 10 pmol/L vs. 86 ± 18 pmol/L for the hippocampus ($n = 4$), $p = 0.14$; 191 ± 23 pmol/L vs. 128 ± 37 pmol/L for the cortex ($n = 4$), $p = 0.20$; 199 ± 43 pmol/L vs. 112 ± 17 pmol/L for the striatum ($n = 4$), $p = 0.11$). Specific labeling (WT versus KO) was 1517 ± 36.4 fmol/mg vs. 785 ± 45.9 fmol/mg for the hippocampus ($n = 4$), $p < 0.001$; 1116 ± 26.6 fmol/mg vs. 678.8 ± 2.3 fmol/mg for the cortex ($n = 4$), $p < 0.001$ and

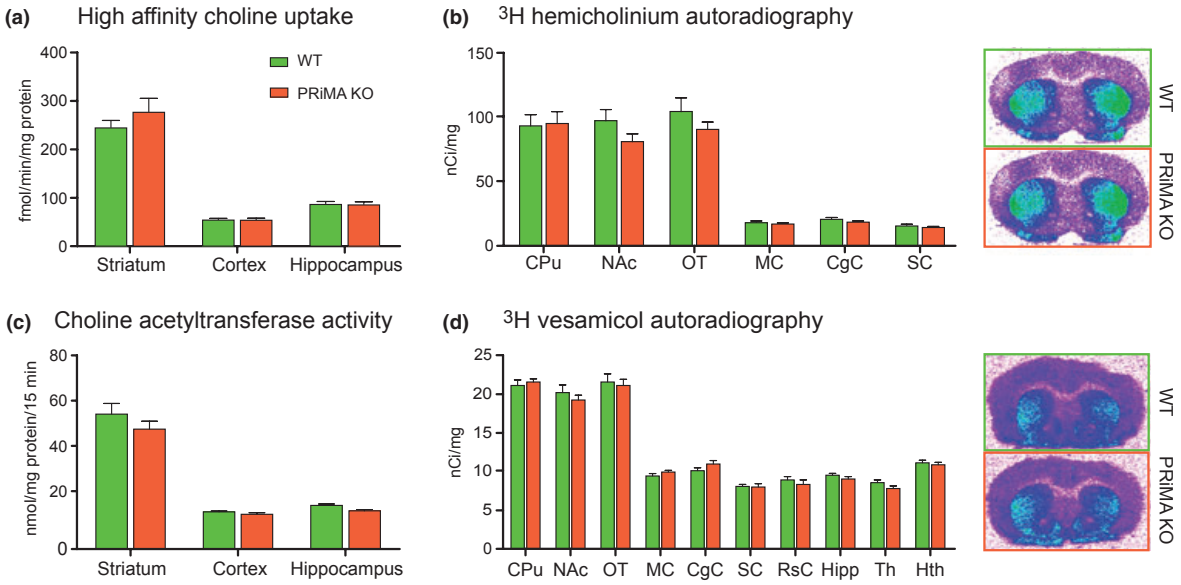

Fig. 3 ACh production is unaffected (a) Choline uptake was evaluated with synaptosomes purified from various areas of the brain (striatum, cortex and hippocampus) of WT (green) and PRiMA KO mice (red). The concentration of ^{3}H choline can be used to assess the activity of the high-affinity choline transporter. No difference between the two groups was observed. (b) Binding of ^{3}H hemicholinium to the high-affinity choline transporter Density was quantified in various parts of the brain. A selected section is presented with the WT at the top and PRiMA KO mice below. (c) Choline acetyltransferase activity: ChAT activity was assessed in extracts of the striatum, cortex and hippocampus. No difference was found between WT and PRiMA KO mice. (d) Binding of ^{3}H vesamicol to the vesicular ACh transporter: The binding of ^{3}H vesamicol to a section encompassing all forebrain regions was assessed by autoradiography. Brain areas: CPu – caudate putamen; NAc nucleus accumbens; OT – olfactory tubercle; MC/CgC/SC -motor/cingulate/somatosensory retrosplenial cortex; Hipp – hippocampus, Th – thalamus. A selected section is presented with the WT at the top and PRiMA KO mice below.

© 2012 The Authors

2243 ± 91.6 fmol/mg vs. 1078 ± 89.8 fmol/mg for the striatum ($n = 4$), $p < 0.001$.

We completed these experiments by comparing the binding of [^{3}H]-QNB, a ligand that does not distinguish between mAChR subtypes, with the binding of specific mAChR ligands: [^{3}H]-pirenzepine, an M_1-like mAChR ligand, and [^{3}H]-AFDX 384, an M_2-like mAChR ligand. We found that mAChR binding in all PRiMA KO and AChEdelE5 + 6 mouse brain regions was much weaker than that in controls, but we were able to identify three types of brain regions defined on the basis of the decrease in mAChR binding (Fig. 4). The first class, which included the caudate putamen (Cpu), nucleus accumbens (NAcc), and olfactory tubercle (OT), displayed the largest decrease in mAChR binding (≈60%), with a larger decrease in binding recorded for m2AChRs (≈70%) than for M_1AChRs (≈50%). The second class of regions, which included the thalamus (Th) and hypothalamus (Hth), displayed the smallest decrease in mAChR binding (≈20%). The third class, which included the hippocampus and cortical areas (motor and somatosensory cortex), displayed an intermediate decrease in mAChR binding (≈40%) (Fig. 4).

We characterized the functional role of mAChRs in PRiMA KO mice, by analyzing the effects of scopolamine (a mAChR antagonist) on motor activity in open-field conditions and of oxotremorine (a mAChR agonist) on central temperature. Scopolamine injection is known to increase basal motor activity in open-field conditions, in a

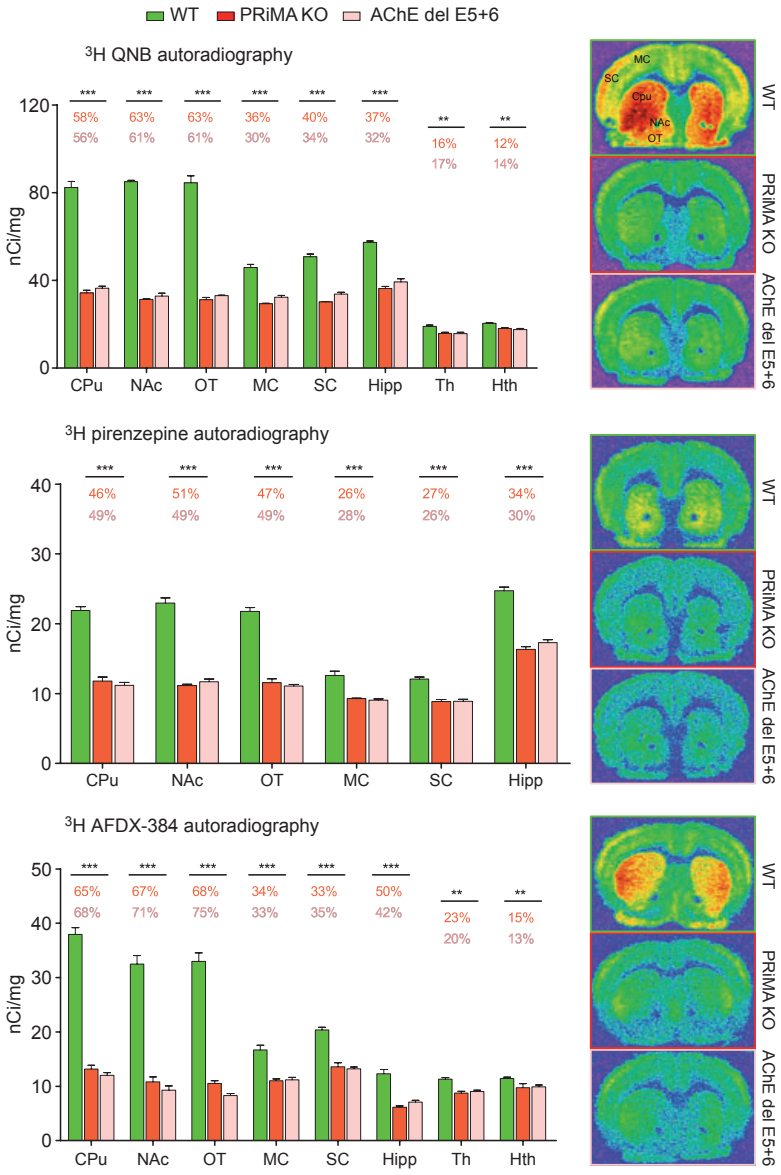

Fig. 4 Decrease in mAChR density Specific binding of [^{3}H] QNB, [^{3}H] pirenzepine and [^{3}H] AFDX 384 to various regions of the brain of WT ($n = 6$), PRiMA KO ($n = 6$) and AChEdelE5+6 mice ($n = 6$). All the brain areas studied displayed significantly lower levels of binding in PRiMA KO and AChEdelE5+6 mice. The values indicate the percentage difference between PRiMA KO (above) or AChEdelE5+6 (below) and WT mice. The images on the left correspond to examples of brain sections, in false colors. CPu – caudate putamen, NAc nucleus accumbens, OT – olfactory tubercle, Hipp – hippocampus, CA1/CA3 – CA1/CA3 hippocampal field, DG – dentate gyrus Th – thalamus, Hth – hypothalamus MC/CgC/SC/RsC – motor/cingulate/somatosensory/retrosplenial cortex. Statistical significance was evaluated with Student's *t*-test, *** is $p < 0.001$, ** is $p < 0.01$.

© 2012 The Authors

dose-dependent manner, in WT mice, by increasing the release of dopamine (Sipos *et al.* 1999). This effect was also observed in PRiMA KO mice, in which it was actually stronger than in WT mice (Fig. 5a). A similar increase in scopolamine sensitivity was also observed in AChE-KO mice (Volpicelli-Daley *et al.* 2003b). This suggests that the increase in extracellular ACh levels in the two mutants is not completely offset by the decrease in mAChR density.

The injection of oxotremorine (a mAChR agonist) into WT mice triggers a significant decrease in central temperature (Clement 1993). The central temperature of WT mice in our study decreased from 36.9 ± 0.5°C to 30.3 ± 0.6°C ($n = 4$ $p < 0.001$) (Fig. 5), half an hour after the injection of oxotremorine (0.2 mg/kg). The injection of the same amount of oxotremorine into PRiMA KO mice decreased central temperature from 36.2 ± 0.5°C to only 33.0 ± 0.2°C ($n = 4$ $p < 0.001$). We also calculated the time spent at a temperature below 34°C, which was found to be 125 ± 33 min for WT and 44 ± 25 min for PRiMA KO mice. The weaker response to oxotremorine in PRiMA KO mice indicates that the decrease in muscarinic drug binding reflects a decrease in the number of functional mAChRs.

Slight changes to nAChRs

We first investigated the way in which PRiMA KO nAChRs cope with excess ACh, by assessing the binding of specific toxins: [^{125}I]- α-bungarotoxin, which labels α7 nAChRs, and [^{125}I]-epibatidine, which labels principally β2-containing nAChRs. We observed a small (less than 20%), but systematic decrease in the levels of β2-containing nAChRs in PRiMA KO mice (Fig. 6a). By contrast, α-bungarotoxin binding was similar in PRiMA KO and WT mice, for most regions of the brain, with the exception of the CA1 region of the hippocampus, for which binding was significantly weaker in the PRiMA KO mice (Fig. 6b).

To analyze the functional status of nAChRs in PRiMA KO mice, we chose to compare the nicotinic synaptic currents of WT mice treated with neostigmine with those of PRiMA KO mice at the motoneuron - Renshaw cell (MN-RC) synapse. This synapse expresses both homomeric and heteromeric post-synaptic nAChRs, which can be blocked separately by methyllycaconitine (MLA) or dihydro-β-erythroidine (DHβE) (Lamotte d'Incamps and Ascher 2008). The inhibition of AChE by neostigmine prolongs the excitatory postsynaptic currents (EPSCs) mediated by heteromeric nAChRs, but not those mediated by homomeric nAChRs. This differential effect of AChE inhibitors on homomeric and heteromeric nAChRs has also been observed in the ciliary ganglion (Zhang *et al.* 1996) and hippocampal CA1 interneurons (Fayuk and Yakel 2004). Then, if AChE inhibition by neostigmine is prolonged, both responses gradually disappear (Lamotte d'Incamps *et al.* 2012).

The nicotinic EPSCs of the MN-RC synapse in PRiMA KO mice (Fig. 7, upper part) resembled strikingly those observed in the first few minutes after application of neostigmine in WT mice. They consisted of a fast EPSC (Fig. 7, α7), the amplitude of which decreased during the train, a slower component (Fig. 7, hetero), the amplitude of which increased during the train and an ''ultra-slow'' component (decay time with a time constant in the second range) eliminated by the addition of exogenous AChE (Lamotte d'Incamps *et al.* 2012). The addition of DHβE (10 μM) eliminated the slow and ultraslow components and

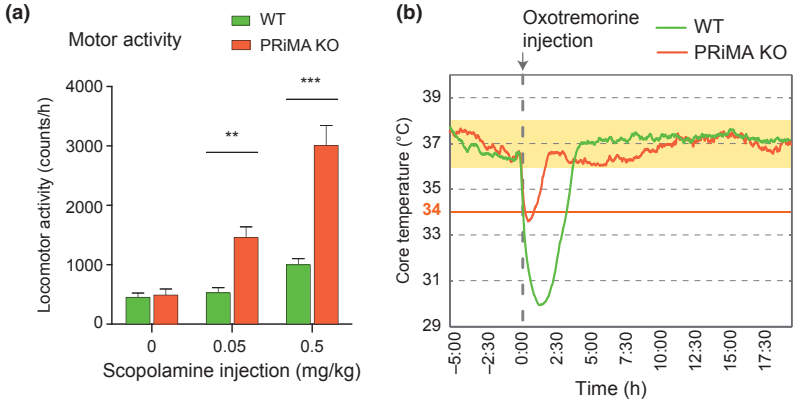

Fig. 5 Decrease in the number of functional mAChRs (a) Scopolamine injections had no effect (520 ± 81, $p = 0.54$) at a dose of 0.05 mg/kg and mild effects (966 ± 107, $p < 0.01$) at a dose of 0.5 mg/kg in WT mice. By contrast, injections of 0.05 and 0.5 mg/kg scopolamine significantly increased (1430 ± 179, $p < 0.01$ and 2954 ± 331, $p < 0.001$, respectively) the locomotor activity of the PRiMA KO mice. Basal levels were WT vs. PRiMA KO for saline 447 ± 69 ($n = 5$) vs. 481 ± 101 ($n = 5$) $p = 0.78$, for scopolamine 0.05 mg/kg 520 ± 81 ($n = 8$) vs. 1430 ± 179 ($n = 8$) ** is $p < 0.001$, for scopolamine 0.5 mg/kg 966 ± 107 ($n = 8$) vs. 2954 ± 33 ($n = 8$) *** is $p < 0.001$. (b) The subcutaneous injection of oxotremorine (0.2 mg/kg) reduced the central temperature in WT mice (green line) and PRiMA KO mice (red line). Both the intensity and the duration of hypothermia were lower in PRiMA KO mice than in WT mice.

© 2012 The Authors

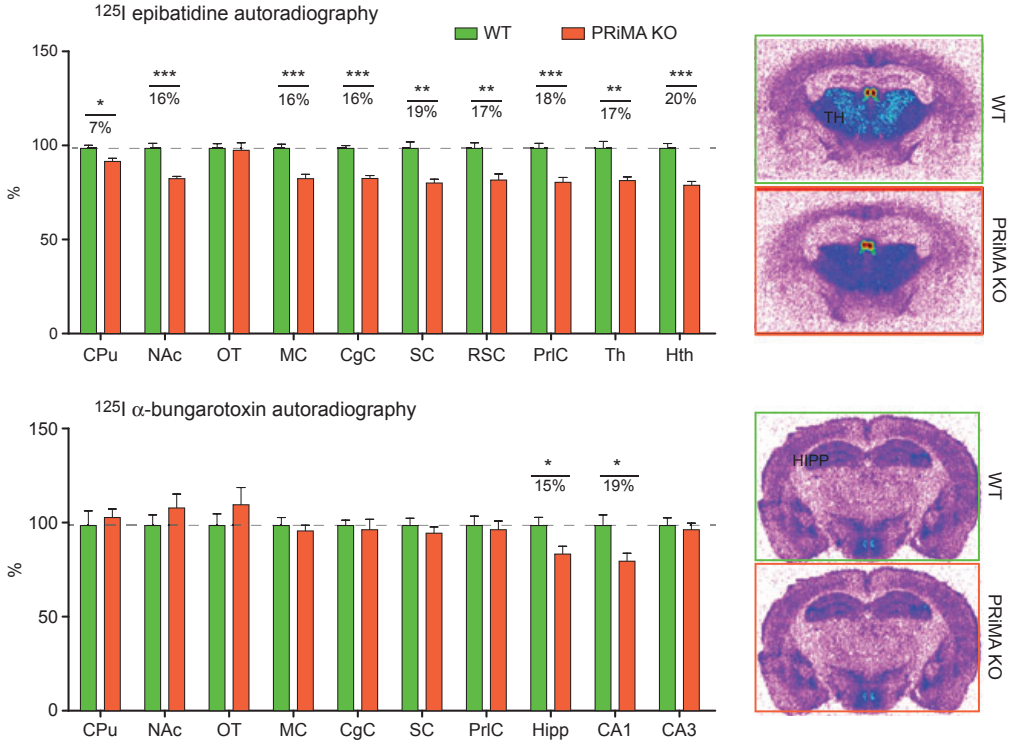

Fig. 6 Nicotinic receptors Nicotinic receptors in coronal brain sections were labeled with [^{125}I]-epibatidine (β2 subunit-containing receptors) and [^{125}I]-α-bungarotoxin (α7 receptors) and relative autoradiographic densities for each brain area were normalized taking the WT value as 100%. CPu – caudate putamen, NAc nucleus accumbens, OT – olfactory tubercle, Hipp – hippocampus, CA1/CA3 – CA1/CA3 hippocampal field, DG – dentate gyrus Th – thalamus, Hth – hypothalamus MC/CgC/SC/RsC/PrlC – motor/cingulate/somatosensory/retrosplenial/prelimbic cortex. We analyzed 6 mice of each genotype. Statistical significance was evaluated with Student's *t*-test: * is $p < 0.05$, ** is $p < 0.01$, *** is $p < 0.001$.

revealed the fast component (Fig. 7, α7), which had a decay time constant of 3–5 ms, similar to that previously characterized as being mediated by α7 receptors in WT mice, (Lamotte d'Incamps and Ascher 2008) and which was abolished by MLA (10 nM). The EPSC suppressed by DHβE (and therefore attributed to heteromeric receptors) was similar in every way to the response observed in WT mice just after the application of neostigmine. Thus, the kinetics of nAChRs does not seem to be changed by the persistent presence of ACh in the extracellular space, as also reported by Sun (Sun *et al.* 2007) for the nAChRs of the sympathetic ganglia of AChE-KO mice.

An important difference between WT mice treated with neostigmine and PRiMA KO mice was that, despite a similar prolonged presence of ACh in the extracellular space in PRiMA KO mice, the response did not disappear as they do in the continued presence of neostigmine in WT mice. This suggests a homeostatic adaptation (Lamotte d'Incamps *et al.* 2012). A possible explanation of this difference is suggested by the experiments of Sun (Sun *et al.* 2007) who showed that in the sympathetic ganglia, mAChRs inhibit nAChRs. If the progressive depression of nAChRs in WT treated with neostigmine resulted from the activation of muscarinic receptors by the « background » ACh induced by neostigmine, this effect would be greatly reduced in PRiMA KO as a result of the reduction of the density of mAChRs.

Our electrophysiological experiments did not allow a quantification of the density of nAChRs and we would not have been be able to detect a less than 20% reduction of density such as that observed, in some regions, in binding experiments (Fig. 5). Overall, the physiological data can be reconciled with the binding data by assuming in PRiMA KO a reduction of nAChRs which is less marked than that of mAChRs.

No change in the distribution of dopamine, GABA and glutamate receptors

We explored potential changes in the distribution of non-cholinergic receptors in the brain of PRiMA KO mice, by analyzing the distributions of labeled specific ligands: [^{3}H]-SCH 23390 for D_1 dopamine receptors and [^{125}I]-iodosulpride for D_2 dopamine receptors, [^{3}H]-muscimol for γ-aminobutyric acid -A receptors, [^{3}H]-CGP 39653 for NMDA receptors,

© 2012 The Authors

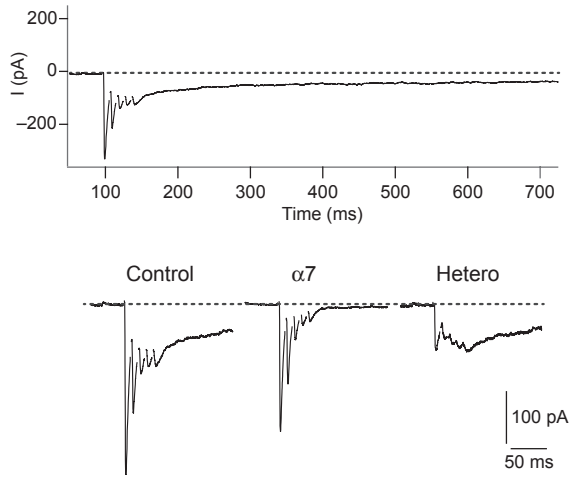

Fig. 7 Functional changes to synaptic transmission at the motoneuron-Renshaw cell synapse Recordings were obtained with spinal cord slices from P8 PRiMA KO mice. Excitatory post-synaptic currents were triggered by a train of five pulses applied to the ventral root at a frequency of 100 Hz in the presence of D-APV (50 μM) and NBQX (2 μM). The membrane potential was held at −45 mV. The upper traces correspond to the control recording obtained before (black, left) and after (middle, gray) the addition of 10 μM dihydro-β-erythroidine (DHβE). DHβE eliminated both an early component (present in WT mice) and a very slowly decaying current, which is induced by the application of neostigmine (0.1–1 μM) in WT mice. The current persisting after the addition of DHβE displayed rapid kinetics (rapid rise, rapid decay) and the repetition of the stimulus at 100 Hz induced a depression. This pattern is characteristic of α7 responses. The response persisting after the addition of DHβE was blocked by MLA (10 nM; data not shown). The lower right trace (gray, hetero) indicates the difference between control and DHβE and corresponds to the response of heteromeric nicotinic receptors. The ratio of the DHβE-sensitive and MLA-sensitive components was markedly different, and such differences are also observed in WT mice.

[^{3}H]-AMPA for AMPA receptors and [^{3}H]-kainate for kainate receptors. The labeling patterns in the various areas of the brain were identical in PRiMA KO mice and WT mice, indicating a lack of effect of high levels of extracellular ACh on non-cholinergic receptors (not shown). These results contrast with the observations made in AChE-KO mice, in which there was a dramatic decrease of both D_1 and D_2 receptors in the striatum (Hrabovska *et al.* 2010).

Sensitivity to AChE inhibitors of PRiMA KO mice

The behavioral data indicated that PRiMA KO mice have adapted well to the ACh overload resulting from the AChE deficiency. This overload is similar in AChEdelE5 + 6 mice, which have a similar brain AChE deficiency, a similar increase in extracellular ACh concentration (Fig. 2), and a similar decrease in the number of mAChRs (Fig. 4), and yet are smaller in size and display tremor and muscle weakness (Camp *et al.* 2010). These clinical manifestations are likely to be caused to the additional deficiency of muscle AChE (anchored by ColQ). However, this difference cannot account for the surprising effects observed after injection of the specific AChE inhibitor, donepezil, used to treat Alzheimer's disease.

AChE inhibitors have been known to induce hypothermia in WT adult mice and this effect has been shown to involve the activation of the same central (hypothalamic) muscarinic receptors, which are responsible for the hypothermia induced by oxotremorine (Clement 1993). Given the expected reduction in density of the muscarinic receptors in AChE-deficient mice ((Bernard *et al.* 2003; Volpicelli-Daley *et al.* 2003b) and Fig. 4) as well in PRiMA KO mice (Fig. 4), one could expect that the hypothermia induced by AChE inhibitors be reduced in both mice mutants. For evaluating this prediction we used donepezil, a specific inhibitor of AChE known to induce a large decrease in central temperature in wild-type mice, and which had been shown to have no effect on AChE-KO mice (Duysen *et al.* 2007; Naik *et al.* 2009). In both WT and PRiMA KO mice, central temperature was variable, but always above 34°C before donepezil injection. Surprisingly, the injection of donepezil into PRiMA KO mice led to a decrease of the central temperature as large as that observed in WT mice (Fig. 8).

The severity of the hypothermia induced by donepezil was assessed by measuring how long the temperature remained below 34°C. After a single injection of 10 mg/kg donepezil, hypothermia lasted 173 ± 5 min in WT mice and 172 ± 13 min in PRiMA KO mice (n = 4). For donepezil injections at a lower dose (2 mg/kg), hypothermia lasted 42 ± 23 min in WT mice and 57 ± 21 min in PRiMA KO mice (n = 4). In AChEdelE5+6 mice, donepezil induced a weaker hypothermia, lasting only 66 ± 20 min (n = 4) when a dose of 10 mg/kg was administered, and 0 ± 0 min (n = 4) when a dose of 2 mg/kg was administered (Fig. 8).

These observations are particularly surprising in view of the observation (Fig. 5b) that the hypothermia induced by oxotremorine (agonist of mAChR) is reduced in PRiMA KO. It suggests that the hypothermia induced by donepezil in PRiMA KO mice is mostly mediated by peripheral AChE, as was observed in neonates of AChE-KO mice (Sun *et al.* 2007). Since the peripheral AChE persisting in PRiMA KO is ColQ-anchored, we could test its involvement by injecting donepezil into ColQ KO mice. Central temperature fell below 34°C for 127 ± 44 min following the administration of 10 mg/kg donepezil. The lower dose (2 mg/kg) had no effect, as in AChEdelE5+6 mice (Fig. 8).

Discussion

Our main findings are that the CNS of PRiMA KO mice has adapted so well to the challenge created by the genetically induced excess of ACh that these mice display spontaneously nearly no behavioral phenotype. The strong behavioral

© 2012 The Authors

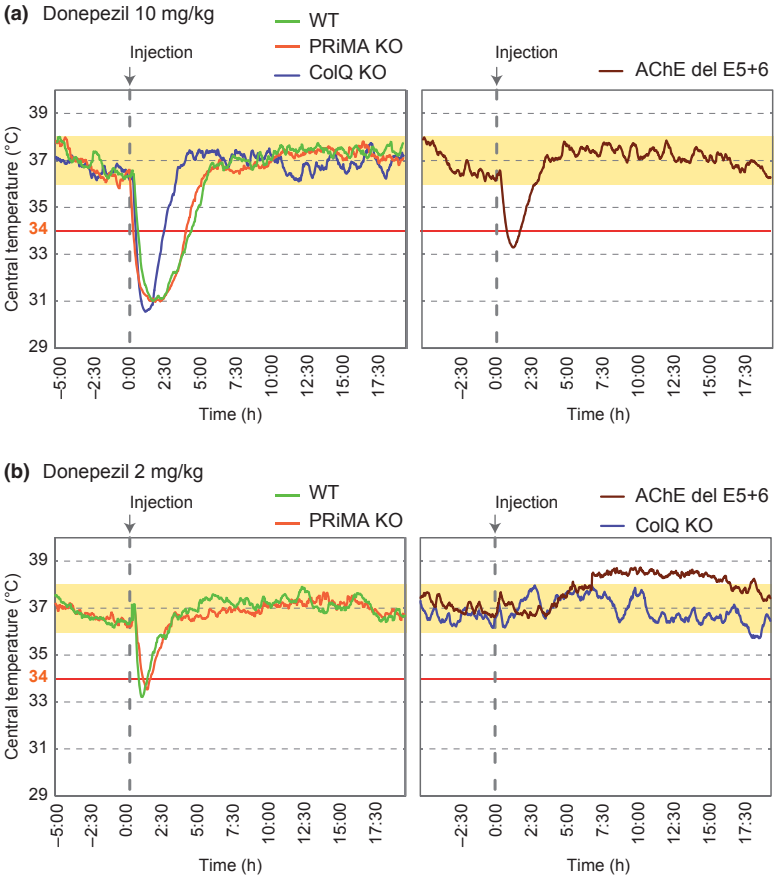

Fig. 8 Changes in central temperature. The graphs show changes in central temperature (mean values for four animals of the same genotype) over time. The yellow band marks the limits of the fluctuation of normal central temperature. (a) 10 mg/kg of donepezil was injected into WT, PRiMA KO, collagen Q (ColQ) KO and AChEdelE5+6 mice. The left shows the deep hypothermia in three genotypes; note the faster recovery of ColQ KO mice than of WT mice. The right illustrates the partial resistance of AChEdelE5+6 mice to hypothermia after the injection of donepezil. (b) 2 mg/kg of donepezil was injected into WT, PRiMA KO, ColQ KO and AChEdelE5+6 mice. The left shows similar hypothermia in PRiMA KO mice and WT mice. The right shows the absence of a decrease in central temperature in AChEdelE5+6 and ColQ KO mice.

phenotype of AChE-deficient mice may thus be mostly the consequence of a peripheral deficiency of AChE.

The adaptations of the brain cholinergic synapses to the high extracellular ACh concentration are very similar in PRiMA KO mice and AChE-deficient mice

Our microdialysis experiments indicated that the ambient concentration of ACh in the striatum of PRiMA KO mice reached 3 μM, a value consistent with the observation of sustained nAChR activation in the spinal cord (Lamotte d'Incamps *et al.* 2012). These high extracellular ACh concentrations exceed the EC50 of mAChRs, but not that of most nAChRs. It is therefore not surprising that the main adaptation of ACh receptors concerns the mAChRs. In PRiMA KO mice a decrease in mAChR density was observed in all regions of the CNS (Fig. 4) and was associated with a decrease in the functional effects of both the muscarinic agonist oxotremorine and the muscarinic antagonist scopolamine (Fig. 5). These observations are similar to those made for AChE-KO mice (Bernard *et al.* 2003; Li *et al.* 2003; Volpicelli-Daley *et al.* 2003a,b). In contrast the nAChRs display a less marked adaptation to the high ACh concentration. Binding studies indicated a widespread but small decrease in the density of heteromeric receptors containing β2 chain and a small, well delimited decrease in the density of homomeric receptors (Fig. 6). The EPSCs of the motoneuron–Renshaw cell synapse indicated that both heteromeric and the homomeric nAChRs were functional in the PRiMA KO mice, with no change in kinetics (Fig. 7). The long tail of the synaptic current involving heteromeric receptors is identical to that observed immediately after the administration of neostigmine in WT mice. Overall in PRiMA KO mice, the nAChRs do not undergo a global marked down-regulation. This is in agreement with the situation described in AChE-KO mice, for which Volpicelli-Daley *et al.* (2003a) reported that there were no alterations in β2-containing receptors while Sun *et al.* (2007) observed a significant decrease of responses to nicotine in the sympathetic ganglia.

The role of AChE in the CNS

The role of AChE in the CNS has often been considered in the framework of anatomical observations indicating that, in some typical synapses, the active zone of the cholinergic terminal faces a well-defined post-synaptic density but that, in many cases, there is a long distance between the release sites and ACh receptors, consistent

© 2012 The Authors

with the occurrence of volume transmission (Descarries 1998; Lendvai 2008).

In the interneuronal cholinergic synapses, the presynaptic and postsynaptic elements are usually much smaller than those in the NMJ or the ciliary ganglion. Given the small size of the synaptic boutons and the low density of postsynaptic AChRs, diffusion may be the principal driving force eliminating ACh from the synaptic cleft (Eccles 1944; Descarries 1998; Barbour 2001), and the inhibition of ACh hydrolysis in the brain may not have the severe consequences observed at the NMJ. Experimental support for this hypothesis has been provided by Rang (1981) and Bennett *et al.* (1997), who reported that in ganglia mEPSCs are less prolonged by AChE inhibition than those at the NMJ. The notion that AChE plays no major role in shaping rapid nicotinic responses is also supported by the theoretical calculations of Wathey *et al.* (1979). Finally, our observations are consistent with the fact that in the Renshaw cells of PRiMA KO mice, neither the fast decay of nicotinic mEPSCs nor the fast component of the decay of evoked EPSCs is longer than that in WT mice (Lamotte d'Incamps *et al.* 2012).

When there is a long distance between release sites and ACh receptors, we can assume that a large proportion of the ACh released can escape hydrolysis by AChE, which is mostly tethered to the presynaptic boutons (Dobbertin *et al.* 2009). Once it leaves the synaptic cleft, ACh diffuses in an AChE-free extracellular space and can thus reach distant receptors at a sufficiently high concentration to activate them (Descarries 1998). This hypothesis has received strong support in the case of the high-affinity mAChRs but is probably also valid for the presumably lower affinity nicotinic α7 receptor (e.g. (Jones and Wonnacott 2004). It is consistent with the very long tail observed for the synaptic current mediated by heteromeric nAChRs in PRiMA KO mice (Fig. 6).

Our results are thus consistent with the hypothesis (Descarries 1998; Lendvai 2008) that the principal role of AChE in the CNS is not to terminate the synaptic transmission, but to keep extracellular ACh concentrations low.

Central versus peripheral changes in cholinergic function

PRiMA KO mice, AChE-KO mice and AChEdelE5+6 mice have similar major AChE deficiencies in the CNS. All these mutants have high levels of ambient extracellular ACh (Fig. 2) (Hartmann *et al.* 2007) and display similar decreases in the number of mAChRs evaluated by binding studies (Bernard *et al.* 2003; Volpicelli-Daley *et al.* 2003a,b) and by functional assays (AChE-KO mice: (Li *et al.* 2003); PRIMA KO mice: Fig. 5).

Despite all these similarities, the behavior of PRiMA KO mice appears normal, whereas AChE KO and AChEdelE5+6 mice have a poor locomotor activity, high levels of fatigability, are affected by tremor. Notably only AChE-KO mice develop seizures in response to very slight changes to their environment (Duysen *et al.* 2002). PRiMA KO mice have a normal respiratory function (Boudinot *et al.* 2009), whereas AChE-KO mice display several respiratory abnormalities similar to those observed after the administration of AChE inhibitors (Chatonnet *et al.* 2003). AChEdelE5+6 mice are less strongly affected than AChE-KO mice, but nonetheless have a clear pathological phenotype (Boudinot *et al.* 2009; Camp *et al.* 2010).

Butyrylcholinesterase (BChE), the other cholinesterase, moderates the ACh level in AChE KO mouse brain (Hartmann *et al.* 2007), and may contribute to the survival mechanism in AChE-KO mice. However, the respiration of AChE-KO mice is blocked by a BChE inhibitor that does not cross the blood–brain barrier (Chatonnet *et al.* 2003), suggesting a toxic effect at the periphery but not in CNS. In PRiMA KO mice, central BChE is absent as is central AChE (Dobbertin *et al.* 2009) and our preliminary results of microdialysis do not show change of ACh after inhibition of BChE (Mohr, unpublished observations).

The normal levels of AChE/ColQ at the NMJ in PRiMA KO mice may account for some of their differences from AChE KO and AChEdelE5+6 mice, including, in particular, the lower levels of motor activity of AChE-KO mice. However, the presence of AChE in muscle cannot account for the milder CNS defects or the marked effects of donepezil on central temperature in PRiMA KO mice. PRiMA KO mice must therefore have a source of AChE other than the NMJ. The two most plausible and nonexclusive hypotheses are the presence of residual AChE activity in the CNS and a contribution of the autonomic nervous system AChE.

We cannot exclude the possibility that a small amount of residual AChE in PRiMA KO mouse CNS has a disproportionately large effect, accounting for the absence in PRiMA KO mice of an increase in hChT density (Volpicelli-Daley *et al.* 2003b) and the smaller number of dopamine receptors (Hrabovska *et al.* 2010) in AChE-KO mice. Further investigation of these aspects is required. Nevertheless, the most plausible explanation for the differences between PRiMA KO mice on the one hand, and AChE-KO mice and AChEdel5+6 on the other, is that ColQ-anchored AChE is present not only at the NMJ, but also in the cholinergic synapses of the autonomic nervous system (Skau and Brimijoin 1980; Koelle *et al.* 1987). This hypothesis is supported by the effects of donepezil on PRiMA KO mice, which cannot be explained by residual central AChE (similar in PRiMA KO mice and AChEdelE5+6 mice) and are much larger than those observed in AChEdelE5+6 mice and ColQ KO mice. We thus propose that the major targets of donepezil in PRiMA KO mice are the cholinergic synapses of the PNS and, more generally that the persistence of AChE at these synapses may at least partially account for the mild phenotype of PRiMA KO mice. Indeed, AChE-KO mice are by far the most strongly affected, as they die within the first 3 weeks of development. Some of the defects in these mice

© 2012 The Authors

may be accounted for by a loss of brown adipose tissue thermoregulation, which involves the autonomic nervous system (Sun *et al.* 2007). Many ColQ KO mice (50%) die in the same period (Feng *et al.* 1999) and are rescued effectively by increasing the rearing temperature or energy intake, as in AChE-KO mice. Skeletal muscle AChE does not seem to be involved, because AChE1irr KO mice, which lack AChE specifically in the skeletal muscle, display no growth deficit (Camp *et al.* 2008; Bernard *et al.* 2011).

These results suggest that, when interpreting the effects of AChE inhibitors, the inhibition of autonomic nervous system and NMJ AChE may be more important than the inhibition of central AChE, contrary to previous explicit assumptions (Duysen *et al.* 2002, 2007), or implicit assumptions such as those underlying the search for new antidotes for treating AChE inhibitors induced poisoning, e.g. by targeting oximes into the CNS (Wagner *et al.* 2010). The phenotype of the PRiMA knockout mice thus highlights the need for a change in paradigm in the search for new treatments of intoxications caused by cholinesterase inhibitors.

Acknowledgements

This study was partly funded by the Grant Agency of the Czech Republic (JM, GACR 309/09/0406), Goethe University, Frankfurt (JK, start-up grant), Paris Descartes University (EK, BLI and PA, collaborative project), Association française contre les myopathies (EK) and Ministère des affaires étrangères (France) (EK and AH : SK-FR-0031-09/Stefanik, SK-FR-0048-11/Stefanik, VF ''bourse de co-tutelle''), APVV grants SK-CZ-0028-09, and VEGA 1/1139/12 (AH). There are no financial or conflicts of interest.

References

Albin R. L., Howland M. M., Higgins D. S. and Frey K. A. (1994) Autoradiographic quantification of muscarinic cholinergic synaptic markers in bat, shrew, and rat brain. *Neurochem. Res.* **19**, 581–589.

Andersson D. R., Björnsson E., Bergquist F. and Nissbrandt H. (2010) Motor activity-induced dopamine release in the substantia nigra is regulated by muscarinic receptors. *Exp. Neurol.* **221**, 251–259.

Araki T., Tanji H., Fujihara K., Kato H., Imai Y., Mizugaki M. and Itoyama Y. (2000) Sequential changes of cholinergic and dopaminergic receptors in brains after 6-hydroxydopamine lesions of the medial forebrain bundle in rats. *J. Neural Transm.* **107**, 873–884.

Ayata C., Ayata G., Hara H. *et al.* (1997) Mechanisms of reduced striatal NMDA excitotoxicity in type I nitric oxide synthase knock-out mice. *J. Neurosci.* **17**, 6908–6917.

Barbour B. (2001) An Evaluation of Synapse Independence. *J. Neurosci.*, **21**, 7969–7984.

Bennett M. R., Farnell L., Gibson W. G. and Lavidis N. A. (1997) Synaptic transmission at visualized sympathetic boutons: stochastic interaction between acetylcholine and its receptors. *Biophys. J.* **72**, 1595–1606.

Bernard V., Brana C., Liste I., Lockridge O. and Bloch B. (2003) Dramatic depletion of cell surface m2 muscarinic receptor due to limited delivery from intracytoplasmic stores in neurons of acetylcholinesterase-deficient mice. *Mol. Cell. Neurosci.* **23**, 121–133.

Bernard V., Girard E., Hrabovska A., Camp S., Taylor P., Plaud B. and Krejci E. (2011) Distinct localization of collagen Q and PRiMA forms of acetylcholinesterase at the neuromuscular junction. *Mol. Cell. Neurosci.* **46**, 272–281.

Berrard S., Varoqui H., Cervini R., Israël M., Mallet J. and Diebler M. F. (1995) Coregulation of two embedded gene products, choline acetyltransferase and the vesicular acetylcholine transporter. *J. Neurochem.* **65**, 939–942.

Bon S., Coussen F. and Massoulié J. (1997) Quaternary Associations of Acetylcholinesterase. *J. Biol. Chem.* **272**, 3016–3021.

Boudinot E., Emery M. J., Mouisel E., Chatonnet A., Champagnat J., Escourrou P. and Foutz A. S. (2004) Increased ventilation and CO2 chemosensitivity in acetylcholinesterase knockout mice. *Respir Physiol Neurobiol* **140**, 231–241.

Boudinot E., Bernard V., Camp S., Taylor P., Champagnat J., Krejci E. and Foutz A. S. (2009) Influence of differential expression of acetylcholinesterase in brain and muscle on respiration. *Respir Physiol Neurobiol* **165**, 40–48.

Camp S., Zhang L., Marquez M., de la Torre B., Long J. M., Bucht G. and Taylor P. (2005) Acetylcholinesterase (AChE) gene modification in transgenic animals: functional consequences of selected exon and regulatory region deletion. *Chem. Biol. Interact.*, **157-158**, 79–86.

Camp S., De Jaco A., Zhang L., Marquez M., De la Torre B. and Taylor P. (2008) Acetylcholinesterase expression in muscle is specifically controlled by a promoter-selective enhancesome in the first intron. *J. Neurosci.* **28**, 2459–2470.

Camp S., Zhang L., Krejci E., Dobbertin A., Bernard V., Girard E., Duysen E. G., Lockridge O., De Jaco A. and Taylor P. (2010) Contributions of selective knockout studies to understanding cholinesterase disposition and function. *Chem. Biol. Interact.* **187**, 72–77.

Chatonnet F., Boudinot É., Chatonnet A., Taysse L., Daulon S., Champagnat J. and Foutz A. S. (2003) Respiratory survival mechanisms in acetylcholinesterase knockout mouse. *Eur. J. Neurosci.* **18**, 1419–1427.

Clement J. G. (1993) Pharmacological nature of soman-induced hypothermia in mice. *Pharmacol. Biochem. Behav.* **44**, 689–702.

Dean B., Hussain T., Hayes W., Scarr E., Kitsoulis S., Hill C., Opeskin K. and Copolov D. L. (1999) Changes in serotonin2A and GABA(A) receptors in schizophrenia: studies on the human dorsolateral prefrontal cortex. *J. Neurochem.* **72**, 1593–1599.

Descarries L. (1998) The hypothesis of an ambient level of acetylcholine in the central nervous system. *J. Physiol. Paris* **92**, 215–220.

Dobbertin A., Hrabovska A., Dembele K., Camp S., Taylor P., Krejci E. and Bernard V. (2009) Targeting of acetylcholinesterase in neurons *in vivo*: a dual processing function for the proline-rich membrane anchor subunit and the attachment domain on the catalytic subunit. *J. Neurosci.* **29**, 4519–4530.

Duysen E. G., Stribley J. A., Fry D. L., Hinrichs S. H. and Lockridge O. (2002) Rescue of the acetylcholinesterase knockout mouse by feeding a liquid diet; phenotype of the adult acetylcholinesterase deficient mouse. *Brain Res. Dev. Brain Res.* **137**, 43–54.

Duysen E. G., Li B., Darvesh S. and Lockridge O. (2007) Sensitivity of butyrylcholinesterase knockout mice to (–)-huperzine A and donepezil suggests humans with butyrylcholinesterase deficiency may not tolerate these Alzheimer's disease drugs and indicates butyrylcholinesterase function in neurotransmission. *Toxicology* **233**, 60–69.

Eccles J. C. (1944) The nature of synaptic transmission in a sympathetic ganglion. *J. Physiol.* **103**, 27–54.

Fayuk D. and Yakel J. L. (2004) Regulation of Nicotinic Acetylcholine Receptor Channel Function by Acetylcholinesterase Inhibitors in Rat Hippocampal CA1 Interneurons. *Mol. Pharmacol.* **66**, 658–666.

© 2012 The Authors

Feng G., Krejci E., Molgo J., Cunningham J. M., Massoulié J. and Sanes J. R. (1999) Genetic analysis of collagen Q: roles in acetylcholinesterase and butyrylcholinesterase assembly and in synaptic structure and function. *J. Cell Biol.* **144**, 1349–1360.

Fernagut P.-O., Chalon S., Diguet E., Guilloteau D., Tison F. and Jaber M. (2003) Motor behaviour deficits and their histopathological and functional correlates in the nigrostriatal system of dopamine transporter knockout mice. *Neuroscience* **116**, 1123–1130.

Fonnum F. (1969) Radiochemical micro assays for the determination of choline acetyltransferase and acetylcholinesterase activities. *Biochem. J.* **115**, 465–472.

Hamers F. P. T., Koopmans G. C. and Joosten E. A. J. (2006) CatWalk-assisted gait analysis in the assessment of spinal cord injury. *J. Neurotrauma* **23**, 537–548.

Hartmann J., Kiewert C., Duysen E. G., Lockridge O., Greig N. H. and Klein J. (2007) Excessive hippocampal acetylcholine levels in acetylcholinesterase-deficient mice are moderated by butyrylcholinesterase activity. *J. Neurochem.* **100**, 1421–1429.

Hartmann J., Kiewert C., Duysen E. G., Lockridge O. and Klein J. (2008) Choline availability and acetylcholine synthesis in the hippocampus of acetylcholinesterase-deficient mice. *Neurochem. Int.* **52**, 972–978.

Hrabovska A., Farar V., Bernard V., Duysen E. G., Brabec J., Lockridge O. and Myslivecek J. (2010) Drastic decrease in dopamine receptor levels in the striatum of acetylcholinesterase knock-out mouse. *Chem. Biol. Interact.* **183**, 194–201.

Jones I. W. and Wonnacott S. (2004) Precise Localization of α7 Nicotinic Acetylcholine Receptors on Glutamatergic Axon Terminals in the Rat Ventral Tegmental Area. *J. Neurosci.* **24**, 11244–11252.

Koelle G. B., Massoulié J., Eugène D., Melone M. A. and Boulla G. (1987) Distributions of molecular forms of acetylcholinesterase and butyrylcholinesterase in nervous tissue of the cat. *Proc. Natl. Acad. Sci. USA* **84**, 7749–7752.

Krejci E., Thomine S., Boschetti N., Legay C., Sketelj J. and Massoulié J. (1997) The mammalian gene of acetylcholinesterase-associated collagen. *J. Biol. Chem.* **272**, 22840–22847.

Kristofiková Z., Rícný J., Kozmiková I., Rípová D., Zach P. and Klaschka J. (2006) Sex-dependent actions of amyloid beta peptides on hippocampal choline carriers of postnatal rats. *Neurochem. Res.* **31**, 351–360.

Lamotte d'Incamps B. and Ascher P. (2008) Four Excitatory Postsynaptic Ionotropic Receptors Coactivated at the Motoneuron–Renshaw Cell Synapse. *J. Neurosci.* **28**, 14121–14131.

Lamotte d'Incamps B., Krejci E. and Ascher P. (2012) Mechanisms shaping the slow nicotinic synaptic current at the motoneuron-Renshaw cell synapse. *J. Neurosci.* **32**, 8413–8423.

Lendvai B.. (2008) Cholinergic Transmission, in *Handbook of Neurochemistry and Molecular Neurobiology* (Lajtha A. and Vizi E. S., eds), pp. 113–127. Springer US, Boston, MA.

Li B., Duysen E. G., Volpicelli-Daley L. A., Levey A. I. and Lockridge O. (2003) Regulation of muscarinic acetylcholine receptor function in acetylcholinesterase knockout mice. *Pharmacol. Biochem. Behav.* **74**, 977–986.

Machová E., Jakubík J., Michal P., Oksman M., Iivonen H., Tanila H. and Dolezal V. (2008) Impairment of muscarinic transmission in transgenic APPswe/PS1dE9 mice. *Neurobiol. Aging* **29**, 368–378.

Martres M. P., Sales N., Bouthenet M. L. and Schwartz J. C. (1985) Localisation and pharmacological characterisation of D-2 dopamine receptors in rat cerebral neocortex and cerebellum using [125I]iodosulpride. *Eur. J. Pharmacol.* **118**, 211–219.

Mihaylova V., Müller J. S., Vilchez J. J. *et al.* (2008) Clinical and molecular genetic findings in COLQ-mutant congenital myasthenic syndromes. *Brain* **131**, 747–759.

Morris R. (1984) Developments of a water-maze procedure for studying spatial learning in the rat. *J. Neurosci. Methods* **11**, 47–60.

Naik R. S., Hartmann J., Kiewert C., Duysen E. G., Lockridge O. and Klein J. (2009) Effects of rivastigmine and donepezil on brain acetylcholine levels in acetylcholinesterase-deficient mice. *J. Pharm. Pharm. Sci.* **12**, 79–85.

Paxinos G. and Watson C.. (2007) *The Rat Brain in Stereotaxic Coordinates: hard Cover Edition*, Academic Press, Sydney, Australia.

Pepeu G. and Giovannini M. G. (2010) Cholinesterase inhibitors and memory. *Chem. Biol. Interact.* **187**, 403–408.

Perrier A. L., Massoulié J. and Krejci E. (2002) PRiMA: the membrane anchor of acetylcholinesterase in the brain. *Neuron* **33**, 275–285.

Perry D. C. and Kellar K. J. (1995) [3H]epibatidine labels nicotinic receptors in rat brain: an autoradiographic study. *J. Pharmacol. Exp. Ther.* **275**, 1030–1034.

Rang H. P. (1981) The characteristics of synaptic currents and responses to acetylcholine of rat submandibular ganglion cells. *J. Physiol.* **311**, 23–55.

Schumacher M., Camp S., Maulet Y., Newton M., MacPhee-Quigley K., Taylor S. S., Friedmann T. and Taylor P. (1986) Primary structure of Torpedo californica acetylcholinesterase deduced from its cDNA sequence. *Nature* **319**, 407–409.

Sipos M. L., Burchnell V. and Galbicka G. (1999) Dose-response curves and time-course effects of selected anticholinergics on locomotor activity in rats. *Psychopharmacology (Berl)* **147**, 250–256.

Skau K. A. and Brimijoin S. (1980) Multiple molecular forms of acetylcholinesterase in rat vagus nerve, smooth muscle, and heart. *J. Neurochem.* **35**, 1151–1154.

Spurden D. P., Court J. A., Lloyd S., Oakley A., Perry R., Pearson C., Pullen R. G. L. and Perry E. K. (1997) Nicotinic receptor distribution in the human thalamus: autoradiographical localization of [3H]nicotine and [125I][alpha]-bungarotoxin binding. *J. Chem. Neuroanat.* **13**, 105–113.

Sun M., Lee C. J. and Shin H.-S. (2007) Reduced nicotinic receptor function in sympathetic ganglia is responsible for the hypothermia in the acetylcholinesterase knockout mouse. *J. Physiol. (Lond.)* **578**, 751–764.

Taylor P. (1996) Anticholinesterase agents. *The pharmacol. basis of ther.* **9**, 161–176.

Volpicelli-Daley L. A., Duysen E. G., Lockridge O. and Levey A. I. (2003a) Altered hippocampal muscarinic receptors in acetylcholinesterase-deficient mice. *Ann. Neurol.* **53**, 788–796.

Volpicelli-Daley L. A., Hrabovska A., Duysen E. G., Ferguson S. M., Blakely R. D., Lockridge O. and Levey A. I. (2003b) Altered striatal function and muscarinic cholinergic receptors in acetylcholinesterase knockout mice. *Mol. Pharmacol.* **64**, 1309–1316.

Wagner S., Kufleitner J., Zensi A., Dadparvar M., Wien S., Bungert J., Vogel T., Worek F., Kreuter J. and von Briesen H. (2010) Nanoparticulate Transport of Oximes over an *In Vitro* Blood-Brain Barrier Model. *PLoS One* **5**, e14213.

Wathey J. C., Nass M. M. and Lester H. A. (1979) Numerical reconstruction of the quantal event at nicotinic synapses. *Biophys. J.* **27**, 145–164.

Wolff S. C., Hruska Z., Nguyen L. and Dohanich G. P. (2008) Asymmetrical distributions of muscarinic receptor binding in the hippocampus of female rats. *Eur. J. Pharmacol.* **588**, 248–250.

Xie W., Stribley J. A., Chatonnet A., Wilder P. J., Rizzino A., McComb R. D., Taylor P., Hinrichs S. H. and Lockridge O. (2000) Postnatal developmental delay and supersensitivity to organophosphate in gene-targeted mice lacking acetylcholinesterase. *J. Pharmacol. Exp. Ther.* **293**, 896–902.

Yamamura H. I. and Snyder S. H. (1974) Muscarinic Cholinergic Binding in Rat Brain. *Proc. Natl. Acad. Sci. USA* **71**, 1725–1729.

Zhang Z., Coggan J. S. and Berg D. K. (1996) Synaptic Currents Generated by Neuronal Acetylcholine Receptors Sensitive to α-Bungarotoxin. *Neuron* **17**, 1231–1240.

© 2012 The Authors

* **Supplement 2**

Chemico-Biological Interactions 183 (2010) 194–201

Contents lists available at ScienceDirect

Chemico-Biological Interactions

journal homepage: www.elsevier.com/locate/chembioint

Drastic decrease in dopamine receptor levels in the striatum of acetylcholinesterase knock-out mouse

Anna Hrabovska[a,*], Vladimir Farar[a,e], Veronique Bernard[b,1], Ellen G. Duysen[c,2], Jiri Brabec[d,3], Oksana Lockridge[c,2], Jaromir Myslivecek[e,4]

[a] Department of Pharmacology and Toxicology, Faculty of Pharmacy, Comenius University, Bratislava, Slovakia
[b] INSERM U686, Biologie des Jonctions Neuromusculaires, 45 rue des Saints-Pères, 75006 Paris, France
[c] University of Nebraska Medical Center, Eppley Institute, Omaha, NE 68198-6805, United States
[d] Institute of Anatomy, 1st Faculty of Medicine, Charles University, U Nemocnice 3, 128 00 Prague, Czech Republic
[e] Institute of Physiology, 1st Faculty of Medicine, Charles University, Prague, Czech Republic

ARTICLE INFO

Article history:
Received 22 July 2009
Received in revised form
29 September 2009
Accepted 30 September 2009
Available online 8 October 2009

Keywords:
AChE−/− mouse
Cholinergic system
Dopaminergic system
Adaptation changes
Striatum

ABSTRACT

Background: The acetylcholinesterase knock-out mouse lives to adulthood despite 60-fold elevated acetylcholine concentrations in the brain that are lethal to wild-type animals. Part of its mechanism of survival is a 50% decrease in muscarinic and nicotinic receptors and a 50% decrease in adrenoceptor levels.
Hypothesis: The hypothesis was tested that the dopaminergic neuronal system had also adapted.
Methods: Radioligand binding assays measured dopamine receptor level and binding affinity in the striatum. Immunohistochemistry of brain sections with specific antibodies visualized dopamine transporter. Effects on the intracellular compartment were measured as cAMP content, PI-phospholipase C activity.
Results: Dopamine receptor levels were decreased 28-fold for the D_1-like, and more than 37-fold for the D_2-like receptors, though binding affinity was normal. Despite these huge changes in receptor levels, dopamine transporter levels were not affected. The intracellular compartment had normal levels of cAMP and PI-phospholipase C activity.
Conclusion: Survival of the acetylcholinesterase knock-out mouse could be linked to adaptation of many neuronal systems during development including the cholinergic, adrenergic and dopaminergic. These adaptations balance the overstimulation of cholinergic receptors caused by high acetylcholine concentrations and thus maintain homeostasis inside the cell, allowing the animal to live.
© 2009 Elsevier Ireland Ltd. All rights reserved.

1. Introduction

Acetylcholinesterase (AChE; E.C. 3.1.1.7) has a crucial role in termination of cholinergic action by hydrolyzing the neurotransmitter acetylcholine (ACh). Inhibition of this enzyme leads to severe pathological changes or even death. Therefore it was considered to be an essential enzyme for life.

However, generation of the AChE−/− mouse disproved the dogma that life without AChE is not possible [1]. Mutant mice develop a characteristic phenotype but survive under special care to adulthood [2,3]. Nullizygotes die during spontaneous myoclonic seizures, with peak mortality around age 30 days [4].

Despite numerous studies, it is not yet fully understood why AChE−/− mice are viable. One of the first hypotheses to explain their survival was a compensating role of butyrylcholinesterase in the cholinergic action. Indeed, nullizygous mice are more sensitive to butyrylcholinesterase inhibitors than their wild-type and heterozygous littermates. However, neither protein expression level nor butyrylcholinesterase activity is changed [1]. Another hypothesis suggested possible modification of synthesis and release of ACh as an adaptation to zero AChE activity. The key players in ACh synthesis and release were studied in striatum. Activity of choline acetyltransferase, which catalyzes formation of ACh from endogenous precursors, was the same for all AChE genotypes. The protein level of vesicular ACh transporter, responsible for storing the neurotransmitter in presynaptic vesicles, was not changed in the mutant mouse. On the other hand the level of the high-affinity choline transporter was significantly increased in AChE−/− mice [5]. The rate-limiting step in neuronal ACh-synthesis is the reuptake of choline by the high-affinity choline transporter. The increased

Abbreviations: AChE, acetylcholinesterase; ACh, acetylcholine; Arc, activity-regulated cytoskeletal-associated gene; DAT, dopamine transporter; PLC, phospholipase C.

* Corresponding author. Tel.: +421 250117376; fax: +421 250117100.
E-mail address: anna.hrabovska@gmail.com (A. Hrabovska).
[1] Tel.: +33 142864353; fax: +33 142863399.
[2] Tel.: +1 4025596032; fax: +1 4025594651.
[3] Tel.: +420 224965771; fax: +420 224965770.
[4] Tel.: +420 224968485; fax: +420 224918816.

0009-2797/$ – see front matter © 2009 Elsevier Ireland Ltd. All rights reserved.
doi:10.1016/j.cbi.2009.09.025

level of this transporter is most likely a response to low levels of synaptic choline caused by absence of ACh hydrolysis.

Based on these observations, increased levels of synaptic ACh were expected and an impact on cholinergic receptors was proposed. Microdialysis experiments demonstrated that extracellular ACh levels were 60-fold higher in the hippocampus of AChE−/− mice than in AChE+/+ mice [6]. Additionally, in agreement with observation from striatum, high-affinity choline uptake was shown to be more than doubled in corticohippocampal synaptosomes in AChE−/− mice [7]. Down-regulation of muscarinic receptors in the CNS was shown, using different experimental approaches [5,8]. Adrenoceptors that oppose the action of muscarinic receptors are reduced by 50% in the lung [9]. The muscarinic and adrenoceptor changes are likely a part of the regulatory mechanism that rescues AChE−/− mice.

This supports the idea of interconnectivity between different neurotransmitter systems and the hypothesis that in accordance with homeostasis, modifications of one system will be reflected by changes in another. We hypothesize that other non-cholinergic adaptations have developed in AChE−/− mice in response to cholinergic changes or as a consequence of changes in other neurotransmitter systems.

The tight connection between the dopaminergic and cholinergic systems in striatum is well known. Cholinergic interneurons express both D_1-like and D_2-like dopamine receptors through which complex modulation of the cholinergic tonus is achieved (activation or inhibition) [10]. On the other hand, cholinergic receptors are expressed on striatal dopaminergic terminals and their activation controls dopamine release [11]. A balance between these two neurotransmitter systems is involved mostly in motor functions, cognitive functions and reward action (linked to addiction). Challenging one system can cause a reaction in the other system. For example, cholinergic receptors stimulated by nicotine cause dopamine-mediated addiction to this agonist [11,12].

In this work, we studied adaptation changes in the dopaminergic system in AChE−/− striatum. We focused on the receptor system itself, as well as on possible changes inside the cell.

2. Methods

2.1. AChE knock-out mice

Animal work was carried out in accordance with the Guide for the Care and Use of Laboratory Animals as adopted by the National Institutes of Health. Formal approval to conduct the experiments was obtained from the animal subjects review board. AChE−/− mice with no AChE activity and no AChE protein in any tissue were made by gene-targeting [1] and raised to adulthood on a liquid diet of Ensure [2]. The AChE−/− mice are isogenic in strain 129S6/SvEvTac. AChE−/− mice do not breed. Therefore the colony is maintained by breeding heterozygotes. The mating of AChE+/− mice yields littermates that are AChE−/−, AChE+/−, and AChE+/+. The mice were genotyped by phenotype and by PCR as previously reported [1].

2.2. Radiolabeled ligand binding study of D_1-like dopamine receptors

D_1-like dopamine receptors in the striatum of AChE−/− ($n = 5$) and AChE+/+ ($n = 4$) mice were quantified by radioligand binding. Adult (over 60 days old) AChE−/− mice and AChE+/+ mice were euthanized by asphyxiation with carbon dioxide. D_1-like receptor analysis was carried out following Hyttel's protocol [13]. The striatum was dissected, homogenized with a Teflon glass homogenizer in 20 volumes of ice cold 50 mM TrisCl, pH 7.4, containing 2 mM EGTA and 10% sucrose. Cell debris was removed by centrifugation at $800 \times g$ for 5 min (1900 rpm in a microcentrifuge). The supernatant was centrifuged at $49{,}000 \times g$ for 20 min (20,000 rpm in Sorvall rotor SS34). The pellet was washed twice in 50 mM TrisCl, pH 7.4, and suspended in 50 mM TrisCl, pH 7.4. After the protein concentration was determined with the BCA method (Pierce), the suspension was frozen at −70 °C. The ligand [^{3}H]SCH23390 ((R)-(+)-7-chloro-8-hydroxy-3-methyl-1-phenyl-2,3,4,5-tetrahydro-1H-3-benzazepine hydrochloride), specific for D_1-like dopamine receptors [13,14] was from PerkinElmer Life Science (specific activity = 3.2 TBq/mmol). The binding reaction contained 120 mM NaCl, 5 mM KCl, 2 mM $CaCl_2$, 1 mM $MgCl_2$, 50 mM TrisCl, pH 7.4, 10 μM mesulergine to block serotonin receptors, 0.5–15 nM [^{3}H]SCH23390, and 0.4 mg protein in a total reaction volume of 250 μl. Non-specific binding was measured in the presence of 10 μM cis-flupentixol to block D_1-like receptor binding. The reactions were incubated for 30 min at 30 °C without radioligand to allow binding of cisflupentixol to D_1-like receptor. Then the radioligand was added and the tubes were incubated an additional 30 min at 30 °C. The reaction mixtures were filtered through Whatman GF/B glass fiber filters to wash out unbound radioligand. The filters were washed three times with 4 ml of ice-cold 50 mM Tris–HCl, pH 7.4, then placed in scintillation vials, covered with scintillation cocktail and stored overnight in the dark to minimize chemiluminescence, before being counted the next day. Non-specific binding was subtracted from total binding to yield specific binding.

For determination of the dissociation constant, K_D, and the number of receptors, B_{max}, the data were fit to Eq. (1) using SigmaPlot software (Jandel Scientific).

$$\text{Bound} = \frac{B_{max} \times \text{Total}}{K_D + \text{Total}} \quad (1)$$

where Bound is proportional to the radioactivity specifically bound to D_1-like receptors and Free is the concentration of radioligand.

2.3. Radioligand binding of D_2-like dopamine receptors

As the generation of large numbers of AChE−/− mice is costly, we slightly modified the protocol for analysis of D_2-like dopamine receptors to reduce the amount of striata necessary for an experiment. In pilot experiments, we compared binding to membranes and to homogenates. Striatal homogenates were prepared by two or three pulses of 20–30 s in homogenizer (Ultra-Turrax® T25 basic IKA®-Werke 24,000 r.p.m.) in ice cold Tris–EDTA buffer (Tris–HCl 50 mmol/l, EDTA 2 mmol/l, pH adjusted to 7.4). Although binding to membranes was comparable to binding to homogenates the dpm per mg of original tissue was higher in homogenates, thus requiring less tissue. This difference is probably due to the partial loss of receptors during purification, higher non-specific binding and/or binding to intracellular receptors. For D_2-like assays (AChE+/+, $n = 4$; AChE−/−, $n = 3$) we used 2 mg tissue homogenate. Protein content in the homogenates was determined by the BCA method (Pierce). The specific D_2-like ligand [^{3}H]spiperone (8-[4-(p-fluorophenyl)-4-oxo[2,3(n)-^{3}H]butyl]-1-[4-^{3}H]phenyl1,3,8-triazaspiro[4,5]decan-4-one) (specific activity = 0.56 TBq/mmol) was purchased from PerkinElmer Life Science. Binding was performed in duplicate in Tris–EDTA buffer (Tris–HCl 50 mmol/l, EDTA 2 mmol/l, pH adjusted to 7.4), in a final volume of 500 μl. Incubation with [^{3}H]spiperone lasted 90 min at 25 °C. Ligand concentration from 6 pM to 4 nM ([^{3}H]spiperone) was used to analyze K_D values and determine the saturating concentration of ligand. One saturating concentration of radioligand was used to determine the receptor density (B_{max}). The single concentration which was close to the full saturation was 4 nM [^{3}H]spiperone (94% receptor saturation). Non-specific binding was

examined in the presence of sulpirid (final concentration 4 μM). Incubation was terminated by filtration through Whatman GF/B glass fiber filters pre-soaked with distilled water in a Brandel cell harvester (Brandel Inc., Gaithersburg, USA). Filters were washed three times with ice cold distilled water and placed in scintillation vials, air-dried overnight, then covered with scintillation cocktail and stored in the dark to minimize chemiluminescence before being counted.

2.4. Immunohistochemistry of dopamine transporter

Adult wild-type ($n = 2$) and AChE−/− ($n = 2$) mice were deeply anesthetized with sodium chloral hydrate and were perfused transcardiacally with a mixture of 2% paraformaldehyde and 0.2% glutaraldehyde as previously described [15]. Sections from the neostriatum were cut on a vibrating microtome at 70 μm and collected in phosphate-buffered saline (PBS). The sections were cryoprotected, freeze-thawed and stored in PBS until use.

Dopamine transporter (DAT) was detected at the light microscopic level on brain sections by immunofluorescence using a rabbit polyclonal antibody raised against rabbit DAT [16]. Specificity of the antibody was previously confirmed by zero binding in DAT knock-out mouse (unpublished data). Sections were incubated in 4% normal donkey serum (NDS) for 30 min and then in DAT (1:2000) antibody supplemented with 1% NDS for 15 h at room temperature. Washed sections were incubated with Alexa 568 donkey anti-rabbit secondary antibody. Washed sections were mounted in Vectashield mounting medium (Vector Laboratories, Burlingame, CA, USA) and examined in an epifluorescence microscope. Images of striatum were collected using an Olympus upright microscope (BX61) equipped with an oil-immersion lens (×60) and a cooled video camera (Qimaging, Retiga 2000R, Burnaby, Canada). Digitizing was performed with a PC computer using the image analysis system Image-Pro Plus (Silver Spring, USA).

2.5. cAMP assay

cAMP content was measured with a competitive enzyme immunoassay kit (Cayman Chemical, Inc., MI, USA). Extraction and analysis of cAMP was conducted in accordance with the package instructions accompanying the assay kit. Samples ($n = 3$ for each genotype) were prepared from trichloroacetic acid (TCA)-extracted tissue (10% TCA). All samples, as well as standards were acetylated using 4 M KOH and acetic anhydride following the instructions. Absorbance was read on a spectrophotometer at 420 nm. A standard curve was drawn for each experiment. The mean value was calculated from duplicate measurements of each sample.

2.6. Determination of PI-PLC activity

The phosphoinositide-phospholipase C (PI-PLC) activity was measured by the enzymatic assay of Dwivedi and Pandey [17] ($n = 3$ for each genotype). Briefly, tissue was homogenized at 4 °C in homogenizing buffer containing 20 mM Tris–HCl, pH 7.4, 2 mM EGTA, 5 mM EDTA, 1.5 mM pepstatin, 2 mM leupeptin, 0.5 mM phenylmethylsulfonylfluoride, 0.2 U/ml aprotinin, and 2 mM dithiothreitol using Ultra-Turrax homogenizer (2 short pulses of 10 s with a 30 s pause). 5 μg of protein per tube was used in the assay. Tissue was incubated for 10 min at 37 °C in incubation buffer (20 mM Tris–HCl, pH 7.4, 1 mM $CaCl_2$, and 100 mM KCl) containing 10 mM lithium chloride, PIP_2 substrate (50 μM unlabeled PIP_2, 2.0 μCi/ml [^{3}H]PIP_2) and protease inhibitor cetrimide (0.5 mg/ml) in a total volume of 100 μl (Thermoblock Biometra T1). The reaction was terminated by acidification with 500 μl of 1 M HCl and addition of 500 μl of chloroform/methanol (1:1, v/v). The tubes were vigorously mixed and centrifuged at 1000 × g for 10 min. The aqueous (upper) phase was transferred to a scintillation vial containing scintillation fluid, and the radioactivity was counted in a liquid scintillation counter. Each experiment had a blank in which the protein suspension was added after the reaction was stopped.

2.7. DNA specific staining

Adult AChE−/− mice ($n = 3$) and wild-type mice ($n = 3$) were perfused with 4% paraformaldehyde in 0.1 M phosphate buffer, pH 7.4 while under anaesthesia. Brains were removed, post-fixed for 1 h in 4% buffered paraformaldehyde and then submerged for 1 h in 20% sucrose for cryoprotection. Brains were cryostatically sliced in frontal plane to 40 μm thin sections free-floating in 0.1 M phosphate buffer. Tissue sections were mounted onto gelatinized slides and allowed to dry at room temperature. Slides were used for DNA specific staining and immunohistochemistry. Sections were then stained with the DNA specific dye bis-benzimide (0.01% solution; Hoechst) and examined under the epifluorescent microscope Olympus AX-70 [18]. Samples were handled in the dark. All the images were acquired under the same conditions.

2.8. Evaluation of data

Data are expressed as a mean ± standard error of the mean for at least three independent experiments, while binding assays were performed in duplicates. Statistical significance of differenced in the mean values was evaluated with unpaired two-tailed Student t-test. Significance was determined as $p < 0.05$.

3. Results

3.1. Dopamine receptor levels

In the first step we examined possible changes in the binding properties of dopamine receptors in AChE−/− striatum. Affinity of each ligand towards a receptor, expressed as K_D was determined and compared for both studied genotypes. For saturation curves see Fig. 1. The K_D value for [^{3}H]SCH23390, a specific ligand for D_1-like dopamine receptors, was the same in AChE−/− (3.1 ± 0.2 nM) and wild-type striatum (2.9 ± 0.5 nM) and was comparable with literature values [19–22]. The K_D value for [^{3}H]spiperone, a specific ligand for D_2-like dopamine receptors, was 0.27 ± 0.06 nM for wild-type striatum. No K_D value was obtained for AChE−/− striatum because the binding of radioligand at low concentrations was below detection limits. However, the K_D value for [^{3}H]spiperone determined in other brain regions (cortex) indicated no change in affinity towards D_2-like dopamine receptors in mutant mouse (data not shown).

The number of receptors was quantified by maximal binding, numerically expressed as the B_{max} value. The D_1-like dopamine receptors had $B_{max} = 550 \pm 29$ fmol/mg protein in wild-type ($n = 4$) and $B_{max} = 19 \pm 13$ fmol/mg protein in AChE−/− striatum ($n = 5$). The D_2-like dopamine receptors had $B_{max} = 221.4 \pm 21.54$ fmol/mg protein in wild-type ($n = 4$) and almost undetectable binding, less than 6 fmol/mg protein, in AChE−/− striatum ($n = 5$). These significant decreases in ligand binding in both receptor subsystems suggest that the number of dopamine receptors is drastically reduced in AChE−/− striatum.

3.2. DNA-specific staining in striatum

To examine possible depletion of striatal neurons, brain sections were stained for DNA. As illustrated in Fig. 2, no differences in density or distribution of cells were observed between AChE−/− and wild-type genotypes.

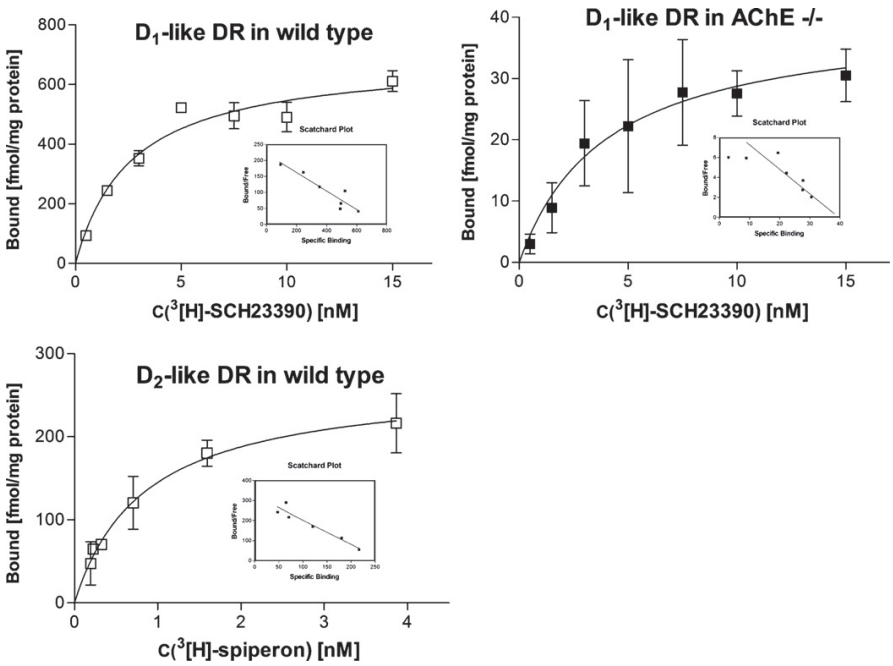

Fig. 1. Saturation curves for radioligand binding to dopamine receptors. Substrate ^{3}[H]-SCH23390 was used as a ligand for D_1-like dopamine receptors and [^{3}H]spiperone as a ligand for D_2-like dopamine receptors. Saturation curves for D_2-like dopamine receptors in AChE−/− striatum were impossible to obtain due to elusiveness of low ligand concentrations binding.

3.3. Immunohistochemistry of dopamine transporter

Dopamine transporter (DAT) in striatum was visualized by immunohistochemistry with a specific antibody. The signal was localized in caudate putamen at the neuron terminals of striatonigral projection in both genotypes. We did not observe any differences in labelling between wild-type and AChE−/− striatum (Fig. 3). Based on our observation, DAT was not affected in AChE−/− striatum.

3.4. Second messengers in AChE−/− vs. wild-type striatum

The hypothesis was tested that the adaptation changes due to hypercholinergic stimulation represented by decreased muscarinic and dopamine receptor levels might affect cell signaling. Therefore cAMP level and phospholipase C (PLC) activity were determined and compared between two genotypes (Fig. 4). Results showed no differences in cAMP content in AChE−/− and wild-type striatum. Similarly, activity of PLC was the same in mutant and wild-type striatum. Both key players of cell signaling mediated by dopamine receptors remained unchanged in AChE−/− mouse.

3.5. Mechanism of dopamine receptors regulation

We developed two hypotheses to explain the mechanism of dopamine receptor level decrease in the striatum of the AChE−/− mouse. Both hypotheses are schematically described in Fig. 5, using a striatal dopaminergic neuron co-expressing M_5 muscarinic receptor and D_1-like and D_2-like dopamine receptors as a model.

(1) In the homologous regulation hypothesis we assume that overstimulation of muscarinic receptors on striatal dopaminergic neurons leads to increased dopamine release [23,24]. This could increase dopamine receptor stimulation and consequently desensitize or down-regulate dopamine receptors. Fig. 5 demonstrates odd-numbered muscarinic receptor G-protein mediated PLC activation which produces calcium-mobilizing IP_3 (by capacitative calcium entry [25]). Increased cytoplasmic calcium serves as a signal for dopamine release. Dopamine discharge is similarly controlled by cAMP signaled calcium influx after even-numbered muscarinic receptor activation.

(2) In the heterologous regulation hypothesis, overstimulated M_1, M_3 and M_5 muscarinic receptors could induce phosphorylation of dopamine receptors by activation of protein kinase C as shown in Fig. 5. Similarly, overstimulation of M_2 and M_4 muscarinic receptors could induce phosporylation of dopamine receptors by cAMP-activated phosphokinase A. The hypothesis predicts that phosphorylated dopamine receptors are desensitized and internalized [26].

4. Discussion

4.1. Receptor balance

The CNS as an integrated complex system consists of many different pathways responsible for different actions. Interconnectivity and mutual communication is characteristic of the nervous system organization and is essential for proper physiology. As a consequence, pathological change of one system can (and probably will) modify another system(s) in the same or related regions. Examples include: the dopaminergic/cholinergic pathway pathology in Parkinson's disease [27], NMDA/dopaminergic pathology in schizophrenia [28], and disturbances in multiple systems besides the serotonin system in the pathology of depression [29,30].

We know that acute inhibition of AChE leads to death [31] while the mouse in which AChE is knocked-out, survives until adulthood. This could be explained by non-selectivity of AChE inhibitors that could affect multiple targets in the body [32,33] and thus their

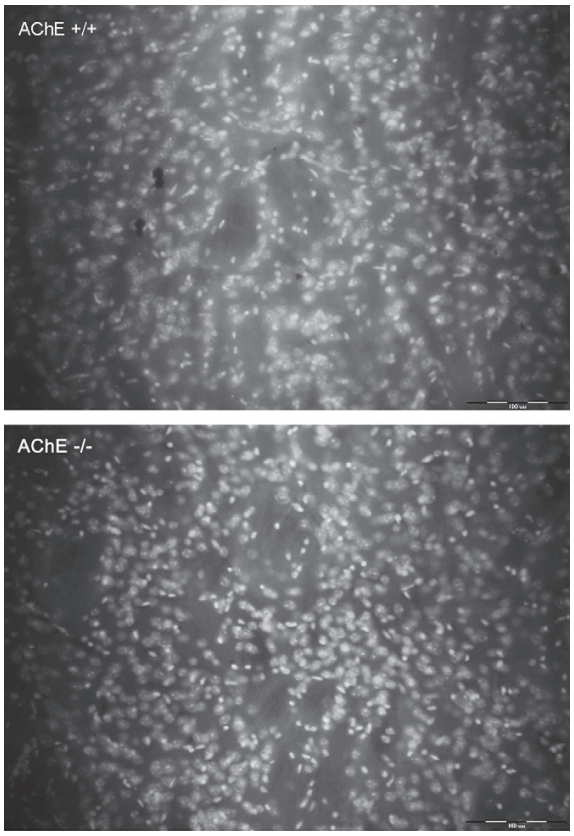

Fig. 2. DNA-specific staining. Modified Hoechst method showed no difference in the neuronal composition of striatum of wild-type and AChE−/− mouse.

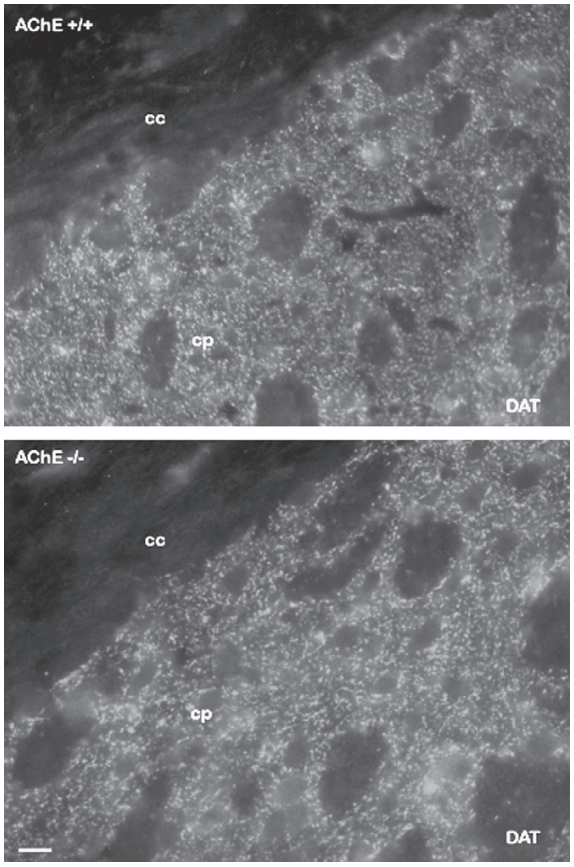

Fig. 3. Immunofluorescent detection of the dopamine transporter (DAT) in caudate putamen (cp) of normal and AChE−/− mice. In AChE+/+ and AChE−/− animals, immunolabelling for DAT was detected in caudate putamen as expected in small structures corresponding to terminals of striato-nigral neurons. No difference in the intensity or distribution of the labelling was shown in mutant compared to normal animals. Cc: Corpus callosum, bar: 15 μm.

lethality could rise from non-cholinergic action. Another possible explanation of the AChE mutant survival is lack of the enzyme during embryonic development that allows adaptation in the AChE−/− mouse. However, it is difficult to conclude whether this adaptation is a consequence of the lack of AChE or the high ACh level. Similarly, adaptation changes were described in a transgenic mouse over-expressing human AChE. In order to maintain the required force of receptors stimulation, increased turnover of the ACh by an increased high-affinity choline transporter in hippocampus and striatum was reported [34].

4.2. Adaptations in AChE−/− mouse

To date it is known that muscarinic receptors in the brain [5], adrenoceptors in the lung [9], and nicotinic receptors in the muscle [35] of AChE−/− mice are downregulated. Despite the high importance of the cholinergic–dopaminergic system in many physiological brain functions only little attention was paid to dopaminergic system in AChE−/− mouse. Indeed, impaired motor functions (e.g. tremor at rest; postural tremor; rigidity; bradykinesia) in AChE−/− mice could suggest a shift in the cholinergic/dopaminergic balance.

As we have shown before in immunohistochemistry and radiolabelled binding studies; striatal muscarinic receptor numbers are dramatically reduced in AChE−/− mice (40–64% reduction) [5,49]. On the other hand, immunoblotting of dopamine receptors in striatal homogenates did not show any changes in the mutant mice [5]. However, in the radiolabelled binding study we obtained different results for dopamine receptors in AChE−/− striatum. They showed drastically decreased binding of specific ligands for D_1-like dopamine receptors (to 5% of the wild-type value). As the K_D value was the same for both genotypes, we conclude that the AChE−/− striatum has lower amounts of available receptors. D_2-like dopamine receptors were almost undetectable in AChE−/− striatum under our conditions. This means that changes in cholinergic system have a great impact on the dopaminergic system and on that homeostasis in the dopaminergic receptor system in AChE−/− striatum is more affected than cholinergic receptor system. The difference in our results could be explained by different binding properties of antibody and ligand. While antibody is selective to the epitope on the surface of the protein that in the case of a linear epitope can be recognized even on inactive or partially degraded protein, the ligand binds strictly to the binding site with an intact conformation. This dramatic decrease in the numbers of dopamine receptors and muscarinic receptors in striatum could suggest diminished numbers of neurons. Our results from DNA-specific staining suggest no changes in the number of the striatal cells. This result, together with observation from electron microscopy from other authors [8,36], showed no differences at the cellular level in striatum of both genotypes. It is concluded that the low dopamine receptor levels in the striatum of AChE−/− mice is not due to changes in the number of cells expressing dopamine

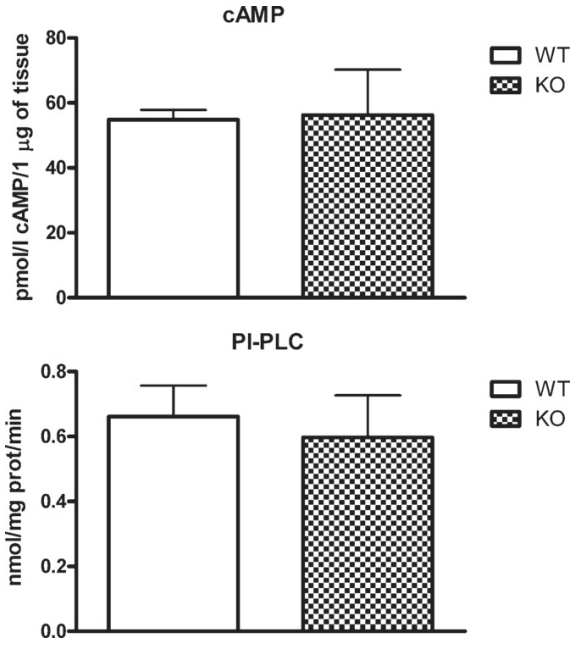

Fig. 4. Cell signaling markers in wild-type and AChE−/− striata. cAMP content ($n = 3$ for each genotype) and PLC activity ($n = 3$ for each genotype) were not changed in the mutant mouse striatum; $p < 0.05$; WT: wild-type.

receptors but that receptors must have been internalized or down-regulated. The literature confirms such complex changes in the cholinergic–dopaminergic balance. For example over-expression of AChE is affected by interference with the dopaminergic system [37]. On the other hand D_5−/− mice have decreased hippocampal ACh level and up-regulated M_1-like receptors [38].

4.3. Proposed scheme of cholinergic regulation of the dopaminergic neurons in striatum

To explain the cause of changes in the dopamine receptor level in AChE−/− striatum, we hypothesize two mechanisms: (1) homologous receptor regulation via increased dopamine release due to muscarinic receptor stimulation [23,24]; (2) heterologous receptor regulation, based on mechanisms different than direct receptor activation by its natural ligand [39].

However, one would expect that dopamine levels causing the drastic down-regulation of dopamine receptors that we observed would influence other dopamine-regulated proteins, e.g. DAT. Our experiments did not confirm any changes in DAT which makes us skeptical about but does not rule out the first hypothesis. Hypothetically, changes observed in AChE−/− mouse could be related to the loss of interaction of AChE with partner proteins. AChE has many partner interactions which are essential for location and function of AChE. These interactions are involved in other cell processes and molecular interactions as well. One can imagine that the lack of AChE would shift the balance in cells and secondarily affect other distant molecules. Examples of AChE assembly partners include: the Proline Rich Membrane Anchor (PRiMA) that is essential for targeting and stabilization of AChE in neurons [40,41]; a collagen tail (ColQ) which anchors AChE tetramers to the basal lamina [42]; a laminin which could affect a cell–cell or cell–basal lamina interactions in the AChE−/− mouse [43,44]; a RACK1 scaffold protein that interacts with $AChE_R$ form [45] and CtB transcriptional regulator interacting with the $AChE_S$ form [46]. It has been suggested that these two AChE forms influence dopamine/cholinergic balance based on the *in vivo* exposure tests of mice expressing either of these variants to the dopaminergic neurotoxin MPTP [37].

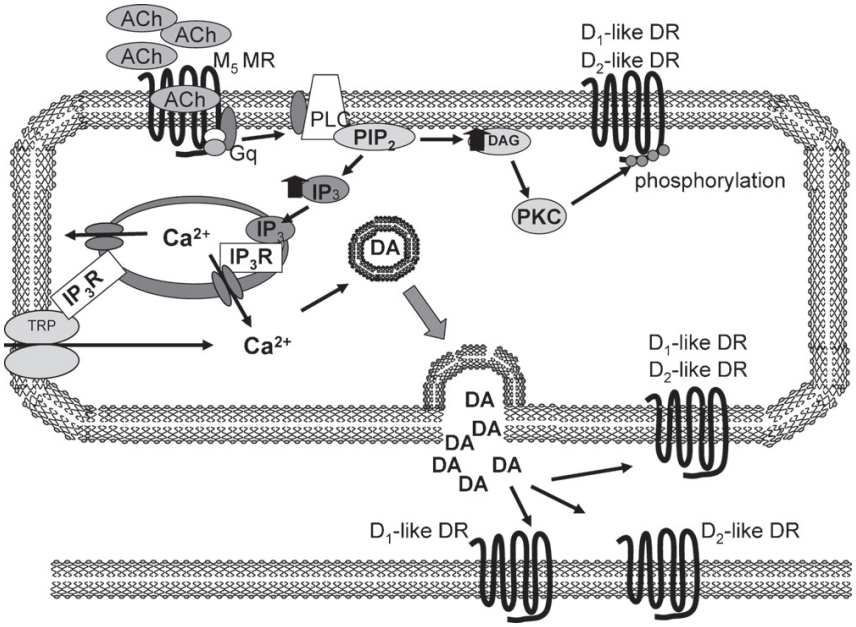

Fig. 5. Scheme of hypotheses of dopamine receptor regulation at the striatal dopaminergic neuron. (1) In homologous regulation, overstimulation of muscarinic receptors on the cell body of the dopaminergic neuron leads to increased release of dopamine (DA); consequent overstimulation of (pre- and post-synaptic) dopamine receptors leads to their desensitization or down-regulation. (2) In heterologous regulation, overstimulated muscarinic receptors activate protein kinase C (PKC) through a secondary intracellular pathway; the kinase phosphorylates pre-synaptic dopamine receptors. Such a modification in the receptor structure can lead to changes in its binding characteristic or in receptor number.

4.4. Intracellular impact of dopamine receptors changes

Our next concern was whether changes in the dopamine receptor and muscarinic receptor levels were reflected within the cell. This question was studied in cell signaling pathways, we did not find an intracellular impact of receptor numbers decrease.

While stimulation of D_1-like receptors coupled with G_s increases cAMP level by activating adenylyl cyclase, D_2-like dopamine receptors activation through its G_i inhibits this enzyme and thus decreases the level of cAMP. Similarly, the cAMP level is decreased by activation of even-numbered muscarinic receptors coupled to G_q/G_{11} but can be as well secondarily increased by M_2 muscarinic receptors coupled with G_s family. D_2-like dopamine receptors can be coupled with G_q and activate PLC as well. Similarly, odd numbered muscarinic receptors activate PLC through G_q/G_{11}. When coupled to the same protein, M_2 muscarinic receptor can affect PLC as well. Obviously, the mechanism of the receptor signaling in the cell is very complex. Therefore it is difficult to conclude why the changes in dopamine receptors and muscarinic receptors do not reflect within the cell. It is possible that such a controversial action of the receptors activations on the secondary messenger results into balanced level of cAMP and PLC activity.

Our result for animals completely devoid of AChE activity contrasts with results on animals with partially inhibited AChE activity due to chronic exposure to dichlorvos. The latter had reduced muscarinic receptor levels as well as reduced cAMP levels [47]. One could therefore explain this difference by postulating that the AChE−/− mouse gradually adapted to excess ACh during development, whereas the acutely poisoned mouse did not adapt. Similarly, downregulation of dopamine receptors in AChE−/− mice was not accompanied by changes in cell signaling, whereas cocaine-induced dopamine receptor downregulation enhanced signal transduction [48].

In conclusion, our results confirm interconnectivity of the nervous systems in the striatum. Primary disruption of the cholinergic system caused by its hyperactivity is reflected in adaptation of multiple receptor systems, including the adrenergic and dopaminergic systems. This is probably due to homeostasis on the intracellular level. By a similar "rescue" action one may explain receptor changes in pathology of some diseases, as similar receptor system correlations were described in patients with Alzheimer's disease and Parkinson's disease.

Conflict of interest

The authors declare that there are no conflicts of interest.

Acknowledgements

Supported by grants VEGA 1/2271/05 (to A.H.); SK-CZ-08706 (to A.H and J.M); GAUK 519/07 (to J.M.); GACR 309/090406 (to J.M.); DAMD17-01-2-0036 (to O.L.). Authors are grateful to Dr. Zsolt Csaba for his comments on the manuscript.

References

[1] W. Xie, J.A. Stribley, A. Chatonnet, P.J. Wilder, A. Rizzino, R.D. McComb, P. Taylor, S.H. Hinrichs, O. Lockridge, Postnatal developmental delay and supersensitivity to organophosphate in gene-targeted mice lacking acetylcholinesterase, J. Pharmacol. Exp. Ther. 293 (2000) 896–902.
[2] G. Duysen, J.A. Stribley, D.L. Fry, S.H. Hinrichs, O. Lockridge, Rescue of the acetylcholinesterase knockout mouse by feeding a liquid diet; phenotype of the adult acetylcholinesterase deficient mouse, Brain Res. Dev. Brain Res. 137 (2002) 43–54.
[3] E.G. Duysen, O. Lockridge, Phenotype comparison of three acetylcholinesterase knockout strains, J. Mol. Neurosci. 30 (2006) 91–92.
[4] A. Hrabovska, E.G. Duysen, J.D. Sanders, L.C. Murrin, O. Lockridge, Delivery of human acetylcholinesterase by adeno-associated virus to the acetylcholinesterase knockout mouse, Chem. Biol. Interact. 157–158 (2005) 71–78.
[5] L.A. Volpicelli-Daley, A. Hrabovska, E.G. Duysen, S.M. Ferguson, R.D. Blakely, O. Lockridge, A.I. Levey, Altered striatal function and muscarinic cholinergic receptors in acetylcholinesterase knockout mice, Mol. Pharmacol. 64 (2003) 1309–1316.
[6] J. Hartmann, C. Kiewert, E.G. Duysen, O. Lockridge, N.H. Greig, J. Klein, Excessive hippocampal acetylcholine levels in acetylcholinesterase-deficient mice are moderated by butyrylcholinesterase activity, J. Neurochem. 100 (2007) 1421–1429.
[7] J. Hartmann, C. Kiewert, E.G. Duysen, O. Lockridge, J. Klein, Choline availability and acetylcholine synthesis in the hippocampus of acetylcholinesterase-deficient mice, Neurochem. Int. 52 (2008) 972–978.
[8] V. Bernard, C. Brana, I. Liste, O. Lockridge, B. Bloch, Dramatic depletion of cell surface m2 muscarinic receptor due to limited delivery from intracytoplasmic stores in neurons of acetylcholinesterase-deficient mice, Mol. Cell. Neurosci. 23 (2003) 121–133.
[9] J. Myslivecek, E.G. Duysen, O. Lockridge, Adaptation to excess acetylcholine by downregulation of adrenoceptors and muscarinic receptors in lungs of acetylcholinesterase knockout mice, Naunyn Schmiedebergs Arch. Pharmacol. 376 (2007) 83–92.
[10] A. Pisani, P. Bonsi, D. Centonze, P. Calabresi, G. Bernardi, Activation of D_2-like dopamine receptors reduces synaptic inputs to striatal cholinergic interneurons, J. Neurosci. 20 (2000) RC69.
[11] F.M. Zhou, Y. Liang, J.A. Dani, Endogenous nicotinic cholinergic activity regulates dopamine release in the striatum, Nat. Neurosci. 4 (2001) 1224–1229.
[12] R. Exley, S.J. Cragg, Presynaptic nicotinic receptors: a dynamic and diverse cholinergic filter of striatal dopamine neurotransmission, Br. J. Pharmacol. 153 (Suppl. 1) (2008) S283–297.
[13] J. H3yttel, SCH 23390—the first selective dopamine D-1 antagonist, Eur. J. Pharmacol. 91 (1983) 153–154.
[14] W. Billard, V. Ruperto, G. Crosby, L.C. Iorio, A. Barnett, Characterization of the binding of 3H-SCH 23390, a selective D-1 receptor antagonist ligand, in rat striatum, Life Sci. 35 (1984) 1885–1893.
[15] V. Bernard, A.I. Levey, B. Bloch, Regulation of the subcellular distribution of m4 muscarinic acetylcholine receptors in striatal neurons in vivo by the cholinergic environment: evidence for regulation of cell surface receptors by endogenous and exogenous stimulation, J. Neurosci. 19 (1999) 10237–10249.
[16] C. Gras, B. Amilhon, E.M. Lepicard, O. Poirel, J. Vinatier, M. Herbin, S. Dumas, E.T. Tzavara, M.R. Wade, G.G. Nomikos, N. Hanoun, F. Saurini, M.L. Kemel, B. Gasnier, B. Giros, S. El Mestikawy, The vesicular glutamate transporter VGLUT3 synergizes striatal acetylcholine tone, Nat. Neurosci. 11 (2008) 292–300.
[17] Y. Dwivedi, G.N. Pandey, Repeated administration of dexamethasone increases phosphoinositide-specific phospholipase C activity and mRNA and protein expression of the phospholipase C beta 1 isozyme in rat brain, J. Neurochem. 73 (1999) 780–790.
[18] V. Riljak, M. Milotova, K. Jandova, M. Langmeier, D. Maresova, J. Pokorny, S. Trojan, Repeated kainic acid administration and hippocampal neuronal degeneration, Prague Med. Rep. 106 (2005) 75–78.
[19] J. Drago, C.R. Gerfen, J.E. Lachowicz, H. Steiner, T.R. Hollon, P.E. Love, G.T. Ooi, A. Grinberg, E.J. Lee, S.P. Huang, et al., Altered striatal function in a mutant mouse lacking D1A dopamine receptors, Proc. Natl. Acad. Sci. U.S.A. 91 (1994) 12564–12568.
[20] E.M. Nikulina, J.A. Skrinskaya, D.F. Avgustinovich, N.K. Popova, Dopaminergic brain system in the quaking mutant mouse, Pharmacol. Biochem. Behav. 50 (1995) 333–337.
[21] K.V. Niessen, G. Hofner, K.T. Wanner, Competitive MS binding assays for dopamine D_2 receptors employing spiperone as a native marker, Chembiochem 6 (2005) 1769–1775.
[22] H. Houchi, D. Babovic, O. Pierrefiche, C. Ledent, M. Daoust, M. Naassila, CB1 receptor knockout mice display reduced ethanol-induced conditioned place preference and increased striatal dopamine D_2 receptors, Neuropsychopharmacology 30 (2005) 339–349.
[23] P. Calabresi, B. Picconi, L. Parnetti, M. Di Filippo, A convergent model for cognitive dysfunctions in Parkinson's disease: the critical dopamine-acetylcholine synaptic balance, Lancet Neurol. 5 (2006) 974–983.
[24] G.L. Forster, J.S. Yeomans, J. Takeuchi, C.D. Blaha, M_5 muscarinic receptors are required for prolonged accumbal dopamine release after electrical stimulation of the pons in mice, J. Neurosci. 22 (2002) RC190.
[25] J.W. Putney Jr., TRP, inositol 1,4,5-trisphosphate receptors, and capacitative calcium entry, Proc. Natl. Acad. Sci. U.S.A. 96 (1999) 14669–14671.
[26] R.J. Lefkowitz, Seven transmembrane receptors: something old, something new, Acta Physiol. (Oxford, England) 190 (2007) 9–19.
[27] A.H. Schapira, E. Bezard, J. Brotchie, F. Calon, G.L. Collingridge, B. Ferger, B. Hengerer, E. Hirsch, P. Jenner, N. Le Novere, J.A. Obeso, M.A. Schwarzschild, U. Spampinato, G. Davidai, Novel pharmacological targets for the treatment of Parkinson's disease, Nat. Rev. Drug Discov. 5 (2006) 845–854.
[28] B. Gisabella, V.Y. Bolshakov, F.M. Benes, Regulation of synaptic plasticity in a schizophrenia model, Proc. Natl. Acad. Sci. U.S.A. 102 (2005) 13301–13306.
[29] M. Beneyto, L.V. Kristiansen, A. Oni-Orisan, R.E. McCullumsmith, J.H. Meador-Woodruff, Abnormal glutamate receptor expression in the medial temporal lobe in schizophrenia and mood disorders, Neuropsychopharmacology 32 (2007) 1888–1902.
[30] D.F. Wong, G.D. Pearlson, L.E. Tune, L.T. Young, C.C. Meltzer, R.F. Dannals, H.T. Ravert, J. Reith, M.J. Kuhar, A. Gjedde, Quantification of neuroreceptors in the living human brain. IV. Effect of aging and elevations of D_2-like receptors inschizophrenia and bipolar illness, J. Cereb. Blood Flow Metab. 17 (1997) 331–342.

[31] J.H. McDonough Jr., T.M. Shih, Neuropharmacological mechanisms of nerve agent-induced seizure and neuropathology, Neurosci. Biobehav. Rev. 21 (1997) 559–579.
[32] S. Wieseler, L. Schopfer, O. Lockridge, Markers of organophosphate exposure in human serum, J. Mol. Neurosci. 30 (2006) 93–94.
[33] S.J. Ding, J. Carr, J.E. Carlson, L. Tong, W. Xue, Y. Li, L.M. Schopfer, B. Li, F. Nachon, O. Asojo, C.M. Thompson, S.H. Hinrichs, P. Masson, O. Lockridge, Five tyrosines and two serines in human albumin are labeled by the organophosphorus agent FP-biotin, Chem. Res. Toxicol. 21 (2008) 1787–1794.
[34] C. Erb, J. Troost, S. Kopf, U. Schmitt, K. Loffelholz, H. Soreq, J. Klein, Compensatory mechanisms enhance hippocampal acetylcholine release in transgenic mice expressing human acetylcholinesterase, J. Neurochem. 77 (2001) 638–646.
[35] M. Adler, H.A. Manley, A.L. Purcell, S.S. Deshpande, T.A. Hamilton, R.K. Kan, G. Oyler, O. Lockridge, E.G.E.G. Duysen, R.E. Sheridan, Reduced acetylcholine receptor density, morphological remodeling, and butyrylcholinesterase activity can sustain muscle function in acetylcholinesterase knockout mice, Muscle Nerve 30 (2004) 317–327.
[36] M.M Mesulam, A. Guillozet, P. Shaw, A. Levey, E.G. Duysen, O. Lockridge, Acetylcholinesterase knockouts establish central cholinergic pathways and can use butyrylcholinesterase to hydrolyze acetylcholine, Neuroscience 110 (2002) 627–639.
[37] Y. Ben-Shaul, L. Benmoyal-Segal, S. Ben-Ari, H. Bergman, H. Soreq, Adaptive acetylcholinesterase splicing patterns attenuate 1-methyl-4-phenyl-1,2,3,6-tetrahydropyridine-induced Parkinsonism in mice, Eur. J. Neurosci. 23 (2006) 2915–2922.
[38] F. Laplante, D.R. Sibley, R. Quirion, Reduction in acetylcholine release in the hippocampus of dopamine D_5 receptor-deficient mice, Neuropsychopharmacology 29 (2004) 1620–1627.
[39] E.M. Hur, K.T. Kim, G protein-coupled receptor signalling and cross-talk: achieving rapidity and specificity, Cell Signal. 14 (2002) 397–405.
[40] A.L. Perrier, J. Massoulie, E. Krejci, PRiMA: the membrane anchor of acetylcholinesterase in the brain, Neuron 33 (2002) 275–285.
[41] A. Dobbertin, A. Hrabovska, K. Dembele, S. Camp, P. Taylor, E. Krejci, V. Bernard, Targeting of acetylcholinesterase in neurons in vivo: a dual processing function for the proline-rich membrane anchor subunit and the attachment domain on the catalytic subunit, J. Neurosci. 29 (2009) 4519–4530.
[42] G. Feng, E. Krejci, J. Molgo, J.M. Cunningham, J. Massoulie, J.R. Sanes, Genetic analysis of collagen Q: roles in acetylcholinesterase and butyrylcholinesterase assembly and in synaptic structure and function, J. Cell Biol. 144 (1999) 1349–1360.
[43] L.E. Paraoanu, P.G. Layer, Mouse AChE binds in vivo to domain IV of laminin-1beta, Chem. Biol. Interact. 157–158 (2005) 411–413.
[44] G. Johnson, C. Swart, S.W. Moore, Interaction of acetylcholinesterase with the G4 domain of the laminin alpha1-chain, Biochem. J. 411 (2008) 507–514.
[45] K.R. Birikh, E.H. Sklan, S. Shoham, H. Soreq, Interaction of "readthrough" acetylcholinesterase with RACK1 and PKCbeta II correlates with intensified fear-induced conflict behavior, Proc. Natl. Acad. Sci. U.S.A. 100 (2003) 283–288.
[46] C. Perry, M. Pick, E. Podoly, A. Gilboa-Geffen, G. Zimmerman, E.H. Sklan, Y. Ben-Shaul, S. Diamant, H. Soreq, Acetylcholinesterase/C terminal binding protein interactions modify Ikaros functions, causing T lymphopenia, Leukemia 21 (2007) 1472–1480.
[47] G. Raheja, K.D. Gill, Altered cholinergic metabolism and muscarinic receptor linked second messenger pathways after chronic exposure to dichlorvos in rat brain, Toxicol. Ind. Health 23 (2007) 25–37.
[48] M. Graziella De Montis, et al., Modifications of dopamine D_1 receptor complex in rats self-administering cocaine, Eur. J. Pharmacol. 362 (1998) 9–15.
[49] B. Li, E.G. Duysen, L.A. Volpicelli-Daley, A.I. Levey, O. Lockridge, Regulation of muscarinic acetylcholine receptor function in acetylcholinesterase knockout mice, Pharmacol. Biochem. Behav. 74 (2003) 977–986.

* Supplement 3

PLoS One. DOI: 10.1371/journal.pone.0068265

Developmental adaptation of central nervous system to extremely high acetylcholine levels

Vladimir Farar[1,2], Anna Hrabovska[3], Eric Krejci[2], Jaromir Myslivecek[1a]

[1]1st Faculty of Medicine, Institute of Physiology, Charles University, Prague, Czech Republic
[2]Centre d'Etude de la Sensorimotricité, Université Paris Descartes, CNRS UMR 8194, Paris, France
[3]Department of Pharmacology and Toxicology, Faculty of Pharmacy, Comenius University, Bratislava, Slovakia

[a]Corresponding author
Jaromir Myslivecek
Institute of Physiology, 1st Faculty of Medicine, Charles University, Albertov 5, 128 00 Prague, Czech Republic, Tel: +420-224 968 485, Fax: +420-224 968 816, E-mail: jmys@lf1.cuni.cz

Abstract
Acetylcholinesterase (AChE) is a key enzyme in termination of fast cholinergic transmission. In brain, acetylcholine (ACh) is produced by cholinergic neurons and released in extracellular space where it is cleaved by AChE anchored by protein PRiMA. Recently, we showed that the lack of AChE in brain of PRiMA knock-out (KO) mouse increased ACh levels 200-300 times. The PRiMA KO mice adapt nearly completely by the reduction of muscarinic receptor (MR) density. Here we investigated changes in MR density, AChE, butyrylcholinesterase (BChE) activity in brain in order to determine developmental period responsible for such adaptation. Brains were studied at embryonal day 18.5 and postnatal days (pd) 0, 9, 30, 120, and 425. We found that the AChE activity in PRiMA KO mice remained very low at all studied ages while in wild type (WT) mice it gradually increased till pd120. BChE activity in WT mice gradually decreased until pd9 and then increased by pd120, it continually decreased in KO mice till pd30 and remained unchanged thereafter. MR number increased in WT mice till pd120 and then became stable. Similarly, MR increased in PRiMA KO mice till pd30 and then remained stable, but the maximal level reached is approximately 50% of WT mice. Therefore, we provide the evidence that adaptive changes in MR happen up to pd30. This is new phenomenon that could contribute to the explanation of survival and nearly unchanged phenotype of PRiMA KO mice.

Keywords: acetylcholinesterase activity; butyrylcholinesterase activity; muscarinic receptors; development; PRiMA

PLoS One. DOI: 10.1371/journal.pone.0068265

Introduction

The central cholinergic system belongs to one of the firstly appearing transmitter system in the brain and has been involved in important functions of central nervous system (CNS) such as cognitive processes [1], motor coordination [2], attention, circadian rhythms [3], food reinforcement and drug addiction [4] and synaptic plasticity [5].

Choline, transported from extracellular space by high affinity choline transporter (ChT), and acetyl coenzyme A (derived from Krebs cycle) form acetylcholine (ACh) [6] in the reaction catalyzed by choline acetyltransferase (ChAT) [7,8]. Then ACh molecules are transported by vesicular acetylcholine transporter (VAChT) into synaptic vesicles [9].

The evoked release of ACh activates two classes of cholinergic receptors. Muscarinic receptors (MR, subtypes M_1-M_5) are G-protein coupled receptors [10]. Nicotinic receptors (NR) are pentameric ligand-gated ion channels of various subunit composition. Nine α subunits: α_1-α_7, α_9, α_{10}, four β subunits: β_1-β_4, and subunits γ, δ, ε were described [11]. In the CNS, the expression of α_2- α_7, and three β subunits: β_2-β_4 were described [12].

ACh action is terminated by acetylcholinesterase (AChE, E.C. 3.1.1.7). ACh can be also cleaved by butyrylcholinesterase (BChE, E.C. 3.1.1.8) [13]. In the CNS, these enzymes are mainly tethered to plasma membrane by anchoring protein PRiMA (**P**roline **Ri**ch **M**embrane **A**nchor) [14,15].

All components of cholinergic system (CHT, VAChT, ChAT, NR, MR, AChE) appear already during the embryonal development in rodents and show a rapid age-related increase during the first three weeks of postnatal development. NR present subtype and brain region developmental differences [16]. In the rat brain, the activity of ChAT and protein level of VAChT increases slowly until postnatal day (pd)7 and then rapidly until pd24 [17]. A similar pattern has been shown for the development of cholinergic innervation in the cortex and hippocampus [18,19].

In murine brain, AChE activity is measurable in embryonic day (E)9 and gradually increases 15-fold to E19 [20]. This increase continues after birth till the pd30 [20,21]. The postnatal increase in AChE activity is also accompanied by increase in expression of PRiMA mRNA and protein [22]. In contrast to AChE, BChE shows only modest changes in activity during the postnatal development [23].

MR are transitorily expressed in the mouse blastoderm and in blastemic tissues during morphogenesis [24]. Between E17 and E18, MR are detectable in the brain, spinal cord and peripheral nerves [24]. After the birth, MR increase by pd25 of age and then become stable [25]. The number of NR in neonatal mouse brain is approximately twice the number in adult mouse brain [25] and the pattern of development differs from MR. There is an increase in NR level by pd10, followed by decrease by pd25 to the level that remain stable until adulthood [25].

In vitro and *in vivo* studies have demonstrated that in the adult rodent brain, the abundance and availability of MR at plasma membrane are controlled by the composition of neurochemical environment and depend on complex intraneuronal trafficking [26]. Overstimulation of MR, whether induced acutely or chronically (repeatedly), leads to the reversible decrease in the density of MR at plasma membrane [26].

Recently, we have found that in PRiMA KO mice, ACh levels are 200-300-times increased in the striatum [27], yet PRiMA KO mice are indistinguishable from (wild type) WT mice and present only marginal changes in behavior, motor skills and gait [27]. The central cholinergic system adapts to this huge increase in ACh by 20-60% decrease in MR level (accompanied by small, less than 20%, decrease in NR number). In the absence of PRiMA, AChE and also

PLoS One. DOI: 10.1371/journal.pone.0068265

BChE, are not delivered to the plasma membrane but are retained in ER, the site of synthesis. Decrease in the number of total MR is similar in hippocampus, somatosensory cortex, motor cortex, olfactory tubercle, nucleus accumbens, and caudate putamen ranging between 37 to 63% reduction. This decrease is not a subtype specific, as we observed similar reduction in pirenzepine binding (usually considered as M_1 MR, 27-51%) and AFDX-384 binding (usually considered as M_2 MR, 33-67%). Although many transmitter systems (cholinergic muscarinic and nicotinic, GABAergic, dopaminergic, glutamatergic: AMPA, kainate, NMDA) and the ACh synthesis machinery were investigated [27], we only found changes in MR and NR levels. Despite low number, MR are still responsive to cholinergic stimulation as it can be deduced from retained thermoregulatory responses to oxotremorine (MR agonist) and also preserved locomotory responses to scopolamine (MR antagonist) in PRiMA KO mice, albeit the degree of responses is changed.

Therefore we suggest that the decrease in MR receptor level is the key adaptation to the lack of membrane anchored AChE and huge increase in ACh level in the brain of PRiMA KO mice. Here we determined when during the development this adaptation occurs. We tested hypothesis that the adaptation to gradually increasing ACh levels would start prenatally. This is important question at least for two reasons: 1) young animals are considered to be more sensitive to AChE inhibition than adults [28]; 2) a minimum of AChE activity necessary for survival [29] ranges between 17.5% (frontal cortex) and 92.1% (basal ganglia) while mice without PRiMA are indistinguishable from WT counterparts through visual inspection., i.e. without any sign of cholinergic hyperactivity with less than 5% of AChE activity. Also it is evident from mathematical model [30] that total AChE inhibition lead to LD_{100}. That means that total inhibition of AChE (and also inhibition with residual AChE activity) is not reconcilable with life.

As a tool for testing our hypothesis, we employed radioligand binding studies together with measurement of AChE and BChE activity. Because of virtually identical changes in different MR subtypes and in different brain region we measured total MR in whole brain preparations.

PLoS One. DOI: 10.1371/journal.pone.0068265

Methods

Ethics Statement

All experiments were performed in accordance with the Czech Republic legislature and were approved by Animal protection Committee of the 1st Faculty of Medicine, Charles University, Prague.

Experimental Animals

Experiments were performed on WT and nullizygous mice for PRiMA (PRiMA KO) of both sexes at specific ages (E18.5, just after the birth (pd0), on pd9, pd30, pd120, and pd425). Concerning the first developmental points (the determination of embryonal day and pd0), we determined these using careful mice observation. Briefly, males were allowed to cover females for five hours in the morning and after 18 days in the evening the embryos were carefully removed from uterus immediately after decapitation of dams (E18.5), the brains were removed (with cerebellum, without adjacent parts), flash frozen in liquid nitrogen and stored at -80 °C until membrane fractions were prepared [27].The newborn litters were decapitated and their brains removed just after birth (pd0). To obtain remaining age points, mice were decapitated at pd9, pd30, pd120 and pd425. The procedure of membrane preparation was the same as described before. Genotypes were determined by PCR with primers described elsewhere [15]. The genetic background of mice was a mixture equivalent to that for an F3 mating of B6D2 strain. Mice were maintained under controlled environmental conditions (12/12 light/dark cycle, 22 ± 1°C, light on at 6 a.m.). Food and water were available *ad libitum*.

Receptor binding

We determined the total amount of MR in membrane preparations as described earlier [27]. The brains were homogenized with Ultra Turrax homogenizer by 3 pulses of 10 seconds in 15 volumes of cold 0.32 M sucrose. The homogenates were centrifugated at 4˚C for 10 min at 1000 g to remove cell debris and nuclear fraction. The supernatant was removed and centrifugated for 55 min at 17 000g to obtain membrane preparation. Supernatant was discarded and the pellet was washed once with cold 50 mM Na/K phosphate buffer ph 7.4, suspended in the same buffer and directly used for binding assay. The total amount of MR binding sites was determined in duplicates using 65 – 1600 pmol/l [^{3}H]-QNB, non-specific binding was determined with 50 µmol/l atropine. The incubation was performed at 25°C and lasted 120 minutes as described previously [31]. The maximal amount of binding sites (B_{max}) per mg protein (determined using BCA a method kit; Sigma) and the affinity constant (K_D) was computed by non-linear regression using GraphPad Prism 5.01 program (GraphPad Software). Affinity constants (K_D) were used for the "single-point" measurement in order to determine the total number of receptors while saving the amount of tissue, using saturating concentration of radioligand (2000 pmol/l [^{3}H]QNB).

Acetylcholinesterase and butyrylcholinesterase activity

Activity of AChE and BChE was determined by Ellman's colorimetric method [32] modified for a 96-well microtiter plate reader (Tecan Sunrise) [33]. Briefly, the activity of AChE was assayed with 0.75 mM acetylthiocholine and 0.5 mM 5,5-dithiobis(2-nitrobenzoic acid) (DTNB) in 5 mM HEPES buffer pH 7.5.The total assay volume was 200 µl. 10 µg of membrane preparation was preincubated first with DTNB to saturate free sulfhydryl groups and with tetra(monoisopropyl)pyrophosphortetramide (iso-OMPA) (final concentration 0.1 mM) to block BChE activity during 30 min. The activity was measured at 412 nm. BChE activity was assayed as described for AChE except that butyrylthiocholine was used as

PLoS One. DOI: 10.1371/journal.pone.0068265

substrate and AChE activity was blocked with 1,5-bis(4-allyldimethylammoniumphenyl) pentan-3-one dibromide (BW284C51) (final concentration 5 μM).

Statistical evaluation

Results are presented as mean±S.E.M. and each group represents an average of 3-9 animals. The binding data were evaluated using GraphPad Prism software (San Diego, USA). Statistical differences among groups were determined by two-way analysis of variance (ANOVA): for multiple comparisons an adjusted t-test modified SNK (Student-Newman-Keuls) correction was used.

PLoS One. DOI: 10.1371/journal.pone.0068265

Results

AChE activity

The brain AChE activity did not differ between WT and PRiMA KO mice on E18.5 (see Figure 1). From the pdo (zero), the AChE activity was significantly higher in WT animals than in PRiMA KO animals. AChE activity remained unchanged from the E18.5 till pd425 in PRiMA KO brain. In contrast, AChE activity steeply increased till pd30 of postnatal development, further increase occurred between pd30 and pd120 and the activity was stable up to the 1st year of postnatal life in WT mice.

BChE activity

In the brain of WT mice, BChE activity decreased (see Figure 1) from prenatal period to pd9 then increased steeply until pd120 and remained stabilized thereafter. In PRiMA KO brain, BChE activity decreased drastically until the pd30 while it represented 42% of the WT value. It remained at the same value at all of following age points, but represented less than 30 % of WT values.

Receptor binding

The affinity of receptors (K_D) was not altered in membrane preparations of PRiMA KO mice (183.8±18.2 pmol/l vs. 143.2±27.6 pmol/l for WT and PRiMA KO mice, respectively) suggesting that we observed changes in receptor levels but not in their affinities to radioligand.

The number of MR copied the development of AChE activity (see Figure 2). While the level of MR in WT brain increased steeply up to day pd30 and then less dramatically up to day pd120, in PRiMA KO brains, increase in the MR number stabilized at the level of pd30 (49% of WT value) and remained unchanged during further ageing.

PLoS One. DOI: 10.1371/journal.pone.0068265

Discussion

Here we provide the data on gradual changes in MR level showing that the adaptation in brains of PRiMA KO mice is finished by pd30. This observation could contribute to the explanation of the viability and nearly unchanged phenotype of PRiMA KO mice [27]. Further it suggests how the organism could adapt to the conditions that are considered to be contradictory to the survival (like in AChE KO mice, [34]). Importantly, the AChE KO mice were indistinguishable from their littermates at birth by naked eye till pd7 when a clear difference was noticeable between AChE KO and WT mice [34] what supports the hypothesis about postnatal (and not prenatal) adaptation to increased ACh levels.

It is important to note that the development of AChE and MR in WT mice was similar as previously reported [16,20,24,25] although we noticed subtle increase in AChE activity between pd30 and pd120 (9.7%).

BChE in brain is also associated with PRiMA [14]. Our data on postnatal BChE activity development in WT mice are similar to that previously published [23,35-37]. BChE is expressed in white matter [38]. As the myelination starts during the postnatal development, decrease of BChE activity in PRiMA KO brain during an early development may be linked to the timing of myelin development. As far as we are aware, there is no other report on BChE prenatal development and in that view our data are new. Importantly, AChE and BChE (see Figure 1) activity developmental profile described here indicate that PRiMA becomes the main anchoring mechanism after birth.

The increase in MR level slowed down from pd30 to pd120 (7.5% only). Therefore, it is possible to conclude that the development of AChE and MR is finished before pd30. Importantly, there is a clear correlation between AChE activity and MR density in WT mice (see Figure 3) which is not apparent in PRiMA KO mice due to almost null AChE activity in these mice.

As we have mentioned in Methods, we measured the total number of MR. Although five subtypes of MR exist, it is very difficult to characterize the changes of specific subtypes. The limitations are methodological. Muscarinic antagonist usually do not differ more than one order of magnitude [39] in pKi for M_1-M_5 subtypes and have similar pKi for two or more subtypes. Thus, it is possible to resolve it by multiple competition binding experiments but this makes the experiments extremely difficult. Another possibility how to determine MR subtype is determination using M_1-M_5 specific antibodies but validity of this methodological approach was challenged multiple times [40,41]. Moreover, radioligand binding has also advantage that intact binding pocket (into G protein-coupled receptors transmembrane zones) is necessary for binding while antibodies can bind on cleaved receptor parts. As we have previously found similar changes in M_1 and M_2 MR here we demonstrate the changes in total number of MR what undoubtedly reflects the changes in specific subtypes.

In contrary to our hypothesis, the adaptation to extremely low AChE activity is not apparent during the prenatal period but the mechanisms occur during the postnatal development. Indeed, the MR density increases by 61% between pd9 and pd30 in WT mice while only by 13% in PRiMA KO. There are different hypotheses that may explain the adaptation delay of the MR density during the prenatal development. The production of ACh is still low and do not interfere with the regulation of MR localization and/or the development of blood-brain barrier is unfinished [42]. This would allow ACh to pass through blood-brain barrier into blood circulation where AChE activity is present [43]. Moreover, BChE activity is high in the serum, and could also contribute to ACh removal between E18.5 and pd30 before the blood-brain barrier is closed.

PLoS One. DOI: 10.1371/journal.pone.0068265

It is also possible to hypothesize that the degree of change in MR density reflects the excess of ACh. If the accumulation of ACh occurs then MR decrease should be gradual. But, as it is apparent form our data, MR do not change from day 30 to day 425 what suggest no accumulation of ACh after the pd30. Another explanation is increased MR synthesis and recycling in the presence of accumulated ACh.

Despite lower MR density in PRiMA KO mice after birth, the development pattern of MR in PRiMA KO mice is similar to that of WT mice. The age-related differences in total MR density in PRiMA KO mice are likely shaped by actual strengthening of cholinergic signaling. More generally, it can be suggested that gradual inhibition of AChE, such as treatment strategy in Alzheimer disease, or intoxication by AChE inhibitors present in environment, may be accompanied by gradual changes in MR abundance.

We can conclude that although it was shown multiple times that cholinergic system starts to develop in early prenatal stages, the development of cholinergic system in PRiMA KO mice is similar to that of WT mice. The differences in cholinergic system of PRiMA KO mice begin to be obvious after the birth in accordance with the maturation of the brain functions.

PLoS One. DOI: 10.1371/journal.pone.0068265

References

1. Pepeu G, Giovannini MG (2010) Cholinesterase inhibitors and memory. Chemico-Biological Interactions 187: 403-408.
2. Guzman MS, De Jaeger X, Raulic S, Souza IA, Li AX, et al. (2011) Elimination of the Vesicular Acetylcholine Transporter in the Striatum Reveals Regulation of Behaviour by Cholinergic-Glutamatergic Co-Transmission. PLoS Biol 9: e1001194.
3. Hut RA, Van der Zee EA (2011) The cholinergic system, circadian rhythmicity, and time memory. Behavioural Brain Research 221: 466-480.
4. Williams MJ, Adinoff B (2007) The Role of Acetylcholine in Cocaine Addiction. Neuropsychopharmacology 33: 1779-1797.
5. Aosaki T, Miura M, Suzuki T, Nishimura K, Masuda M (2010) Acetylcholine–dopamine balance hypothesis in the striatum: An update. Geriatrics & Gerontology International 10: S148-S157.
6. Bazalakova MH, Blakely RD (2006) The high-affinity choline transporter: a critical protein for sustaining cholinergic signaling as revealed in studies of genetically altered mice. Handb Exp Pharmacol: 525-544.
7. Oda Y (1999) Choline acetyltransferase: The structure, distribution and pathologic changes in the central nervous system. Pathology International 49: 921-937.
8. Brandon EP, Lin W, D'Amour KA, Pizzo DP, Dominguez B, et al. (2003) Aberrant Patterning of Neuromuscular Synapses in Choline Acetyltransferase-Deficient Mice. The Journal of Neuroscience 23: 539-549.
9. de Castro BM, De Jaeger X, Martins-Silva C, Lima RDF, Amaral E, et al. (2009) The Vesicular Acetylcholine Transporter Is Required for Neuromuscular Development and Function. Molecular and Cellular Biology 29: 5238-5250.
10. Wess J, Han S-J, Kim S-K, Jacobson KA, Li JH (2008) Conformational changes involved in G-protein-coupled-receptor activation. Trends in Pharmacological Sciences 29: 616-625.
11. Le Novère N, Corringer P-J, Changeux J-P (2002) The diversity of subunit composition in nAChRs: Evolutionary origins, physiologic and pharmacologic consequences. Journal of Neurobiology 53: 447-456.
12. Marks M, Laverty D, Whiteaker P, Salminen O, Grady S, et al. (2010) John Daly's Compound, Epibatidine, Facilitates Identification of Nicotinic Receptor Subtypes. Journal of Molecular Neuroscience 40: 96-104.
13. Massoulié J, Perrier N, Noureddine H, Liang D, Bon S (2008) Old and new questions about cholinesterases. Chemico-Biological Interactions 175: 30-44.
14. Perrier AL, Massoulie J, Krejci E (2002) PRiMA: the membrane anchor of acetylcholinesterase in the brain. Neuron 33: 275-285.
15. Dobbertin A, Hrabovska A, Dembele K, Camp S, Taylor P, et al. (2009) Targeting of Acetylcholinesterase in Neurons In Vivo: A Dual Processing Function for the Proline-Rich Membrane Anchor Subunit and the Attachment Domain on the Catalytic Subunit. The Journal of Neuroscience 29: 4519-4530.
16. Abreu-Villaça Y, Filgueiras CC, Manhães AC (2011) Developmental aspects of the cholinergic system. Behavioural Brain Research 221: 367-378.
17. Holler T, Berse B, Cermak JM, Diebler M-F, Blusztajn JK (1996) Differences in the developmental expression of the vesicular acetylcholine transporter and choline acetyltransferase in the rat brain. Neuroscience Letters 212: 107-110.

PLoS One. DOI: 10.1371/journal.pone.0068265

18. Aznavour N, Watkins KC, Descarries L (2005) Postnatal development of the cholinergic innervation in the dorsal hippocampus of rat: Quantitative light and electron microscopic immunocytochemical study. The Journal of Comparative Neurology 486: 61-75.
19. Mechawar N, Descarries L (2001) The cholinergic innervation develops early and rapidly in the rat cerebral cortex: a quantitative immunocytochemical study. Neuroscience 108: 555-567.
20. Moreno RD, Campos FO, Dajas F, Inestrosa NC (1998) Developmental regulation of mouse brain monomeric acetylcholinesterase. Int J Dev Neurosci 16: 123-134.
21. Sawyer TW, Weiss MT (1993) Parallel development of acetylcholinesterase in vivo and in primary neuron surface culture. Brain Res Dev Brain Res 71: 147-149.
22. Xie HQ, Leung KW, Chen VP, Chan GKL, Xu SL, et al. (2010) PRiMA directs a restricted localization of tetrameric AChE at synapses. Chemico-Biological Interactions 187: 78-83.
23. Svedberg MM, Svensson A-L, Bednar I, Nordberg A (2003) Neuronal nicotinic and muscarinic receptor subtypes at different ages of transgenic mice overexpressing human acetylcholinesterase. Neuroscience Letters 340: 148-152.
24. Lammerding-Koppel M, Greiner-Schroder A, Drews U (1995) Muscarinic receptors in the prenatal mouse embryo. Comparison of M35-immunohistochemistry with [3H]quinuclidinyl benzylate autoradiography. Histochem Cell Biol 103: 301-310.
25. Fiedler EP, Marks MJ, Collins AC (1987) Postnatal development of cholinergic enzymes and receptors in mouse brain. J Neurochem 49: 983-990.
26. Bernard V, Decossas M, Liste I, Bloch B (2006) Intraneuronal trafficking of G-protein-coupled receptors in vivo. Trends Neurosci 29: 140-147.
27. Farar V, Mohr F, Legrand M., Lamotte d'Incamps B, Cendelin J, et al. (2012) Near complete adaptation of the PRiMA knockout to the lack of central acetylcholinesterase. Journal of Neurochemistry 122: 1065-1080.
28. Zheng Q, Olivier K, Won YK, Pope CN (2000) Comparative Cholinergic Neurotoxicity of Oral Chlorpyrifos Exposures in Preweanling and Adult Rats. Toxicological Sciences 55: 124-132.
29. Bajgar J, Fusek J, Kassa J, Jun D, Kuca K, et al. (2008) An attempt to assess functionally minimal acetylcholinesterase activity necessary for survival of rats intoxicated with nerve agents. Chemico-Biological Interactions 175: 281-285.
30. Maxwell D, Brecht K, Koplovitz I, Sweeney R (2006) Acetylcholinesterase inhibition: does it explain the toxicity of organophosphorus compounds? Archives of Toxicology 80: 756-760.
31. Myslivecek J, Duysen EG, Lockridge O (2007) Adaptation to excess acetylcholine by downregulation of adrenoceptors and muscarinic receptors in lungs of acetylcholinesterase knockout mice. Naunyn Schmiedebergs Arch Pharmacol 376: 83-92.
32. Ellman GL, Courtney KD, Andres V, Jr., Feather-Stone RM (1961) A new and rapid colorimetric determination of acetylcholinesterase activity. Biochem Pharmacol 7: 88-95.
33. Mrvova K, Obzerova L, Girard E, Krejci E, Hrabovska A (2012) Monoclonal antibodies to mouse butyrylcholinesterase. Chemico-Biological Interactions 203: 348-353.

PLoS One. DOI: 10.1371/journal.pone.0068265

34. Xie W, Stribley JA, Chatonnet A, Wilder PJ, Rizzino A, et al. (2000) Postnatal developmental delay and supersensitivity to organophosphate in gene-targeted mice lacking acetylcholinesterase. J Pharmacol Exp Ther 293: 896-902.
35. Lassiter TL, Barone Jr S, Padilla S (1998) Ontogenetic differences in the regional and cellular acetylcholinesterase and butyrylcholinesterase activity in the rat brain. Developmental Brain Research 105: 109-123.
36. Geula C, Nagykery N (2007) Butyrylcholinesterase activity in the rat forebrain and upper brainstem: Postnatal development and adult distribution. Experimental Neurology 204: 640-657.
37. Bullock R, Lane R (2007) Executive dyscontrol in dementia, with emphasis on subcortical pathology and the role of butyrylcholinesterase. Curr Alzheimer Res 4: 277-293.
38. Mesulam MM, Guillozet A, Shaw P, Levey A, Duysen EG, et al. (2002) Acetylcholinesterase knockouts establish central cholinergic pathways and can use butyrylcholinesterase to hydrolyze acetylcholine. Neuroscience 110: 627-639.
39. Alexander S, Mathie A, Peters J (2011) Guide to Receptors and Channels (GRAC), 5th edition. British Journal of Pharmacology 164: 1-324.
40. Michel MC, Wieland T, Tsujimoto G (2009) How reliable are G-protein-coupled receptor antibodies? Naunyn Schmiedebergs Arch Pharmacol 379: 385-388. doi: 310.1007/s00210-00009-00395-y. Epub 02009 Jan 00227.
41. Jositsch G, Papadakis T, Haberberger R, Wolff M, Wess J, et al. (2009) Suitability of muscarinic acetylcholine receptor antibodies for immunohistochemistry evaluated on tissue sections of receptor gene-deficient mice. Naunyn-Schmiedeberg's Archives of Pharmacology 379: 389-395.
42. Yamada N, Sasaki S, Ishii H, Sato J, Kanno T, et al. (2011) Dark cell change of the cerebellar Purkinje cells induced by terbutaline under transient disruption of the blood-brain barrier in adult rats: morphological evaluation. Journal of Applied Toxicology.
43. Massoulie J (2002) The origin of the molecular diversity and functional anchoring of cholinesterases. Neurosignals 11: 130-143.

PLoS One. DOI: 10.1371/journal.pone.0068265

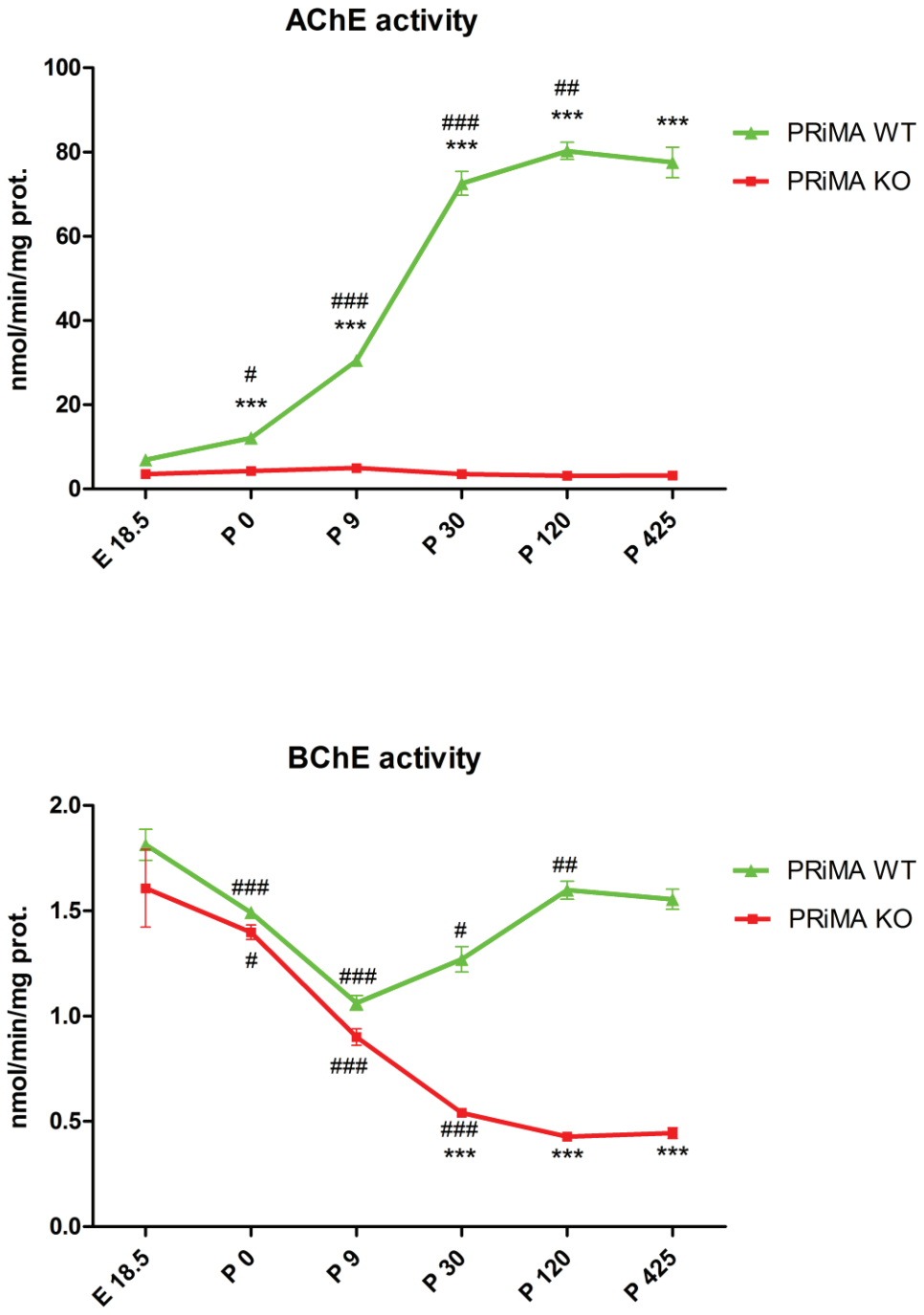

Figure 1:
The development of acetylcholinesterase activity in the brain of PRiMA WT and PRiMA KO mice. **Bottom:** The development of butyrylcholinesterase activity in the brain of PRiMA WT and PRiMA KO mice. Abscissa: day of the development (E18.5, embryonal day 18.5; P0, postnatal day 0; P9, postnatal day 9; P30, postnatal day 30; P120, postnatal day 120; P425, postnatal day 425). Ordinate: the activity of acetylcholinesterase express as nmol/min/ mg of protein. ***p<0.001, significantly different from PRiMA +/+. #p<0.05, significantly different from previous day of development, ##p<0.01, significantly different from previous day of development. ##p<0.01, significantly different from previous day of development. ###p<0.001 significantly different from previous day of development.

PLoS One. DOI: 10.1371/journal.pone.0068265

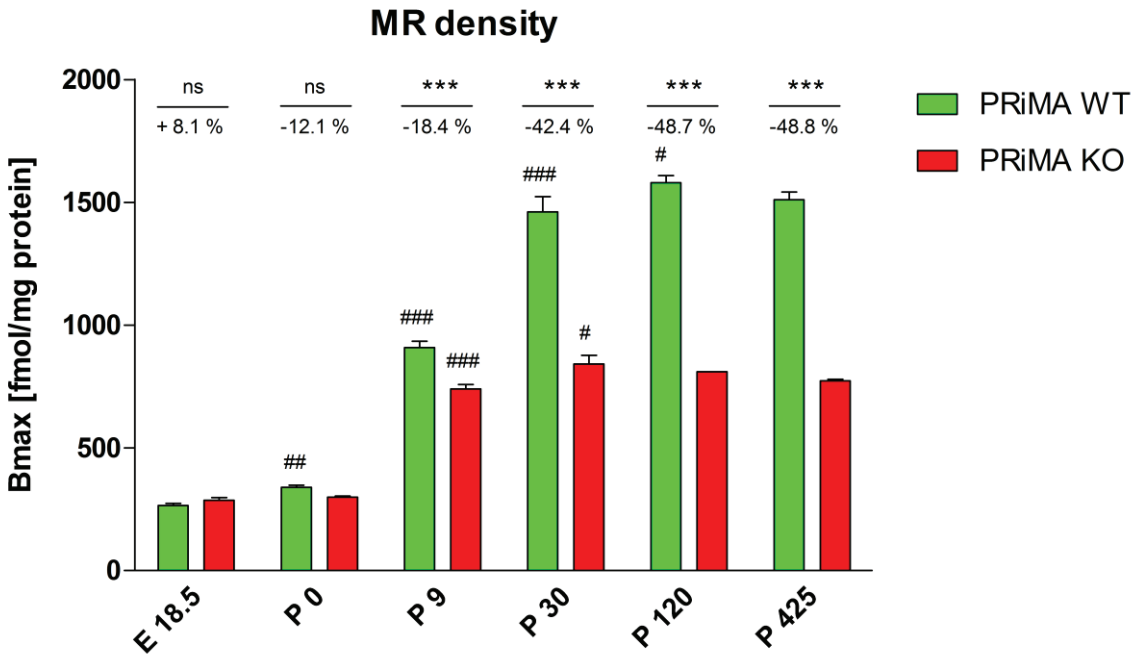

Figure 2: The development of number of binding sites in the brain of PRiMA WT and PRiMA KO mice. Abscissa: day of the development (E18.5, embryonal day 18.5; P0, postnatal day 0; P9, postnatal day 9; P30, postnatal day 30; P120, postnatal day 120; P425, postnatal day 425). Ordinate: the number of muscarinic receptor binding sites expressed as Bmax [fmol/mg protein]. ***p<0.001, significantly different from PRiMA +/+. #p<0.05, significantly different from previous day of development, ##p<0.01, significantly different from previous day of development. ###p<0.001 significantly different from previous day of development.

PLoS One. DOI: 10.1371/journal.pone.0068265

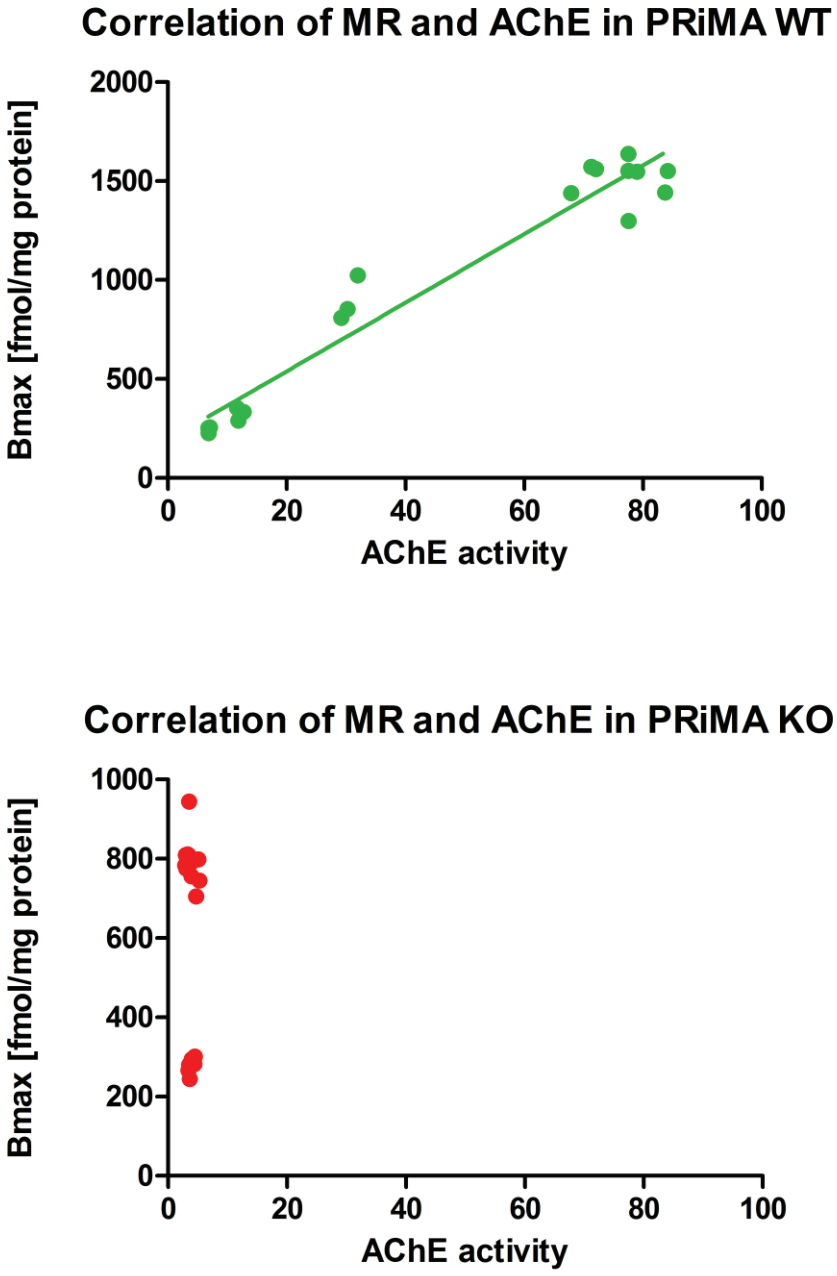

Figure 3: Correlation between AChE activity (abscissa) and MR density (ordinate). Top: Correlation in WT animals, bottom correlation in KO animals. In KO, there were no correlation, in WT we have able to discover significant correlation $p<0.0001$, Pearson $r=0.9727$.